



Miriam Trigo López se licenció en Química en la Universidad de Burgos, en 2009. Tras haber cursado el Máster Oficial en Química Avanzada en la especialidad de Nuevos Materiales se incorporó en el año 2011 al Grupo de Polímeros como Personal Docente Investigador. En el año 2012 obtuvo una Beca FPI (Formación de Personal Investigador) del Ministerio de Ciencia e Innovación, llevando a cabo, hasta finales de 2015, los trabajos para la obtención del título de Doctora.



Miriam Trigo López

TESIS DOCTORAL

Año 2015

POLÍMEROS FUNCIONALES

**APLICACIONES COMO SENSORES Y
MATERIALES DE ALTAS PRESTACIONES**

Directores:

Prof. Dr. José Miguel García Pérez

Prof. Dr. Félix Clemente García García

Universidad de Burgos

DEPARTAMENTO DE QUÍMICA

Área de Química Orgánica

Grupo de Polímeros



D. José Miguel García Pérez, Catedrático, y **D. Félix Clemente García García**, Profesor Titular, del Área de Química Orgánica del Departamento de Química de la Universidad de Burgos,

INFORMAN:

La presente Memoria titulada **“Polímeros funcionales. Aplicaciones como sensores y materiales de altas prestaciones”** se ha realizado en el Departamento de Química de la Universidad de Burgos, bajo su dirección, por **Dña. Miriam Trigo López**, y autorizan su presentación para que sea calificada como **TESIS DOCTORAL**.

Burgos, 16 de septiembre de 2015.

Fdo.: Prof. Dr. José Miguel García Pérez

Fdo.: Prof. Dr. Félix Clemente García García

Agradecimientos

Quisiera expresar mi más sincero agradecimiento a todas las personas que me han apoyado y ayudado, de manera que sin su contribución no hubiera sido posible culminar este trabajo con satisfacción:

A mis directores José Miguel García y Félix García, por su calidad científica, su trabajo intenso, su dedicación personal, y por su orientación y dirección; pero sobre todo por apostar por mi hace tiempo y darme la oportunidad de realizar esta Tesis y trabajar en el Grupo de Polímeros.

A Asun, Satur y Felipe por sus consejos y su ayuda en esta Tesis.

A los integrantes del Centro de I+D+i de la Universidad de Burgos, por la ayuda y contribución prestada en este Trabajo de Investigación.

A Craig Hawker, a su grupo de investigación y a la gente que conocí allí, por acogerme tan bien durante mi estancia en Santa Bárbara, California.

A mis compañeros de laboratorio (tanto a los actuales como a los que ya han terminado o simplemente han pasado por aquí un tiempo), a los analíticos, a mis químicos (frustrados y no frustrados), a mis amigas de toda o casi toda la vida y a Álvaro; a todos ellos les doy las gracias por los buenos momentos que hemos pasado juntos, y por las terapias de grupo durante las comidas y los cafés, las quedadas, las fiestas, los viajes, las celebraciones, los momentos buenos y menos buenos, por su amistad y su apoyo en todo momento.

A mis padres y a mis hermanos Elena, Álvaro, Pablo, Javier, Miguel y Mariola, que siempre han estado a mi lado, les quiero decir que sin ellos nada de lo que hoy en día he logrado hubiera sido posible, ni tampoco tendría sentido.

Resumen

El trabajo que conforma la Tesis se encuadra en el ámbito científico y tecnológico de los materiales avanzados para aplicaciones específicas. En este marco se han diseñado materiales funcionales con aplicaciones en protección y seguridad civil, industria y medio ambiente. Concretamente se han elaborado sensores químicos poliméricos cromogénicos y fluorogénicos de explosivos (TNT), cationes metálicos, alta acidez y agua. Los receptores orgánicos utilizados son insolubles en agua, pero su incorporación a polímeros con el grado de hidrofilia adecuada ha permitido la obtención de polímeros solubles en este medio, así como geles capaces de detectar a las moléculas de interés en entornos acuosos. Además, se han preparado materiales de altas prestaciones, concretamente poliamidas aromáticas, con grupos funcionales que aportan características de interés como color, potencial funcionalización adicional, o mejores propiedades mecánicas y térmicas.

Abstract

The work constituting this Thesis lies within the scientific and technological field of advanced materials for specific applications. In this framework, functional materials with applications in civil protection and security, industry and environment have been designed. Specifically, fluorogenic and chromogenic polymeric chemosensors towards explosives (TNT), metal cations, high acidity and water were developed. The organic receptors used were insoluble in water, but their incorporation into polymers with the appropriate degree of hydrophilicity allowed for the preparation of water soluble polymers, as well as gels capable of detecting target molecules in aqueous environments. In addition, high performance materials were prepared, particularly aromatic polyamides containing functional groups that provide interesting features, such as color, additional functionalization potential, or better mechanical and thermal properties.

CAPÍTULO 1 Introducción general	
1.1. Antecedentes históricos de los polímeros	1
1.2. Diseño de estructuras poliméricas	6
1.3. Polímeros funcionales	7
1.3.1. Polímeros vinílicos	8
1.3.2. Poliamidas aromáticas	11
1.3.3. Polímeros vinílicos y poliamidas aromáticas en el marco del trabajo realizado	14
1.4. Objetivos	15
1.5. Estructura de la memoria	16
CAPÍTULO 2 Polímeros sensores	
2.1. Introducción	19
2.1.1. Sensores químicos ópticos	20
2.1.2. Diseño y síntesis de polímeros como sensores químicos y dosímetros	25
2.2. Sensores fluorogénicos de agua y humedad	30
2.2.1. Derivados de la fluorenona y del 1,2,3-triazol	30
2.2.2. Polímeros con grupos fluorenona y 1,2,3-triazol en su estructura	32
2.2.3. Aplicaciones	33
2.2.4. Resultados	33
<i>Solid sensory kit for the easy and rapid determination of the concentration of water in organic solvents and ambient humidity</i>	35
2.3. Sensores cromogénicos de cationes metálicos	52
2.3.1. Derivados de la terpiridina	53
2.3.2. Polímeros con derivados de terpiridina en su estructura	53
2.3.3. Aplicaciones	55
2.3.4. Resultados	56
<i>Colorimetric detection of Fe(III), Co(II), Cu(II), and Sn(II) in 100% water by acrylic polymers with pendant terpyridine motifs for analytical and forensic applications</i>	57
2.4. Sensores cromogénicos de explosivos (TNT)	83
2.4.1. Complejos de Meisenheimer	83
2.4.2. Polímeros con aminas primarias, secundarias y terciarias	84
2.4.3. Aplicaciones	87
2.4.4. Resultados	87
<i>Water soluble polymers, solid polymer membranes, and coated fibres as smart sensory materials for the naked eye detection and quantification of TNT in aqueous media</i>	89
<i>Solid polymer substrate and smart fibres for the selective visual detection of TNT both in vapor and in aqueous media</i>	101

2.5. Sensores cromogénicos de alta acidez	122
2.5.1. Azoderivados	122
2.5.2. Polímeros con derivados de azobencenos en su estructura.	124
2.5.3. Aplicaciones	125
2.5.4. Resultados.....	126
<i>Aromatic polyamides and acrylic polymers as solid sensory materials and smart coated fibres for high acidity colorimetric sensing</i>	127
CAPÍTULO 3 Polímeros de altas prestaciones	
3.1. Introducción	157
3.1.1. Poliamidas aromáticas como materiales de altas prestaciones...	159
3.1.2. Propiedades de las poliamidas aromáticas	160
3.1.3. Diseño y síntesis de nuevos polímeros de altas prestaciones.....	162
3.2. Poliamidas aromáticas con coloración azul inherente	164
3.2.1. Coloración de fibras de aramida y moléculas derivadas de azadipirrometenos	164
3.2.2. Poliamidas con derivados de azadipirrometeno en su estructura	166
3.2.3. Aplicaciones	168
3.2.4. Resultados.....	168
<i>Intrinsically colored wholly aromatic polyamides (aramids)</i>	169
3.3. Poliamidas con grupos reactivos	194
3.3.1. Azidas aromáticas.....	194
3.3.2. Poliamidas aromáticas con grupos azida en su estructura	196
3.3.3. Aplicaciones	198
3.3.4. Resultados	199
<i>Crosslinked aromatic polyamides: a further step in high-performance materials</i>	201
<i>Functional aramids: Aromatic polyamides with reactive azido and amino groups in the pendant structure</i>	223
Conclusions	245
Anexo – Resumen de méritos	247

CAPÍTULO 1

Introducción general

Los polímeros son materiales que forman parte de nuestra vida cotidiana. La irrupción de los polímeros sintéticos y la variedad de sus usos ha afectado tan profundamente a la vida moderna que nuestro mundo es prácticamente inimaginable sin ellos. Actualmente, la Ciencia y Tecnología de Polímeros dirige su investigación a la profundización en la relación estructura-propiedades de las macromoléculas con el objetivo de diseñar materiales de altas prestaciones que satisfagan las necesidades que demanda el desarrollo socioeconómico y las nuevas tecnologías. En este marco tecnológico se inscribe este trabajo desarrollado en el Grupo de Polímeros de la Universidad de Burgos. Concretamente en el diseño, síntesis y caracterización de nuevos polímeros que incorporan modificaciones en su estructura para su aplicación como sensores o su mejora como materiales de altas prestaciones.

1.1. Antecedentes históricos de los polímeros

Los polímeros son tan antiguos como la vida misma; el ADN y el ARN, la base de la vida tal cual la entendemos, son macromoléculas naturales. Desde los albores de la humanidad, se han utilizado polímeros naturales como alimento, ropa y refugio, y se ha ido incrementado su capacidad de uso y transformación a medida que el hombre aprendía a tallar la madera, hilar el algodón y la lana, y

a curtir el cuero. Hace unos dos mil años, en China dieron un paso adelante con la manufactura del papel a partir de fibras vegetales naturales y los nativos centroamericanos incluso encontraron la manera de transformar el látex vegetal en un material útil. Todos estos desarrollos fueron importantes para la creación de la civilización moderna, aunque no afectaron a la estructura original de los polímeros.^{1,2}

En 1839 se produjo un salto cualitativo con la conversión de polímeros naturales en productos más útiles, cuando Charles Goodyear trató el caucho natural con azufre para producir caucho vulcanizado, que no se congelaba en invierno ni fundía en verano, a diferencia del caucho natural. Poco después, Christian Schönbein convirtió el algodón, una forma de la celulosa, en nitrocelulosa, polímero soluble y moldeable en artículos acabados. Posteriormente, a finales del siglo XIX la nitrocelulosa se convirtió en el material de fabricación de las películas fotográficas, barnices, etc. y contribuyó a la mejora de las dinamitas, lo que supuso el inicio de la demanda efectiva de materiales orgánicos por parte de la sociedad.

Los primeros estudios sobre polímeros acrílicos se realizaron en Alemania, en 1901, por Otto Röhm³ y se comercializaron por primera vez en 1931 como recubrimientos y formando parte de vidrios de seguridad. El más conocido es el polimetacrilato de metilo (PMMA), que se comercializó en 1933 bajo el nombre de Plexiglas®.^{4,5} Su producción aumentó considerablemente durante la Segunda Guerra Mundial al utilizarse como sustituto del vidrio, debido principalmente a su elevada resistencia al impacto y a su transparencia.

El primer polímero sintético usado a escala industrial fue una resina de fenol-formaldehído conocida como baquelita, desarrollada en 1907 por Leo

¹ H. Morawetz, *Polymers-The Origins and Growth of a Science*, Wiley-Interscience, Nueva York, 1985.

² P. J. T. Morris, *Polymer Pioneers*, Centre for the History of Chemistry, Filadelfia, 1986.

³ O. Röhm, *Ber. Dtsch. Chem. Ges.* **1901**, *34*, 573.

⁴ O. Röhm, *Chemische Fabrik* **1936**, 529.

⁵ O. Röhm, E. Trommsdorff, Patente EEUU 2171765, 1939.

Baekland. La baquelita es un material termoestable, aislante térmico y eléctrico y resistente al agua y a los ácidos, por lo que se utilizó rápidamente en numerosos objetos de uso doméstico y componentes eléctricos de uso general.

A pesar de estos avances significativos, en ese momento todavía no se tenía conocimiento de la estructura de los polímeros y eran considerados materiales mal definidos. Sin embargo, en 1920 se produjo un acontecimiento que supuso la primera etapa en el desarrollo efectivo de los materiales orgánicos. Hermann Staudinger⁶ propuso por primera vez el concepto de polímero tal y como lo conocemos hoy en día, sugiriendo que los polímeros eran cadenas de gran tamaño constituidas por unidades repetitivas unidas por enlaces covalentes. Recibió el Premio Nobel en 1953 por su trabajo en este campo. Además esta idea fue confirmada por los trabajos de Wallace Carothers^{7,8} en el campo de la policondensación y por las aportaciones de Paul Flory⁹ a la comprensión del comportamiento de los polímeros en disolución y en fundido, por las que le otorgaron el Premio Nobel en Química en 1974. Sus trabajos pusieron los cimientos científicos, tanto teóricos como experimentales, del desarrollo de la física y la química de las macromoléculas.

Los resultados alcanzados con los primeros polímeros llevaron a los investigadores y a la industria química a buscar otras moléculas sencillas que pudieran enlazarse para formar polímeros. En la década de 1930, en el Reino Unido se descubrió que el gas etileno polimerizaba por la acción del calor y la presión, formando un termoplástico, el polietileno. En estas fechas surgieron también el policloruro de vinilo, el politetrafluoroetileno y el poliestireno; y en la década de los 50 surgió el polipropileno. También en los años 30, Carothers,¹⁰ considerado el gran impulsor de los polímeros de condensación, se percató de

⁶ H. Staudinger, *From Organic Chemistry to Macromolecules*, Wiley-Interscience, Nueva York, 1970.

⁷ W. H. Carothers, G. J. Berchet, *J. Am. Chem. Soc.* **1930**, *52*, 5289.

⁸ W. H. Carothers, *J. Am. Soc.* **1929**, *51*, 2548; *Chem. Rev.* **1931**, *8*, 353; *Collected Papers of Wallace Hume Carothers on High Polymeric Substances*, H. Marck, G.S. Whitby, eds., Wiley-Interscience, Nueva York, 1926.

⁹ P. J. Flory, *Principles of Polymer Chemistry*, Cornell University Press, Ítaca, 1951.

¹⁰ W. H. Carothers, J. W. Hill, *J. Am. Soc.* **1932**, *54*, 1566.

que la reacción entre diácidos y diaminas daba lugar a la formación de poliamidas, que en general se podían hilar en fibras, y fueron denominados *nylons* (nailons) por la empresa DuPont.¹¹ Su primer uso fue la fabricación de paracaídas para las fuerzas armadas estadounidenses durante la Segunda Guerra Mundial, extendiéndose rápidamente a la industria textil.

Durante la Segunda Guerra Mundial se produjo un vertiginoso crecimiento en la utilización de algunos polímeros como sustitutos de otros materiales de difícil adquisición debido a los cortes en los suministros de materias primas. Como ejemplo, Alemania perdió sus fuentes naturales de látex e impulsó un programa que llevó al desarrollo del caucho sintético. La entrada de Japón en el conflicto cortó los suministros de caucho natural, seda y muchos metales asiáticos a EEUU. La respuesta fue la intensificación del desarrollo y la producción de polímeros. Las poliamidas se convirtieron en una de las fuentes principales de fibras textiles, los poliésteres se utilizaron para la fabricación de blindajes y otros materiales bélicos, y se produjeron varios tipos de cauchos sintéticos en grandes cantidades. Durante los años de la posguerra se mantuvo el elevado ritmo de los descubrimientos y desarrollos de la industria de los plásticos, y la investigación se derivó hacia la física de polímeros, lo que supuso un avance importante en el conocimiento de la relación entre la estructura, la morfología y las propiedades de estos materiales.

En la década de 1950, el químico alemán Karl Ziegler y el italiano Giulio Natta, desarrollaron catalizadores para la síntesis estereoespecífica de poliolefinas, por lo que recibieron el Premio Nobel de Química en 1963. La relevancia de sus descubrimientos se refleja en los volúmenes de producción a nivel mundial, 57 y 55 millones de toneladas al año de polietileno de alta densidad y de polipropileno, respectivamente.^{12,13}

¹¹ W. H. Carothers, Patente EEUU 2130948, 1938.

¹² Ceresana Market Intelligence. Consulting, *Market Study: Polyethylene-HDPE*. 3ª ed. Constanza, Alemania, 2015.

Las poliamidas aromáticas, o aramidias, también se desarrollaron en los años 60. Algunas de ellas se comercializaron a principios de la década de 1970 por DuPont bajo los nombres de Nomex® [poli(*m*-fenilen isoftalamida)] y el Kevlar® [poli(*p*-fenilen tereftalamida)]. Estos materiales destacan por su alta resistencia térmica y mecánica, lo que permite su utilización en aplicaciones de altas prestaciones, como trajes para bomberos, chalecos antibalas, ropa de protección anti-corte, por ejemplo.

A partir de los años 70 tuvo lugar una multitud de descubrimientos científicos y tecnológicos debido al mayor número de investigadores en este ámbito, así como al desarrollo y mejora de las herramientas científicas. Así, se produjo un avance importante de los métodos de síntesis, transformación y producción de los polímeros generales en sus aplicaciones finales.

Actualmente, la investigación se dirige hacia la obtención de polímeros especiales, preparados directamente mediante síntesis de nuevos monómeros, o bien a través de modificaciones químicas y físicas de polímeros preexistentes. La Ciencia y Tecnología de Polímeros requiere conocimientos sobre síntesis, caracterización estructural, procesado, propiedades y comportamiento de los materiales, y se ha convertido en una ciencia puntera e interdisciplinar entre las fronteras de la Química, la Física, la Ingeniería y la Biología. Hoy en día, se investiga en la producción de materiales con alto módulo de Young, alta resistencia térmica, fotosensibles, biopolímeros, polímeros electroactivos, polímeros con propiedades ópticas no lineales, nanomateriales, sistemas multicomponente, materiales selectivos para técnicas de separación o análisis, entre otros.¹⁴

¹³ Ceresana Market Intelligence. Consulting, *Market Study: Polypropylene*. 3ª ed. Constanza, Alemania, 2014.

¹⁴ *New Trends in Polymer Sciences*, Macromolecular Symposia, Vol. 283-284, Eds.: K. Matyjaszewski, R. C. Advincula, E. Saldivar-Guerra, G. Luna-Bárcenas, R. González-Núñez, John Wiley & Sons, Nueva York, 2009.

La producción mundial anual de polímeros es de 300 millones de toneladas.¹⁵ Su campo de aplicación es variado, como por ejemplo en la industria de la construcción, la aeronáutica, la automovilística, el envasado y embalaje, en adhesivos y pinturas, electrónica, medicina, y aislamiento térmico y eléctrico. Por tanto, han adquirido una enorme importancia económica y social. La diversidad de aplicaciones de los materiales poliméricos se debe a la variedad de propiedades físicas y químicas que pueden presentar, que se encuentran relacionadas con su estructura, la cual deriva del monómero y del enlace que forma a lo largo de la cadena polimérica, además de los grupos laterales que puedan incorporar. Esta serie de factores confieren distintos grados de rigidez a las cadenas y distintas fuerzas de interacción entre las mismas que determinan las propiedades que presenta finalmente el material.

1.2. Diseño de estructuras poliméricas

Las numerosas posibilidades de diseño de estructuras poliméricas permiten la obtención de materiales con propiedades muy distintas, como materiales químicamente inertes, mecánica y térmicamente resistentes, hidrofílicos, hidrofóbicos, solubles en medios acuosos, etc. lo que posibilita el empleo de estos polímeros en cualquier tipo de medio y condiciones. De entre todas estas posibilidades de diseño, en el Grupo de Investigación se ha planteado la preparación de dos tipos distintos de estructuras poliméricas:

- *Estructuras vinílicas, específicamente tipo polimetacrilato o polimetacrilamida*: polímeros de adición, con resistencia térmica baja y mecánica moderada. Se pueden obtener materiales con distintos grados de hidrofilia, así como polímeros completamente solubles en agua.
- *Estructura tipo poliamida aromática*: polímeros de condensación, térmica y químicamente estables, mecánicamente resistentes e

¹⁵ J. M. García, *La Edad de los Polímeros. Un mundo de plástico*. Universidad de Burgos, Burgos, 2014.

insolubles en la mayoría de los disolventes, que poseen además cierto grado de hidrofilia. Los materiales derivados de las poliamidas aromáticas pueden emplearse en condiciones extremas, tanto en medios acuosos, orgánicos, o al aire.

1.3. Polímeros funcionales

Los polímeros se pueden dividir en dos subgrupos atendiendo a sus aplicaciones: polímeros con aplicaciones estructurales, y polímeros que tienen alguna funcionalidad específica, es decir, polímeros funcionales. Aunque ambos juegan un papel importante en la Ciencia y Tecnología de Polímeros, los segundos se caracterizan por su utilidad específica que viene determinada por la presencia de grupos funcionales o grupos de átomos con alguna función.

La IUPAC define *polímero funcional* como un polímero que tiene unas propiedades físicas, biológicas, farmacológicas o de otro tipo que dependen de grupos químicos específicos.¹⁶ Por ejemplo, estos polímeros pueden tener átomos o grupos de átomos que interaccionen con disolventes, iones, células, superficies, otros polímeros, etc. y pueden tener funcionalidades especiales como actividad catalítica, unión selectiva de ciertas especies, transporte de fármacos o transporte de carga. También pueden tener propiedades ópticas, eléctricas, térmicas o mecánicas específicas o mejoradas respecto a los polímeros estructurales similares.¹⁷

Un polímero funcional posee una combinación de las propiedades relativas a la naturaleza de la cadena principal, y a la reactividad química o funcionalidad de los átomos o grupo de átomos unidos a la cadena, por lo que la elección de la naturaleza del polímero es clave para la aplicación final del material. En este sentido, en el Grupo de Polímeros se trabaja en el diseño y

¹⁶ IUPAC. Compendium of Chemical Terminology, 2ª ed. Compiled by A.D. McNaught and A. Wilkinson. Blackwell Scientific publications, Oxford, 1997.

¹⁷ D. Braun, H. Cherdrón, M. Rehahn, H. Ritter, B. Voit, *Functional polymers* en "Polymer synthesis: theory and practice", 5ª Ed. Springer-Verlag Berlin Heidelberg, 2012.

síntesis de polímeros funcionales con aplicación como materiales sensores y materiales de altas prestaciones, empleando para ello polímeros con estructuras vinílicas y estructuras tipo poliamidas aromáticas.

Desde el punto de vista químico, a la hora de preparar nuevos polímeros funcionales se puede seguir una doble vía:

- Modificación de polímeros comerciales o preparados previamente en el laboratorio.
- Síntesis integral de nuevos monómeros y su posterior polimerización.

Ambas metodologías tienen sus ventajas y sus inconvenientes. La modificación de polímeros implica el diseño y síntesis de un polímero base, o la utilización de uno comercial, a partir del cual se pueden preparar de forma rápida y barata una serie de materiales derivados, ya que las reacciones de modificación que generalmente se utilizan son sencillas desde el punto de vista de la química orgánica. Por el contrario, los polímeros presentan una solubilidad limitada en los disolventes habituales utilizados en la síntesis orgánica, el rendimiento suele estar condicionado por la estructura macromolecular en disolución o en fundido, y los productos secundarios permanecen en la propia estructura de la macromolécula.

En cuanto a la síntesis integral de nuevos monómeros, permite un diseño específico de las estructuras, así como una purificación previa a la polimerización, pero supone un coste más elevado. Otra dificultad añadida, en el caso de monómeros diseñados con grupos laterales, es que estos grupos pueden ser sensibles a las condiciones de polimerización.

1.3.1. Polímeros vinílicos

Los polímeros vinílicos son los que poseen en su cadena principal uniones exclusivas carbono-carbono que provienen de la polimerización en cadena de

dobles enlaces. Entre ellos se encuentran las poliolefinas, los polímeros estirénicos, los vinílicos halogenados y los acrílicos.

Esta familia de polímeros es muy amplia, lo que hace difícil una discusión general más allá de su amplio uso, versatilidad y, en general, costes bajos de producción. Por este motivo nos centraremos en los polímeros acrílicos.

Los polímeros acrílicos y metacrílicos se obtienen por reacciones de adición de dobles enlaces en monómeros vinílicos. Resumidamente, el proceso de polimerización implica la ruptura del enlace π del doble enlace etilénico de la especie monomérica de partida por parte de un iniciador, seguida por su reacción en cadena con sucesivas incorporaciones de moléculas de monómero.¹⁸ La etapa de propagación finaliza cuando las cadenas activas en crecimiento se desactivan a través de procesos de distinta naturaleza.

La facilidad de preparación de nuevas estructuras con la funcionalidad adecuada, junto con la versatilidad de la copolimerización, ha hecho que estas familias sean de las más estudiadas entre los polímeros sintéticos. La modificación química del ácido (met)acrílico o sus derivados, fundamentalmente el cloruro de (met)acrilato, es una fuente prácticamente inagotable de monómeros que da lugar a materiales polímeros como polimetacrilatos, poliácridatos, polimetacrilamidas, o poliácridamidas, cuyas propiedades están condicionadas por la naturaleza química del grupo lateral unido covalentemente al grupo carbonilo. Como caso particular, se encuentran los polímeros que incorporan grupos funcionales hidroxilo o amino en su cadena lateral, ya que por su carácter hidrófilo se utilizan en la preparación de materiales de aplicación en medicina y cirugía. Por ejemplo, para la preparación de lentes de contacto se utilizan los polímeros derivados de metacrilatos de 2-hidroxietilo o de 3-hidroxipropilo.

¹⁸ G. Odian, *Principles of Polymerization*, 4ª Ed., Wiley-VCH, Nueva York, 2004.

La naturaleza química de los grupos laterales unidos al grupo carbonilo determina, por tanto, la hidrofilia, la solubilidad y la rigidez del polímero acrílico lineal. Este tipo de estructuras se emplean en nuestro Grupo de Investigación para la preparación de materiales solubles en agua y membranas densas con comportamiento de gel y buenas propiedades mecánicas tanto en seco como en hinchado. De este modo se pueden modificar las propiedades del material en función de la aplicación a la que se quiera destinar, pudiendo obtener así sistemas con grados variables de hidrofilia, rigidez o flexibilidad, etc. Como ejemplo de modulación de propiedades se puede mencionar los distintos grados de hinchamiento de acuerdo con la proporción de los monómeros 1-vinil-2-pirrolidona (VP, hidrofílico), metacrilato de metilo (MMA, hidrofóbico) y el entrecruzante (E) de distintas membranas (Tabla 1.1).

Tabla 1.1. Propiedades de las membranas en función de la proporción de los monómeros y el entrecruzante

VP	MMA	E	Hinchamiento	Propiedades
100%	0%	10%	150%	Rígida, frágil
75%	25%	5%	65%	Flexible, resistente
50%	50%	1%	20%	Ligeramente flexible, muy resistente

El trabajo desarrollado por el Grupo de Polímeros en el campo de los polímeros lineales solubles en agua y los reticulados en forma de membrana densa con alta capacidad de absorción de agua incluye la preparación de materiales que incorporan grupos éter corona y podandos,¹⁹⁻²¹ triazol,²² grupos

¹⁹ P. Tiemblo, F. García, J. M. García, E. Riande, J. Guzmán, *Polymer* **2003**, *44*, 6773.

²⁰ F. García, J. M. García, F. Rubio, P. Tiemblo, J. Guzmán, E. Riande, *Polymer* **2004**, *45*, 1467.

²¹ J. Rey, F. C. García, J. M. García, *React. Funct. Polym.* **2011**, *71*, 948.

²² A. Gómez-Valdemoro, M. Trigo, S. Ibeas, F. C. García, F. Serna, J. M. García, *J. Polym. Sci. Part A: Polym. Chem.* **2011**, *49*, 3817.

derivados de la piperazinodiona,^{23,24} del fluoreno,²⁵ ácido fenilborónico,²⁶ 2,4,6-trinitrobenceno,²⁷ hidroxiquinolona,²⁸ etc. Estos polímeros, además de ser un buen soporte, permiten controlar el carácter hidrofílico/hidrofóbico del material mediante la selección y el empleo de la proporción adecuada de los monómeros utilizados, posibilitando, por ejemplo, la optimización de la capacidad sensora de moléculas ancladas a una matriz polimérica. Porcentajes de hinchamiento mayores de 40% y menores de 100% son óptimos para la aplicación de los polímeros como sensores en medios acuosos, ya que porcentajes más bajos de hinchamiento se traducen en una menor difusión del agua y los analitos solvatados hacia el interior, y un porcentaje mayor perjudica las propiedades mecánicas de la membrana, y por lo tanto, su manejabilidad. De esta forma se ha conseguido preparar materiales sensores en medios acuosos hacia aniones (como hidrogenocarbonato,²⁹ cianuro,²⁵ etc., hacia cationes (como mercurio,³⁰ hierro,^{22,28} cromo,²³ etc.), y hacia moléculas neutras (como glucosa,²⁶ aminas²⁷ y aminoácidos²⁴).

1.3.2. Poliamidas aromáticas

Una poliamida es una macromolécula que contiene enlaces de tipo amida. Las poliamidas pueden ser naturales, como las proteínas, la lana o la seda; o artificiales. Las poliamidas artificiales son polímeros de ingeniería que se utilizan como textiles y como piezas para diversos sectores debido a sus buenas propiedades de resistencia y durabilidad. Las poliamidas aromáticas

²³ S. Vallejos, A. Muñoz, F. C. García, F. Serna, S. Ibeas, J. M. García, *Hazard. Mater* **2012**, 227-228, 480.

²⁴ S. Vallejos, P. Estévez, S. Ibeas, F. García, F. Serna, J. M. García, *Sensors* **2012**, 12, 1969.

²⁵ S. Vallejos, P. Estevez, F. C. García, F. Serna, J. L. de la Peña, J. M. García, *Chem. Commun.* **2010**, 46, 7951.

²⁶ J. L. Pablos, S. Vallejos, S. Ibeas, A. Muñoz, F. Serna, F. C. García, J. M. García, *ACS Macro Lett.* **2015**, 4, 979.

²⁷ J. L. Pablos, S. Vallejos, A. Muñoz, M. J. Rojo, F. Serna, F. C. García, J. M. García, *Chem. Eur. J.* **2015**, 21, 8733.

²⁸ S. Vallejos, A. Muñoz, S. Ibeas, F. Serna, F. C. García, J. M. García, *J. Mater. Chem.* **2013**, 1, 15435.

²⁹ B. García-Acosta, F. García, J. M. García, R. Martínez-Mañez, F. Sancernón, N. San-José, J. Soto, *Org. Lett.* **2007**, 9, 2429.

³⁰ S. Vallejos, P. Estevez, S. Ibeas, A. Muñoz, F. C. García, F. Serna, J. M. García, *Sens. Actuators B* **2011**, 157, 686.

sintéticas difieren de las poliamidas alifáticas (nailons) en la naturaleza aromática de su cadena principal. De acuerdo con la *US Federal Trade Commission* (FTC), las poliamidas aromáticas son poliamidas sintéticas que contienen al menos un 85% de grupos amida unidos directamente a dos anillos aromáticos.³¹

Las poliamidas aromáticas se sintetizan generalmente a partir de monómeros difuncionales: diaminas y diácidos, o derivados reactivos de éstos.³² En concreto, los métodos más comunes son la polimerización de dicloruros de diácido con diaminas a baja temperatura, y la condensación directa en disolución de diácidos aromáticos con diaminas a elevada temperatura.

La reacción suele producirse en fase homogénea, por lo que monómero y polímero han de ser solubles en el disolvente empleado a la temperatura de polimerización. Los disolventes utilizados son disolventes polares apróticos como la *N,N*-dimetilformamida (DMF), la *N,N*-dimetilacetamida (DMA) o la *N*-metil-2-pirrolidona (NMP). Se emplean asimismo sales, como LiCl, CaCl₂ o mezclas de ambas, que actúan como promotores de la solubilidad, ya que los cationes al interactuar con los grupos amida disminuyen la fuerza de interacción por enlaces de hidrógeno entre cadenas.

El procedimiento a baja temperatura, que se desarrolló en primer lugar, permite la polimerización de dicloruros de diácido con diaminas a temperaturas inferiores a la ambiente.³³⁻³⁵ Presenta varias ventajas, entre las que se encuentran la mezcla homogénea y rápida de reactivos, así como una

³¹ Rules and regulations under the textile fiber products identification act (<http://www.ftc.gov/os/statutes/textile/rr-textil.pdf>), Part 303.7 (Generic names and definitions for manufactured fibers), US Federal Trade Commission (FTC).

³² H. Sekiguchi, B. Countin, H. R. Kricheldorf, *Polyamides* en "Handbook of Polymer Synthesis", Ed. Dekker, Nueva York, 1992.

³³ H. R. Kricheldorf, G. Schwarz, *Makromol. Chem.* **1983**, *184*, 475.

³⁴ Y. Oishi, M. Kakimoto, Y. Imai, *Macromolecules* **1987**, *20*, 703.

³⁵ A. E. Lozano, J. G. de la Campa, J. de Abajo, *Macromolecules* **1997**, *30*, 2507.

eliminación eficiente del calor de reacción, lo que permite minimizar las reacciones secundarias de los cloruros de ácido con el disolvente. Este método se utiliza generalmente cuando es posible obtener el cloruro del correspondiente diácido aromático de forma sencilla.

Una modificación de este método incluye la sililación de diaminas para aumentar la reactividad de los grupos amino, que se realiza normalmente *in situ* para evitar el aislamiento y la purificación de las diaminas sililadas, sensibles a la humedad.³⁶

La reacción de polimerización también puede llevarse a cabo en un sistema de dos fases a baja temperatura, por el método de polimerización interfacial.³⁷ En este caso la reacción tiene lugar en la interfase de dos disolventes no miscibles.

Cuando no es posible obtener el cloruro del correspondiente diácido aromático, es difícil obtenerlo con la pureza adecuada, o bien es sensible al calor o a la humedad, se puede recurrir a la policondensación en disolución a alta temperatura. Esta técnica, desarrollada en la década de 1970 por Yamazaki e Higashi,³⁸ permite la condensación directa de diaminas y diácidos mediante la activación de estos últimos empleando difenil o triaril fosfitos y piridina, así como NMP como disolvente. Además de la necesidad de una gran pureza de los monómeros, se ha de tener en cuenta que las elevadas temperaturas favorecen muchas reacciones secundarias. Por tanto, para obtener poliamidas aromáticas con cadenas laterales que incluyan grupos funcionales sensibles, es importante verificar la ausencia de reacciones secundarias en las condiciones de polimerización, lo cual puede llevarse a cabo mediante la preparación previa de compuestos modelo.

³⁶ Y. Imai, Y. Oishi, *Prog. Polym. Sci.* **1989**, *14*, 173.

³⁷ P. W. Morgan. *Condensation polymers*, Interscience, Nueva York, 1965.

³⁸ N. Yamazaki, F. Higashi, J. Kawataba. *J. Polym. Sci. Polym. Chem. Ed.* **1974**, *12*, 2149.

Las aramidas se caracterizan por tener un comportamiento térmico y mecánico excepcional, y se les considera aptas para aplicaciones tecnológicas avanzadas.³⁹ Las poliamidas aromáticas procesadas son materiales que se caracterizan por ser resistentes a la llama, al corte y de gran resistencia a la tracción, encontrando aplicaciones en tejidos avanzados: chalecos antibalas, equipamientos protectores y deportivos, filtros industriales y fibras de refuerzo en materiales compuestos empleados en la industria aeroespacial, entre otros.

No obstante, los mismos factores estructurales que confieren a las poliamidas aromáticas unas propiedades térmicas y mecánicas únicas, limitan su campo de aplicación debido a su baja solubilidad y elevada temperatura de fusión, que está incluso por encima de su temperatura de descomposición. Por ello, la investigación básica, y en concreto la que realiza nuestro Grupo de Investigación, se enfoca a la mejora de sus características físicas o químicas y de su procesabilidad, con intención de expandir sus aplicaciones.

1.2.3. Polímeros vinílicos y poliamidas aromáticas en el marco del trabajo realizado

El Grupo de Polímeros en el que se ha realizado este trabajo ha llevado a cabo numerosos estudios en cuanto al diseño de monómeros con grupos receptores selectivos de aniones, cationes y moléculas neutras, que tras su polimerización con otros monómeros comerciales se transforman en sensores químicos poliméricos o polímeros quimiosensores.²¹⁻²⁹ Otra de las líneas de investigación del Grupo trata de la mejora de las propiedades de las poliamidas aromáticas mediante la modificación química de la composición de poliamidas convencionales, y más concretamente poliisofalamidas. Se han realizado en el pasado estudios exhaustivos de la influencia de las modificaciones en la

³⁹ J. M. García, F. C. García, F. Serna, J. L. de la Peña, *Aromatic Polyamides (Aramids)* en "Handbook of Engineering and Specialty Thermoplastics", S. Thomas, Visakh P.M., Eds., Wiley/Scrivener Publishing, Salem, 2012.

estructura química en propiedades muy específicas, como la solubilidad, absorción de agua, así como el comportamiento térmico y mecánico.⁴⁰⁻⁴⁴

El trabajo desarrollado por el Grupo de Polímeros de la Universidad de Burgos, en el seno del cual se circunscribe esta Tesis, está orientado a la preparación de nuevos polímeros funcionales para su utilización como sensores o como materiales de altas prestaciones.

1.4. Objetivos

El trabajo que se recoge en esta Memoria se integra en el realizado hasta el momento en el Grupo de Polímeros y supone la continuación natural de los llevados a cabo por otros investigadores. En este sentido, se encuadra dentro de la línea de general de *investigación, diseño, síntesis y caracterización de polímeros para aplicaciones especiales*, que incluye, implícitamente, el estudio de la relación entre estructura y propiedades de los nuevos materiales.

Más concretamente, la investigación que se recoge en esta Memoria está dirigida hacia dos vías. En primer lugar el diseño, síntesis y caracterización de nuevos polímeros funcionales que incorporan en su estructura grupos receptores selectivos para su aplicación como polímeros sensores, membranas densas y tejidos inteligentes en tecnologías de sensores y dosímetros químicos. En segundo lugar, el diseño, síntesis y caracterización de nuevos polímeros funcionales de altas prestaciones que incorporan grupos en la cadena que proporcionan unas características físicas y/o químicas especiales a los materiales de altas prestaciones (poliamidas aromáticas) para ampliar o mejorar su aplicabilidad.

⁴⁰ J. M. García, J. G. de la Campa, J. de Abajo, *J. Polym. Sci. Part A. Polym. Chem.* **1996**, *34*, 659.

⁴¹ J. M. García, J. C. Álvarez, J. G. de la Campa, J. de Abajo, *Macromol. Chem. Phys.* **1997**, *198*, 727.

⁴² J. M. García, J. C. Álvarez, J. G. de la Campa, J. de Abajo, *J. Appl. Polym. Sci.* **1998**, *67*, 975.

⁴³ J. M. García, J. G. de la Campa, G. Schwarz, J. de Abajo, *Macromol. Chem. Phys.* **2001**, *202*, 1298.

⁴⁴ J. M. García, F. García, R. Sanz, J. G. de la Campa, A. E. Lozano, J. de Abajo, *J. Polym. Sci. Part A. Polym. Chem.* **2001**, *39*, 1825.

Los objetivos del trabajo se pueden resumir de la siguiente manera:

- Diseñar, sintetizar y caracterizar nuevos copolímeros de adición (vinílicos) lineales y entrecruzados, portadores de grupos receptores selectivos, como materiales sensores con potenciales aplicaciones en la detección visual y fluorogénica de especies químicas de interés.
- Diseñar, sintetizar, y caracterizar nuevos copolímeros de condensación (poliamidas aromáticas) que incorporen grupos en la cadena que proporcionen características especiales a los polímeros de altas prestaciones.
- Relacionar la estructura química de todos los polímeros preparados con las propiedades específicas, como los comportamientos térmico y mecánico, la solubilidad y la absorción de agua.
- Relacionar la capacidad sensora de los materiales poliméricos sintetizados frente a diversos analitos de interés con la estructura química.

1.5. Estructura de la Memoria

La Memoria se ha ordenado en cuatro capítulos, comenzado con esta Introducción General en la que se ha abordado el encuadre del trabajo y la presentación de los objetivos.

La metodología y los trabajos realizados para la consecución de estos objetivos se describen en los dos capítulos siguientes, estructurados por aplicación de los polímeros funcionales, como sensores o como materiales de altas prestaciones.

En el Capítulo 2 se describe la síntesis y caracterización de polímeros como sensores de explosivos, concretamente TNT, agua, alta acidez y cationes metálicos.

En el Capítulo 3 se describe la síntesis y caracterización de polímeros de altas prestaciones con color azul inherente, poliamidas entrecruzadas y poliamidas con grupos reactivos.

La memoria finaliza con las conclusiones que se derivan del trabajo realizado.

Por su parte, los procedimientos experimentales, los resultados y su discusión, así como las conclusiones parciales se aportan mediante la transcripción íntegra de los artículos publicados en las correspondientes revistas científicas. Esta Tesis se presenta, por tanto, como compendio de publicaciones.

CAPÍTULO 2

Polímeros sensores

Para el seguimiento en tiempo y espacio reales de la concentración de analitos de interés biológico, clínico, medioambiental, químico o industrial se necesitan sensores selectivos y de bajo umbral de detección. Una de las líneas de investigación del Grupo de Polímeros se basa en el diseño y síntesis de nuevos polímeros con grupos receptores en su estructura, capaces de interactuar selectivamente con cationes, aniones y moléculas neutras en distintos medios. El estudio concreto de la interacción de analitos con diversos grupos anclados a una matriz polimérica ha conducido al desarrollo de materiales sensores cromogénicos y fluorogénicos. Así, en el marco de esta Tesis se han desarrollado polímeros sensores de explosivos (TNT), de alta acidez, de agua y humedad, así como de cationes (hierro (III), cobalto (II), cobre (II) y estaño (II)).

2.1. Introducción

El fenómeno del reconocimiento molecular, que se da entre dos o más moléculas cuando éstas son química y geoméricamente complementarias, es habitual en el medio natural. Se trata de una interacción espacial debida a fuerzas moleculares consideradas débiles, como por ejemplo las

electrostáticas e hidrofóbicas, los puentes de hidrógeno y las coordinaciones débiles metal-ligando.^{45,46}

En la naturaleza se encuentran ejemplos de estas interacciones, como la interacción enzima/sustrato,⁴⁷ fármaco/diana biológica,^{48,49} antígeno/anticuerpo,^{50,51} y la síntesis del ARNm a partir del ADN,⁵² entre otros. De la observación de este tipo de fenómenos surgió la Química Supramolecular, o química *anfitrión-huésped*, tratando de imitar la efectividad, la simplicidad y los resultados de estos procesos biológicos. Cuando la interacción *anfitrión-huésped* es muy específica se utiliza el término *reconocimiento*; y de este modo surgió la utilización del *anfitrión* para el desarrollo de dispositivos tipo sensores, membranas permselectivas, catalizadores, sistemas de extracción, etc.

Sin embargo, a escala macromolecular, es importante combinar el fenómeno del reconocimiento con la transducción de la señal para el desarrollo de sistemas capaces de detectar moléculas de interés. Por lo tanto, el término *sensor* se utiliza únicamente para los fenómenos de reconocimiento *anfitrión-huésped* que dan lugar a la variación de una propiedad macroscópica fácilmente detectable y cuantificable.

2.1.1. Sensores químicos ópticos

Un sensor químico es un dispositivo que transforma una información química en una señal analítica de utilidad (IUPAC). Más concretamente, una molécula sensora es una estructura química con, al menos, dos subgrupos o

⁴⁵ N. M. Bergmann, N. Peppas, *Prog. Polym. Sci.* **2008**, *33*, 271.

⁴⁶ B. N. Chen, S. Piletsky, A. P. F. Turner, *Comb. Chem. High Throughput Screen* **2002**, *5*, 409.

⁴⁷ A. Tulinsky, *Sem. Thromb. Hemostasis* **1996**, *22*, 117.

⁴⁸ M. Britschgi, S. von Greyerz, C. Burkhart, W. J. Pichler, *Curr. Drug. Targets* **2003**, *4*, 1.

⁴⁹ P. Cudic, D. C. Behenna, J. K. Kranz, R. G. Kruger, A. J. Wand, Y. I Veklich, J. W. Weisel, D. G. McCafferty, *Chem. Biol.* **2002**, *9*, 897.

⁵⁰ E. J. Sundberg, R. A. Mariuzza, *Adv. Protein. Chem.* **2002**, *61*, 119.

⁵¹ R. Jimenez, G. Salazar, K. K. Baldrige, F. E. Romesberg, *Proc. Natl. Acad. Sci. USA* **2003**, *100*, 92.

⁵² S. A. Hofstadler, R. H. Griffery, *Chem. Rev.* **2001**, *101*, 377.

subunidades integrados, dónde uno de ellos actúa como *unidad receptora* y el otro como *unidad indicadora*.

La *unidad receptora* tiene la capacidad de interactuar con un *analito* o sustancia objetivo. Si esta interacción tiene lugar de forma reversible y selectiva hablamos de sensor químico o quimiosensor, mientras que si la interacción es irreversible estamos ante un dosímetro químico (en relación con la terminología, conviene aclarar que desde el punto de vista práctico cuando se habla de sensores se incluye asimismo a los dosímetros). Sobre la *unidad indicadora* o *transductora* recae el fenómeno de la detección, relacionado con la variación detectable de una propiedad macroscópica.^{53,54} Cuando además la transducción de la información se produce a través de un cambio de las propiedades fluorescentes, o mediante un cambio de color, se habla de sondas fluorogénicas o cromogénicas, respectivamente. En este proceso, la información de cambios producidos a nivel molecular, como puede ser la presencia o no de un determinado *analito*, se amplifica y se observa macroscópicamente.

En general, se puede decir que las fuerzas que gobiernan las interacciones entre las *unidades coordinantes* y los *analitos* pueden ser:

- Interacciones electrostáticas.
- Interacciones por formación de enlaces de hidrógeno.
- Interacciones covalentes con centros metálicos.

Atendiendo a la naturaleza de la unión entre la *unidad coordinante* y la *unidad indicadora* hay dos tipos de diseños de sondas moleculares (Figura 2.1). Si ésta es covalente se habla de *aproximación unidad coordinante-unidad indicadora* y si no lo es, de *aproximación por ensayos de desplazamiento*.

⁵³ J. P. Desvergne, A. W. Czarnik, *Chemosensors for Ion and Molecule Recognition*, NATO ASI Series, Kluwer Academic Publishers, Londres, 1997.

⁵⁴ M. D. Marcos, R. Martínez-Mañez, F. Sancenón, J. Soto, L. A. Villaescusa, *Anales de la Real Sociedad Española de Química* **2004**, *100*, 20.

La relación entre la especie coordinada y libre viene determinada por los cambios en la concentración del *analito*, y por lo tanto se trata de una reacción reversible del *analito* con el *receptor*.



Figura 2.1. Representación esquemática de la *aproximación unidad coordinante-unidad indicadora* (izquierda), y de la *aproximación por ensayos de desplazamiento* (derecha).

La mayoría de los quimiosensores descritos en la literatura se basan en la *aproximación unidad coordinante-unidad indicadora*, es decir, son sistemas que contienen un centro de coordinación unido covalentemente a una unidad generadora de señal o *unidad indicadora*. Mediante un diseño adecuado del *receptor* se puede conseguir que la interacción del *analito* con la *unidad coordinante* produzca cambios en las propiedades de la *unidad indicadora*, como por ejemplo, variaciones en la intensidad de emisión (sondas fluorogénicas) o variación del color (sondas cromogénicas).

En los *ensayos de desplazamiento* también se utiliza una *unidad coordinante* y una *unidad indicadora*, pero en este caso no están unidas por medio de un enlace covalente, sino formando un complejo de coordinación. Cuando se añade un determinado *analito* a la disolución de este conjunto, se produce una reacción de desplazamiento por la que la *unidad coordinante* pasa a formar un complejo con la especie añadida, desplazando a la *unidad indicadora* hacia la disolución. Si las características espectroscópicas de la *unidad indicadora* cuando está formando el complejo y cuando se encuentra libre son distintas, se obtiene una respuesta que está relacionada con la presencia del *analito*.

Además de los quimiosensores moleculares, hay otra aproximación a la detección química selectiva, como son los sistemas denominados dosímetros químicos o quimidosímetros. En la *aproximación del dosímetro químico*, la idea última no es utilizar sistemas selectivos de coordinación, como en los casos anteriores, sino reacciones químicas altamente específicas, y generalmente irreversibles, inducidas por un determinado *analito*, asociadas a un cambio en alguna propiedad macroscópica medible del sistema, en nuestro caso óptica.⁵⁵⁻⁵⁷ En la Figura 2.2 se muestra un ejemplo donde el *analito* induce una reacción que da lugar a la liberación de una molécula con color o fluorescente.

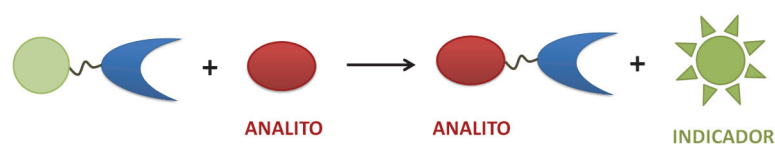


Figura 2.2. Representación esquemática de la *aproximación del dosímetro químico*.

Los sensores o sondas más habituales son los ópticos, en los que la propiedad macroscópica detectable es la fotoluminiscencia y el color.

La fotoluminiscencia es la emisión espontánea de la radiación, de luz, desde un estado electrónico excitado por parte de cualquier sustancia. En función de la naturaleza del estado excitado se divide en dos categorías, fluorescencia y fosforescencia. En fluorescencia la molécula excitada tiene la misma multiplicidad que la molécula en el estado fundamental. Tras ser irradiada a una determinada longitud de onda, una molécula emite radiación a longitudes de onda mayores que la empleada.⁵⁸ Se denomina fluoróforo a la subestructura de la molécula responsable de la fluorescencia.

⁵⁵ M. Y. Chae, A. W. Czarnik, *J. Am. Chem. Soc.* **1992**, *114*, 9704.

⁵⁶ V. Dujols, F. Ford, A. W. Czarnik, *J. Am. Chem. Soc.* **1997**, *119*, 7386.

⁵⁷ F. García, J. M. García, B. García-Acosta, R. Martínez-Máñez, F. Sancenón, J. Soto, *Chem. Commun.* **2005**, 2790.

⁵⁸ J. R. Lakowicz, *Principles of Fluorescence Spectroscopy*, Cap. 1, Ed. 3, Kluwer Academic/Plenum Publishers, Nueva York, 2006.

Tras la coordinación, son varios los procesos que permiten utilizar la variación de la intensidad de fluorescencia como señal de respuesta. Entre ellos está la transferencia electrónica fotoinducida (PET, Photoinduced Electron Transfer) y la desactivación por transferencia de energía (EET, Electronic Energy Transfer), los excímeros, o los efectos asociados a variaciones en la rigidez de los fluoróforos.

Los procesos PET pueden dar lugar tanto al desarrollo de la fluorescencia (“apagado-encendido”, “encendido”, “turn-on”, o “OFF-ON”) como al amortiguamiento (“encendido-apagado”, “apagado”, “turn-off” o “ON-OFF”). Un excímero es un complejo formado por la interacción de una molécula de fluoróforo en el estado excitado con otra en el estado fundamental, y presentan bandas desplazadas hacia el rojo cuando se compara con la emisión del propio fluoróforo.

Por otro lado, las sondas colorimétricas se basan en cambios de color provocados por la unión *grupo coordinante-analito*. Los sistemas coloreados están formados por estructuras conjugadas con diferencias de energía entre el HOMO y el LUMO correspondientes a las de la radiación electromagnética visible. Un incremento en la extensión del sistema conjugado disminuye la diferencia de energía HOMO-LUMO dando lugar a un desplazamiento hacia el rojo, o batocrómico, de la banda de absorción. La longitud de onda absorbida se puede variar tanto por el control de la extensión o del diseño del sistema conjugado, como mediante la introducción de grupos dadores (p.ej., -NR₂, -OR, -O⁻) y aceptores de (p.ej., -NO₂, -CN, -SO₃H, -SO₃⁻, -COR) de electrones en el sistema conjugado. La conjugación extendida entre un grupo dador y uno aceptor da lugar a complejos de transferencia de carga (CT) que se asocian generalmente a colores intensos debido a que estos complejos poseen coeficientes de extinción molar elevados. La interacción de la molécula cromófora, que actúa como *anfitrión*, con un *huésped* varía generalmente las características dadoras o receptoras de los grupos, modificando al CT, con la consiguiente transducción por cambio de color.

Las variaciones en el espectro de absorción de radiación ultravioleta y visible se pueden medir de forma muy precisa y económica con espectrofotómetros de UV/Visible, o con equipos UV/Visible de fotodiodos portátiles conectados asimismo a ordenadores portátiles, a tabletas o a teléfonos móviles. Pero sobre todo es interesante desde un punto de vista práctico la detección y cuantificación de analitos a simple vista, a través de variaciones en el color, y es clave en el desarrollo de sensores colorimétricos para uso por personal no especializado.

2.1.2. Diseño y síntesis de polímeros como sensores químicos y dosímetros

La gran mayoría de las investigaciones básicas que se realizan en el ámbito de los sensores se llevan a cabo con moléculas discretas, que por lo general tienen baja masa molecular, una resistencia química y térmica limitada y su separación y recuperación es laboriosa y cara. Además suelen ser insolubles en agua, y su aplicación en la detección de analitos se limita en la mayor parte de los casos a medios orgánicos u orgánico-acuosos, lo que restringe su futura aplicación clínica, biológica y medioambiental.

En este sentido, uno de los objetivos de las investigaciones más recientes en este campo se dirige al soporte de los sensores en diferentes matrices sólidas, lo que posibilita su empleo como materiales sensores sólidos, inmoviliza a los *receptores* selectivos impidiendo su migración, favorece su reutilización y mejora sus propiedades mecánicas. Como materiales sólidos para el anclaje de sensores se han utilizado materiales inorgánicos,^{59,60} como materiales silíceos, y materiales orgánicos poliméricos.²²⁻²⁹

⁵⁹ M. Comes, M. D. Marcos, R. Martínez Mañez, F. Sancenón, J. Soto, L. A. Villaescusa, P. Amorós, D. Beltrán, *Adv. Mater.* **2004**, *16*, 1783.

⁶⁰ A. B. Descalzo, R. Martínez Mañez, F. Sancenón, K. Hoffmann, K. Rurack, *Angw. Chem. Int. Ed.* **2006**, *45*, 5294.

El diseño y síntesis de polímeros con subunidades *anfitrión* ancladas químicamente a la cadena principal, o como parte integral de ésta, ofrece una vía inmejorable de inmovilización. Además, los polímeros se pueden transformar de forma sencilla en materiales acabados ya que habitualmente poseen buenas propiedades mecánicas y térmicas. De esta forma se pueden obtener sensores baratos, como recubrimientos, películas o films sensores colorimétricos, o integrar los mismos en equipos portátiles de espectroscopia de UV/Vis o fluorescencia, empleando fibras ópticas recubiertas en su extremo con los polímeros sensores.⁶¹⁻⁶⁵

Como es natural, los fenómenos de detección en sistemas biológicos se dan en medios acuosos, en los que la interacción *grupo receptor-analito* se basa en enlaces débiles que tienen lugar debido a los dominios hidrofóbicos en un entorno hidrofílico proporcionado por la constitución química y por la estructura cuaternaria de las proteínas. Es decir, la competitividad de las moléculas de agua para establecer estas interacciones débiles disminuye localmente, o se altera drásticamente, según sea el microentorno de los sitios activos.

La estructura polimérica no sólo actúa como soporte del *receptor*, sino que juega un papel importante en el proceso de detección. El anclaje de *receptores* insolubles en agua, lipofílicos, a cadenas lineales o reticuladas de polímeros hidrofílicos, da lugar a polímeros sensores solubles en agua o a materiales sensores hinchados en este medio, con comportamiento tipo gel. La hidrofilia del polímero se puede controlar mediante la naturaleza de los comonomeros y por medio del incremento o disminución de la densidad de nudos, denominada relación nominal de entrecruzamiento si es un material

⁶¹ J. M. García, F. C. García, F. Serna, J. L. de la Peña, *Prog. Polym. Sci.* **2010**, *35*, 623.

⁶² K. C. Persaud, *Mater. Today* **2005**, *8*, 38.

⁶³ P. Anzenbacher Jr, Y. Liuand, M. E. Kozelkova, *Curr. Opin. Chem. Biol.* **2010**, *14*, 1.

⁶⁴ K. E. Geckeler, *Advanced Macromolecular and Supramolecular Materials and Processes*, Ed., Kluwer Academic/Plenum Publishers, Nueva York, 2003.

⁶⁵ V. Rotello, S. Thayumanavan, *Molecular Recognition and Polymers. Control of Polymer Structure and Self-Assembly*, Wiley, Hoboken, 2008.

entrecruzado. La densidad de entrecruzamiento permite modular la absorción de agua de las redes hidrofílicas mecánicamente. La constitución química de los polímeros se puede diseñar de forma que los *receptores* anclados químicamente a la cadena lateral, o formando parte de la cadena principal, posean microentornos hidrofóbicos o hidrofílicos independiente de la naturaleza del disolvente. Este hecho permite el fenómeno de la detección, tal como ocurre en medios biológicos en los sitios activos de los enzimas, a causa de la estructura terciaria y cuaternaria de las proteínas. Así, los analitos solvatados penetran en la membrana hinchada en agua, por difusión general en el entorno hidrofílico, interaccionando selectivamente con los *receptores* orgánicos situados en los microdominios hidrofóbicos. A escala macroscópica, y con menor sofisticación, se trata de intentar imitar a la naturaleza y eliminar el inconveniente general de la mayoría de los *receptores* sintéticos, que solo funcionan en medios orgánicos. El polímero permite de esta forma que el receptor se comporte como tal en estado sólido y genera el microentorno hidrofóbico necesario para que se maximicen las interacciones entre *receptor* y *analito*, con la consiguiente transducción de la señal.

Los quimiosensores poliméricos exhiben generalmente una sensibilidad muy superior a la de las moléculas discretas por dos motivos principales. En primer lugar los polímeros muestran propiedades colectivas que son sensibles a perturbaciones menores, es decir, la interacción de una molécula de *receptor* con un único *analito* puede dar lugar a cambios como por ejemplo el amortiguamiento de la fluorescencia en toda la cadena de un polímero conjugado, en relación al cambio de únicamente ese centro. También se observa, al igual que en las proteínas, el efecto alostérico, que en general conduce al incremento de sensibilidad a medida que se produce la interacción *receptor-analito*.

Los polímeros como sensores se pueden clasificar, en función del tipo de respuesta asociada al fenómeno de la detección, en sensores

piezoeléctricos,⁶⁶ sensores quimio-mecánicos,⁶⁷ sensores electroquímicos⁶⁸ sensores colorimétricos,⁶⁹⁻⁷¹ y sensores fluorescentes.⁷² En lo que respecta a este trabajo, se han diseñado materiales quimiosensores colorimétricos y fluorogénicos. Nuestro interés se centra realmente en la detección a simple vista mediante sensores colorimétricos, así como en la cuantificación por espectroscopía UV/Vis y fluorescencia, ya que son técnicas sencillas, rápidas, baratas y disponibles en la mayoría de los laboratorios.

No obstante, a la hora de elegir o diseñar un polímero que pueda ser utilizado como material selectivo en un sensor, se necesita que tenga las siguientes características:

- El polímero ha de poseer una alta capacidad de absorción de los compuestos específicos, y fundamentalmente una selectividad hacia éstos.
- En aplicaciones acuosas, el material debe ser resistente a la hidrólisis por agua caliente y disoluciones acuosas ligeramente ácidas y básicas. En otros medios, el polímero ha de ser resistente a disolventes orgánicos y aceites.
- Deberá tener una adecuada resistencia química y, en polímeros de condensación, una solubilidad moderada, de forma que pueda ser transformado por los métodos convencionales de *casting* y que mantenga a su vez su integridad frente a disolventes comunes.
- En el caso de membranas densas, el material debe presentar una absorción de agua suficiente para permitir la difusión del disolvente en la red tridimensional y de esta forma el acceso de los *analitos* a la

⁶⁶ M. Ávila, M. Zougagh, A. Escarpa, A. Ríos, *Trends Anal. Chem.* **2008**, *27*, 54.

⁶⁷ H. J. Schneider, K. J. Kato, *Mater. Chem.* **2009**, *19*, 569.

⁶⁸ L. J. Fan, Y. Zhang, C. B. Murphy, S. E. Angell, M. F. L. Parker, B. R. Flynn, W. E. Joner Jr., *Coord. Chem. Rev.* **2009**, *253*, 410.

⁶⁹ R. Martínez-Máñez, F. Sancenón, *Coord. Chem. Rev.* **2006**, *250*, 3081.

⁷⁰ H. N. Kim, Z. Guo, W. Zhu, J. Yoon, H. Tian, *Chem. Soc. Rev.* **2011**, *40*, 79.

⁷¹ A. B. Descalzo, R. Martínez-Máñez, F. Sancenón, K. Hoffmann, K. Rurack, *Angew. Chem. Int. Ed.* **2006**, *45*, 5924.

⁷² P. Bosch, F. Catalina, T. Corrales, C. Peinado, *Chem. Eur. J.* **2005**, *11*, 4314.

subestructura receptora. Además tiene que tener buenas propiedades mecánicas que permitan su manejabilidad.

- El polímero ha de estar libre de contaminación de cualquier tipo, en particular trazas de metales o iones metálicos.
- El porcentaje del compuesto específico absorbido en equilibrio debe ser alto, pero ha de mostrar un balance cinético equilibrado en los ciclos de absorción-desorción en medios acuosos u orgánicos.
- El comportamiento del polímero no debe verse afectado sensiblemente con los cambios de temperatura.

Además, las numerosas posibilidades de diseño de estructuras poliméricas permiten la preparación de materiales con propiedades muy diversas, como materiales químicamente inertes, mecánicamente y térmicamente resistentes, hidrofílicos, hidrofóbicos, solubles en medios acuosos, etc., lo que posibilita, en principio, el empleo de estos polímeros en cualquier tipo de medio y condiciones.

Así, desde la experiencia previa se orientó el trabajo hacia un diseño de estructuras poliméricas con *unidades receptoras* selectivas introducidas en polímeros acrílicos y en poliamidas aromáticas. Para ello, con la especie objetivo que se quiere detectar en mente, se realiza una búsqueda bibliográfica para encontrar *receptores* selectivos de las mismas, que generalmente son moléculas discretas insolubles en agua. A continuación se modifica ligeramente la estructura química del *receptor* añadiendo un grupo polimerizable, y finalmente se polimeriza con otros monómeros para obtener un material sensor con las propiedades térmicas y mecánicas que interese. De este modo se sintetizaron polímeros sensores cromogénicos de TNT, alta acidez, Cu(II), Fe(III), Sn(II) y Co(II), y un sensor fluorogénico de agua y humedad, tal y como se describen a lo largo de este capítulo.

2.2. Sensores fluorogénicos de agua y humedad

La presencia de agua en los disolventes orgánicos es un problema en la química, y el control de la humedad es importante desde el punto de vista industrial. Así se ha diseñado un material sensor fluorogénico con grupos fluorenona y 1,2,3-triazol en su estructura capaz de cuantificar el contenido de agua en distintos medios de forma rápida, barata y en tiempo real, evitando los problemas asociados a otras técnicas que se usan actualmente, como el método de Karl Fisher.

2.2.1. Derivados de la fluorenona y del 1,2,3-triazol

La fluorenona es un compuesto aromático con fluorescencia azul sintetizado a partir de la oxidación del fluoreno. La fluorenona se utiliza en la preparación de compuestos químicos más complejos, como remedios contra la malaria, y tiene propiedades antivíricas. Los derivados de la fluorenona tienen propiedades espectroscópicas y fotoquímicas muy interesantes desde el punto de vista de la investigación.⁷³

Por otro lado, el 1,2,3-triazol es un heterociclo aromático de tres nitrógenos que puede obtenerse mediante una cicloadición 1,3-dipolar de un grupo alquino terminal y un grupo azida. Los derivados de este compuesto se utilizan en investigación como componente básico de compuestos químicos más complejos como el fármaco tazobactam.

Los tres nitrógenos contiguos en el ciclo heteroaromático le proporcionan al grupo 1,2,3-triazol 1,4 sustituido unas características únicas.⁷⁴ El nitrógeno en posición 3 del ciclo se comporta como aceptor de enlaces de hidrógeno y el C-H como dador de enlaces de hidrógeno. Por otro lado, con el grupo fluorenona sucede algo similar, el carbonilo actúa

⁷³ R. Heldt, J. Heldt, M. Józefowicz, J. Kamiński, *J. Fluoresc.* **2001**, *11*, 65.

⁷⁴ W. Dehaen, *Calix[n]phyrins: Synthesis and molecular recognition* en "Anion recognition in supramolecular chemistry". Springer, Heidelberg, 2010.

como grupo aceptor de enlaces de hidrógeno y los C-H del lado opuesto de la molécula como dadores de enlaces de hidrógeno (Figura 2.3).

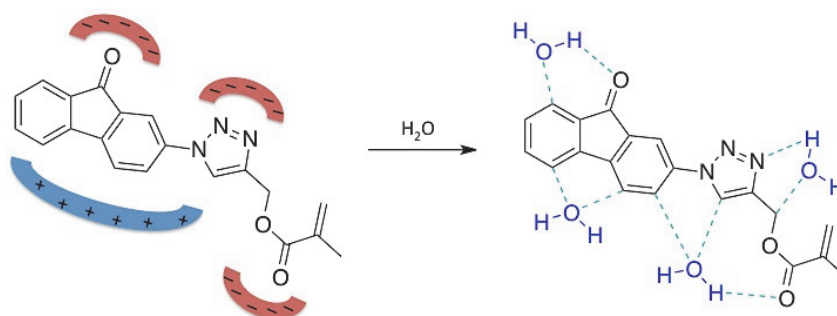


Figura 2.3. Esquema simplificado de la estructura y formación de enlaces de hidrógeno entre el agua y el monómero sensor.

La formación de estos enlaces de hidrógeno amortigua la fluorescencia inicial de la molécula, pudiendo establecerse una relación entre la cantidad de agua presente en un medio y la intensidad de la fluorescencia. En este sentido se ha preparado una membrana sólida con la molécula sensora que se muestra la Figura 2.3. Esta membrana se maneja bien, sin cuidados especiales tanto en seco como en hinchado, y es capaz de detectar cantidades muy bajas de agua en medios orgánicos y en el ambiente (humedad).

2.2.2. Polímeros con grupos fluorenona y 1,2,3-triazol en su estructura

En este trabajo se ha preparado una membrana acrílica hidrofílica con un monómero sensor de agua hidrofóbico, basado en un derivado de la fluorenona y el grupo 1,2,3-triazol, por copolimerización de este monómero con el monómero hidrofílico acrilato de 2-hidroxietilo y un entrecruzante, obteniéndose una membrana de color rojizo transparente con buenas propiedades mecánicas y térmicas.

Al sumergir esta membrana en distintos disolventes orgánicos el agua presente penetra en la membrana mediante un mecanismo de difusión y alcanza el grupo quimiosensor, dando lugar al fenómeno sensor. En este sistema, la interacción selectiva entre el agua y las unidades fluorescentes derivadas de la fluorenona y el triazol causan un amortiguamiento cuantificable de la fluorescencia de la membrana. De esta manera, la membrana se puede utilizar como un “kit” de detección de agua por fluorescencia.

El límite de detección por fluorescencia de esta membrana es bajo, aunque depende del disolvente. Por ejemplo, en acetona es $1 \times 10^{-2}\%$, en THF de $7 \times 10^{-3}\%$ y en tolueno $2 \times 10^{-4}\%$. La membrana también detecta la humedad ambiental con variaciones entre el 20% y el 100%. Además se puede reutilizar sin pérdida de la capacidad sensora.

Para conocer el mecanismo sensor de la membrana se estudió por fluorescencia la molécula sensora discreta frente a los disolventes, con apoyo de la resonancia magnética nuclear de protón y de cálculos teóricos *ab-initio*. Los estudios pusieron de manifiesto una interacción con formación de un complejo con estequiometría 1:4 (monómero sensor: agua). La interpretación está relacionada con la capacidad del monómero para establecer enlaces de hidrógeno, como se ha comentado anteriormente.

2.2.3. Aplicaciones

El desarrollo de métodos de determinación y cuantificación de la presencia de agua es importante en aplicaciones industriales, en la viabilidad y reproducibilidad experimental de muchas reacciones orgánicas en las que los reactivos son sensibles al agua y para prevenir el deterioro de aparatos mecánicos que utilizan aceites de transmisión por corrosión, por poner algunos ejemplos. Por este motivo hemos desarrollado un método de cuantificación de agua sencillo, barato y en tiempo real, que evita los

aspectos problemáticos de otros métodos de detección de agua que se utilizan actualmente, que en general son caros, lentos, tediosos, y que requieren personal especializado. Además, el límite de detección de esta membrana es considerablemente inferior que el de las técnicas convencionales. También hay que destacar que la membrana es reutilizable.

2.2.4. Resultados

A continuación se describen los resultados obtenidos a través de la transcripción íntegra del trabajo publicado.

- ❖ *Solid sensory polymer kit for the easy and rapid determination of the concentration of water in organic solvents and ambient humidity*

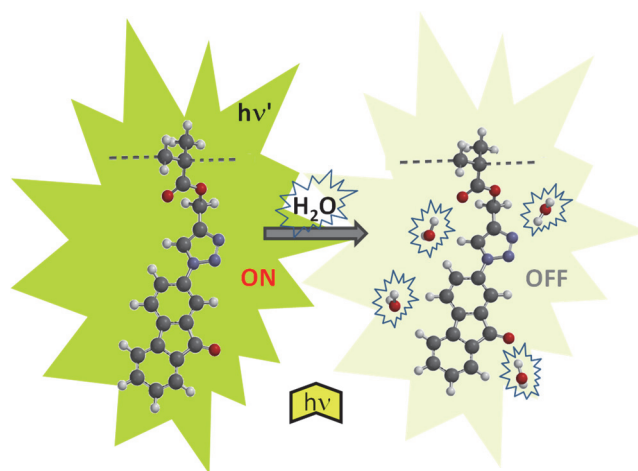
Los detalles experimentales y de caracterización se encuentran en el material suplementario, cuya copia está disponible en el CD adjunto.

Solid sensory polymer kit for the easy and rapid determination of the concentration of water in organic solvents and ambient humidity

Solid sensory polymer kit for the easy and rapid determination of the concentration of water in organic solvents and ambient humidity

Miriam Trigo-López, Asunción Muñoz, Saturnino Ibeas, Félix C. García, Felipe Serna, and José M. García*

Departamento de Química, Facultad de Ciencias Universidad de Burgos
Plaza de Misael Banuelos s/n, E-09001 Burgos, Spain. Fax: (+) 34 947 258 831. E-mail: jmiguel@ubu.es. Homepage: <http://sites.google.com/site/grupodepolimeros/>



We have prepared a solid sensory polymer kit to detect and quantify the water in organic solvents, as well as the ambient humidity; these determinations are cheap, easy and rapid with our new material. The limit of detection of water is 6×10^{-5} % in acetone, 4×10^{-3} % in THF, and 3×10^{-4} % in toluene. Additionally, the relative humidity in air can be measured between 20 and 100%.

Keywords: polymers; dense membranes; gels; sensory materials; water sensor; humidity sensor.

1. Introduction

The determination and quantification of the water present in organic fluids is currently an important topic. For example, in synthetic chemistry, dehydration procedures are often performed on water-sensitive reagents to ensure experimental reproducibility. Additionally, the determination of moisture in lubricants is routinely carried out because the presence of water affects the lubricants' efficiency and causes detrimental reactions that can degrade machinery efficiency and performance, such as corrosion. The determination of water content is also important within other industries, such as the sugar, food, ground water and petroleum industries. The standard process for the determination of water contamination is the Karl Fischer method, which requires a highly skilled operator to obtain reliable results. It does not provide reliable results at very low concentrations of water, cannot be used with samples containing redox active substances and its color change is not straightforward to quantify. Moreover, the Karl Fischer reagent is expensive and has a very short shelf life; The Standard Test Method for Water in Petroleum Products and Bituminous Materials by Distillation, ASTM D 95-05, is another widely used method for the quantification of water. The distillation process used in this method is very slow and is only effective for water concentrations above 0.5-1%. Other water quantification methods include infrared spectroscopy (IR) and ultraviolet spectroscopy (UV) [1]. Infrared spectroscopy is not accurate because it is based on the correlation of the intensity of the oxygen-hydrogen stretch of water, which occurs at approximately 3400 cm^{-1} , and the water concentration; other diagnostic resonances indicative of a reaction between any substance with the contaminating water may be used in place of the resonance at 3400 cm^{-1} . The method utilizing ultraviolet spectroscopy requires the addition of a solvatochromic substance and the calculation of a complex calibration curve, the molar extinction coefficient of the additive and other tedious empirical calculations. Moreover, undesirable secondary reactions may occur between the solvent and the solvatochromic substance. D.T. Benedyk introduced a

method that used a pigment to quantitatively determine of the presence of water in different solvents and fluids; however, in concentrations between 0.001% and 0.1%, the quantification of water was not possible [2]. Other techniques have been described, such as a ^{19}F -NMR-based method, which is very tedious, or a photo-induced electron transfer method, in which the sensitivity depends on the polarity of the solvent [3].

The measurement of humidity determines the amount of water vapor present in a gas, which can be a mixture, such as air, or pure. Most humidity sensors are relative humidity sensors and can be classified into ceramic, semiconductor, and polymer humidity sensors [4,5].

Ceramic materials, such as Al_2O_3 , TiO_2 , SiO_2 , LiCl-doped MnWO_4 and spinel compounds, detect water based on the decrease in the conductivity and the increase in the dielectric constant when the humidity increases; this mechanism was reported approximately 200 year ago. In wide-gap semiconductor materials, such as SnO_2 , In_2O_3 , ZnO , or perovskite compounds, water is adsorbed on the surface, which results in an increase in the conductivity of n-type materials and a decrease in the conductivity of p-type materials. This effect might be caused by the donation of electrons from the chemically adsorbed water molecules to the ceramic material or the replacement of the previously adsorbed and ionized oxygen (O^- , O^{2-} , etc.) by water molecules, which would trigger the release of the electrons from the ionized oxygen.

Polymeric sensors are thin films with micropores in which a change in a physical property can be attributed to water absorption. There are two categories of polymeric sensors: resistive- and capacitive-types. The former responds to moisture variations by changing its conductivity, while the latter responds to water vapor by varying its electric constant. A recent work by Ohira *et al.* describes the potential application of these materials to the trace moisture measurement in gases and organic solvents [6].

To facilitate the detection of substances, the development of molecules acting as chromogenic or fluorogenic sensors is currently a topic of scientific and technological interest [7,8]. The design, synthesis and optimization of new sensors led to new analyte detection technologies that are inexpensive, highly sensitive and easy to handle, which enables the use of the sensors by non-specialized individuals. Within this context, water is an incredibly important target molecule, but there are few examples of successful water samples because strong and selective water:host interactions are both elusive and difficult to establish [9,10].

Sensors for water [11-13] and humidity [14-16] can be prepared via the physical immobilization of discrete sensory molecules onto different surfaces or materials; this interesting approach generates manageable sensors with improved selectivity and sensitivity toward water. Moreover, the design, preparation and eventual polymerization of functional monomers generates dense hydrophilic membranes that may function as sensory materials and advance the development of this field [17,18]. In this regard, the preparation of solid films with sensory motifs, which are chemically anchored to polymer structure to avoid migration, that can be handled easily in both dry or swelled states would open new avenues within this field.

2. Results and discussion

We prepared a fluorescent methacrylic monomer containing fluorenone and 1,2,3-triazole moieties for the fluorogenic water sensing motif (**2**) and copolymerized it with a hydrophilic monomer (**1**) (Figure 1). The monomer (**2**) was prepared in a straightforward manner following four high-yielding and easy synthetic steps (Supplementary Data –SD-, Section SD.1 and Scheme SD1). A crosslinker (**3**) was used to obtain solid materials with good mechanical properties. Structural monomer 2-hydroxyethyl acrylate, as well as the ethylene glycol dimethacrylate crosslinker, were fully miscible and could be mixed in any molar ratio. Preparation of the dense membrane

began with a solution of the photochemical initiator, the crosslinker and 2-hydroxyethyl acrylate (solution total volume = 600 μL); the functional monomer (**2**) was added to this solution. The homogeneous polymerization mixture was subsequently treated with bubbling nitrogen to eliminate any dissolved oxygen and immediately injected into silanized glass molds; the polymerization was conducted smoothly under a UV light lamp. The silanization of the glass mold facilitated the unmolding of the plasticized material. The structure of the copolymer network of the membrane and the sensing material are depicted in Figure 1, in addition to a digital picture of the membrane that demonstrates its good optical properties. The content of (**2**) was quite low (0.5%, mole), and the other comonomers, (**1**) and (**3**), are widely used in industry and are therefore commercially available and inexpensive, which means that these materials can be used to make an inexpensive material that might have practical applications.

The membrane's hydrophilic or hydrophobic character was correlated with the water-swelling percentage (WSP); it was related to the weight percentage of water uptaken by the films after soaking until equilibrium was reached in pure water at rt. The prepared membrane has a water-swelling percentage (WSP) of 84%. WSPs higher than 40% and lower than 100% are optimal for sensory materials designed for applications in aqueous environments because low water uptake means a low diffusion rate of water and of other water solvated target molecules, and higher water uptake can impair the mechanical performance of the swelled materials [17].

The membrane demonstrated reasonably good thermal resistance under both nitrogen and air atmospheres when observed via thermogravimetric analysis. A 5% weight loss was observed at 288°C and 298°C under nitrogen and dry synthetic air atmospheres, respectively.

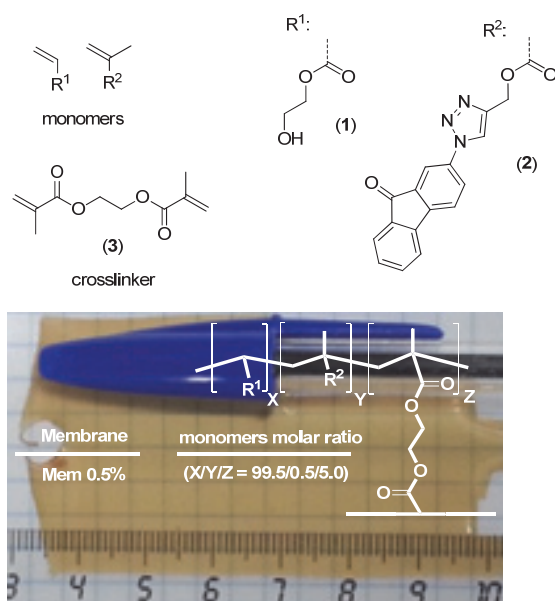


Figure 1. Chemical structures of the monomers and the copolymer. The copolymer structure and code are shown over a digital picture of the sensory film. For the detailed experimental synthetic procedure, see the Supplementary Data.

All of the membranes, both dry (Young's modulus of 4 MPa and a tensile strength of 3 MPa) and solvent-swelled materials, were highly tractable and transparent and had good mechanical properties. Membranes with dimensions of 80x50x0.1 mm were easy to handle and could be cut into appropriate sensing strips with dimension of approximately 20x5x0.1 mm using a home cutter or scissors.

When the monomer was dissolved in a dry solvent, the dry membrane swelled in a dry solvent or the dry membrane exposed to a gas phase, an intense fluorescence band was observed at approximately 515 nm when excited at 410 nm. In the SD, Figure SD7 depicts the fluorescence activity of monomer (2) in different solvents. After the addition of water (miliQ), the fluorescence at 515 nm displayed by the monomer or membrane

was quenched. This behavior was also observed when the membrane was in contact with increasingly humid environments. In addition, the membrane could be dried and re-used at least 10 times (for testing purposes we have reused the membrane 10 times without any apparent loss of performance).

Table 1. Water quantification (weight percentage) in organic solvents using the sensing monomer (**2**) (5×10^{-4} M), or the membrane as water sensory solid kits as probes. Excitation wavelength = 410 nm.

Solvent	Probe (2) in solution [#]			Sensory membrane [#]		
	LOD(%)	LOQ(%)	UML(%)	LOD(%)	LOQ(%)	UML(%)
Acetone	6×10^{-5}	2×10^{-4}	8	1×10^{-2}	1×10^{-6}	8
THF	4×10^{-3}	1×10^{-2}	2.2	7×10^{-3}	2×10^{-2}	6
Toluene	3×10^{-4}	1×10^{-3}	0.03	2×10^{-4}	7×10^{-4}	0.003
Air ^{&}	--	--	--	20 ^{&}		100 ^{&}

[#] Limit of detection (LOD), limit of quantification (LOQ), and upper measuring limit (UML).

[&] Relative humidity (RH).

To test the fluorimetric sensing ability of the monomer and the membrane, increasing amounts of water were added to a fluorimeter cell already containing a solution of the monomer in dry acetone (Figure 2) or the film swelled in dry acetone (Figure 3), resulting in a gradual diminishment in the intensity of the 510 nm band with increased water content. The membrane was previously dried for 24h under vacuum in a vacuum oven containing a beaker with the drying agent P_2O_5 . The detection limit of the monomer dissolved in dry acetone was 0.0007% water, while the detection limit of the membrane swelled in dry acetone was 0.01% water. The membrane sensitivity was also tested at increasing relative humidity (RH) levels. The detection limit was 20% of the RH (Figure 3). The results are summarized in Table 1. At low water concentrations, both the sensory molecule (**2**) and the membrane follow the quenching pattern described by the Stern-Volmer equation ($F_0/F = 1 + K_{SV}[Q]$, where [Q] is the concentration of the quencher (water), F_0 and F are the initial and experimental fluorescence intensity of the uncomplexed fluorophore (**2**), respectively, and K_{SV} is the Stern-Volmer quenching constant). Therefore, the concentration of water vs $F_0/F - 1$ is represented as a straight line, which has a slope of K_{SV} (see SD,

Figure SD13) [19]. Though the quenching process may have a dynamic, a static, or a combined dynamic and static nature, a static quenching process caused by the formation of (2):water complexes can be envisaged because of a binding mechanism that will be discussed later. The calculated K_{SV} are 2.87 ± 0.04 and $13.6 \pm 0.2 \text{ M}^{-1}$ for the quenching of (2) in solution and membrane **Mem0.5%** dipped in acetone, respectively.

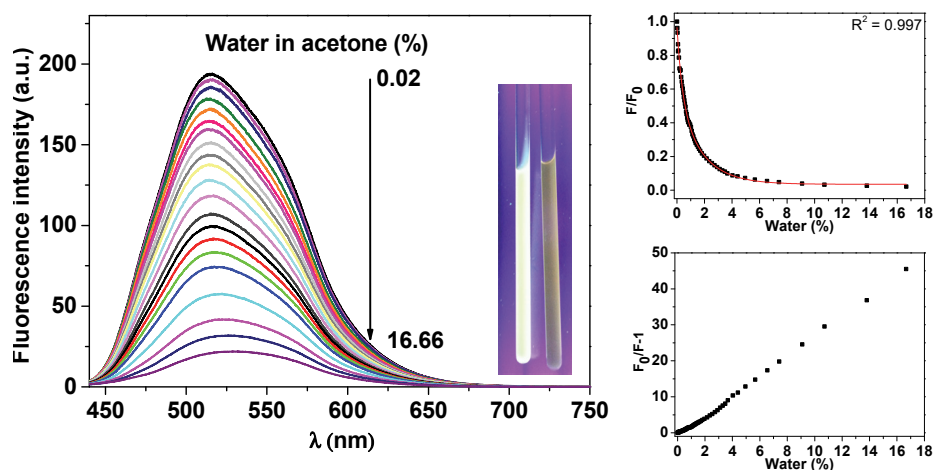


Figure 2. Titration of the water content in acetone. Left: selected emission curves of a solution of monomer (2) ($5 \times 10^{-4} \text{ M}$) in dry acetone after increasing the water (milli-Q) content (inset: picture of NMR tubes containing (2) in dry and 1% water in acetone, left and right, respectively, upon irradiation with 365 nm UV light). Right: water titration curves (water content vs. relative fluorescence intensity –top– and quenching efficiency –bottom– at $\lambda = 515 \text{ nm}$). Excitation wavelength = 410 nm.

The limit of detection (LOD) and the limit of quantification (LOQ) were estimated with the following equation: $\text{LOD} = 3.3 \times \text{SD}/s$ and $\text{LOQ} = 10 \times \text{SD}/s$, where SD is the standard deviation of the blank sample and s is the slope of the calibration curve in the region with the lowest water content.

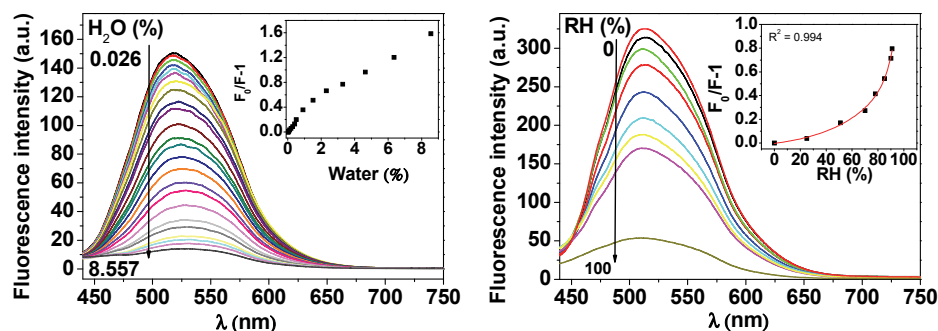


Figure 3. Titration curves of the water content in acetone using the film **Mem0.5%** (left, inset: water content in acetone vs. quenching efficiency at $\lambda = 518$ nm) and in the environment as relative humidity (RH) (right, inset: RH vs. quenching efficiency at $\lambda = 512$ nm). Excitation wavelength = 410 nm.

The interaction mechanism between **(2)** and water was studied by fluorescence spectroscopy, ^1H NMR, and by *ab-initio calculations*. The fluorescence studies highlighted an interaction leading to the initial formation of a complex, which had a stoichiometry of 1:4 [**(2)**: H_2O], as depicted with the Yoe-Jones' method illustrated in Figure SD19 [20,21]. The interpretation of this mechanism is obviously related to the hydrogen bonding capabilities of **(2)**, i.e., with the inter- or intra-molecule and water-**(2)** hydrogen bonds. Therefore, the H-bonding of **(2)** has been studied with 1D and 2D ^1H NMR spectroscopy because the ^1H chemical shift (δ) changes relative to the strength of H bonds. Inter-molecule hydrogen bonds in **(2)** were disregarded because the chemical shifts for the all of the C-H protons were not affected by variations of the concentration of **(2)** in any of the three deuterated solvents utilized in this study ($\text{DMSO-}d_6$, $\text{acetone-}d_6$ and CDCl_3) [22-25]. However, these δ depend on the sample temperature, as demonstrated in Figure 4, and the protons experience downfield shifts ($\Delta\delta$) with a decrease in the temperature, which was related to the strength of the hydrogen bonds the relevant protons established [26]. As illustrated in Figure 4, nucleus H7 exhibits a higher $\Delta\delta$ within the range of the studied temperatures in

acetone- d_6 (with negligible water content, lower than 0.05 %). However, a major change in the spectra was related to variations in the frequency resonance of water ($\delta_{\text{H}_2\text{O}}$) after increasing the molar fraction of water in the samples, as depicted in SD, Figure SD9. The $\delta_{\text{H}_2\text{O}}$ observed is much higher than the corresponding to binary mixtures of water/acetone [27]. We ascribe this behavior to the water-(**2**) H-bonds, which are stronger than the water-acetone interactions. The experimental evidence of the water-(**2**) interaction was achieved in a solvent that exhibited weak interactions with water, such as CDCl_3 [26], under selected experimental conditions: low concentration of (**2**), 2 mg in 0.5 mL of CDCl_3 , and high water content, 0.03 % (v/v). Therefore, a COSY spectrum exhibiting a cross-peak representing the interaction between H7 and H_2O was recorded, as depicted in Figure 5. Additionally, Abraham et al. reported that the strength of the hydrogen bonds in a molecule can be linearly correlated with the differences in protons chemical shifts collected using different solvents [28-32]. Following this strategy, $\Delta\delta_{\text{DMSO-}d_6/\text{CDCl}_3} = \delta_{\text{DMSO-}d_6} - \delta_{\text{CDCl}_3}$ was calculated (Figure 5 and SD, Figure SD8). The results agreed with the theoretical studies described below.

Geometric optimizations and energy evaluations of (**2**), as well as the interaction of 4 water molecules with (**2**) [(**2**): H_2O], using density functional theory (DFT) and the B3LYP/6-31G* hybrid functional in acetone (SM8 model) were carried out. The geometric optimization was run from the lowest energy conformer obtained after the optimization of 18 conformers with constrained fluorenone-triazole angles (see SD, Figure SD17), and the 4 water molecules were allowed to interact with the electron poor and rich regions indicated by the electrostatic potential maps (see SD, Figure SD18 and movie). The water molecules establish 3 hydrogen bonds and an electrostatic interaction with energies ranging 12.6 to 33.0 kJ/mol (Figure 5). These values agreed with the measured $\Delta\delta_{\text{DMSO-}d_6/\text{CDCl}_3}$, as presented in Figure 5, with the experimental energy of attraction between water

molecules (hydrogen bond enthalpy, which is the energy required for breaking and completely separating the bond, being approximately 23.3 kJ mol⁻¹, as reported by Suresh et al., which equals about half the enthalpy of vaporization (44 kJ/mol at 25°C)) [33-36]. A video showing the interaction of (2) with water can be found in the SD.

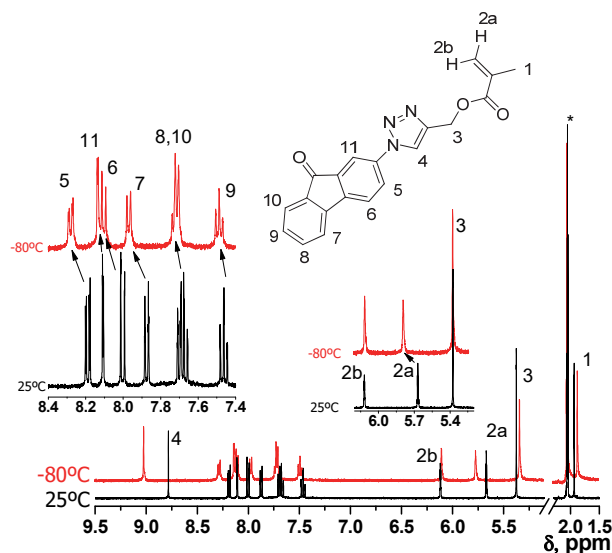


Figure 4. ¹H NMR spectra of the monomer in acetone-*d*₆ (*) at 80 °C (red lines) and at 25 °C (black lines) [(2):H₂O ratio = 4 - estimated by the aromatic to H₂O signal ratio-].

The strongest interaction of water with (2) was found in the cross-peak of the COSY experiment depicted in Figure 5, having arisen from the dipolar coupling of H7 with H₂O; the magnitude of $\Delta\delta_{\text{DMSO-}d_6/\text{CDCl}_3}$ validates these theoretical calculations.

Aside from alcohols, no material interfered with the water sensing of the sensory molecules, and the quenching of the fluorescence of (2) by an alcohol, such as ethanol, was ascribed to a similar mechanism as the pathway described for water. Regarding this point, the concentration of water could be determined with these methodologies in any non-protic

solvent. To demonstrate this versatility, we have titrated the water content in toluene and THF with sensory strips cut from **Mem0.5%**, as well as with **(2)** in solution; the results are summarized in Table 1 (see the emission curves

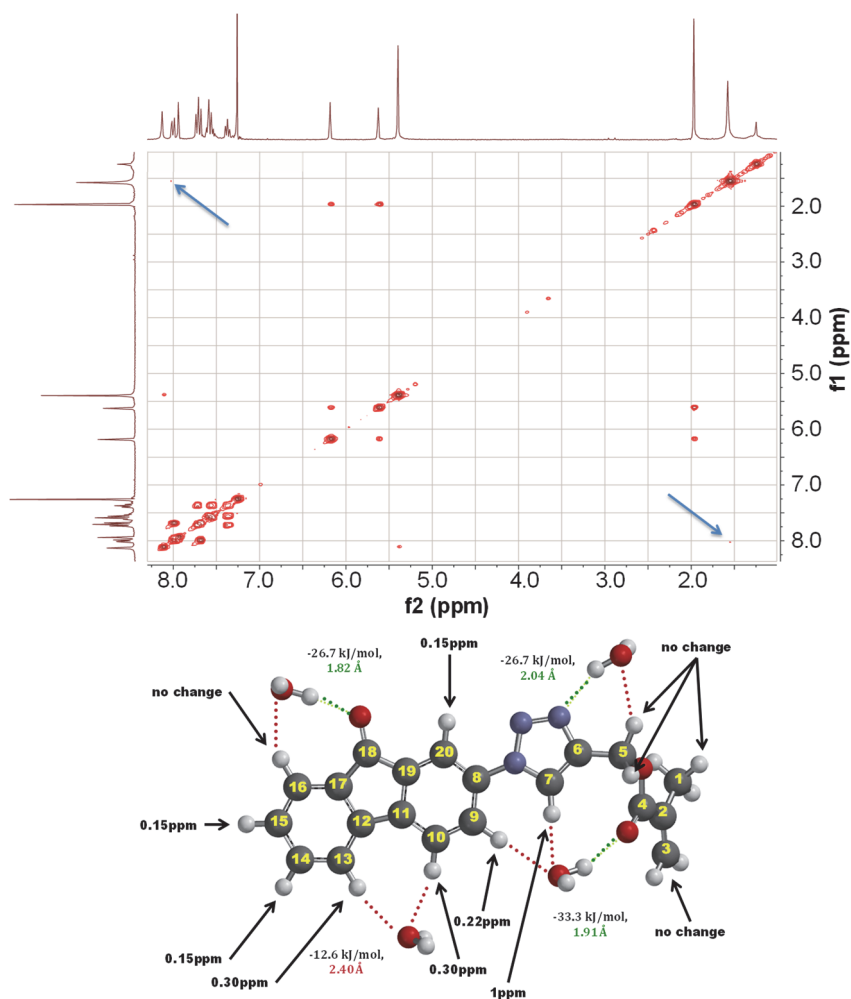


Figure 5. Interaction of monomer **(2)** with water. Top: COSY experiment (400 MHz, 25°C, 2 mg of **(2)** in 0.5 mL of CDCl₃). The cross-peaks caused by the dipolar coupling between H9 and H₂O are involved in a “relatively strong” H-bond (see arrows). The molar fraction of water seems to be critical for the observation of this cross-peak. Bottom: Model of the interaction between 4 water molecules and **(2)** in acetone (DFT B3LYP/6-31G*). Dashed lines represent hydrogen bonds (acceptor: green; donor: red). The distances and the interaction energies are written close to the appropriate water molecules. Arrows indicate $\Delta\delta_{\text{DMSO-}d_6/\text{CDCl}_3}$ ($\Delta\delta_{\text{DMSO-}d_6/\text{CDCl}_3} = \delta_{\text{DMSO-}d_6} - \delta_{\text{CDCl}_3}$).

in the SD, Figures SD14 and SD16). Moreover, the conditions for the fluorescence experiments can be adjusted to suit different needs. For instance, the ratiometric titration of water in THF after irradiation at 310 nm is depicted in the SD, Figure SD15. Ratiometric methods measure the ratio of the fluorescence intensities at two wavelengths, overcoming the drawbacks of conventional intensity-based measurements using an internal correction for the intensity of the two emission bands.

3. Conclusions

In summary, a water-insoluble organic molecule (**2**), which acts as a water sensor, was incorporated into the lateral chain of a methacrylic copolymer to furnish a dense membrane. The membrane composition generated a solid material that was easy to handle. After swelling with different organic solvents, the membrane facilitated the fluorimetric detection of water with an extremely low detection limit (by weight in toluene: 9×10^{-4} %). The membrane can also be used for the rapid and cheap determination of the relative humidity within a gas phase.

Spanish provisional patent application P2012001139 was filed 16 November 2012.

Acknowledgements

We gratefully acknowledge the financial support provided by the Spanish Ministerio de Economía y Competitividad-Feder (MAT2011-22544) and by the Consejería de Educación - Junta de Castilla y León.

Appendix A. Supplementary data

Full experimental details and characterization data used for the present study are given, along with a video showing the modelization of the interaction of the sensory molecule with water.

References

- [1] F.R. Van de Voort, J. Sedman, V. Yaylayan, C. Saint Laurent, C. Mucciardi, Quantitative Determination of Moisture in Lubricants by Fourier Transform Infrared Spectroscopy, *Appl. Spectrosc.* 58 (2004) 193-198.
 - [2] D. T. Benedyk, US Patent 4962039, 1990.
 - [3] H. Sun, B. Wang, S. G. DiMagno, A Method for Detecting Water in Organic Solvents, *Org. Lett.* 10 (2008) 4413-4416.
 - [4] Z. Chen, C. Lu, Humidity Sensors: A Review of Materials and Mechanisms, *Sens. Lett.*, 3 (2005) 274-295.
 - [5] M. M. F. Choi, O. L. Tse, Humidity-sensitive optode membrane based on a fluorescent dye immobilized in gelatin film, *Anal. Chim. Acta* 378 (1999) 127-134.
 - [6] S. I. Ohira, K. Goto, K. Toda, P. K. Dasgupta, A Capacitance Sensor for Water: Trace Moisture Measurement in Gases and Organic Solvents, *Anal. Chem.* 84 (2012) 8891-8897.
 - [7] R. Martínez-Mañez, F. Sancenon, Fluorogenic and Chromogenic Chemosensors and Reagents for Anions, *Chem. Rev.* 103 (2003) 4419-4476.
 - [8] J. Janata, Introduction: Modern Topics in Chemical Sensing, *Chem. Rev.*, 2008, 108, 327-328.
 - [9] Y. Ooyama, M. Sumomogi, T. Nagano, K. Kushimoto, K. Komaguchi, I. Imae, Y. Harima, Detection of water in organic solvents by photo-induced electron transfer method, *Org. Biomol. Chem.* 9 (2011) 1314-1316.
 - [10] Y. Ooyama, A. Matsugasako, T. Nagano, K. Oka, K. Kushimoto, K. Komaguchi, I. Imae, Y. Harima, Fluorescence PET (photo-induced electron transfer) sensor for water based on anthracene-amino acid, *J. Photochem. Photobiol. A* 222 (2011) 52-55.
 - [11] C. G. Niu, A. L. Guan, G. M. Zeng, Y. G. Liu, Z. W. Li, Fluorescence water sensor based on covalent immobilization of chalcone derivative, *Anal. Chim. Acta* 577 (2006) 264-240.
 - [12] C. G. Niu, P. Z. Qin, G. M. Zeng, X. Q. Gui, A. L. Guan, Fluorescence sensor for water in organic solvents prepared from covalent immobilization of 4-morpholinyl-1, 8-naphthalimide, *Anal. Bioanal. Chem.* 387 (2007) 1067-1074.
 - [13] F. Galindo, J. C. Lima, S. V. Luis, M. J. Melo, A. J. Parola, F. Pina, Water/humidity and ammonia sensor, based on a polymer hydrogel matrix containing a fluorescent flavylum compound, *J. Mater. Chem.* 15 (2005) 2840-2847.
 - [14] P. G. Su, C. C. Shiu, Electrical and sensing properties of a flexible humidity sensor made of polyamidoamine dendrimer-Au nanoparticles, *Sens. Actuators B: Chem.* 165 (2012) 151-156.
 - [15] J. Liu, F. Sun, F. Zhang, Z. Wang, R. Zhang, C. Wang, S. Qiu, In situ growth of continuous thin metal-organic framework film for capacitive humidity sensing, *J. Mater. Chem.* 21 (2011) 3775-3778.
 - [16] Y. Li, C. Deng, M. Yang, A novel surface acoustic wave-impedance humidity sensor based on the composite of polyaniline and poly(vinyl alcohol) with a capability of detecting low humidity, *Sens. Actuators B: Chem.* 165 (2012) 7-12.
 - [17] J. M. García, F. C. García, F. Serna, J. L. de la Peña, Fluorogenic and Chromogenic Polymer Chemosensors, *Polym. Rev.* 51 (2011) 341-390.
 - [18] S. Vallejos, H. El Kaoutit, P. Estévez, F. C. García, F. Serna, J. L. de la Peña, Working with water insoluble organic molecules in aqueous media: fluorene derivative-containing polymers as sensory materials for the colorimetric sensing of cyanide in water, *Polym. Chem.* 2 (2011) 1129-1138.
 - [19] J. R. Lakowicz, *Principles of Fluorescence Spectroscopy*, 2nd Ed., Kluwer Academic/Plenum Publishers, NY, 1999, ch 8.
 - [20] J. H. Yoe, A.L. Jones, Colorimetric Determination of Iron with Disodium-1,2-dihydroxybenzene-3,5-disulfonate, *Ind. Eng. Chem. Anal. Ed.* 16 (1944) 111-115.
-

-
- [21] J. M. Bosque-Sendra, E. Almansa-López, A. M. García-Campaña, L. Cuadros-Rodríguez, *Data Analysis in the Determination of Stoichiometries and Stability Constants of Complexes*, *Anal. Sci.* 19 (2003) 1431-1439.
- [22] G. R. Desiraju, T. Steiner, *The Weak Hydrogen Bond: In Structural Chemistry and Biology*, Oxford University Press, Oxford, 2001, ch 2.
- [23] R. J. Abraham, M. Mobli, *Modelling 1H NMR Spectra of Organic Compounds: Theory, Applications and NMR prediction software*, John Wiley & Sons, Chichester, 2008, pp 78-80.
- [24] H. Friebolin, *Basic one- and two-dimensional NMR spectroscopy*, 5th completely rev. and enlarged ed., Wiley-VCH, Weinheim, 2011, pp 60, 69 and 334
- [25] R. J. Abraham, M. Mobli, An NMR, IR and theoretical investigation of 1H Chemical Shifts and hydrogen bonding in phenols, *Magn. Reson. Chem.* 45 (2007) 865–877.
- [26] B. García, F. Secco, S. Ibeas, A. Muñoz, F. J. Hoyuelos, J.M. Leal, M.L. Senent, M. Venturini, Structural NMR and ab Initio Study of Salicylhydroxamic and p-Hydroxybenzohydroxamic Acids: Evidence for an Extended Aggregation, *J. Org. Chem.* 72 (2007) 7832-7840.
- [27] K. Mizuno, S. Imafuji, T. Ochi, T. Ohta, S. Maeda, Hydration of the CH Groups in Dimethyl Sulfoxide Probed by NMR and IR, *J. Phys. Chem. B* 104 (2000) 11001-11005.
- [28] M. H. Abraham, Scales of solute hydrogen-bonding: their construction and application to physicochemical and biochemical processes, *Chem. Soc. Rev.* 22 (1993) 73-83.
- [29] M. H. Abraham, P. L. Grellier, D. V. Prior, P. P. Duce, J. J. Morris, P. J. Taylor, Hydrogen bonding. Part 7. A scale of solute hydrogen-bond acidity based on log K values for complexation in tetrachloromethane, *J. Chem. Soc. Perkin Trans. 2* (1989) 699-711.
- [30] M. H. Abraham, P. L. Grellier, J. J. Morris, P. J. Taylor, Hydrogen bonding. Part 10. A scale of solute hydrogen-bond basicity using log K values for complexation in tetrachloromethane, *J. Chem. Soc. Perkin Trans. 2* (1990) 521-529.
- [31] M. H. Abraham, P. L. Grellier, D. V. Prior, R. W. Taft, J. J. Morris, P. J. Taylor, C. Laurence, M. Berthelot, R.M. Doherty, M.J. Kamlet, J.L.M. Abboud, K. Sraidi, G. Guiheneuf, A general treatment of hydrogen bond complexation constants in tetrachloromethane, *J. Am. Chem. Soc.* 110 (1988) 8534-8536.
- [32] M. H. Abraham, R. J. Abraham, J. Byrne, L. Griffiths, NMR Method for the Determination of Solute Hydrogen Bond Acidity, *J. Org. Chem.* 71 (2006) 3389-3394.
- [33] S. J. Suresh, V. M. Naik, Hydrogen bond thermodynamic properties of water from dielectric constant data, *J. Chem. Phys.* 113 (2000) 9727-9732.
- [34] L. C. Ch'ng, A. K. Samanta, G. Czako, J. M. Bowman, H. Reisler, Experimental and Theoretical Investigations of Energy Transfer and Hydrogen-Bond Breaking in the Water Dimer, *J. Am. Chem. Soc.* 134 (2012) 15430–15435.
- [35] A. Shank, Y. Wang, A. Kaledin, B. J. Braams, J. M. Bowman, Accurate ab initio and “hybrid” potential energy surfaces, intramolecular vibrational energies, and classical ir spectrum of the water dimer, *J. Chem. Phys.* 130 (2009) 144314.
- [36] C. Leforestier, K. Szalewicz, A. van der Avoird, Spectra of water dimer from a new ab initio potential with flexible monomers, *J. Chem. Phys.* 137 (2012) 014305.
-

2.3. Sensores cromogénicos de cationes metálicos

La presencia de metales en distintos medios puede ser tanto beneficiosa como perjudicial para la salud y el medio ambiente, por lo que es necesaria su detección y cuantificación. En este apartado se describe la estrategia seguida para preparar un material sensor visual selectivo de cuatro cationes de metales de transición (Fe(III), Co(II), Sn(II) y Cu(II)) en agua. Para ello se ha incorporado un derivado de la terpiridina como monómero sensor a una membrana entrecruzada con comportamiento de gel y a un polímero lineal soluble en agua.

2.3.1. Derivados de la terpiridina

La terpiridina (2,2':6',2''-terpiridina, tpy o terpy) es un heterociclo derivado de la piridina sintetizada por primera vez en 1932 cuando G. Morgan y F.H. Burstall calentaron piridina a 340°C con FeCl₃ anhidro en un autoclave durante 36 horas. Obtuvieron tpy junto con otros productos que contenían nitrógeno.⁷⁵ A continuación se descubrió que la adición de Fe(II) a una disolución de tpy daba lugar a un color morado, como indicación de la formación de un complejo. La molécula de tpy contiene tres átomos de nitrógeno y por lo tanto puede actuar como un ligando tridentado y formar complejos estables con una gran variedad de iones de metales de transición. Estas interacciones fuertes vienen tanto de la retrodonación $d\pi-d\pi^*$ de los cationes al heterociclo, como del efecto quelante. Las características de las tpy les hacen útiles para un gran número de aplicaciones como materiales fotovoltaicos,⁷⁶ diodos emisores de luz,⁷⁷ celdas solares⁷⁸ y principalmente en el desarrollo de quimiosensores para metales.⁷⁹

⁷⁵ H. Hofmeier, U. S. Schubert, *Chem. Soc. Rev.* **2004**, 33, 373.

⁷⁶ V. Duprez, M. Biancardo, H. Span, *Macromolecules* **2005**, 38, 10436.

⁷⁷ E. Holder, V. Marin, M. Meier, U. Schubert, *Macromol. Rapid Commun.* **2004**, 25, 1491.

⁷⁸ S. Zakeeruddin, M. Nazeeruddin, P. Pechy, F. Rotzinger, K. Humphry-Baker, *Inorg. Chem.* **1997**, 36, 5937.

Con el objetivo final de preparar polímero sensor de cationes se utilizó la metacrilamida derivada de la tpy de la Figura 2.4. La metacrilamida es de color blanco, y aunque en presencia de un gran número de metales se producen cambios en la fluorescencia, únicamente con 4 de ellos (Fe(III), Co(II), Sn(II) y Cu(II)) se observa el desarrollo de coloración (morado, rojo, amarillo y verde, respectivamente) por la formación de un complejo de estequiometría 1:2 catión:tpy.

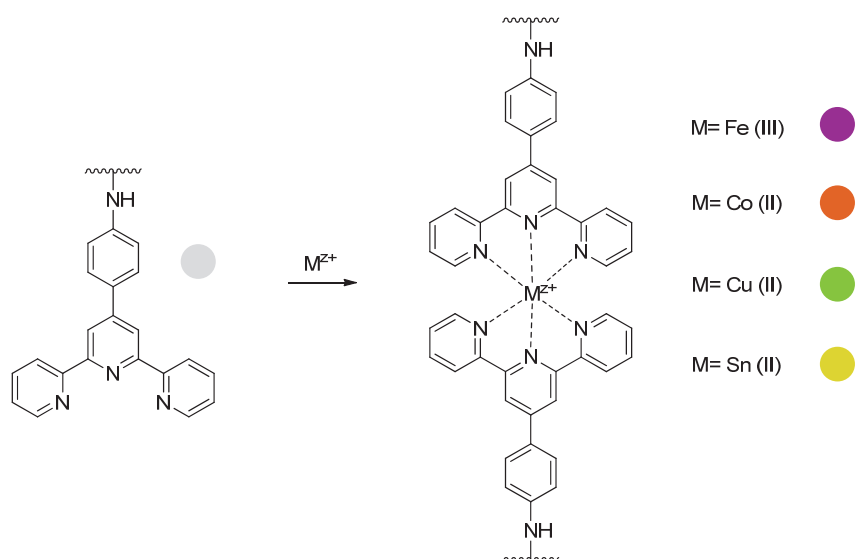


Figura 2.4. Formación de los complejos 1:2 entre el derivado de tpy y los distintos cationes metálicos. Colores observados en la membrana tras la formación de los complejos con los polímeros.

2.3.2. Polímeros con derivados de terpiridina en su estructura

Se diseñó un derivado sensor de la terpiridina capaz de establecer complejos coloreados con Fe(III), Co(II), Cu(II) y Sn(II) con un grupo metacrilamida polimerizable para preparar dos tipos de polímeros sensores:

⁷⁹ L. Hong-Yuan, J. Jian-Hui, Z. Xiao-Bing, L. Chun-Yan, S. Guo, Y. Ru-Qin, Y. *Talanta* **2007**, 72, 575.

- Polímero lineal soluble en agua con 1-vinil-2-pirrolidona como matriz inerte, por polimerización radical en disolución con iniciación térmica.
- Polímero reticulado como membrana densa con comportamiento de gel, por polimerización radical térmica, utilizando 1-vinil-2-pirrolidona y metacrilato de metilo como matriz inerte con un balance adecuado de propiedades mecánicas y de hinchamiento en agua.

A partir del polímero lineal se pudo determinar visualmente y cuantificar por espectroscopia UV/vis una concentración sub-micromolar de Fe(III) y de Co(II) ($1,3 \times 10^{-7}$ M y $6,4 \times 10^{-8}$ M, respectivamente), y una cantidad micromolar de Cu(II) y Sn(II) ($1,3 \times 10^{-5}$ M y $1,4 \times 10^{-5}$ M, respectivamente) en agua, pudiéndose construir las correspondientes curvas de calibrado, y demostrándose la formación de los complejos 1:2 (metal:tpy) mediante una representación *Job's plot*.

Las membranas densas permitieron el estudio de las concentraciones de los cationes a simple vista. La menor sensibilidad hacia los cationes de cobre y estaño que a los cationes de hierro y cobalto se resolvió utilizando un mayor porcentaje de monómero sensor en la membrana. Se construyeron curvas de calibrado con los parámetros de color RGB de fotografías digitales de las membranas sensoras por un análisis de componentes principales frente a distintas cantidades de cationes, con el objetivo de poder determinar las concentraciones de los mismos. Se trata de un procedimiento de análisis cuantitativo rápido y sin coste adicional utilizado frecuentemente en nuestro grupo.⁸⁰ Las membranas densas permiten cuantificar visualmente la concentración de Fe(III) y Co(II) entre 1×10^{-7} y 5×10^{-3} M; y entre 9×10^{-5} y 9×10^{-3} M para el caso del Cu(II) y el Sn(II).

⁸⁰ H. El Kaoutit, P. Estevez, F. C. Garcia, F. Serna, J. M. Garcia, *Anal. Methods* **2013**, 5, 54.

Aunque el derivado de la tpy sintetizado únicamente muestra un cambio de color en presencia los cuatro cationes metálicos mencionados anteriormente, también forma complejos con un gran número de cationes como Al(III), Pb(III), Mg(II), Hg (II), Cd(II), Zn(II), etc., pudiéndose observar cambios en la fluorescencia del sistema, por lo que suponen un interferente real. Sin embargo, es posible cuantificar las especies coloreadas en presencia de estos cationes interferentes por espectrofotometría de UV/Vis mediante la técnica de la adición estándar.

2.3.3. Aplicaciones

Un gran número de aplicaciones medioambientales e industriales se basan en la posibilidad de detectar y controlar este tipo de cationes metálicos, ya que estos tienen distintos efectos sobre el hombre y la naturaleza. La presencia de Co(II), Fe(III), Cu(II) y Sn(II) puede ser desde beneficiosa hasta tóxica, dependiendo de la concentración en la que se encuentren. Muchos de estos iones metálicos se hallan en el suelo y en el agua, como consecuencia de la práctica minera y la agricultura, y la cuantificación de esos metales por personal no especializado supone un gran ahorro de tiempo y dinero.

La sensibilidad de estos polímeros sensores hacia el Fe(III) y el Co(II) hace que puedan ser explotados para aplicaciones forenses. Por ejemplo, las partículas metálicas que se depositan en las manos tras estar en contacto con una herramienta permiten revelar su forma tras presionar las manos contra un papel o tejido humedecido con una disolución del polímero lineal al producirse un cambio de color. También es posible detectar el cobalto presente en una herramienta que contiene una punta de carburo de tungsteno con entre un 6 y un 10% de cobalto de este mismo modo; o saber si una pieza metálica tiene hierro simplemente por inmersión de esta pieza en una disolución del polímero sensor.

2.3.4. Resultados

A continuación se describen los resultados obtenidos a través de la transcripción íntegra del trabajo.

- ❖ *Colorimetric detection of e Fe(III), Co(II), Cu(II) and Sn(II) in 100% water by acrylic polymers with pendant terpyridine motifs for analytical and forensic applications*

Los detalles experimentales y de caracterización se encuentran en el material suplementario, cuya copia está disponible en el CD adjunto.

Colorimetric detection of Fe(III), Co(II), Cu(II) and Sn(II) in 100% water by acrylic polymers with pendant terpyridine motifs for analytical and forensic applications

Colorimetric detection of Fe(III), Co(II), Cu(II) and Sn(II) in 100% water by acrylic polymers with pendant terpyridine motifs for analytical and forensic applications

*Miriam Trigo-López, Asunción Muñoz, Saturnino Ibeas, Félix Clemente García, Felipe Serna, and José Miguel García**

Departamento de Química, Facultad de Ciencias Universidad de Burgos
Plaza de Misael Bañuelos s/n, E-09001 Burgos, Spain. Fax: (+) 34 947 258 831. E-mail: jmiguel@ubu.es.

We have designed and prepared colorimetric cation responsive water soluble polymers and manageable films or membranes. The sensory materials respond with a colour change to the presence in water of Fe(III), Co(II), Cu(II), and Sn(II). The colour change is specific of each metal cation, and enable its identification (purple for iron, orange for cobalt, green for copper, and yellow for tin). The design of the materials relies on an addition monomer having a terpyridine moiety, which behaves as a dye in presence of transition metal cations due to its proven chelating capability toward these species and the colour development that always accompany the metallic complex formation. Water solutions of the sensory linear polymers allow for the UV/vis titration of Fe(III), Co(II), Cu(II), and Sn(II) with a limit of detection of 1.3×10^{-7} , 6.4×10^{-8} , 1.3×10^{-5} and 1.4×10^{-5} M, respectively. On the other hand, sensory kits, cut from sensory membranes, permitted the visual quantification of the cations in a dynamic range of five decades (1×10^{-7} - 5×10^{-3} M) for Fe(III) and Co(II) and of two decades (9×10^{-5} - 9×10^{-3} M) for Cu(II) and Sn(II). Titration curves can also be drawn from a picture taken to the sensory kits with a smartphone, by using the digital colour definition of the materials as analytical signal. Also, after entering into contact with hands, shapes of metallic objects (iron and cobalt containing tools) can be colour revealed by pressing the hands on paper or cotton fabrics wetted with water solutions of the linear sensory polymer.

Artículo enviado

Films and water soluble polymers as sensory materials for the detection and quantification of iron, cobalt, copper and tin salts in water, and for forensic applications.



Introduction

The costless, *in-situ*, and fast detection and quantification of transition metal cations in pure water are of the utmost environmental, industrial, and health importance. Traditional techniques, such as atomic absorption spectroscopy (AAS) or inductively coupled plasma mass spectrometry (ICP-MS), enable the selective and precise detection and quantification of the mentioned chemical species. However, they are heavy, bulky, extremely expensive techniques and require trained personnel. On the other hand, chemical sensors have become a simple species detection method for non-trained personnel, especially if the transduction is chromogenic (i.e., by a colour change) and the detection can be carried out visually.

Chemical sensors are an emerging technology with expanding applicability to a number of fields, such as civil security, environmental control and remediation, medicine, and industrial control. Moreover, sensory polymers, which are macromolecules that have receptor motifs (or binding sites) in their structure, represent a step further and show significant advances over discrete (or low molecular mass) chemosensors. Thus, polymers can be prepared or transformed into films, coatings or finished sensory materials with different shapes. Distinct polymer geometries are achievable (linear, spherical, and

tridimensional crosslinked network). They can be easily designed to work in hydrophobic or hydrophilic environments and can be used to sense both vapours and liquids. Also, they exhibit collective properties sensitive to minor perturbations. Finally, their sensory moieties cannot migrate with the concomitant increase in the performance stability along time, improvement in the thermal and chemical resistance, and can be easily reused.

We design and prepare chemosensory polymers and our research methodology is based on a guaranteed of success strategy. That is to say, once we have chemical species to be detected, the so-called targets, we look into the scientific literature to find fully confident receptors for such targets, usually discrete organic molecules that are insoluble in water; then, we slightly modify the chemical structure of the receptor by including a polymerizable group; and finally we copolymerize it with commercial hydrophilic and hydrophobic monomers to have water soluble linear polymers and crosslinked membranes with gel structures that allow for the detection in 100% water. The target species for this work are transition metal cations (Fe(III), Co(II), Cu(II) and Sn(II)), and the receptor core is based on a terpyridine (2,2':6',2''-terpyridine, tpy) motif.

Morgan and Burstal isolated tpy and described its purple complex with iron(II) in the 1930s.¹ Since then tpy has become one of the most used ligands with multiple applications in different research and technological areas, such as coordination polymers;²⁻⁴ sensors for anion,⁵⁻⁸ cations,⁹⁻¹⁵ both,^{16,17} and biomolecules;^{18,19} luminescent converters;²⁰⁻²² photon harvesting;²³ and catalysis.²⁴ Terpyridine derivatives are multivalent pyridine ligands that exhibit strong binding affinity toward a broad set of transition metal cations. This extremely strong interactions come both from the $d\pi-d\pi^*$ back bonding of the cations to the *N*-heterocycle rings and from the chelate effect.^{25,26}

We modified the tpy structure with a polymerizable methacrylamide group and prepared two kind of chromogenic sensory materials: linear polymers and solid film-shaped dense membranes comprised of crosslinked polymer

networks. The tpy-monomer (~1% mol) was copolymerized with a balance of hydrophilic and hydrophobic commercial co-monomers (~99% mol) to give linear copolymers and networks (membranes). The linear polymers are water soluble. The membranes are solid, exhibit gel behaviour, and can be used to prepare manageable solid sensory kits. Both type of materials respond with development of different colour depending on the presence of Fe(III), Co(II), Cu(II) and Sn(II) in 100% water.

Experimental part

Materials

All materials and solvents were commercially available and used as received, unless otherwise indicated: 2-acetylpyridine (98%, Alfa Aesar), iodine ($\geq 99.8\%$, Sigma-Aldrich), 4-nitrobenzaldehyde (99% Alfa Aesar), ammonium acetate (97%, Alfa Aesar), tin chloride anhydrous (98% , Alfa Aesar), methacryloyl chloride (97%, Alfa Aesar), triethylamine (TEA) ($\geq 99\%$, Aldrich), pyridine ($\geq 99\%$, Probus), sodium hydroxide (99.9%, VWR-Prolabo), hydrochloric acid (37%, VWR-Prolabo), *N*-methyl-2-pyrrolidone (NMP) (99%, Aldrich), ethanol (99.97%, VWR-Prolabo), diethyl ether ($\geq 99.5\%$, Aldrich), SnCl₂ anhydrous (98%, Alfa Aesar), Fe(NO₃)₃·9H₂O (VWR-Prolabo), Cu(NO₃)₂·3H₂O (98%, Sigma-Aldrich), Co(NO₃)₂·6H₂O ($\geq 99\%$, Labkem), NaCl ($\geq 99\%$, Sigma-Aldrich), KCl (99.5%, Scharlau), Al(NO₃)₂·9H₂O ($\geq 989\%$, Sigma-Aldrich), Pb(NO₃)₂ ($\geq 99\%$, Fluka), LiCl ($\geq 99\%$, Sigma-Aldrich), Zn(NO₃)₂·6H₂O (98%, Aldrich), Mg(NO₃)₂·6H₂O ($\geq 99\%$, Labkem), Cd(NO₃)₂ (98.5%, Alfa Aesar), Ni(NO₃)₂·6H₂O (98.5%, Sigma-Aldrich), methyl methacrylate (**MMA**) (99%, Aldrich), 1-vinyl-2-pyrrolidone (**VP**) ($\geq 99\%$, Sigma-Aldrich), ethylene glycol dimethacrylate (**EGDMA**) (98%, Sigma-Aldrich), Azo-bis-isobutyronitrile (AIBN, $\geq 98\%$, Aldrich) was recrystallised twice from methanol.

Instruments and measurements

^1H and ^{13}C NMR spectra were recorded with a Varian Inova 400 spectrometer operating at 399.92 and 100.57 MHz, respectively, with deuterated chloroform (CDCl_3) as the solvent.

UV/vis spectra were recorded using a Hitachi U-3900 UV/vis spectrophotometer.

Infrared spectra (FT-IR) were recorded with a FT/IR-4200 FT-IR Jasco spectrometer with an ATR-PRO410-S single reflection accessory. Low-resolution electron impact mass spectra (EI-LRMS) were obtained at 70 eV on an Agilent 6890N mass spectrometer. Thermogravimetric analysis (TGA) data were recorded for a 5-mg sample under a nitrogen or oxygen atmosphere on a TA Instrument Q50 TGA analyser at a scan rate of $10^\circ\text{C min}^{-1}$. The limiting oxygen index (LOI) was estimated using the following experimental Van Krevelen equation: $\text{LOI} = 17.5 + 0.4 \text{ CR}$, where CR is the char yield weight percentage at 800°C , which was obtained from the TGA measurements under a nitrogen atmosphere.

The water-swelling percentage (WSP) of the membrane was obtained from the weights of a dry sample membrane (ω_d) and a water-swelled sample membrane (ω_s) as follows: $100 \times [(\omega_s - \omega_d)/\omega_d]$ (the membrane was immersed in pure water at 20°C until the swelled equilibrium was achieved).

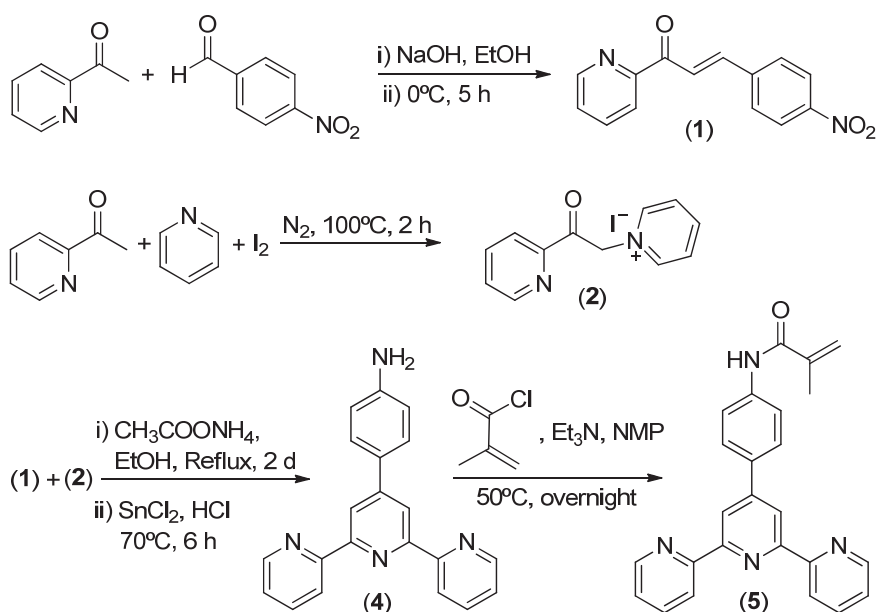
To determine the tensile properties of the polymer films (membranes), strips (5 mm in width and 30 mm in length) were cut from polymer films of 112 and $115\mu\text{m}$ thickness for **Mem1** and **Mem2**, respectively, on a SHIMADZU EZ Test Compact Table-Top Universal Tester at 20°C . Mechanical clamps were used and an extension rate of 5 mm min^{-1} was applied using a gauge length of 9.44 mm. At least 6 samples were tested for each polymer, and the data was then averaged.

The limit of detection (LOD) and limit of quantification were estimated by the following equations: $LOD = 3.3 \times SD/s$ and $LOQ = 10 \times SD/s$, where SD is the standard deviation of a blank sample and s is the slope of the calibration curve in a region of low concentration of target species.

The qualitative and quantitative chromogenic responses of sensory squares (~5x5 mm) cut from membranes (**Mem1** and **Mem2**) toward Fe(III), Co(II), Cu(II) and Sn(II) in water solution were studied by immersing the squares in a number of sealed vials with 1 mL of buffered water, containing each vial a known concentration of one of the target cations (pH = 2, buffer: KCl-HCl). The resident time was 24 hours and the temperature 25 °C. The qualitative evaluation of the sensing performance of the materials was carried out visually. On the other hand, the quantitative study was performed using a digital picture of the sensory squares taken with a smartphone by treatment of the colour definition data of each disc (RGB parameters, R = purple, G = green, B = blue). These parameters were obtained for each square directly after taking the photograph of the set squares through using the app called ColourMeter of a conventional Android smartphone (for each square 121 (11 × 11) pixels were averaged). The three RGB parameters were reduced to one variable (PC1, principal component 1), using principal component analysis (PCA), which provided an account of >78% of the information on the three RGB parameters, thus allowing for the elaboration of simple 2D titration curves ([cation] vs. PC1) with concomitant noise reduction without a significant loss of information.

Synthesis of sensory monomer

The sensory monomer containing the tpy-motif (**5**) was prepared according with the procedure schematically shown in Scheme 1.



Scheme 1. Synthesis of acyclic monomer (5).

Synthesis of 3-(4-nitrophenyl)-1-(pyridine-2-yl)prop-2-en-1-one (1). 2.5 mL of an aqueous solution of 10% NaOH was added to a suspension of 6.25 g (41.4 mmol) of 4-nitrobenzaldehyde in 50 mL of ethanol. To the resulting mixture cooled at 0°C, 5.0 g (41.2 mmol) of 2-acetylpyridine was added dropwise for 3 h. The solution was stirred at 0 °C for 2 h. The precipitate formed was collected by filtration and washed with ethanol. Yield 6.91 g (66%). ^1H NMR δ_{H} (400 MHz, CDCl_3 , Me_4Si): 8.75 (1H, d, J 4.7 Hz, pyridyl-H); 8.42 (1H, d, J 16.1 Hz, CH=CH); 8.26 (2H, d, J 8.8 Hz, Ph); 8.19 (1H, d, J 7.9 Hz, pyridyl-H); 7.91 (1H, d, J 16.1 Hz, CH=CH); 7.90 (1H, td, J 7.7 Hz, 1.7 Hz, pyridyl-H); 7.85 (2H, d, J 8.9 Hz, Ph); 7.52 (1H, ddd, J 7.5 Hz, 4.7 Hz, 1.2 Hz, pyridyl-H). ^{13}C NMR, δ_{C} (100.6 MHz, CDCl_3 , Me_4Si): 189.06, 153.73, 149.11, 148.67, 141.44, 141.36, 137.32, 129.36, 127.46, 124.94, 124.25, 123.20. EI-LRMS (m/z (%)): 255.07 (18), 254.07 (M^+ , 100), 226.07 (23), 225.06 (68), 180.07 (18), 179.07

(31), 130.04 (16), 102.04 (29), 79.03 (19), 78.03 (20). FTIR [Wavenumbers (cm^{-1})]: $\nu_{\text{ar C-H}}$: 3075; $\nu_{\text{C=O}}$: 1671; $\nu_{\text{C=N}}$: 1578; $\nu_{\text{as NO}_2}$: 1511; $\nu_{\text{s NO}_2}$: 1334.

Synthesis of 1-pyridylacetylpyridinium iodide (2). To a solution of 2 g (15.6 mmol) of 2-acetylpyridine in 20 mL of pyridine 4.60 g (17.6 mmol) of I_2 was added and heated at 100°C under N_2 atmosphere for 3 h. The mixture was then cooled at room temperature and filtered off and washed with ether. The dry solid was then washed with ethanol. A black solid was obtained. It was immediately used in the next synthetic step because it is sensitive to ambient conditions. Yield 4.03 g (75%). $^1\text{H NMR } \delta_{\text{H}}$ (300 MHz, CDCl_3 , Me_4Si): 8.75 (1H, d, J 4.7 Hz, pyridyl-H); 8.42 (1H, d, J 16.1 Hz, CH=CH); 8.26 (2H, d, J 8.8 Hz, Ph); 8.19 (1H, d, J 7.9 Hz, pyridyl-H); 7.91 (1H, d, J 16.1 Hz, CH=CH); 7.90 (1H, td, J 7.7 Hz, 1.7 Hz, pyridyl-H); 7.85 (2H, d, J 8.9 Hz, Ph); 7.52 (1H, ddd, J 7.5 Hz, 4.7 Hz, 1.2 Hz).

Synthesis of 2-(4-(4-nitrophenyl)-6-(pyridin-2-yl)pyridin-2-yl)pyridine (3). To a solution of 10% dry ammonium acetate in 20 mL of ethanol, 1 g (3 mmol) of (2) and 0.78 g (3 mmol) (1) were added. The mixture was refluxed for two days, the solvent removed and the product used without further purification. Yield 1.00 g (93%). $^1\text{H NMR } \delta_{\text{H}}$ (400 MHz, CDCl_3 , Me_4Si): 8.75 (2H, pyridyl-H); 8.73 (2H, d, J 4.3 Hz, pyridyl-H); 8.68 (2H, d, J 8.0 Hz, pyridyl-H); 8.36 (2H, d, J 8.8 Hz, Ph); 8.04 (2H, d, J 8.8 Hz, Ph); 7.90 (2H, td, J 7.8 Hz, 1.6 Hz, pyridyl-H); 7.38 (2H, pyridyl-H). $^{13}\text{C NMR}, \delta_{\text{C}}$ (100.6 MHz, CDCl_3 , Me_4Si): 156.53, 155.81, 149.35, 148.33, 148.02, 145.12, 137.17, 128.43, 124.34, 124.34, 121.56, 119.07. EI-LRMS (m/z (%)): 355.11 (25), 354.11 (M^+ , 100), 309.12 (20), 308.12 (78), 306.09 (9), 229.07 (57), 203.06 (4), 177.05 (4), 153.54 (5), 78.02 (5). FTIR [Wavenumbers (cm^{-1})]: $\nu_{\text{C=N}}$: 1585; $\nu_{\text{as NO}_2}$: 1514; $\nu_{\text{s NO}_2}$: 1351.

Synthesis of 4-(2,6-di(pyridin-2-yl)pyridin-4-yl)benzenamine (4). A mixture of 3.66 g (10.3 mmol) of (3) and 12.24 g (64.5 mmol) of anhydrous tin(II) chloride in concentrated hydrochloric acid (100 mL) was heated at 70°C for 6 h.

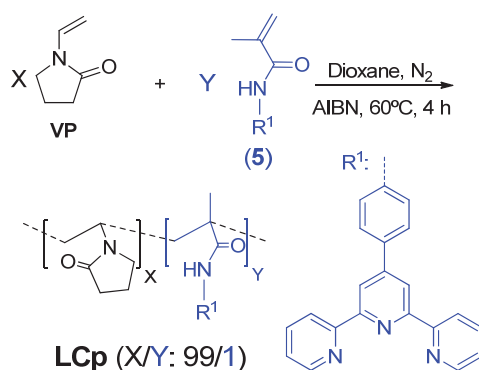
The solid was filtered off and stirred in a 10% aqueous solution of sodium hydroxide for 1 hour. Then it was filtered off and washed with water. Yield 3.07 g (92%). ^1H NMR δ_{H} (400 MHz, CDCl_3 , Me_4Si): 8.73 (2H, ddd, J 4.8 Hz, 1.8 Hz, 0.9 Hz, pyridyl-H); 8.69 (2H, s, pyridyl-H); 8.67 (2H, dt, J 8.0 Hz, 1.1 Hz, pyridyl-H); 7.87 (2H, td, J 7.7 Hz, 1.8 Hz pyridyl-H); 7.78 (2H, d, J 8.5 Hz, Ph); 7.35 (2H, ddd, J 7.5 Hz, 4.8 Hz, 1.2 Hz, pyridyl-H); 3.87 (2H, s, NH_2). ^{13}C NMR, δ_{C} (100.6 MHz, CDCl_3 , Me_4Si): 156.70, 155.88, 150.14, 149.22, 147.67, 136.95, 128.53, 128.38, 123.81, 121.49, 117.93, 115.37. EI-LRMS (m/z (%)): 325.13 (24), 324.13 (M^+ , 100), 323.12 (19), 296.11 (6), 246.10 (15), 219.09 (6), 162.09 (6), 78 (4). FTIR [Wavenumbers (cm^{-1})]: ν_{NH_2} : 3481, 3387; $\nu_{\text{C=N}}$: 1599; δ_{NH_2} : 1338; $\nu_{\text{C-N}}$: 1185.

Synthesis of *N*-(4-(2,4-di(pyridin-2-yl)pyridine-4-yl)phenyl)methacrylamide

(5). A solution of 2.60 g (8 mmol) of **(4)** in 20 mL of NMP was stirred at room temperature for 5 min. Then, 1 g (9.6) mmol of methacryloyl chloride was added dropwise for 20 min. After that, 1.05 g (10.4 mmol) of TEA was added and the mixture is stirred for 4 hs at 50°C under nitrogen atmosphere. The solution thus formed was precipitated in water, the solid filtered off and washed with water. Yield 3.07 g (98%). ^1H NMR δ_{H} (400 MHz, CDCl_3 , Me_4Si): 8.73 (2H, d, J 4.3 Hz, pyridyl-H); 8.72 (2H, s, pyridyl-H); 8.66 (2H, d, J 8.0 Hz, pyridyl-H); 7.91 (2H, d, J 8.7 Hz, Ph); 7.87 (2H, td, J 7.8 Hz, 1.6 Hz, pyridyl-H); 7.73 (2H, d, J 8.7 Hz, Ph); 7.68 (1H, s, NH); 7.35 (2H, m, pyridyl-H); 5.83 (1H, s, $=\text{CH}_2$), 5.49 (1H, s, $=\text{CH}_2$), 2.09 (3H, s, CH_3). ^{13}C NMR, δ_{C} (100.6 MHz, CDCl_3 , Me_4Si): 171.38, 166.68, 156.40, 156.08, 149.55, 149.25, 141.00, 138.86, 137.01, 134.35, 128.12, 123.96, 121.52, 120.26, 118.55, 18.91. EI-LRMS (m/z (%)): 393.17 (29), 392.16 (M^+ , 100), 391.14 (23), 337.14 (6), 351.12 (5), 323.13 (6), 233.09 (19), 78.02 (21), 62.99 (18). FTIR [Wavenumbers (cm^{-1})]: $\nu_{\text{N-H}}$: 3301; $\nu_{\text{C=O}}$: 1665; $\nu_{\text{C=N}}$: 1585; $\delta_{\text{N-H}}$: 1519.

Polymer synthesis

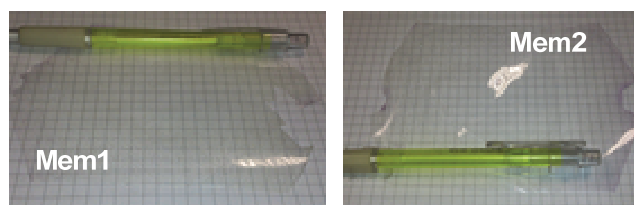
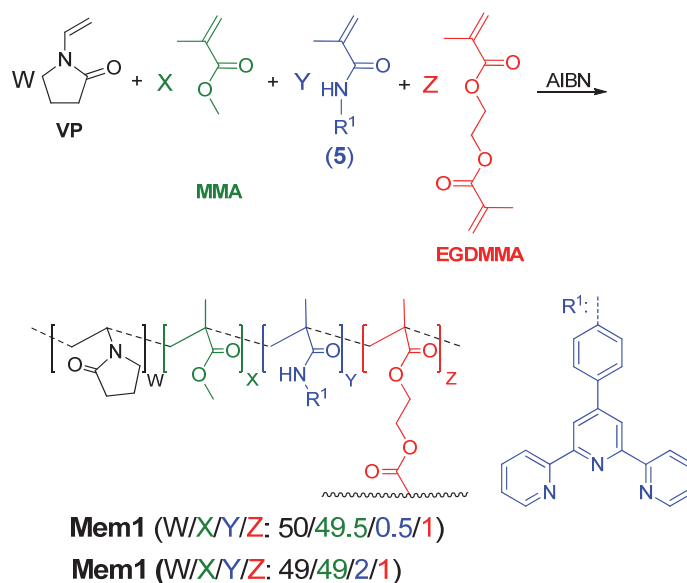
The linear copolymer (**LCp**) was prepared by thermally initiated radical polymerization of the hydrophilic monomer **VP** and the tpy-derivative monomer (**5**) in a 99/1 (**VP**/**5**) molar ratio (Scheme 2). A 100-mL three-necked flask equipped with a magnetic stirrer, a nitrogen inlet, and a reflux condenser was charged with a solution of 0.18 mmol (0.071 g) of (**5**) and 17.9 mmol (2.0 g) of **VP** in 18 mL of dioxane. Subsequently, AIBN (0.29 g, 1.8 mmol) was added, and the solution was heated to 60 °C. After stirring for 4 h under nitrogen, the solution was allowed to cool. The, it was poured dropwise to hexane (200 mL) with vigorous stirring, yielding a white precipitate (Yield 1.61 g (79%)).



Scheme 2. Synthesis and chemical structure of sensory linear polymer (**LCp**).

The film-shaped sensory membranes were prepared by the bulk radical polymerization of the hydrophilic monomer **VP**, the hydrophobic monomer **MMA**, and the tpy-containing monomer (**5**). **EGDMMA** was used as cross-linking agent (Scheme 3). The co-monomer molar ratio **VP/MMA/5/EGDMMA** was 50/49.5/0.5/1 and 49/49/2/1 for **Mem1** and **Mem2**, respectively. AIBN (1 wt%) was employed as a thermal radical initiator. The bulk radical polymerization

reaction was carried out in a silanized glass mould that was 100 mm thick in an oxygen-free atmosphere at 60 °C overnight.



Scheme 3. Synthesis and chemical structure of sensory membranes **Mem1** and **Mem2**. The picture shows the membranes after removal from the mould.

Solid sensory substrates

The solid sensory substrates were manufactured from **Mem1** and **Mem2** films by using plastic scissors to cut out 5x5 mm sensory squares. Plastic scissors were used to avoid the presence of iron. Conventional steel scissors turned the membrane coloured. The solely contact of an iron containing object with the membrane surface turns it purple in colour.

Results and discussion

Sensing target cations in pure water

Our objective is the exploitation of organic molecules in pure water. Organic molecules are usually highly hydrophobic and water insoluble. Their properties in this medium are unknown although they can be envisaged by studying the molecules in organic/aqueous mixtures. Accordingly, we choose an interesting molecule, slightly modify its structure by including a polymerizable group, and prepare hydrophilic polymers. The polymers are both linear, soluble in water, and crosslinked membranes with gel behaviour as manageable solid kits. With these materials we reach our goal of exploiting water insoluble molecules in pure water.

Design of the colorimetric chemosensory terpyridine unit

Firstly we had metal cations and water as target species and measuring medium, respectively. We also had in mind a chromogenic response as transduction of the recognition phenomena. This is because we seek sensory materials to be used as sensory devices for non-specialized personnel, and the naked eye is the best antenna for this purpose. For meeting this criteria, we chose a proven multivalent chelating ligand, terpyridine, which was isolated in 1932,¹ as a guarantee of success.⁵⁻¹⁷ Thus, a tpy derivative containing an amine group was used to prepare the acrylamide monomer **(5)**, which was copolymerized with the hydrophilic **VP** and the hydrophobic **MMA** co-monomers.

Materials preparation and characterisation

The acrylamide sensory monomer **(5)** was conventionally prepared by the straightforward reaction of methacryloyl chloride with the amine group of the intermediate containing the tpy motif **(4)**. The preparation of **(4)** was previously reported, and the steps we have followed to prepare products **(1)** to **(4)** have

been adapted from those described by a number of authors looking for inexpensiveness of the chemicals, optimization of the reaction steps, higher reaction yields, easy or no further purification of products.²⁷⁻³¹ The ¹H and ¹³C NMR and FTIR data and the spectra of the intermediates and monomers can be found in the experimental section and in the ESI, Section S1. The potential applicability of the designed acrylic soluble polymer **LCp** and sensory membranes, **Mem1**, and **Mem2** is highlighted by the fact that a small quantity ($\leq 6.8\%$ (**Mem2**), $\leq 1.8\%$ (**Mem1**)) by weight of the sensory synthetic monomer is used in the preparation of the sensory materials, as will be described below, using ($\geq 93.1\%$ (**Mem2**), $\geq 98.2\%$ (**Mem1**)) by weight of widely available and very inexpensive commercial co-monomers.

The mechanical and thermal behaviour are key parameters of every material. The membranes, or films, have good physical appearance and were creasable and handleable. Mechanically, they had tensile strength and moduli ranging 33-39 and 660-730 MPa, respectively (Table 1). These results are excellent for lab-made acrylic membranes. The thermal resistance was evaluated using TGA. The degradation temperatures that resulted in a 5% weight loss under a nitrogen atmosphere (T_5) were $\sim 240^\circ\text{C}$ for membranes and much higher, $\sim 390^\circ\text{C}$, for **LCp**. The ester content of the membranes, from the **MMA** co-monomer, lowered the thermal resistance compared with **LCp**. The methyl ester moieties are hydrophobic and counterbalance the hydrophilic nature of **VP** in the membranes in order to control the water-swelling percentage (WSP). Gel behaviour is relevant for the membrane to sense in pure water because the target species enter into the material as solvated species by diffusion. However, the water uptake has to be modulated in order to keep good mechanical properties in the swelled state. For this purpose, a moderate WSP around 40% is desirable. The membranes constitution was designed to meet this criterion. Accordingly, WSP of **Mem1** and **Mem2** was 48% and 36 %, respectively. The hydrophobic nature of the tpy motifs is the responsible of the

12% water uptake decrease upon increasing 1.5% the monomer containing the tpy groups (5).

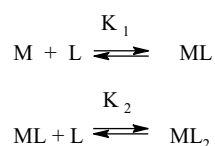
Table 1. Thermal (TGA) and mechanical properties of materials. The thermal properties were evaluated in inert (N₂) and oxidizing (synthetic air) atmospheres.

Polymer	Thermal properties						Mechanical properties		
	Atmosphere			LOI ^(c)	Tensile strength MPa	Young's Modulus MPa	Elongation %		
	N ₂		Air						
T ₅ , ^{a)} °C	T ₁₀ , ^{b)} °C	CR, ^{b)} %	T ₅ , ^{a)} °C	T ₁₀ , ^{b)} °C					
Mem1	242	344	4	224	318	19.1	33	660	9
Mem2	241	342	4	245	333	19.1	39	730	8
LCp	389	408	1	353	399	17.9	n.a. ^{d)}	n.a. ^{d)}	n.a. ^{d)}

^{a)} 5% weight loss (T₅), 10% weight loss (T₁₀); ^{b)} CR: char yield at 800 °C; ^{c)} limiting oxygen index, calculated from the TGA data (LOI = 17.5 + 0.4 CR, CR at 800 °C under nitrogen); ^{d)} n.a.: not applicable.

The chemosensing mechanism

The chemosensing mechanism can be described as the complexation processes of one cation (*M*) and two tpy motifs (*L*) in water. The complex stoichiometry was estimated with a Job's plot obtained from the UV/vis titration of Fe(III) with water solutions of the sensory polymer **LCp** (Figure 1). The process is governed by two stability constants *K*₁ and *K*₂, where *L* is the moles of sensory tpy-motifs per water volume of linear copolymer,



L represents really not a conventional concentration because the sensory motifs are chemically anchored to the linear copolymer chains. The formation of *ML* and *ML*₂ is clearly depicted in the UV/vis titration spectra (Figure 1). Considering the stability constants definition, the UV/vis

spectroscopic data, and the mass balance ($C_M = [M] + [ML] + [ML_2]$; $C_L = [L] + [ML] + 2[ML_2]$), the stability constants can be calculated by non-linear curve fit of Eq. (1), where A is the absorbance, ε_L is calculated initially by $\varepsilon_L = A_0/C_L$, and ε_{ML_2} at the end with a huge excess of metal by $\varepsilon_{ML_2} = 2A_{\text{final}}/C_L$ (at this point $[M] \cong C_M$).³²

$$A = \frac{-1 - K_1[M] + \sqrt{(1 + K_1[M])^2 + 8C_L K_1 K_2 [M]}}{4K_1 K_2 [M]} \left(\varepsilon_L + \varepsilon_{ML} K_1 [M] \right) + \varepsilon_{ML_2} \frac{-1 - K_1[M] + \sqrt{(1 + K_1[M])^2 + 8C_L K_1 K_2 [M]}}{4} \quad (1)$$

The fitting of Eq. (1) to complexation of iron(III) with **LCp** is shown in Figure 1, giving rise to $K_1 = 51,000 \pm 6,000$ and $K_2 = 2,000 \pm 1,000$. The analysis of other cations gave no clear result because all species absorb in the same UV/vis region. This interferes with the constants calculation but not with the titration.

Sensing Fe(III), Co(II), Cu(II) and Sn(II) in aqueous media

The addition of transition metal cations to water solutions of **LCp** give rise to the development of clearly visible and nice colours (purple (Fe(III)), orange (Co(II)), green (Cu(II)) and yellow (Sn(II))) (Figure 2). The UV/vis titration curves are depicted in Figures 3 and 4. The response to Fe(III) and Co(II) is conventional (Figure 3), with LOD and LOQ in the sub-micromolar level (1.3×10^{-7} and 3.9×10^{-7} for the Fe(III) and 6.4×10^{-8} and 1.9×10^{-7} for Co(II)). On the other hand, the response to Cu(II) and Sn(II) was rather complex with LOD and LOQ in the sub millimolar level (1.3×10^{-5} and 3.8×10^{-5} for Cu(II) and 1.4×10^{-5} and 4.2×10^{-5} for Sn(II)). Only the low concentration region is shown in Figure 4. Full titration curves and UV/vis titration spectra are shown in Figures S6 to S9, ESI.

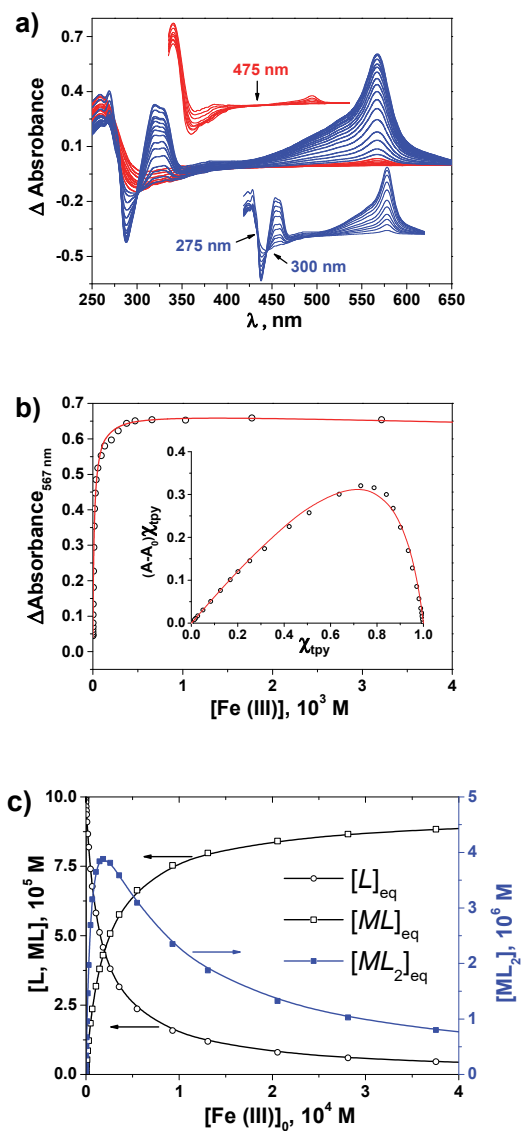


Figure 1. UV/vis study of the interaction of Fe(III) (M) with tpy-motif (L) of **LCp** in water ($\text{pH} = 2$, buffer = HCl-KCl): a) absorbance variation spectra. Blue and red spectra correspond to formation of 1:1 (ML) and 1:2 (ML_2) complexes tpy motif:Fe(III), respectively (inset: separation of processes with indication of the isobestic points); b) absorbance at 567 nm vs Fe(III) concentration. The continuous line is the fitting of the data according with Eq. (1) (inset: Job's plot (χ_{tpy} is molar fraction of tpy sensory motifs, absorbance at 567 nm)); and c) the species distribution.

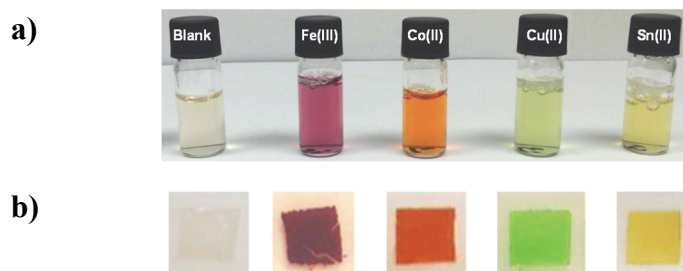


Figure 2. Colour development sensory materials upon entering into contact with Fe(III), Co(II), Cu(II) and Sn(II): a) **LCp** in water solution (pH = 2, buffer = KCl-HCl, concentration of cations = 5×10^{-4} M). The concentration of sensory motifs in water was 0.01 M (equivalents of pendant sensory motifs per litre); and b) **Mem1** after immersion in water (pH = 2, buffer = KCl-HCl, concentration of cations = 5×10^{-4} M, immersion time = 24 h).

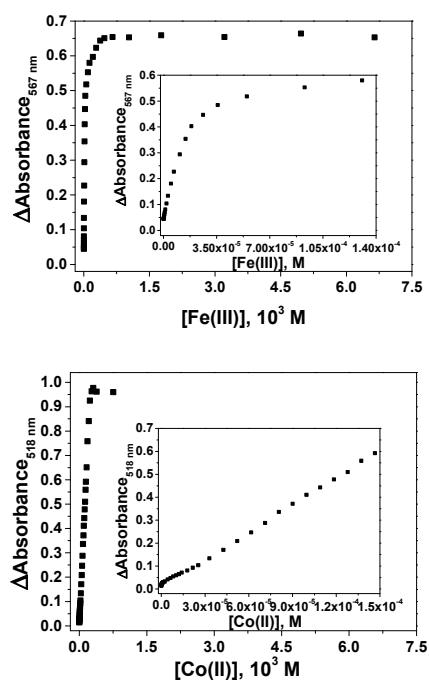


Figure 3. Titration curves of Fe(III) and Co(II) with aqueous solutions of **LCp** (pH = 2, buffer = KCl-HCl, concentration of cations ranging from 6.75×10^{-8} to 6.57×10^{-4} M for Fe(III) and $7 \times 99 \cdot 10^{-8}$ to $7 \times 54 \cdot 10^{-4}$ M for Co(II). Insets: expansion of the low concentration region. The concentration of sensory motifs in water was 1×10^{-4} M for the Fe(III) titration and 1×10^{-3} M for the Co(II) titration (equivalents of pendant sensory motifs per litre).

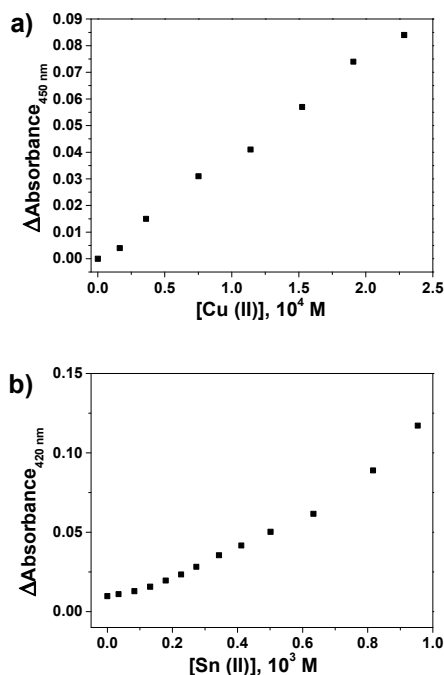


Figure 4. Titration curves of: a) Cu(II); and b) Sn(II) with aqueous solutions of **LCp** (pH = 2, buffer = KCl-HCl, concentration of cations ranging from 1.64×10^{-5} to 1.46×10^{-3} M for Cu(II) and 3.44×10^{-5} to 1.50×10^{-3} M for Sn(II) M. The concentration of sensory motifs in water was 1×10^{-3} M (equivalents of pendant sensory tpy motifs per litre).

Solid sensory materials permitted the preparation of solid titration kits for the visual detection and quantification of cations. Accordingly, squares cut from **Mem1** allowed for the naked eye study of Fe(III) and Co(II) content by analysing the purple and orange colour development, respectively (Figure 5a). The lower sensitivity of the sensory polymers toward Cu(II) and Sn(II), compared with the sensitivity toward Fe(III) and Co(II), was resolved by increasing the tpy sensory motifs within the membranes. Therefore, **Mem2**, which have a molar tpy content four times higher than **Mem1**, permitted the visual titration of Cu(II) and Sn(II) by following the green and yellow colour development, respectively. The digital colour of pictures of sensory squares (sensory kits) shown in Figures 5a and 5b were used to build titration curves

with quantification purposes, as previously described and shown for Fe(III) in Figure 5c (the data and titration curves for Co(II), Cu(II) and Sn(II) are depicted in the ESI, Tables S1-S12 and Figures S10-S13).^{33,34}

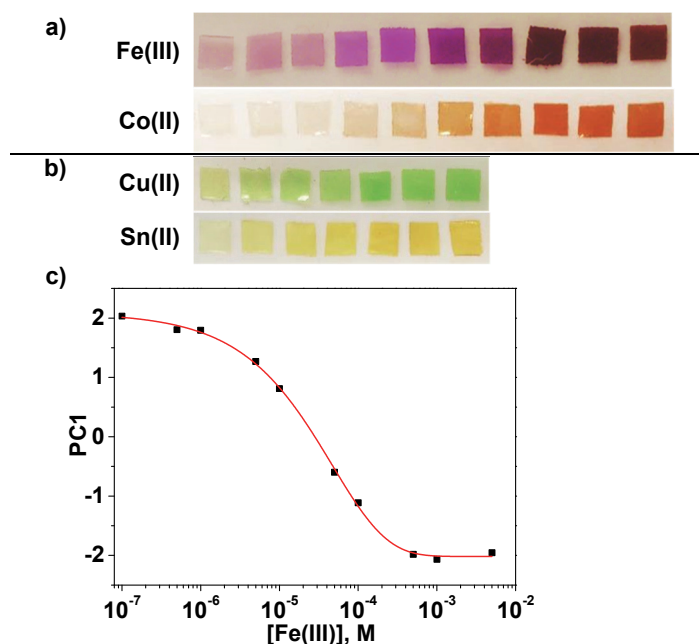


Figure 5. Visual titration of Fe(III), Co(II), Cu(II) and Sn(II) in water (pH = 2, buffer = KCl-HCl) with squares cut from **Mem1** or **Mem2**. Each square was dipped in the water solution containing each cation for 24 h. The sensory membrane and the cation concentration of the water solution was: a) membranes = **Mem1**, Fe(III) and Co(II) concentration, from left to right: 1 × 10⁻⁷, 5 × 10⁻⁷, 1 × 10⁻⁶, 5 × 10⁻⁶, 1 × 10⁻⁵, 5 × 10⁻⁵, 1 × 10⁻⁴, 5 × 10⁻⁴, 1 × 10⁻³, 5 × 10⁻³ M; b) membranes = **Mem2**, Cu(II) and Sn(II) concentration, from left to right: 9 × 10⁻⁵, 3 × 10⁻⁴, 6 × 10⁻⁴, 9 × 10⁻⁴, 3 × 10⁻³, 6 × 10⁻³, 9 × 10⁻³ M; and c) Fe(III) titration curve obtained from the picture taken to the squares immersed in water with Fe(III) (PC1: principal component 1 that encompass three digital colour parameters (RGB) of each sensory square).

Response time

There are key parameters for sensor performance for real live measurements: reliability, accurateness, environmental inertness, and short response time. We

have evaluated the response time for **LCp** solutions by UV/vis spectroscopy as the time needed to achieve 99% of the absorbance variation (ESI, Figure S14). This time was 10, 6, 2, and 12 min for Fe(III), Co(II), Cu(II), Sn(II) respectively (cations concentration of 5×10^{-6} , 5×10^{-5} , 1×10^{-4} , 7.5×10^{-4} M, respectively). The apparent response time of the sensory films (membranes) was slower because of the diffusion of the species into the membrane, and the sensory squares were left immersed overnight.

Interference study

The selectivity of the sensory materials as colorimetric transition metal cation sensors was tested in the presence of a broad set of cations (NaCl, KCl, $\text{Cu}(\text{NO}_3)_2 \cdot 3\text{H}_2\text{O}$, $\text{Co}(\text{NO}_3)_2 \cdot 6\text{H}_2\text{O}$, $\text{Al}(\text{NO}_3)_3 \cdot 9\text{H}_2\text{O}$, $\text{Pb}(\text{NO}_3)_2$, LiCl, $\text{Zn}(\text{NO}_3)_2 \cdot 6\text{H}_2\text{O}$, $\text{Mg}(\text{NO}_3)_2 \cdot 6\text{H}_2\text{O}$, $\text{Cd}(\text{NO}_3)_2$, SnCl_2 and $\text{Ni}(\text{NO}_3)_2 \cdot 6\text{H}_2\text{O}$, SnCl_2 , $\text{Fe}(\text{NO}_3)_3 \cdot 9\text{H}_2\text{O}$, $\text{Cu}(\text{NO}_3)_2 \cdot 3\text{H}_2\text{O}$, $\text{Co}(\text{NO}_3)_2 \cdot 6\text{H}_2\text{O}$). Thus, a solution of **LCp** in water (pH = 2, buffer: KCl-HCl, concentration of sensory motifs in water was 1×10^{-3} M -equivalents of pendant sensory tpy motifs per litre-) with a cocktail of these cations (concentration of each cation = 9.09×10^{-4} M) was used in this study. The UV/vis spectra show that the set of cations are true interferents (ESI, Figure S15). This is a cause of the broad chelating effect of tpy motifs. This means that a full range of complexes are formed, though only a few are coloured. However, the target cations can also be evaluated in presence of these interferents by the standard addition procedure. For instance, by adding increasing and known quantities of Fe(III) to the sample containing the cocktail of 13 cations (concentration of each cation = 1×10^{-6} M), the Fe(III) concentration calculated was 1.3×10^{-6} M, similar to the real content, 1.0×10^{-6} M (ESI, Figure S16).

Forensic applications and metal recognition

Iron containing tools leave a small amount of metal upon entering into contact with other surfaces. This is relevant in forensic applications where it is important

to detect the imprint of certain objects in hands, like knives. In this sense, we show in a video the shape of a lag screw in a finger after holding it with two fingers. After pressing lag screw with the fingers, the index finger is pressed on a filter paper impregnated with an aqueous solution of **LCp**. The iron particles are oxidized by the oxygen of the air, the sweat and water and recognized by the tpy motifs giving rise to the complex formation with the concomitant purple colour development (see video, ESI).

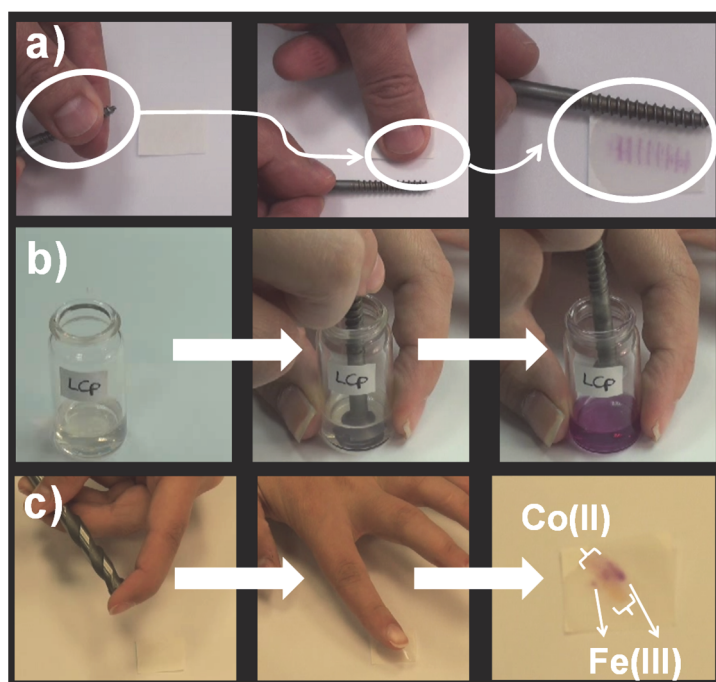


Figure 6. Detecting iron and cobalt with a water solution of **LCp** (pH = 2, buffer: KCl-HCl, 1.14 mg/mL (concentration of sensory motifs was 1.75×10^{-3} M -equivalents of pendant sensory tpy motifs per litre-)): a) shape of a lag screw in a finger; b) coloration of the **LCp** solution caused by the iron of the lag screw; and c) shape of a widia blade (tungsten carbide + 6-10% of cobalt) of a drill bit.

Moreover, it is possible to know if a tool has iron in its composition by dipping in a water solution of **LCp**. Immediately after immersion, the solution turn purple (see video, ESI).

Cobalt, a critical raw material,³⁵ can also be analysed in a similar way. The video (ESI) also shows how a widia drill bit, which has an iron-based shaft with a tungsten carbide (with 6-10% of cobalt) blade at the tip off the drill. After being touched with a finger, the widia blade leave on the filter paper wet with the water solution of **LCp** its orange imprint surrounded by the purple imprint of the iron holding the widia tip.

Conclusions

We have used terpyridine, a proven chelating agent for monoatomic metallic cations, to prepare colorimetric sensory solid polymers both as water soluble linear polymers and as solid films (membranes). Water solution of the linear polymer turned purple, orange, green or yellow upon being in contact with Fe(III), Co(II), Cu(II) and Sn(II), respectively. The colour development permitted the visual differentiation of the cations and the titration with the UV/vis technique. The limit of detection was sub-micromolar for Fe(III) and Co(II), and micromolar for Cu(II) and Sn(II). In a similar fashion, the solid films have gel behaviour and turn coloured upon immersing in water containing the aforementioned cations. Squares cut from the membranes (5x5 mm) behaved as solid sensory kits from which the cations could be differentiated and their concentration estimated by the naked eye. Pictures taken to the kits permitted the titration using the colour definition of the sensory squares as analytical input. The dynamic range was of five decades (lower concentration = 1×10^{-7} M) for Fe(III) and Co(II) and of two decades (lower concentration = 9×10^{-5} M) for Cu(II) and Sn(II). The chosen of proven organic chelating agents and their chemical anchorage to polymer backbones have proven to be successful strategies to prepare sensory materials for water environments. The colour output of the sensory systems and the manageable solid kits allowed for the visually use of these materials by non-specialized personnel and, concomitantly, portable devices such as smartphones permit the fast and costless quantification of target species. Moreover, forensic applications are

envisaged, e.g., the shape of metallic objects after entering into contact with hands can be colour revealed by pressing the hands on paper or cotton fabrics wetted with water solutions of the linear sensory polymer.

Acknowledgments

We gratefully acknowledge the financial support provided by the Spanish Ministerio de Economía y Competitividad-Feder (MAT2014-54137-R) and by the Consejería de Educación – Junta de Castilla y León (BU232U13).

Supporting information

A file and a video. The file containing experimental part (intermediates and monomer characterization); study of interaction of **LCp**, **Mem1** and **Mem2** with Fe(III), Co(II), Cu(II), and Sn(II); interference study; and response time. The video showing the forensic applications and metal recognition of metallic goods with solutions of **LCp**.

References and notes

- 1 G. T. Morgan and F. H. Burstall, *J. Chem. Soc.*, **1932**, 20-30
- 2 C. E. Housecroft, *Dalton Trans.*, 2014, **43**, 6594-6604.
- 3 E. C. Constable, C. E. Housecroft, M. Neuburger, S. Schaffner and L. J. Scherer, *Dalton Trans.*, 2004, 2635-2642.
- 4 P. Wang, T. Okamura, H.-P. Zhou, W.-Y. Sun and Y.-P. Tian, *Chin. Chem. Lett.*, 2013, 24, 20-22.
- 5 B. Zhang, Y. Li and W. Sun, *Eur. J. Inorg. Chem.*, 2011, 4964-4969.
- 6 C. Bhaumik, D. Maity, S. Das and S. Baitalik, *Polyhedron*, 2013, **52**, 890-899.
- 7 Q.-Y. Cao, M. Li, L. Zhou and Z.-W. Wang, *RSC Adv.*, 2014, **4**, 4041-4046.
- 8 S. Bhowmik, B. N. Ghosh, V. Marjomäki and K. Rissanen, *J. Am. Chem. Soc.* 2014, **136**, 5543-5546.
- 9 A. Fermi, G. Bergamini, M. Roy, M. Gingras and P. Ceroni, *J. Am. Chem. Soc.* 2014, **136**, 6395-6400.
- 10 C. Goze, G. Ulrich, L. Charbonnière, M. Cesario, T. Prangé and R. Ziessel, *Chem. Eur. J.* 2003, **9**, 3748-3755.

- 11 C. Fan, X. Wang, P. Ding, J. Wang, Z. Liang and X. Tao, *Dyes Pigm.*, 2012, **95**, 757-767.
 - 12 H. Li, S.-J. Zhang, C.-L. Gong, Y.-F. Li, Y. Liang, Z.-G. Qi and S. Chen, *Analyst*, 2013, **138**, 7090-7093.
 - 13 Y. Hong, S. Chen, C. W. T. Leung, J. W. Y. Lam, J. Liu, N.-W. Tseng, R. T. K. Kwok, Y. Yu, Z. Wang and B. Z. Tang, *ACS Appl. Mater. Interfaces* 2011, **3**, 3411-3418.
 - 14 M. Zheng, H. Tan, Z. Xie, L. Zhang, X. Jing and Z. Sun, *ACS Appl. Mater. Interfaces*, 2013, **5**, 1078-1083.
 - 15 M. E. Padilla-Tosta, J. M. Lloris, R. Martínez-Máñez, A. Benito, J. Soto, T. Pardo, M. A. Miranda and M. D. Marcos, *Eur. J. Inorg. Chem.*, 2000, 741-748.
 - 16 Z.-B. Zheng, Z.-M. Duan, J.-X. Zhang, K.-Z. Wang, *Sens. Actuators B*, 2012, **169**, 312-319.
 - 17 C. Bhaumik, S. Das, D. Maity and S. Baitalik, *Dalton Trans.*, 2011, **40**, 11795-11808.
 - 18 C. Y.-S. Chung and V. W.-W. Yam, *J. Am. Chem. Soc.* 2011, **133**, 18775-18784.
 - 19 H.-L. Kwong, W.-L. Wonga, C.-S. Lee, C.-T. Yeung and P.-F. Teng, *Inorg. Chem. Commun.* 2009, **12**, 815-818.
 - 20 R. Shunmugam and G. N. Tew, *Polym. Adv. Technol.* 2007, **18**, 940-950.
 - 21 Etienne Baranoff, Jean-Paul Collin, Lucia Flamigni and Jean-Pierre Sauvage, *Chem. Soc. Rev.*, 2004, **33**, 147-155.
 - 22 E. G. Moore, M. Benaglia, G. Bergamini and P. Ceroni, *Eur. J. Inorg. Chem.* 2015, 414-420.
 - 23 S. Caramori, J. Husson, M. Beley, C. A. Bignozzi, R. Argazzi and P. C. Gros, *Chem. Eur. J.*, 2010, **16**, 2611-2618.
 - 24 A. Winter, G. R. Newkome and U. S. Schubert, *ChemCatChem* 2011, **3**, 1384-1406.
 - 25 H. Hofmeiera and U. S. Schubert, *Chem. Soc. Rev.*, 2004, **33**, 373-399.
 - 26 P. R. Andres and U. S. Schubert, *Adv. Mater.*, 2004, **16**, 1034-1068.
 - 27 P. Lainé, F. Bedioui, P. Ochsenbein, V. Marvaud, M. Bonin and E. Amouyal, *J. Am. Chem. Soc.*, 2002, **124**, 1364-1377.
 - 28 F. Tessore, D. Roberto, R. Ugo and M. Pizzotti, *Inorg. Chem.*, 2005, **44**, 8967-8978.
 - 29 E. Zysman-Colman, J. D. Slinker, J. B. Parker, G. G. Malliaras and S. Bernhard, *Chem. Mater.* 2008, **20**, 388-396.
 - 30 G. A. Koohmareh and M. Sharifi, *J. Appl. Polym. Sci.*, 2010, **116**: 179-183.
 - 31 W. Y. Ng, X. Gong and W. K. Chan, *Chem. Mater.*, 1999, **11**, 1165-1170.
 - 32 S. Vallejos, P. Estévez, S. Ibeas, F. C. García, F. Serna, J. M. García, *Sensors*, 2012, **12**, 2969-2982.
 - 33 H. El Kaoutit, P. Estevez, F. C. Garcia, F. Serna and J. M. Garcia, *Anal. Methods*, 2013, **5**, 54-58.
 - 34 S. Vallejos, A. Muñoz, S. Ibeas, F. Serna, F. C. Garcia and J. M. Garcia, *J. Mater. Chem. A*, 2013, **1**, 15435-15441.
 - 35 *Report on critical raw materials for the EU*, Report of the Ad hoc Working Group on defining critical raw materials, European Commission, May 2014. Downloaded: July 14, 2015 (http://ec.europa.eu/enterprise/policies/raw-materials/files/docs/crm-report-on-critical-raw-materials_en.pdf).
-

2.4. Sensores cromogénicos de explosivos (TNT)

La preocupación social por la detección de explosivos está relacionada con la seguridad nacional y se sostiene en el miedo a los ataques terroristas. Dentro de estos explosivos el más común es el 2,4,6-trinitrotolueno o TNT, que además es tóxico para los seres vivos. Aunque existen diversos métodos de detección de este nitrocompuesto, el desarrollo de un sensor que permita la detección a simple vista supone un gran avance para la seguridad, la investigación criminal y forense y para la protección medioambiental. De acuerdo con esto, se han diseñado polímeros acrílicos con grupos amina primaria, secundaria y terciaria en su estructura para la detección y cuantificación de TNT mediante el desarrollo de un color rojo en el material sensor. Estos materiales se han preparado como polímeros lineales solubles en agua, membranas densas y tejidos inteligentes, y se puede utilizar tanto en medio acuoso como en fase vapor.

2.4.1. Complejos de Meisenheimer

El complejo de Meisenheimer, también conocido como complejo- σ , es el intermedio que se genera en una reacción de sustitución nucleófila sobre un anillo aromático (Figura 2.5).⁸¹ Esta reacción consta de dos etapas, una primera de adición, consistente en la adición de un nucleófilo (Nu) a un anillo aromático convenientemente activado, es decir, sustituido con grupos electrón-atradores, en la que se consigue el compuesto aniónico denominado complejo de Meisenheimer, y una segunda etapa de eliminación, en la que dicho complejo libera un anión X⁻.

Los complejos de Meisenheimer se describieron por primera vez por Jackson y Gazzolo en el año 1900,⁸² al observar disoluciones intensamente

⁸¹ E. Buncl, J. M. Dust, F. Terrier, *Chem. Rev.* **1995**, 95, 2261.

⁸² J. C. Jacson, F. H. Gazzolo, *J. Am. Chem. Soc.* **1900**, 23, 376.

coloreadas como consecuencia de la mezcla de bases con compuestos aromáticos deficientes electrónicamente. Dos años más tarde, los estudios de Meisenheimer confirmaron la estructura que se había propuesto.⁸³ Más adelante se pudo confirmar que la carga negativa estaba deslocalizada a través del anillo mediante experimentos de resonancia magnética nuclear de protón y carbono.⁸⁴

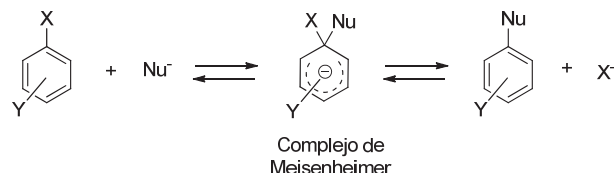


Figura 2.5. Reacción de sustitución nucleófila aromática y formación del complejo de Meisenheimer.

Estos complejos coloreados que se forman por transferencia de carga entre un anillo aromático deficiente en electrones, como el TNT, con bases de Lewis (aminas, alcoxidos y grupos hidróxido) se han utilizado ampliamente para la detección de compuestos nitroaromáticos utilizando la espectroscopia UV/Vis. En este sentido, desde el grupo de investigación se ha trabajado en el diseño y síntesis de polímeros sensores que contienen monómeros con grupos amina primaria, secundaria o terciaria en su estructura como unidades sensoras de TNT.

2.4.2. Polímeros con aminas primarias, secundarias y terciarias en su estructura

La preparación de materiales sólidos para la detección de TNT, tanto en fase gas como en medios acuosos de manera simple, directa y a partir de monómeros comerciales supone un método muy ventajoso desde el punto de vista práctico y económico. En este caso se pensó en una triple aproximación desde el enfoque macromolecular para la preparación de estos materiales:

⁸³ J. Meisenheimer, *Justus Liebigs Ann. Chem.* **1902**, 323, 205.

⁸⁴ G. A. Artamkina, M. P. Egorov, I. P. Beletskaya, *Chem. Rev.* **1982**, 82, 427.

- Polímero lineal sensor soluble en agua.
- Polímero reticulado sensor como membrana densa con comportamiento gel.
- Tejidos inteligentes formados a partir de recubrimientos de telas de algodón con polímero sensor.

En un primer trabajo, se propuso la utilización del monómero comercial metacrilato de 2-(dimetilamino)etilo (AEMA) como amina sensora para la preparación de un material sensor, obteniéndose polímeros lineales, membranas densas y tejidos inteligentes como materiales sensores de TNT en medio acuoso. Sin embargo, estos polímeros no cambiaban de color en presencia de vapores de TNT. Aunque al incrementar el carácter básico de las aminas se esperan complejos de Meisenheimer más estables, y por lo tanto, mayor desarrollo del color y sensibilidad del material sensor, en este caso el volumen de los tres grupos alquilo afecta negativamente a la fortaleza de las bases de Lewis en la amina. Se pensó entonces en utilizar aminas primarias y secundarias.

Por ello, en un trabajo posterior se propuso la utilización de 4-(aminometil)estireno como monómero de síntesis sencillo que contiene una amina primaria, y el 4-[N-(2-(metilamino)-etil)aminometil]estireno como monómero comercial con dos aminas secundarias, con el objetivo de preparar membranas densas y tejidos inteligentes con mayor sensibilidad sin que la selectividad se viera afectada, permitiendo la detección de TNT no solo en medio acuoso sino también en fase vapor.

Cabe destacar la elevada selectividad de las tres aminas hacia al TNT, ya que no se produjo cambio en la coloración por formación del complejo de Meisenheimer frente a otros compuestos nitroaromáticos como el 2,4-dinitrotolueno y el 4-nitrotolueno. En la Figura 2.6 se muestran los monómeros y polímeros utilizados como materiales sensores, así como los complejos de Meisenheimer formados en los polímeros.

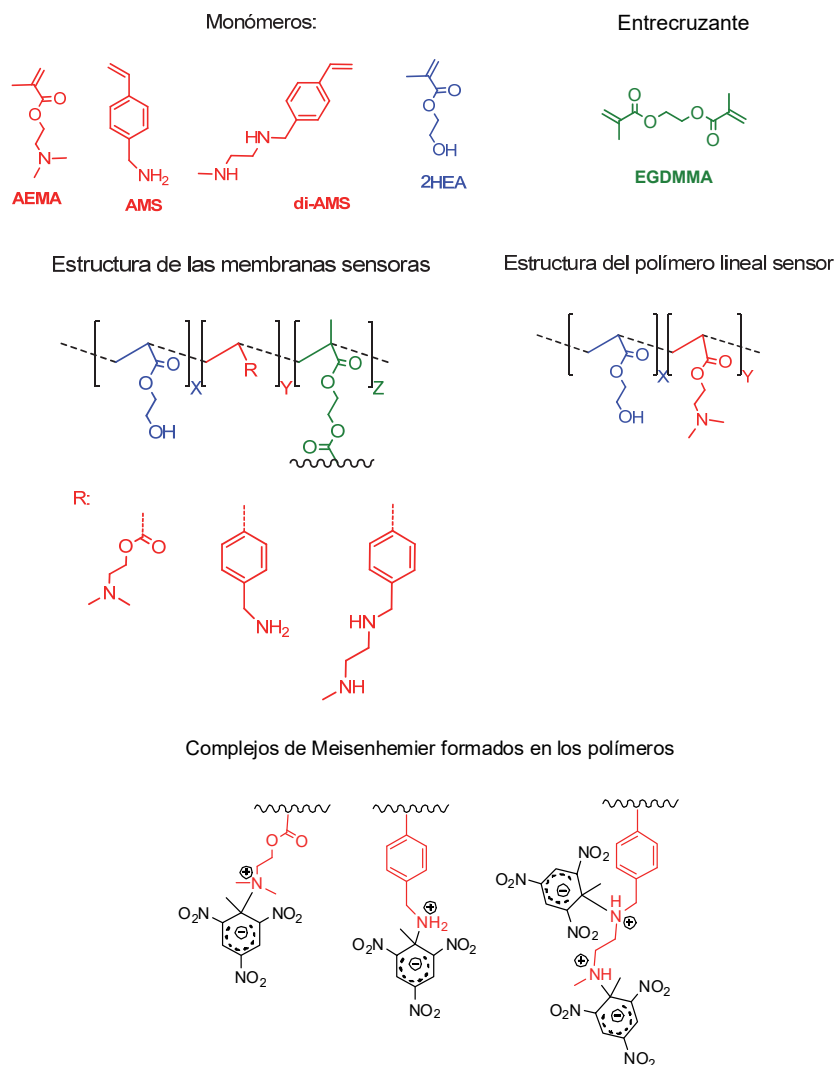


Figura 2.6. Estructura de los monómeros y los polímeros sensores de TNT, así como de los complejos de Meisenheimer que se forman por interacción de los monómeros sensores con el TNT.

En los trabajos se compara la capacidad sensora de los monómeros y los materiales (polímero lineal, membrana densa y tejido inteligente) hacia el TNT en distintas condiciones, construyendo curvas de calibrado mediante espectroscopia de UV/vis y utilizando los parámetros de definición de color

RGB de una imagen digital obtenida con un teléfono inteligente. La formación de los complejos de Meisenheimer se confirmó por resonancia magnética de protón de los monómeros en presencia de TNT.

2.4.3. Aplicaciones

El TNT es explosivo y tóxico por lo que su detección y cuantificación en medios acuosos presenta un gran interés, tanto en aplicaciones técnicas, como ambientales. Así, por ejemplo, la detección de la presencia de TNT en suelos, tejidos y superficies contaminados de forma rápida y barata es de gran importancia en el ámbito de la salud y del medioambiente, así como dentro del campo de la seguridad civil y del técnico forense para el análisis de zonas afectadas por actos terroristas.

2.4.4. Resultados

A continuación se describen los resultados obtenidos a través de la transcripción íntegra de los trabajos publicados.

- ❖ *Water soluble polymers, solid polymer membranes, and coated fibres as smart sensory materials for the naked eye detection and quantification of TNT in aqueous media*
- ❖ *Solid polymer substrates and smart fibres for the selective visual detection of TNT both in vapour and in aqueous media*

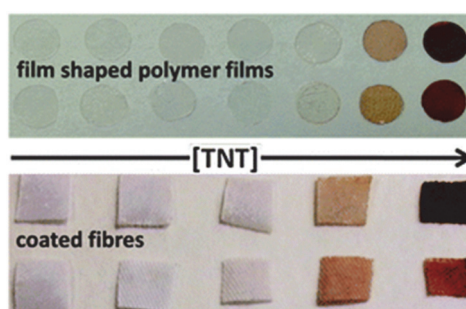
Los detalles experimentales y de caracterización de los trabajos se encuentran en el material suplementario cuya copia está disponible en el CD adjunto.

Water soluble polymers, solid polymer membranes, and coated fibres as smart sensory materials for the naked eye detection and quantification of TNT in aqueous media

Water soluble polymers, solid polymer membranes, and coated fibres as smart sensory materials for the naked eye detection and quantification of TNT in aqueous media

Jesús L. Pablos, Miriam Trigo-López, Felipe Serna, Félix C. García, José M. García*

Departamento de Química, Facultad de Ciencias, Universidad de Burgos. Plaza de Misael Bañuelos s/n, E-09001 Burgos, Spain



This study developed sensory polymeric materials for the colorimetric sensing of TNT in aqueous media. Solid films and coated fabrics permitted the detection of TNT, through colour change, and its quantification, by taking a picture of the materials and processing their RGB parameters to define the evolved colour.

Introduction

The detection of explosives by non-specialised personnel using rapid, cheap techniques is a challenging issue that has arisen from societal concern about their widespread use in mining industries, military endeavours, and

terrorist attacks. The detection and quantification of explosives is twofold, through vapour detection and in solution. The former is related to homeland security and humanitarian efforts such as demining, for instance, and the latter with forensic and criminal investigations and environmental control and remediation. Among the broad set of explosives, 2,4,6-trinitrotoluene (TNT) is one of the most widely used in civil and military applications, and its detection in solution in groundwater or extraction from soil is necessary for the control and remediation of abandoned military sites, industrial waste, and spills by explosive-related industries because nitroaromatics are blood and liver toxins that can be absorbed by the skin or gastrointestinal tract.¹ In the same way, TNT's detection in solutions of washed scrap-metals and residues are essential in terrorist strike investigations. With these needs in mind, we undertook the preparation of water-soluble polymers, solid sensory polymer membranes with gel behaviour, and smart fibres made from polymer-coated yarns as colorimetric chemosensing materials for the naked eye detection and quantification of TNT in aqueous solutions.²⁻⁶ Furthermore, the colour changes arising from the interaction of the sensory materials with solutions containing TNT were analysed using the colour definition (RGB parameters; R = red; G = green; B = blue) of digital photographs of the materials permitting the quantification of the explosive.

The well-known formation of highly coloured complexes of the electron-deficient aromatic ring of TNT with Lewis bases, such as amines, alkoxy, and hydroxyl groups, under mild conditions, also called the Meisenheimer complexes,⁷⁻¹¹ has been exploited for the detection of nitroaromatics using colour changes through UV/Vis spectroscopy. Following this approach, we engaged in the preparation of colorimetric chemosensory polymeric materials using a costless commercial acrylic monomer, 2-(dimethylamino)ethyl methacrylate (**DMAEMA**), which contains an amine group as a colorimetric sensory moiety for TNT. This was a different methodology than that usually followed to achieve sensitivity and

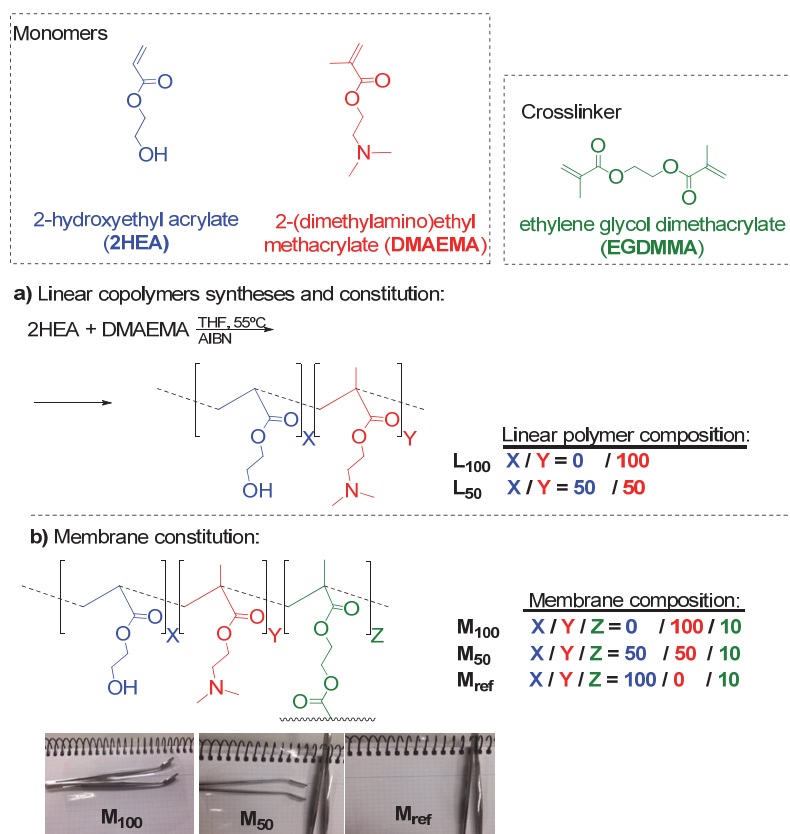
the selectivity challenges encountered in explosive sensing, which is usually carried out using conjugative polymers and is typically based on fluorescence quenching,¹²⁻¹⁵ and not in colour variations. Both the thermally initiated radical homopolymerisation of **DMAEMA** and copolymerisation of **DMAEMA** with the hydrophilic co-monomer 2-hydroxyethyl acrylate (**2HEA**) rendered water soluble linear polymers, **L₁₀₀** and **L₅₀**, respectively (Scheme 1), whose colourless solution in water containing organic solvents developed red colours in the presence of TNT. The addition of a crosslinker to **DMAEMA** or to a mixture of **DMAEMA/DMAEMA** permitted the preparation of film shaped solid membranes with thicknesses of 110 μm , both lipophilic and hydrophilic and with gel and organogel behaviour, named **M₁₀₀** and **M₅₀**, respectively (Scheme 1). The membranes were colourless and transparent and were cut with an office puncher into easily handled sensory discs with diameters of 5 mm. The immersion of the sensory discs in solutions containing TNT turned them reddish in minutes. Moreover, the coating of white cotton fibres and yarns allowed for the preparation of intelligent garment pieces that turned reddish upon coming into contact with organic/aqueous solutions containing TNT. Apart from the visual detection of TNT and its quantification by the UV/Vis technique, the solid materials also permitted its quantification using the colour definition, or the RGB parameters, of a digital picture taken with a conventional camera or smartphone, avoiding the use of time-consuming techniques requiring operation by skilled, specialised personnel.¹⁶⁻¹⁸ A reference membrane **M_{ref}**, without sensory amine motifs, was also prepared for comparative and control purposes (Scheme 1).

The polymers were characterised as materials prior to testing their sensory performance. Thermal resistance is a key parameter of materials for final applications and was evaluated for the membranes using thermogravimetric analysis (TGA) (Table S1 and Figure S1). The decomposition temperatures of membranes that resulted in 5% loss under a nitrogen

atmosphere (T_s) were approximately 250 °C, indicating that the materials had a reasonably good thermal stability for sensing applications. The chemical constitution of the M_{ref} , as derived by FTIR spectra (Figure S2), corresponded to the proposed structure ($\nu_{OH} = 3033\text{-}3696\text{ cm}^{-1}$, broad signal; $\nu_{C=O} = 1721\text{ cm}^{-1}$), and its spectral pattern resembled the structure of the well-known poly(2-hydroxyethyl methacrylate).¹⁹ No significant changes were observed between M_{ref} and M_{50} ; in M_{100} , the absence of the hydroxyl group was in accordance with the absence of ν_{OH} approximately 3400 cm^{-1} . The solvent-swelling percentage (SSP) or solvent uptake, i.e., the hydrophilicity and lipophilicity, is a strategic parameter in the design of solid sensory materials because the target molecules enter the membrane, which is where the sensing event takes place, by diffusion into the solvent-rich membrane gel or organogel phase. The SSPs of the membranes in water were 61% and 54%, and in acetone they were 41% and 38% for M_{100} and M_{50} , respectively. It has been proven that a SSP higher than 40% and lower than 100% is appropriate for both the rapid diffusion of chemicals into the membrane and maintaining the tractability, in terms of mechanical properties, of the water-swelled materials. Furthermore, these data showed that the constitution of the material provided it with an amphiphilic character useful for detection in both organic and aqueous environments. In relation to the linear polymers L_{100} and L_{50} , the characterisation data were in full agreement with those of the membranes (Figures S3-S5 and Table S2). The NMR data confirmed the structure and composition of the copolymer L_{50} in relation to the comonomer feed molar ratio.

After characterisation, the material's performance as a chemosensors was evaluated. It is known that the interaction of an amine with TNT leads to the development of a reddish colour, as was the case with the sensing acrylic monomer **DMAEMA**. However, the sensing was highly specific and no colour change was observed upon the addition of other nitroaromatic compounds, such as 2,4-dinitrotoluene (2,4-DNT) and 4-nitrotoluene (4-NT) (Figure S6). This interaction is based on the Meisenheimer-like complexes, which are species in

equilibrium, including charged species, and the partial transfer of electronic charge from an amine group, behaving as a Lewis base, to the aromatic nucleus of the nitro-compounds.^{8,20} Figure S7 reveals a gradual shift in the proton resonances for the methyl groups of tertiary amine and the methylene group (N-CH₂-) to a lower field, along with the downfield shift of the TNT's aromatic proton resonance, confirming the interaction of **DMAEMA** with the TNT.^{21,22}



Scheme 1. Sensory material preparation and codes: a) linear copolymer and b) membranes, with pictures showing the materials' colourlessness and transparency.

Forensic and environmental samples prepared upon extraction with organic solvents usually contain water, and consequently, the ideal testing

media in lab proof-of-concept sensory systems for this purpose are organic solvents enriched with water. However, the Meisenheimer complex formation is described to be strongly affected by the presence of water,^{11,23} so we analysed the behaviour of the monomer in dry acetone and in acetone:water (80:20, v:v), resulting in an enhanced response in the latter (Figure S8). We chose acetone because it is a common solvent for extraction and forensic applications, it is cheap, samples can be rapidly concentrated at low temperature, it does not present important environmental concerns, and it gave satisfactory TNT titration curves (Figure S9) using the UV/Vis technique, with a limit of detection (LOD) and limit of quantification (LOQ) of 5.7×10^{-5} M and 1.7×10^{-4} M, respectively.²⁴

In a similar fashion, stock water solutions of **L**₁₀₀ and **L**₅₀ were used to prepare sensory acetone:water (80:20, v:v) solutions with a sensory dimethylamino motif concentration of 1.2 mEq/L. The UV/Vis titration curves (Figures S10 and S11) allowed for the detection of TNT with a LOD/LOQ of $4.2 \times 10^{-5}/1.3 \times 10^{-4}$ M and $9.0 \times 10^{-5}/2.7 \times 10^{-4}$ M for **L**₅₀ and **L**₁₀₀, respectively. These limits were reasonably good for the detection of TNT in solutions according to previously reported data.^{11,25} Moreover, the aqueous solutions of **L**₁₀₀ and **L**₅₀ were an environmental friendly tool for preparing sprays with which to detect *in situ* the presence of TNT in surfaces, as demonstrated in the detection of cotton fibres that had been in contact with TNT (shown in the video provided as ESI).

The solid sensory kits were manufactured from the **M**₁₀₀ and **M**₅₀ using a conventional office sheet paper punch to cut out discs 5 mm in diameter. Colour changes were visible to the naked eye after immersing the discs in an acetone:water (80:20, v/v) solution of TNT for 2-3 minutes, indicating the efficient formation of Meisenheimer complexes. Moreover, the rapid visual detection of TNT was highly selective, with the materials remaining silent with other nitroaromatic compounds, such as 2,4-DNT and 4-NT (Figure S12) following the same behaviour that exhibited the sensory monomer **DMAEMA** in solution. To determine the response time of the two sensory membranes,

sensory discs of **M**₁₀₀ and **M**₅₀ were immersed in a quartz cuvette containing a solution of TNT (1×10^{-2} M) in an acetone:water solution (80:20, v:v), and the spectra were recorded periodically every 45 s (Figure S13). A detection time of 25-30 min was adequate, and the optimal time for the sensing experiments was considered to be 1 h when accounting for the instability of Meisenheimer complexes under ambient conditions and the decomposition of TNT in solution.¹⁰ A naked eye titration of the TNT acetone:water (80:20, v/v) solution was carried out by dipping the colourless discs into the solution for 1 h and observing the colour development (Figure 1). A visual colour change was observed at a TNT concentration of 1×10^{-3} M. After photographing the discs, the three RGB parameters of each disc were processed using principal component analysis (PCA), extracting one principal component (PC1), which gave an account of > 96% of the information on the three RGB parameters, thus permitting the simple elaboration of 2D titration curves ([TNT] vs. CP1) with a concomitant noise reduction (the principal component parameters are shown in Table S3-S13). The procedure is shown in a cartoon in Figure S14 and described in depth in recent publications by our Research Group.^{26,27} The LOD/LOQ were $1.1 \times 10^{-4}/3.5 \times 10^{-4}$ M for the sensory material **M**₁₀₀ and $1.4 \times 10^{-4}/4.3 \times 10^{-4}$ M for **M**₅₀. In light of previously reported data, these were concluded to be extremely sensitive sensory materials for the detection of TNT. This conclusion was especially true considering that the quantification was carried out with costless materials, in situ, and using the hardware and software of a smartphone/laptop.

We extended our study to the preparation of smart fibres for the colorimetric detection of TNT, as an attractive class of substrate for fabricating wearable chemical polymeric sensors. Fibres from white cotton fabric were coated with the sensory polymer prepared from **DMAEMA** and **EGDMA**. 1x1 cm cotton fabrics were coated with 61, 47, 27, 12 and 6%, by weight, of the sensory polymer to render smart fabrics with references **F**₆₁, **F**₄₇, **F**₂₇, **F**₁₂, and **F**₆, respectively (see picture in Figure S15). Following the procedure described

for the sensory disc, the fabrics were immersed in acetone:water (80:20, v/v) containing concentrations of TNT ranging from 1×10^{-5} to 5×10^{-2} M. The colour changes were observed in minutes and could be visually related with the TNT concentration and the fabric's sensory polymer content (Figure 2). Similarly, the TNT concentration could be quantified with the colour definition of each fabric taken from a digital picture, giving rise, for instance, to LOD values of 1.1×10^{-3} , 2.4×10^{-3} and 1.8×10^{-3} M for the coated fabrics **F₄₇**, **F₁₂**, and **F₆**, respectively. The picture shown in Figure 2 was taken after immersing the coated fabrics in the media containing TNT for only two minutes, an impressive response time. This time was shorter than that corresponding to the sensory membranes, most likely because of the coated fibres' high sensory surface and the time needed for the diffusion of TNT into the sensory membranes, which was highly diminished when reducing the cross section of the sensory material from one hundred of microns to a thin coating. The coating increased the rigidity of the cotton fabric, with a concomitant loss of garment comfort, though this increase was not apparent to the touch with the lower polymer containing fabrics, **F₁₂** and **F₆**, from which full garments could be prepared. On the other hand, all of the coated fabrics could be used to sew small TNT sensory labels into conventional garments.

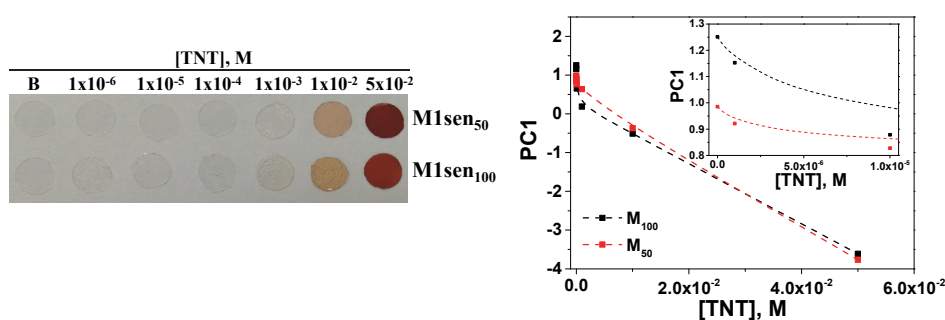


Figure 1. Titration of TNT using the RGB parameters from digital photographs of the sensory discs. These pictures of the sensory films, **M₁₀₀** and **M₅₀**, were taken after immersing the discs in acetone:water (80:20, v/v) for 1 h, and the reduction of the three parameters (R, G, B) to one principal component (PC1) was achieved via principal component analysis. The pictures of the discs depict the colour variations caused by differences in the TNT concentrations.

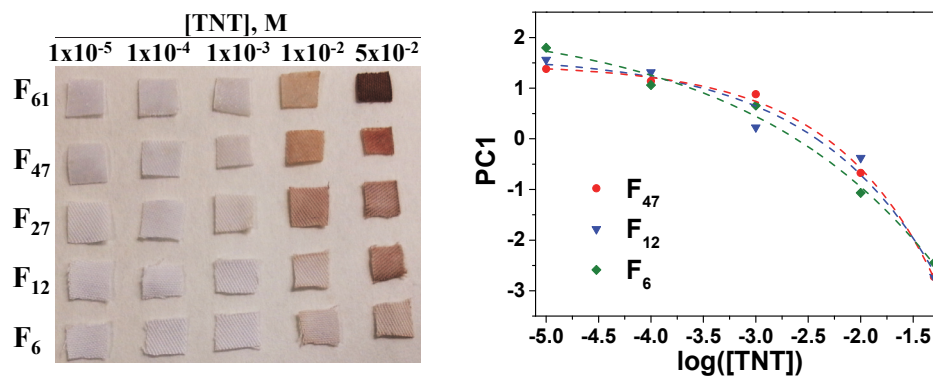


Figure 2. Digital picture taken from squares of lab coat fabric dipped for 2 minutes in TNT solutions of concentrations ranging from 1×10^{-5} M to 5×10^{-2} M, using acetone as a solvent (left), and titration curve using the single principal component (PC1) obtained from the three digital colour parameters via principal component analysis.

In summary, we prepared sensory polymeric materials, both as linear soluble polymers and solid-film shaped networks, and coated fabrics that permitted the colorimetric detection of TNT in solution. Upon putting the sensors into contact with solutions containing TNT, colour development was observed in minutes. Pictures of the sensory films and coated fabrics permitted the explosive's quantification by processing the RGB parameters that defined the digital colours, with limits of detection between the micro and millimolar ranges. Applications in the forensic and environmental remediation fields can be envisaged from these results.

The authors gratefully acknowledge the financial support provided by the Spanish Ministerio de Economía y Competitividad-Feder (MAT2011-22544) and by the Consejería de Educación - Junta de Castilla y León (BU232U13).

† Electronic Supplementary Information (ESI) available: experimental preparation and characterisation of the materials, complementary details of the colorimetric sensory of TNT with linear polymers and with membranes, principal component analysis procedure and data, and demonstrating video. See DOI: 10.1039/c000000x/

Spanish provisional patent application P201301187 was filed December 2013.

Notes and references

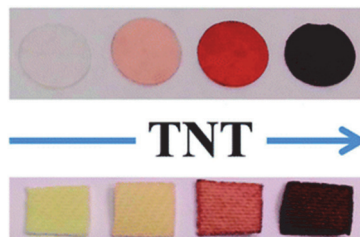
- 1 W.D. McNally, Toxicity, Industrial medicine, Chicago, IL, 1937.
 - 2 Trace chemical sensing of explosives, Ronald L. Woodfin Ed., Wiley-Interscience, Hoboken, 2007.
 - 3 M. E. Germain and M. J. Knapp, *Chem. Soc. Rev.*, 2009, **38**, 2543.
 - 4 Y. Salinas, R. Martínez-Máñez, M. D. Marcos, F. Sancenón, A. M. Costero, M. Parra, S. Gil, *Chem. Soc. Rev.*, 2012, **41**, 1261.
 - 5 S. J. Toal and W. C. Trogler, *J. Mater. Chem.*, 2006, **16**, 2871.
 - 6 M.C. Chuang, J.R. Windmiller, P. Santhosh, G.V. Ramirez, M. Galik, T.Y. Chou, and J. Wang, *Electroanalysis* 21 (2010) 2511-2518.
 - 7 J. Meisenheimer, *Justus Liebigs Ann. Chem.*, 1902, **323**, 205.
 - 8 F. Terrier, *Chem. Rev.*, 1982, **82**, 77.
 - 9 H. Chen, H.W. Chen and G. Cooks, *J. Am. Soc. Mass Spectrom.*, 2004, **15**, 998.
 - 10 Y. Liu, H.H. Wang, J.E. Indacochea and M.L. Wang, *Sens. Actuators B*, 2011, **160**, 1149.
 - 11 E. Ercag, A. Uzer and R. Apak, *Talanta*, 2009, **78**, 772.
 - 12 S. Rochat and T. M. Swager, *ACS Appl. Mater. Interfaces*, 2013, **5**, 4488.
 - 13 A. Alvarez, A. Salinas-Castillo, J. M. Costa-Fernández, R. Pereiro and A. Sanz-Medel, *Trac-Trend. Anal. Chem.*, 2011, **9**, 1513.
 - 14 S. W. Thomas, G. D. Joly and T. M. Swager, *Chem. Rev.*, 2007, **107**, 1339.
 - 15 J. M. García, F. C. García, F. Serna, and J. L. de la Peña, *Polym. Rev.*, 2011, **51**, 341.
 - 16 K. L. Diehl and E. V. Anslyn, *Chem. Soc. Rev.*, 2013, DOI: 10.1039/C3CS60136F.
 - 17 D. S. Moore, *Rev. Sci. Instrum.*, 2004, **75**, 2499.
 - 18 J. Cho, R. Anandakathir, A. Kumar, J. Kumar and P. U. Kurup, *Sens. Actuators B*, 2011, **160**, 1237.
 - 19 S. N. Dobić, J. M. Filipović and S. L. Tomić, *Chem. Eng. J.*, 2012, **179**, 372.
 - 20 E. Buncel, A. R. Norris and K. E. Russell, *Q. Rev. Chem. Soc.*, 1968, **22**, 123.
 - 21 Y. H. Lee, H. Liu, J.Y. Lee, S. H. Kim, S. K. Kim, J. L. Sessler, Y. Kim and J. S. Kim, *Chem. Eur. J.*, 2010, **16**, 5895.
 - 22 H. Kong, J. Sinha, J. Sun and H. E. Katz, *Adv. Funct. Mater.*, 2013, **23**, 91.
 - 23 T.F. Jenkins, M.E. Walsh, *Talanta*, 1992, **39**, 419.
 - 24 The limit of detection (LOD) and the limit of quantification (LOQ) were calculated from the titration curves using the following equation: $LOD=3.3 \times SD/s$ and $LOQ=10 \times SD/s$, where SD is the standard deviation of blank sample and s is the slope of the calibration curve in the region of low analyte content (below 1×10^{-5} M, 1×10^{-4} M and 1×10^{-3} M for linear polymers, membranes and coated fibres, respectively), respectively.
 - 25 G.A. Buttigieg, A.K. Knight, S. Denson, C. Pommier, M.B. Denton, *Forensic Sci. Int.* 135 (2003) 53–59.
 - 26 H. El Kaoutit, P. Estevez, F. C. García, F. Serna and J. M. García, *Anal. Methods*, 2013, **5**, 54.
 - 27 S. Vallejos, A. Muñoz, S. Ibeas, F. Serna, F. C. García and J. M. García, *J. Mater. Chem. A*, 2013, DOI: 10.1039/C3TA12703F.
-

Solid polymer substrates and smart fibres for the selective visual detection of TNT both in vapour and in aqueous media

Solid polymer substrates and smart fibres for the selective visual detection of TNT both in vapour and in aqueous media

Jesús L. Pablos,* Miriam Trigo-López, Felipe Serna, Félix C. García, José M. García*

Departamento de Química, Facultad de Ciencias, Universidad de Burgos. Plaza de Misael Banuelos s/n, E-09001 Burgos, Spain



This work describes the design of efficient, inexpensive and easily prepared selective sensory polymers with chemically anchored amine groups as 2,4,6-trinitrotoluene (TNT)-sensing motifs as materials for the selective visual detection of TNT in aqueous media and as vapours. The materials are prepared as handleable sensory films or dense membranes from which sensory discs are cut, as well as smart fibres by coating conventional and commercial cotton fabrics. Both types of materials exhibited a highly visible colour development from colourless to red upon contact with TNT both in the gas phase and in solution, and the colour change was used to build titration curves using the colour definition parameters of a digital image acquired with a smartphone, i.e., the RGB system. The materials were selective, remaining silent with other nitroaromatic compounds, such as 4-nitrotoluene and 2,4-dinitrotoluene, and the detection limit in solution was close to the micromolar range.

Introduction

The societal concern about the detection of explosives, related to homeland security, stems mainly from the fear of terrorist attacks. However, their detection and quantification are challenging for forensic and criminal investigations after terrorist acts, for reducing the fatalities that occur during humanitarian efforts in demining, and for health and environmental control and remediation of water and contaminated soils in old military areas and in industrial wastes and spills by explosive-related industries.

Among the various explosives, TNT (2,4,6-trinitrotoluene) belongs to the nitroaromatic explosive family and is one of the most widely used explosives in civil and military applications as well as by terrorists worldwide. As a chemical, TNT can easily enter groundwater supplies and is considered toxic at concentrations above 2 ppb, presenting harmful effects to all biota.¹ For humans, it is a liver toxin that can be absorbed by the gastrointestinal track or even by the skin.² Accordingly, the detection and quantification of TNT is of the utmost importance and can be performed using a broad set of analytical techniques, such as high performance liquid chromatography (HPLC) and high-resolution gas chromatography (HRGC) paired with different detectors, including mass spectrometry (MS), electrochemical detection (ED), electron capture detectors (ECD), and ultraviolet detectors (UV).¹ However, the use of recognition processes in supramolecular chemistry and novel selective and sensitive optical probes have arisen as promising techniques for the detection of explosives by non-specialised personnel in an in situ, rapid and inexpensive manner, both for vapour and in-solution detection; the sensitivity is usually achieved using a quenching strategy based on the use of conjugated polymers or supported solids.³⁻¹⁴

In a recent paper, we demonstrated an insanely simple, novel, and straightforward methodology to prepare handleable solid materials for the naked eye detection of TNT in water environments.¹⁵ Using a commercial

monomer containing a tertiary amine, 2-(dimethylamino)ethyl methacrylate (**AEMA**), we prepared the most inexpensive sensory film that changed its colour upon dipping in aqueous media containing a low concentration of TNT. The sensing mechanisms corresponded to the formation, under mild conditions, of colour complexes of Lewis bases, such as the mentioned amine-containing monomer, with electron-deficient aromatic rings, such as TNT, known since the first decade of the former century as Meisenheimer complexes.¹⁶⁻²⁰

The tuning of the amine motif chemical characteristics of sensory monomers permits not only the lowering of the detection limits in aqueous solutions but also the achievement of TNT vapour detection, an especially cumbersome task due to the extremely low vapour pressure of TNT (9.2 ppb_v).²¹ Thus, the use of both commercial and designed sensory monomers with primary and secondary amines, more active towards the formation of Meisenheimer complexes than tertiary amines, would most likely allow for the two-fold detection and quantification of explosives, i.e., as vapours and in solution. From an applied viewpoint, the former is related to homeland security and humanitarian efforts, and the latter is related to forensic and criminal investigations of washed scrap-metals and residues essential in terrorist-strike investigations and environmental control and remediation.

Thus, we have prepared two film-shaped solid sensory membranes: the first one using the commercial monomer 4-{N-(2-(methylamino)-ethyl)aminomethyl}styrene (**di-AMS**) with two secondary amine groups and the second one using the monomer with 4-(aminomethyl)styrene (**AMS**), which have a primary amine that was designed and synthesised by us. The objective was to achieve handleable and tractable materials with the highest sensitivity in the colourimetric detection of TNT. Thus, the materials were cut into manageable sensory discs, and the visual detection of TNT was achieved in situ based on clearly visible colour changes of these discs; its quantification was performed using the UV/Vis technique. Moreover, the

solid sensory materials also allowed for the direct quantification of the TNT concentration within minutes by processing a digital image taken of these discs using a conventional camera or smartphone using the colour definition, i.e., the RGB parameters, thus avoiding the use of time-consuming techniques operated by skilled and specialised personnel.^{1,22-24} Furthermore, cotton fibres were coated with the sensory polymers to render wearable TNT sensory intelligent fabrics.

Results and discussion

Strategy followed for the design of the sensory materials

The drive to success in the design of smart materials relies, in our opinion, on the simple idea of selecting a previously described organic, inorganic, or hybrid molecule with a well-known and highly interesting characteristic, functionalising the molecule with the simplest polymerisable chemical group and exploiting the molecule in any environment by copolymerising it with comonomers that provide the new material with optimal properties, e.g., mechanical and thermal resistance, hydrophilicity or hydrophobicity, or even amphiphilic character.

Using this philosophy, numerous chemosensors have been previously described in the literature, most of which are water insoluble organic molecules that work only in organic media. Thus, our objective was to select a well-known chromogenic organic chemosensor, slightly modify its structure by introducing a polymerisable chemical group, and copolymerise it to yield amphiphilic materials that have sufficient hydrophilicity and lipophilicity to be swelled both in water and in organic solvents to allow the target species dissolved in these media to access, by diffusion, the sensory motifs all along the material. In addition, good lipophilicity usually permits the absorption of gases and vapours, thus permitting their detection.

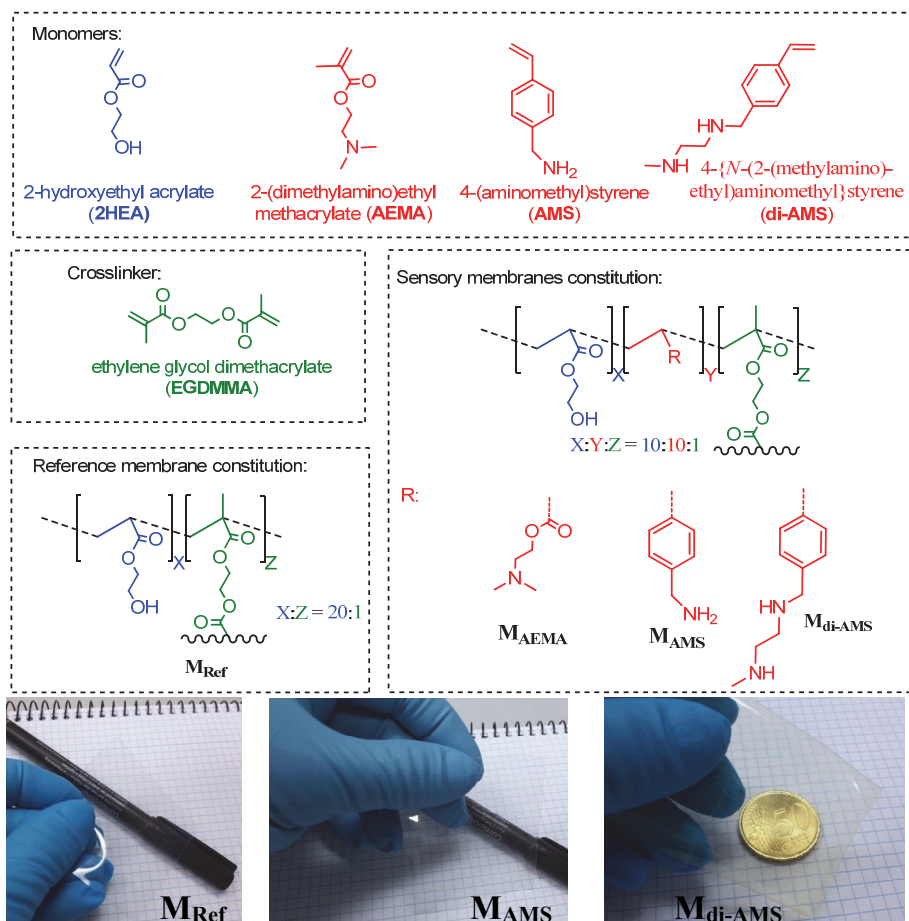
Selecting the colourimetric chemosensory motif for preparing the sensory materials for detecting TNT

As noted in the introduction, Lewis bases, such as amines, alkoxy, and hydroxyl groups form highly coloured Meisenheimer complexes with TNT.¹⁶⁻²⁰ Thus, in a previous paper, we chose a commercial monomer to prepare a chromogenic sensory material for this explosive (**AEMA**, Scheme 1).¹⁵ This selection was the obvious first choice because the monomer is available commercially and is reasonably priced, and the sensory material was very inexpensive. However, the monomer had a tertiary amine that was the sensory motif. It is known that in water the bulkiness of the three alkyl groups usually affects negatively the Lewis base character of the amine group. On the other hand, stronger Meisenheimer complex are expected upon increasing the base character of the amines and, concomitantly, greater colour development and sensitivity of the sensory systems. Thus, in a further step, we have prepared sensory materials with secondary and primary amine groups as sensory motifs, and, as expected, the sensitivity towards TNT has been increased without a penalty in selectivity. Moreover, the colourimetric sensory behaviour of the materials has been extended to TNT vapours, whereas the material derived from AEMA, i.e., MAEMA, was insensitive to these vapours.

Preparation and characterisation of the sensory materials

With simplicity in mind and considering our previous work,¹⁵ the planning of naked eye-sensitive sensory materials towards TNT, both in solution and in the vapour phase, involved the design of monomers with secondary and primary amines, as previously mentioned. Accordingly, we found a styrenic commercial monomer with two secondary amines, **di-AMS** (Scheme 1). Furthermore, using this monomer as a reference, we prepared the simplest styrenic monomer with primary amine groups, **AMS**. Its synthesis was straightforward and performed in two high-yield conventional synthetic

steps, with an overall yield of 84%, starting from the widely used and inexpensive 4-(chloromethyl)styrene (Scheme S1 and Section S1, ESI). A nucleophilic substitution with sodium azide followed by its reduction produced **AMS**, a monomer that was easily purified by vacuum distillation without adding stabilisers to inhibit premature polymerisation.



Scheme 1. Constitution of the sensory film-shaped dense membranes **MAMS** and **M_{di-AMS}** prepared upon the bulk radical copolymerisation of **2HEA** and of the sensory monomers **AMS** or **di-AMS**, using ethylene glycol dimethacrylate (**EGDMMA**) as the cross-linking agent. The structures of the reference membrane (**M_{Ref}**), without sensory moieties and of the membrane with tertiary amines as sensory motifs (**M_{AEMA}**) are also shown.¹⁵ The image of the membranes over a notebook demonstrates the aspect and transparency of the materials.

The constitution of all of the membranes, as derived by FTIR spectra, corresponds to the proposed structure (ν_{OH} , ν_{NH_2} , or $\nu_{\text{NH}} = 3030\text{-}3700\text{ cm}^{-1}$, broad signal; $\nu_{\text{C=O}} \sim 1722\text{ cm}^{-1}$), and its spectral pattern resembles the structure of the well-known poly(2-hydroxyethyl methacrylate).²⁵ The spectra of both **M_{AMS}** and **M_{di-AMS}** show the characteristic bending of the primary and secondary amine groups as two or one medium to weak intensity bands in the range of 700-850 cm^{-1} and weak bands in the region of 1590-1650 cm^{-1} (Figure S3, ESI).

Table 1. Thermogravimetric (TGA) analysis (nitrogen atmosphere) and solvent swelling percentage (SSP) data.

Membrane	T_5 (°C)	T_{10} (°C)	T_{ONSET} (°C)	Char yield (%)	SSP (%)	
					water	acetone
M_{Ref}	315	349	286	2	56	40
M_{di-AMS}	171	191	142	14	40	68
M_{AMS}	180	209	165	14	43	53

Thermal resistance is a key parameter of materials for final applications and was evaluated following the weight loss that occurred during the heating of the material at a constant rate (thermogravimetric analysis, TGA). The decomposition temperatures that resulted in a 5% loss under a nitrogen atmosphere (T_5) were approximately 180 °C, indicating that the materials have a reasonably good thermal stability (Table 1). However, the higher bond energy of the C-O compared with the C-N linkage can be clearly observed in the diminishment of the T_5 at approximately 140 °C of **M_{AMS}** and **M_{di-AMS}** compared with **M_{Ref}**. This negative result is counteracted by the relevant increase of the char yield at 800 °C of **M_{AMS}** and **M_{di-AMS}** compared with **M_{Ref}** due to the partial aromatic structure of the former. The TGA curves are presented in Figure S4, ESI.

The amphiphilic character of the materials was related to the water- and acetone-swelling percentage (SSP); that is, the amphiphilic character

was related to the weight percentage of solvent uptake by the films upon soaking until equilibrium in pure solvent at 20 °C. This character is key because the membranes must be hydrophilic materials to regain enough water in aqueous media to allow for the chemicals dissolved in water to enter the membrane by diffusion to reach the sensory motifs and to yield the macroscopic signal, indicating the presence of the target molecules. In addition, the lipophilicity of the sensory materials must be sufficient to be solvent-swelled with the same purpose. In our previous experiments, we observed that a SSP between 40% and 100% is optimal for both the rapid diffusion of chemicals into the membrane and for maintaining the tractability, in terms of mechanical properties, of the solvent-swelled materials. All of the sensory membranes meet this criterion, as demonstrated in Table 1. The data clearly indicate a decrement of the hydrophilicity of **M_{di-AMS}** and **M_{AMS}** with a parallel increase of the lipophilicity compared with the reference membrane **M_{Ref}**, with this fact being attributed to the hydrophobic nature of the aromatic ring of the former membranes compared with the latter.

Depicting the interaction of TNT with amines, the sensing phenomenon

It is well established that aromatic nitro-compounds undergo the formation of intensely coloured products with Lewis bases, termed Meisenheimer complexes,¹⁶⁻²⁰ as clearly summarised by Buncel et al., with the complex mechanism concerning the interaction also discussed.²⁶

In our work, the ability of the monomers **AMS** and **di-AMS** to sense TNT in solution was tested before the sensory material preparation. Thus, solutions of the monomers in acetone:water (80:20, v:v) immediately turned reddish after adding TNT, as observed in Figure 1. This aqueous system was selected because of two important application fields related to the use of acetone, with water always present, i.e., the detection of TNT in soils for remediation purposes and for the detection of the explosive used by

washing the scrap with acetone after a terrorist attack scenario. The measuring media is important because the water affects the Meisenheimer complex formation by altering the kinetics of these reactions.^{27,28}

The interaction of the monomers **AMS** and **di-AMS** with TNT was confirmed by ¹H NMR. Thus, the addition of TNT to a CDCl₃ solution of the monomers caused the low field shift of the primary and secondary amine protons, demonstrating the participation of these groups in the Meisenheimer complexes (Figures S5 and S6, ESI). This fact is consistent with the ¹H NMR interaction study of TNT with the monomer **AEMA** with a sensory tertiary amine motif in its structure.¹⁵

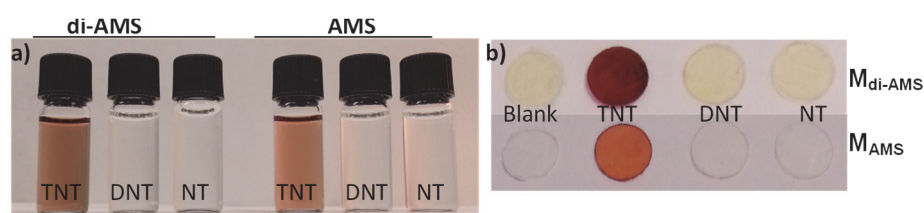


Figure 1. Visual detection of TNT in solution by monomers and sensory membranes: a) images of solutions of **di-AMS** and **AMS** upon addition of TNT, DNT and NT and b) images taken of membranes **M_{di-AMS}** and **M_{AMS}** upon dipping in solutions containing TNT, DNT and NT for 10 min. Conditions: solvent acetone:water (80:20, v:v); the concentration of TNT, DNT and NT was = 1×10^{-2} M; in solution experiments [**di-AMS**] and [**AMS**] = 1.2×10^{-3} M.

The coloured Meisenheimer complexes formed upon interaction in aqueous solution of sensory monomers and TNT in solution permitted the titration of the explosive by UV/Vis, as shown in Figure 2 and Figure S7, ESI. The limit of detection (LOD) and limit of quantification (LOQ)²⁹ of the titration systems were 1×10^{-6} and 3×10^{-6} M, respectively, for the monomers **AMS** and **di-AMS**. Notably, these limits were significantly higher for the monomer with a tertiary amine as the sensory motif, **AEMA** (Table 2), demonstrating the performance increase of the new monomers as sensory probes, as expected.

Sensory membranes for the detection of TNT in solution

Visual preliminary studies with the dense membranes M_{di-AMS} and M_{AMS} revealed an effective colour development upon dipping in solutions containing TNT for only 10 min, thus indicating a rapid and efficient formation of the Meisenheimer complex (Figure 1). However, the reference material, M_{Ref} , produced no colour change, as expected. The colour changes were apparent within the first minute.

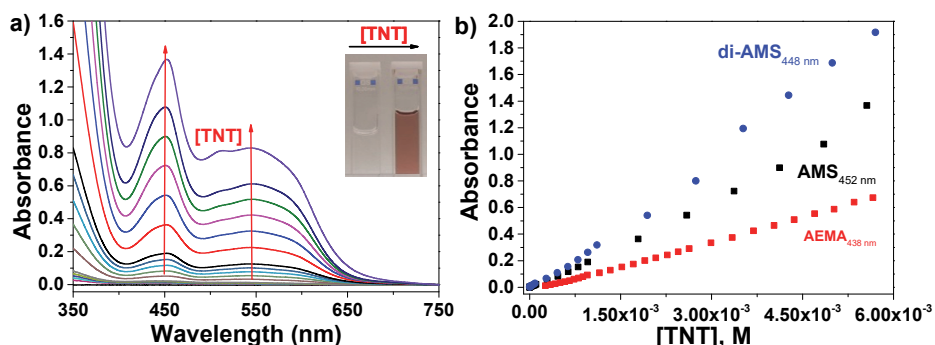


Figure 2. TNT titration by monomers containing amine groups as sensory motifs: a) selected UV/Vis titration curves for monomer **AMS** (inset: image of UV/Vis curves before and after the titration experiments) and b) titration curves for monomers **AMS**, **di-AMS** and **AEMA** (absorbance maxima vs. TNT concentration). Conditions: solvent acetone:water (80:20, v:v); monomer concentration 1.2×10^{-3} M; TNT concentration ranged from 9.9×10^{-8} to 5.5×10^{-3} M.

Table 2. Limit of detection (LOD) and limit of quantification (LOQ) calculated for monomers, membranes and coated fibres.

Monomer	LOD/LOQ $\times 10^6$ M	Membrane	LOD/LOQ $\times 10^5$ M	Coated fibre	LOD/LOQ $\times 10^4$ M
AEMA	19/59	M_{AEMA}	14/43	F_{AEMA}	11/33
di-AMS	1/3	M_{di-AMS}	8/24	F_{di-AMS}	5/16
AMS	1/3	M_{AMS}	9/26	F_{AMS}	4/11

The response time of the materials was evaluated by UV/Vis spectroscopy. Sensory discs of M_{di-AMS} and M_{AMS} were immersed in a quartz

cuvette containing acetone:water (80:20, v:v), and the UV/Vis spectra were recorded. Then, TNT was added to the cuvette from a concentrated stock acetone:water (80:20, v:v) solution, and UV/Vis spectra were recorded as a function of time (Figure S8, ESI). While the absorption maxima due to colour development were noted immediately after the addition of TNT, in our opinion, a better measuring time using the UV/Vis technique would be 20 min because the absorbance maxima is approximately 1. However, for visual and photographic analysis, a dipping time of 1 hour was considered because the colours were more intense and higher sensitivity was envisaged, and longer times were not deemed useful due to the instability of the Meisenheimer complexes under ambient conditions and the decomposition of TNT in solution.

The visual sensing performance of the sensory membranes involved analysing immersed discs of **M_{di}-AMS** and **M_{AMS}** in solutions of various concentrations of TNT for 1 hour, rendering discs of different colour intensities, as depicted in Figure 3. A visible colour change was observed at a TNT concentration of 1×10^{-4} M. After the colour change, digital images of the discs were taken, and the colour definition of each disc was related to the TNT concentration to build the titration curve. As the colour is defined in the RGB system by the three variables red (R), green (G) and blue (B), ranging from 0 to 255, the information regarding these variables were joined in a single result (principal component 1, CP1) using principal components analysis (PCA), accounting for >92% of the information on the three RGB parameters. Using a straightforward mathematical workup, this strategy permits the use of nearly all of the colour information to prepare simple [TNT] vs. CP1 titration curves (the principal component parameters and RGB data are listed in Tables S2–S9, ESI).

The sensitivity was within the millimolar and micromolar range, improving the performance of the previously described sensory membrane **M_{AEMA}** (Table 2). Regarding the selectivity, neither the monomers in solution

nor the sensory membranes changed their colour with other nitro-aromatics besides TNT and especially remained silent with the related NT and DNT, as visually observed in Figure 1.

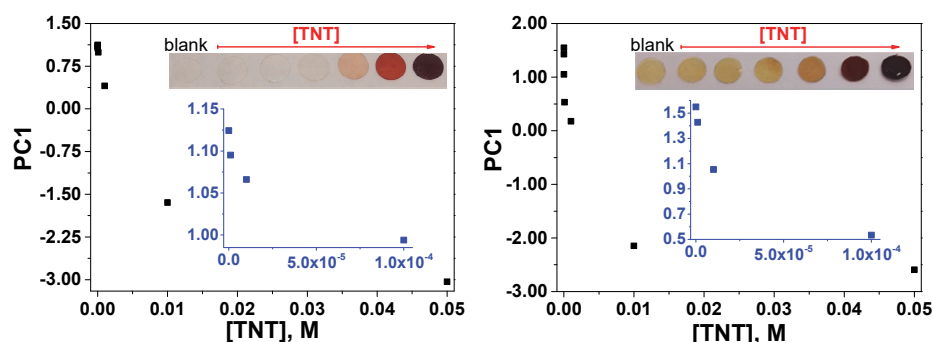


Figure 3. Titration of TNT with sensory discs of membranes **M_{AMS}** (left) and **M_{di-AMS}** (right) using the RGB parameters from digital images taken of the sensory materials. The images were taken after immersing the discs in acetone:water (80:20, v:v) solution for 1 h, and three parameters (R, G and B) defining the colour of each disc were reduced to one principal component (PC1) by principal component analysis. The images of the discs depict the colour variations arising from the differences in the concentration of TNT (Blank, 1×10^{-6} , 1×10^{-5} , 1×10^{-4} , 1×10^{-3} , 1×10^{-2} , 5×10^{-2} M).

Smart fibres for the detection of TNT in solution

Smart or intelligent textiles are stand-alone systems that can be used as sensors, actuators, communication devices, energy sources and storage tools, and even processors and a new generation of textiles made of stimuli-responsive fibres is expected in the near future to contribute significantly to our health and safety.³⁰⁻³²

Within this context, intelligent fabrics capable of detecting TNT represent an attractive class of substrates for fabricating wearable chemical polymeric sensors.³³ Accordingly, we describe herein the coating of cotton fibres of white fabric pieces cut from a lab coat as smart textiles for the colourimetric sensing of TNT. Squares of 1 x 1 cm of the lab coat were coated with sensory polymers prepared from sensing co-monomers **AMS**

and **di-AMS**, fabrics **FAMS** and **Fdi-AMS**, respectively, as well as **2HEA**, **EGDMMA** and a radical photoinitiator. Thus, following the same behaviour as the sensory membrane discs described in the previous section, the smart textiles turned reddish upon interaction with TNT in solution, as observed in Figure 4. Noticeably, the detection time was very short, and the colour change was complete in 5 min, which was significantly less time than that required for the sensory membranes, most likely due to the rapid access of the TNT to the sensory motifs of the thin coating compared with the time needed to diffuse inside the solvent-swelled dense membrane.

Following the same procedure used for the sensory membranes, digital images of the sensory fabric dipped in acetone containing various concentrations of TNT permitted the construction of titration curves (Figure 4) with LOD and LOQ within the micromolar range (Table 2), and this LOD was also clearly visually observed.

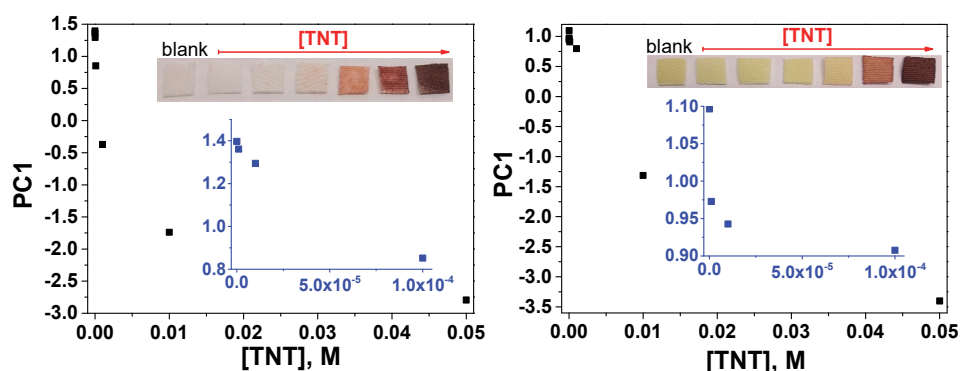


Figure 4. Titration of TNT with cotton coated fibres **FAMS** (left) and **Fdi-AMS** (right) using the RGB parameters from digital images taken of the sensory materials. The images were taken after immersing the lab coat square fabrics in acetone:water (80:20, v:v) solution for 5 min, and three parameters (R, G and B) defining the colour of each square were reduced to one principal component (PC1) using principal component analysis. The images of the squares depict the colour variations arising from the differences in the concentration of TNT (Blank, 1×10^{-6} , 1×10^{-5} , 1×10^{-4} , 1×10^{-3} , 1×10^{-2} , 5×10^{-2} M).

Sensory membranes for the detection of TNT vapours

The detection of nitroexplosive vapours is especially important for many applications related to explosive sensing, for instance in civil security or weapon elimination. However, their detection is cumbersome due to their extremely low vapour pressures, particularly with chromogenic chemical sensing, where a visual signal usually arises from the feeble interaction or from the reaction of the explosive molecules with a receptor.

Thus, a slight colour change is observed at room temperature for the dense membrane M_{di-AMS} and M_{AMS} upon sealing cut sensory discs in small vials containing small quantities of TNT. Noticeably, this behaviour was not observed for the materials with tertiary amines as sensory groups, M_{AEMA} .

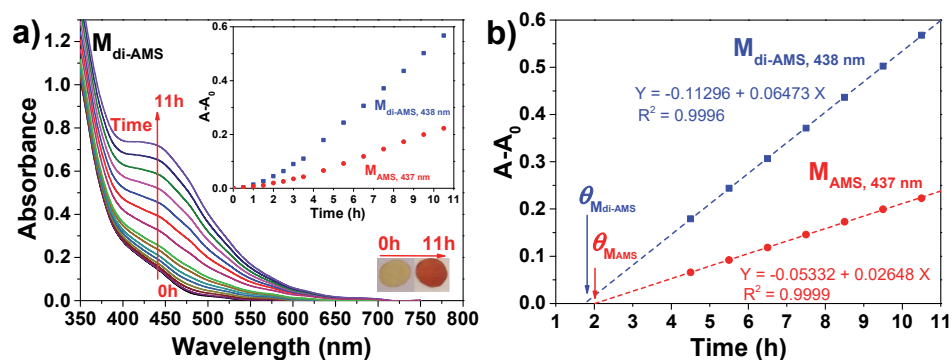


Figure 5. Detection of TNT with sensory membranes M_{AMS} and M_{di-AMS} using a UV/Vis technique as a function of time: a) UV/Vis spectra of membrane M_{di-AMS} in an atmosphere containing TNT vapours (insets: image of the sensory discs and relative absorbance vs. time of membranes M_{AMS} and M_{di-AMS}); b) linear region (steady state) of absorbance increase vs. time of membranes M_{AMS} and M_{di-AMS} , showing the time intercept of the linear regression curve (time lag, θ). Experimental conditions: 50 mg of TNT in a conventional sealed measuring quartz cuvette; temperature: 60 °C.

Based on this observation, the sensory performance of sensory discs cut from M_{di-AMS} and M_{AMS} was analysed. To increase the colourimetric response and to expedite the experimental workup, the experiments were performed at 60 °C, where the vapour pressure of TNT is two orders of

magnitude higher than at 25 °C, i.e., 829 ppb_v according to the equation $\text{Log } P (\text{ppb}_v) = (-5481/T) + 19.37$, where T is the temperature in K.³⁴ The colour development was similar to that observed in the detection of TNT in solution and was clearly observed by the naked eye and followed by UV/Vis spectroscopy, as depicted in Figure 5 and in Figure S9, ESI. As expected, no change was observed for the reference material **M_{Ref}**.

The vapour sensing phenomena occur due to a diffusion/interaction mechanism, i.e., the vapour enters the membrane by diffusion, and in parallel, the interaction to render the Meisenheimer complexes takes place. The behaviour of the system in terms of diffusion clearly resembles that of gas transport through membranes, where the steady state is characterised by a straight line in pressure vs. time curves and is achieved after a time lag (ϕ) calculated at the intersection of the straight line fit corresponding to the straight line region with the abscissa.^{35,36} Thus, the flux of TNT molecules inside the membrane keeps the concentration of TNT in the centre of the membrane near zero because the molecules react with amine groups to yield the coloured complexes. The TNT gradient across the membrane is maintained until all of the amine groups interact with TNT, achieving a steady state at a certain time, and this state is maintained at least throughout the experiment, i.e., 11 h. The time lag is similar for both membranes (Figure 5) and can be related to the diffusion coefficient (D) for Fickian diffusion, with both the solubility coefficient and D independent of concentration, by $D = l^2/6\phi$, where l is the thickness of the membranes in gas transport experiments, where the pressure on one side of the membrane is negligible. In our systems, as the membrane is in a TNT vapour atmosphere, the concentration gradient is from both sides of the membrane to the centre, where the zero concentration of unreacted TNT could be considered, and l would be half of the experimental membrane thickness.³⁵ Thus, ϕ is 1.75 and 2.01 h for **M_{di-AMS}** and **M_{AMS}**, respectively, and D is 8.3×10^{-10} and 8.0×10^{-10} cm²/s. The higher slope of the relative absorbance increase vs. time, visually

observed by a deeper colour development, for **M_{di-AMS}** compared with **M_{AMS}** may arise from the fact that each **di-AMS** monomer has two amine groups, while **AMS** only has one, and the real sensory motif density arising from the same molar feed ratio in each membrane is twice as large in **M_{di-AMS}** compared with **M_{AMS}**. In addition, the lone pair of the secondary amine is more external than that in the primary amine, giving the former a higher nucleophilic character in absence of the hydrogen bonding contribution of a highly solvating solvent as water.

The need to raise the temperature of the experiments to increase the TNT vapour concentration is a clear disadvantage for any practical application, where the explosive must be detected at ambient temperature. However, by working with membranes and smart fabrics that can transport gases by applying a pressure gradient, it is envisaged that a system could be designed to force rt air by pressure or vacuum on one side of the materials to concentrate the explosive vapours inside the membrane or coating, where the molecules would rapidly undergo the Meisenheimer complex formation.

Smart fibres for the detection of TNT vapours

In a similar fashion, the smart fabrics **F_{AMS}** and **F_{di-AMS}** change their colour from white to red upon contact with TNT vapours. The experiments were performed qualitatively at 60 °C, and the slight reddish colour observed in the first two hours of exposure turned deep red in 11 h, as observed in Figure 6.

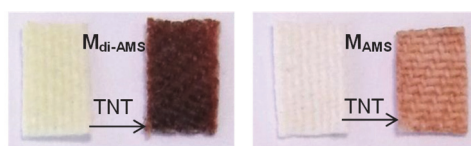


Figure 6. Visual detection of TNT vapours with coated fibres. Conditions: approximately 0.4 x 0.8 cm of each fabric was suspended in a sealed vial with 50 mg of TNT at 60 °C for 11 h.

Conclusions

In this study, we demonstrate the potential of polymers in cutting edge technological applications such as the naked eye detection of explosives following a chemosensory approach. The design of solid sensory polymeric substrates with chemically anchored amine groups as TNT-sensing motifs has been undertaken following a simple, straightforward and inexpensive approach to render usable films or membranes along with coated cotton fibres as smart fabrics for the visual sensitive and selective sensing of TNT both in solution and as a vapour. The visual change of the materials from colourless or white (fibres) to red allowed for the naked eye detection of the explosive, and digital photographs taken of the materials permitted quantification by building titration curves using the colour digital definition, i.e., the RGB parameters, of the materials after being in contact with various concentrations of TNT. Although the detection of TNT vapour is cumbersome, due to its low vapour pressure, we envisage that air forced to permeate through the membranes or fibres could serve as a future system to concentrate the TNT molecules inside of the materials, where the interaction with the sensing motif causes the colour changes, possibly opening the systems to forthcoming security applications.

Acknowledgements

We gratefully acknowledge the financial support provided by the Spanish Ministerio de Economía y Competitividad-Feder (MAT2011-22544) and by the Consejería de Educación-Junta de Castilla y León (BU232U13).

Notes and references

Departamento de Química, Facultad de Ciencias, Universidad de Burgos, Plaza de Misael Bañuelos s/n, 09001 Burgos, Spain. Emails:

jl.pablos@ubu.es (J.L. Pablos), jmiguel@ubu.es (JM García); Tel: +34 947 258 085; Fax: +34 947 258 831.

Electronic Supplementary Information (ESI) available: monomer synthesis and characterisation, sensory membrane preparation and characterisation, fibre coating procedure, measuring conditions, TNT titration data, principal component analysis data. See DOI: 10.1039/b000000x/

NOTES AND REFERENCE

- 1 United States Environmental Protection Agency (EPA), Technical Fact Sheet – 2,4,6-Trinitrotoluene (TNT), May 2012 (http://www.epa.gov/fedfac/pdf/technical_fact_sheet_tnt.pdf). Access data: Feb 27, 2014.
 - 2 W. D. McNally, Toxicology, Industrial medicine Publishing Co.: Chicago, 1937.
 - 3 S. Singh, *J. Hazard. Mater.*, 2007, **144**, 15.
 - 4 S. Rochat and T. M. Swager, *ACS Appl. Mater. Interfaces*, 2013, **5**, 4488.
 - 5 A. Alvarez, A. Salinas-Castillo, J. M. Costa-Fernández, R. Pereiro and A. Sanz-Medel, *Trac-Trend. Anal. Chem.*, 2011, **9**, 1513.
 - 6 S. W. Thomas, G. D. Joly and T. M. Swager, *Chem. Rev.*, 2007, **107**, 1339.
 - 7 J. M. García, F. C. García, F. Serna and J. L. de la Peña, *Polym. Rev.*, 2011, **51**, 341.
 - 8 S. Content, W. C. Trogler and M. J. Sailor, *Chem. Eur. J.*, 2000, **6**, 2205.
 - 9 K. S. Bejoymohandas, T. M. George, S. Bhattacharya, S. Natarajanb and M. L. P. Reddy, *J. Mater. Chem. C*, 2014, **2**, 515.
 - 10 J. L. Novotney and W. R. Dichtel, *ACS Macro Lett.*, 2013, **2**, 423.
 - 11 A. D. Aguilar, E. S. Forzani, M. Leright, F. Tsow, A. Cagan, R. A. Iglesias, L. A. Nagahara, I. Amlani, R. Tsui and N. J. Tao, *ACS Nano Lett.*, 2010, **10**, 380.
 - 12 N. R. Walker, M. J. Linman, M. M. Timmers, S. L. Dean, C. M. Burkett, J. A. Lloyd, J. D. Keelor, B. M. Baughman and P. L. Edmiston, *Anal. Chim. Acta*, 2007, **593**, 82.
 - 13 S. Tao, G. Li and J. Yina, *J. Mater. Chem.*, 2007, **17**, 2730.
 - 14 S. Tao, G. Li and H. Zhub, *J. Mater. Chem.*, 2006, **16**, 4521-4528.
 - 15 J. L. Pablos, M. Trigo-Lopez, F. Serna, F. C. Garcia and J. M. Garcia, *Chem. Commun.*, 2014, **50**, 2484.
 - 16 J. Meisenheimer, *Justus Liebigs Ann. Chem.*, 1902, **323**, 205.
 - 17 F. Terrier, *Chem. Rev.*, 1982, **82**, 77.
 - 18 H. Chen, H.W. Chen and G. Cooks, *J. Am. Soc. Mass Spectrom.*, 2004, **15**, 998.
 - 19 Y. Liu, H.H. Wang, J. E. Indacochea and M. L. Wang, *Sens. Actuators B*, 2011, **160**, 1149.
 - 20 E. Ercag, A. Uzer and R. Apak, *Talanta*, 2009, **78**, 772.
 - 21 R. G. Ewing, M. J. Waltman, D. A. Atkinson, J. W. Grate and P. J. Hotchkiss, *TrAC-Trend. Anal. Chem.*, 2013, **42**, 35.
 - 22 K. L. Diehl and E. V. Anslyn, *Chem. Soc. Rev.*, 2013, **42**, 8596.
 - 23 D. S. Moore, *Rev. Sci. Instrum.*, 2004, **75**, 2499.
 - 24 J. Cho, R. Anandakathir, A. Kumar, J. Kumar and P. U. Kurup, *Sens. Actuators B*, 2011, **160**, 1237.
 - 25 S. N. Dobić, J. M. Filipović and S. L. Tomić, *Chem. Eng. J.*, 2012, **179**, 372.
 - 26 E. Buncel, A.R. Norris and K.E. Rusell, *Q. Rev. Chem. Soc.*, 1968, **22**, 123.
 - 27 E. Ercag, A. Uzer and R. Apak, *Talanta*, 2009, **78**, 772-780.
 - 28 T.F. Jenkins and M.E. Walsh, *Talanta*, 1992, **39**, 419.
-

- 29 The limit of detection (LOD) and the limit of quantification (LOQ) were estimated by the following equation: $LOD = 3.3 \times SD/s$ and $LOQ = 10 \times SD/s$, where SD is the standard deviation of a blank sample and s is the slope of the calibration curve in a region of low TNT content.
 - 30 L. Van Langenhove, C. Hertleer and A. Schwarz, Smart Textiles: An Overview, *in* Intelligent Textiles and Clothing for Ballistic and NBC Protection, NATO Science for Peace and Security Series B: Physics and Biophysics, P. Kiekens and S. Jayaraman (eds.), Springer: Dordrecht, 2012, Ch 6, pp 119-136.
 - 31 P. Westbroek, G. Priniotakis, P. Kiekens, Intelligent/smart materials and textiles: an overview, *in* Analytical electrochemistry in textiles, Woodhead Publishing Limited and CRC Press LLC: Cambridge: 2005, Ch 8, pp 215-243.
 - 32 K. Cherenack and L. van Pieteron, *J. Appl. Phys.*, 2012, **112**, 091301.
 - 33 M.C. Chuang, J.R. Windmiller, P. Santhosh, G. V. Ramrez, M. Galik, T.Y. Chou and J. Wang, *Electroanalysis*, 2010, **21**, 2511.
 - 34 B. C. Dionne, D. P. Rounbehler, E. K. Achter, J. R. Hobbs and D. H. Fine, *J. Energ. Mater.*, 1986, **4**, 447.
 - 35 R. M. Felder, G. S. Huvad, Permeation, diffusion, and sorption of gases and vapors, *in* Polymers, Physical Properties, Methods of Experimental Physics, Vol. 16, Part C, Academic Press: New York, 1980, Ch. 17.
 - 36 S. Matteucci, Y. Yampolskii, B. D. Freeman, and I. Pinnau, Transport of Gases and Vapors in Glassy and Rubbery Polymers, *in* Material Science of Membranes for Gas and Vapor Separation, Y. Yampolskii, B. D. Freeman, and I. Pinnau Eds., Wiley, Chichester: 2006, Ch. 1, pp. 1-47.
-

2.5. Sensores colorimétricos de alta acidez

Las poliamidas aromáticas se caracterizan por sus excelentes propiedades térmicas y mecánicas, mientras que los polímeros acrílicos lo hacen por su versatilidad a la hora de diseñar estructuras con propiedades adecuadas a su aplicación. Aprovechando estas características, se han diseñado materiales de altas prestaciones con estructura de poliamida aromática, así como polímeros hidrofílicos con estructura acrílica, que contienen grupos azobenceno y *N,N*-dimetilamino. Estos grupos se comportan como cromóforos y al mismo tiempo como bases débiles capaces de ser protonadas, lo que ha permitido la preparación de membranas y tejidos inteligentes reutilizables para la detección visual de acidez por debajo de la escala normal de pH, tanto en medios acuosos como no acuosos.

2.5.1. Azoderivados

Un azoderivado, también denominado compuesto azoico o azocompuesto, es un compuesto con el grupo funcional tipo $R-N=N-R'$, donde R y R' suelen ser grupos aromáticos. El $-N=N-$ constituye el grupo azo y es un cromóforo importante debido a la facilidad de excitación por la luz visible.⁸⁵ El derivado más representativo es el que contiene dos grupos fenilo, el azobenceno.

Como consecuencia de la conjugación con los dos anillos aromáticos estos compuestos tienen elevados coeficientes de extinción molar, y son de colores vivos: rojos, naranjas y amarillos. La presencia de distintos grupos en la estructura del compuesto puede provocar que éste absorba a distinta longitud de onda, o que el coeficiente de extinción varíe.

⁸⁵ S. C. Catino, R. E. Farris, *Azo dyes* en "Concise Encyclopedia of Chemical technology", John Wiley and Sons, Nueva York, 1985.

Estos compuestos se utilizan como colorantes en la industria textil, papelera, alimentaria, etc. Por ejemplo, el “rojo congo”, es un colorante azoico, que se utiliza desde 1884 en la industria textil, y el naranja de metilo se utiliza como indicador ácido base en preparaciones farmacéuticas, determinación de la alcalinidad de fangos o en procedimientos petroleros.⁸⁶

Los polímeros que contienen azobencenos se utilizan también como nanopartículas o hidrogeles que responden a cambios de luz y pH, debido a su isomerización *cis-trans* por acción de la luz y el calor, y a la dependencia del pH del medio. De acuerdo con las características de estos compuestos, desde el grupo de Polímeros se ha trabajado en la síntesis de polímeros con estructura de poliamida aromática de altas prestaciones y polímeros acrílicos con comportamiento de gel, que tienen en su estructura grupos azo y amino, y se ha estudiado este sistema desde el punto de vista ácido/base.

El diseño del sensor de acidez se basa en un sistema altamente conjugado que consta de un cromóforo que está unido a un grupo rico en electrones capaz de interactuar con protones, como es el grupo dimetilamino. La protonación causa una variación de la densidad electrónica de la subestructura conjugada y, macroscópicamente, se traduce en una variación de color del sistema. De acuerdo con esto, se diseñaron y sintetizaron los monómeros y polímeros con las estructuras que se muestran en la Figura 2.7.

El grupo azo, además de ser un cromóforo, es una base débil capaz de ser protonada.⁸⁷ Además, el grupo *N,N*-dimetilamino en posición *para* del anillo de azobenceno es una base más fuerte que el grupo azo. De este

⁸⁶ K. Hunger, *Industrial dyes chemistry, properties and applications*, Wiley-VCH Verlag, Weinheim 2003.

⁸⁷ S. Ciccone, J. Halpern, *Can. J. Chem.* **1959**, 37, 1903.

modo ocurrirá una primera protonación a un pH bajo en el grupo amino, y una segunda protonación a un pH más bajo todavía en el grupo azo, de modo que el rango del sensor es más amplio.

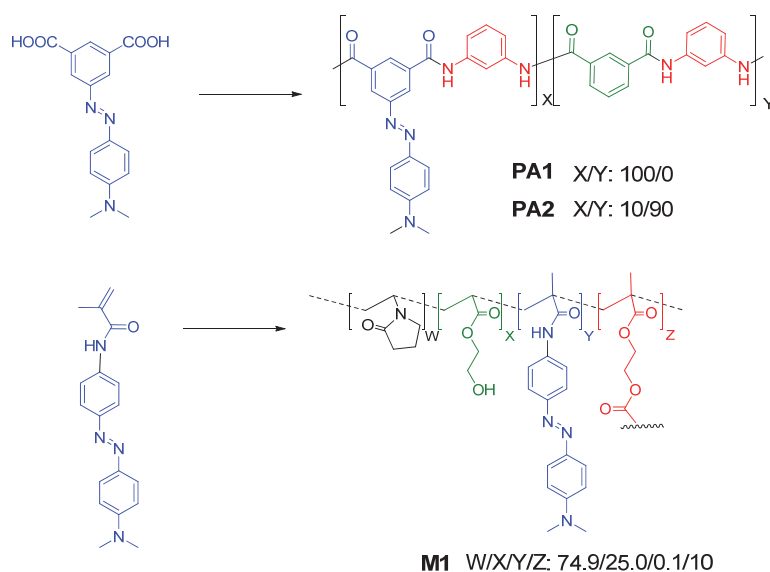


Figura 2.7. Monómeros y polímeros con derivados de azobencenos en su estructura.

2.5.2. Polímeros con derivados azobencenos en su estructura

Como se ha comentado anteriormente en la introducción, en el Grupo de Investigación se trabaja con dos tipos de estructuras poliméricas, las de tipo acrílico y las estructuras tipo poliamida aromática. En este estudio se optó por la preparación de polímeros sensores de alta acidez de los dos tipos aprovechando las ventajas que ofrece cada estructura. Estos materiales se utilizaron en forma de membranas densas y como recubrimientos de fibras y tejidos de *meta* y *para* aramidas y de algodón.

En el caso de los polímeros acrílicos se utilizó acrilato de 2-hidroxietilo y 1-vinil-2-pirrolidona como matriz inerte, para obtener materiales con buenos hinchamientos y buenas propiedades mecánicas.

Las poliamidas aromáticas se sintetizaron por el método de Yamazaki Higashi por homopolimerización del diácido derivado del azobenceno y *meta*-fenilendiamina, o por copolimerización del diácido derivado del azobenceno, ácido isoftálico y *meta*-fenilendiamina, obteniéndose poliamidas con buenas propiedades térmicas y mecánicas, así como con una absorción de agua por encima del 10%. Los recubrimientos se obtuvieron por polimerización radicalaria sobre los tejidos en el caso de los polímeros acrílicos, y por inmersión en una disolución de poliamida en DMA y evaporación del disolvente en el caso de las aramidas.

Tanto los recubrimientos de los tejidos como las membranas obtenidas a partir de los polímeros acrílicos y las poliamidas por *casting* (disolución seguida de evaporación del disolvente) cambiaban de color en presencia de disoluciones ácidas y vapores de ácidos. Este cambio de color era visible a simple vista y cuantificable por espectroscopia de UV/vis. Además, simplemente con lavar con agua los materiales, éstos recuperaban su estado inicial siendo, por tanto, reutilizables.

La membrana acrílica es un material con comportamiento de gel que se hincha en agua y, en menor medida con la humedad ambiental, de modo que los iones hidronio pueden penetrar por difusión dentro de la membrana, alcanzando los grupos básicos. De forma similar ocurre en las poliamidas, que aunque están poco hidratadas son hidrofílicas y también permiten la penetración de los iones hidronio dentro de la membrana, y por tanto la protonación y desprotonación.

2.5.3. Aplicaciones

El control de la acidez o basicidad en distintos medios es fundamental para la industria química y para el control medioambiental. La medida del pH se realiza en la escala normal de pH (1-13), pero a veces es necesario medir este parámetro en sistemas ambientales fuera de este rango, así como en

medios no acuosos, como en aire, por ejemplo. En este estudio se han descrito materiales en forma de filmes o tejidos recubiertos capaces de detectar por cambio de color el pH en distintos ambientes de forma barata, rápida, sencilla y reutilizable. Por otro lado, debido a las excelentes propiedades térmicas y mecánicas de las poliamidas sintetizadas, estos materiales también se pueden utilizar como materiales de altas prestaciones con un valor añadido, como es la capacidad del material de cambiar de color en presencia de ambientes ácidos. De este modo se podría fabricar ropa de trabajo, o batas de laboratorio, con fibra de poliamida y usarse para detectar a simple vista ambientes ácidos en el laboratorio o en la industria.

2.5.4. Resultados

A continuación se describen los resultados obtenidos a través de la transcripción íntegra del trabajo publicado.

- ❖ *Aromatic polyamides and acrylic polymers as solid sensory materials and smart coated fibres for high acidity colorimetric sensing*

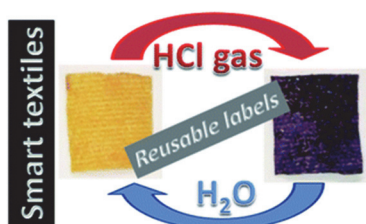
Los detalles experimentales y de caracterización se encuentran en el material suplementario, cuya copia está disponible en el CD adjunto.

*Aromatic polyamides and acrylic polymers as solid sensory materials
and smart coated fibres for high acidity colorimetric sensing*

Aromatic polyamides and acrylic polymers as solid sensory materials and smart coated fibres for high acidity colorimetric sensing

Miriam Trigo-López, Jesús Luis Pablos, Asunción Muñoz, Saturnino Ibeas, Felipe Serna, Félix Clemente García and José Miguel García*

Departamento de Química, Facultad de Ciencias, Universidad de Burgos. Plaza de Misael Banuelos s/n, E-09001 Burgos, Spain. Fax: +34947258831; Tel: +34947258085; E-mail: jmiquel@ubu.es.



Reusable colorimetric acid responsive coated fibres and manageable films or membranes have been successfully designed and prepared herein. The design of the materials rely on condensation and addition monomers

both having the azobenzene group, which is used as a dye moiety as a weak basic motif, and a *N,N*-dimethylamino moiety. The *N,N*-dimethylamino moiety is also used as a weak, albeit stronger, basic group as well as an electron donor or electron withdrawal group, depending on its protonation state. For the sake of applicability, the coated fibres were cotton commodity fabrics, and high-tech aromatic polyamide yarns and fabrics. The high-performance aromatic polyamides and the versatile acrylic structures, along with the pendant weak basic groups, with pK_{as} in water ranging from 1.78 to -0.5 and in air from -1.5 to -3.9, provide the materials with a colorimetric sensing capability over a wide acidity sensing window. This sensing window ranges from 1×10^{-2} to 3 M of perchloric acid in water and from 4×10^{-7} - 9×10^{-2} atm of vapour pressure of hydrogen chloride in air. The colour change of the sensory materials from yellow/blank to red or purple, which occurs upon contact with acidic media, was easily identified using the naked eye. Washing these materials with pure water recovered their original colour and permitted their reuse.

Introduction

Precise control over the acidity or basicity of different media is fundamental in the chemical, cosmetic and household industries; for environmental control and remediation; and in life science. Acidity or basicity in aqueous media is usually monitored using the standard *pH* scale, which ranges from 1 to 13,¹ by different techniques that perform well in covering most of the laboratory requirements. The most popular and easy to use method is that of using *pH* test paper strips, followed by potentiometric techniques based on a proton sensitive membrane, such as a glass membrane electrode. Less extensively used are chemical *pH* sensors.²⁻⁴

For the same reasons, there is a huge need for controlling the acidity or basicity of systems not within range of this scale, both in strongly acidic or basic aqueous media as well as in the environment – in air – where the *pH* scale is not applicable. This need is especially important for a number of important social and economic applications, including work related to the separation of rare-earth metals, nuclear fuel reprocessing, and the recycling and reuse of strong acids in industrial processes.⁵⁻¹⁰ Within this frame, we describe herein colorimetric sensory polymers, which have in their pendant structure azo and amino groups, which are used both as proton receptors and chromogenic moieties. These groups change their colour in highly acidic aqueous media and in air, providing a rapid, precise, and inexpensive measure of the acidity at very low *pH* values, especially values outside of the standard *pH* scale (perchloric acid concentration up to 3 M can be detected). These polymers have a high-performance aromatic polyamide main structure¹¹⁻¹⁴ or an acrylic nature with a gel behaviour,¹⁵⁻¹⁸ which can be prepared or transformed into highly manageable materials including films, membranes, or coatings for cotton commodity or high-tech *meta*- or *para*-aromatic polyamide fibres. To date, the challenge of preparing *pH*-responsive polymeric materials has been mainly undertaken by immobilising

pH responsive organic molecules in polymer matrixes^{7-10,19,20} with only several studies on the preparation of integral polymer chemosensors.^{6,21} However, the latter approach proved to be better^{22,23} than the former²⁴⁻³⁰ because the chemical anchoring of the sensory motifs avoids the migration, leaching and hysteresis of any sensory materials, thus giving rise to an unsurpassed long-term stability. However, although azobenzene polymers have been used as photo- and *pH*-responsive nanoparticles or hydrogels³¹⁻³³ due to their well-known *cis-trans* thermal- and photo-isomerisation and dependence on the medium acidity,³⁴⁻³⁶ to the best of our knowledge, this kind of material has not been fully exploited. Further exploitation includes taking advantage of the colorimetric behaviour of manageable films and coated fibres, which is due to the protonation process of the azo group and more precisely to the two protonation processes corresponding to the 4-dimethylaminoazobenzene dye moiety. These processes have reported second acidity constants (protonation of the azo group) ranging from -4.4 to -3.4 with a first acidity constant (protonation of the amino group) of approximately 3.5.^{37,38}

Thus, we have designed sensory condensation and acrylic monomers from which we have prepared colorimetric sensory materials that respond to acidic environments, both in aqueous solutions and in air, with a clearly visible colour change. For the correct design of colorimetric acidity-responsive materials, the acidity constants of the proton receptors of the monomers were previously considered, along with both the chromogenic and weak basicity of the azobenzene moiety. As a proof of concept for practical applications, the materials have been prepared as manageable transparent membranes, shaped as films, coated fibres of cotton fabrics, and *meta*- and *para*-aromatic polyamides yarns and fabrics (commercial brands: Nomex®, Teijinconex®, and Kevlar®, Twaron®, respectively).

Experimental Part

Instrumentation and measurements

^1H and ^{13}C NMR spectra were recorded with a Varian Inova 400 spectrometer operating at 399.92 and 100.57 MHz, respectively, with deuterated dimethylsulphoxide ($\text{DMSO-}d_6$) as the solvent.

Infrared spectra (FT-IR) were recorded with a FT/IR-4200 FT-IR Jasco spectrometer with an ATR-PRO410-S single reflection accessory. Low-resolution electron impact mass spectra (EI-LRMS) were obtained at 70 eV on an Agilent 6890N mass spectrometer. Thermogravimetric analysis (TGA) data were recorded for a 5-mg sample under a nitrogen or oxygen atmosphere on a TA Instrument Q50 TGA analyser at a scan rate of $10^\circ\text{C min}^{-1}$. The limiting oxygen index (LOI) was estimated using the following experimental Van Krevelen equation: $\text{LOI} = 17.5 + 0.4 \text{ CR}$, where CR is the char yield weight percentage at 800°C , which was obtained from the TGA measurements under a nitrogen atmosphere.

UV/Vis spectra were recorded using a Varian Cary3-Bio UV/Vis spectrophotometer.

The polyamide solubility was determined by mixing 10 mg samples of the **PA1** and **PA2** with 1 mL of a solvent followed by stirring for 24 h at 20°C . The polymer was considered soluble at room temperature if a homogenous solution was obtained. If the polymer was insoluble at room temperature, the system was heated to reflux for 2 h, and the polymer was considered soluble on heating if a homogenous solution was obtained. Otherwise, the polymer was considered insoluble. The inherent viscosities of the polymer were measured with an Ubbelohde viscometer using sulphuric acid (96%) as the solvent at $25^\circ\text{C} \pm 0.1^\circ\text{C}$ and a polymer concentration of 0.5 g dL^{-1} .

Water sorption experiments were conducted gravimetrically. The sample (200 mg) was dried at 60°C for 24 h over phosphorus pentoxide, and the sample was placed in a closed box containing a saturated aqueous solution of NaNO₂ at 20°C, which provided a relative humidity of 65%. The samples were weighed periodically over a period of 8 days until they equilibrated with their surroundings and presented no further changes in weight. The water-swelling percentage (WSP) of the membranes or films was obtained from the weights of a dry sample membrane (ω_d) and a water-swelled (the membrane was immersed in pure water at 20°C until the swelled equilibrium was achieved) sample membrane (ω_s) as follows: $100 \times [(\omega_s - \omega_d) / \omega_d]$.

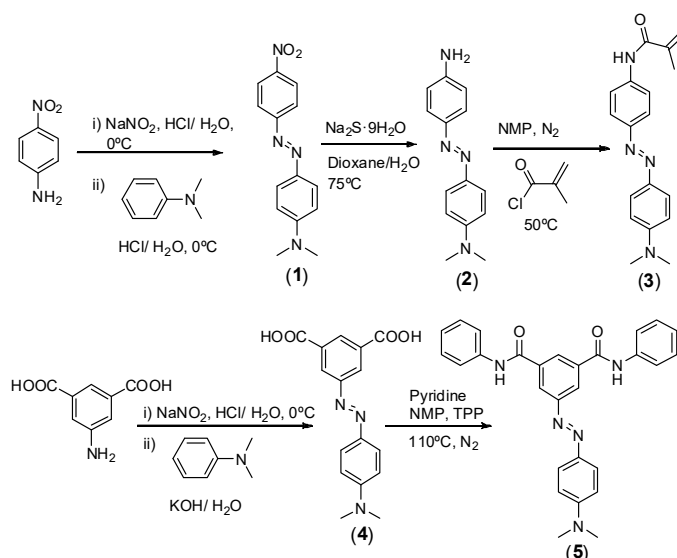
Polyamide films were prepared by evaporation of cast solutions in DMA: solutions 4% by polymer weight for **PA1** and 10% by polymer weight for **PA2** were used. The solvent was eliminated by heating at 60°C overnight. The polymethacrylamide membrane or film, **M1**, was prepared by bulk radical polymerization as described in the ESI (Section S2). To determine the tensile properties of the polyamides, strips (5 mm in width and 30 mm in length) were cut from polymer films of 22 and 71 μm thickness for **PA1** and **PA2**, respectively, on a SHIMADZU EZ Test Compact Table-Top Universal Tester at 20°C. Mechanical clamps were used and an extension rate of 5 mm min⁻¹ was applied using a gauge length of 9.44 mm. The polymethacrylamide membrane, **M1**, 112 μm in thickness, was also tested in the same way. At least 6 samples were tested for each polymer, and the data was then averaged.

The acid titration monitored by UV/Vis both for the vapour and in aqueous phases was performed as follows. The titration in solution with the sensory membranes was performed using perchloric acid as the acid source using the following conditions: 5-mm discs cut from the membrane **M1** and casted films of **PA1** were dipped into 200 mL of water (Millipore-Q) in using a homemade support that also fit the UV/Vis cell holder. Next, the acidity of

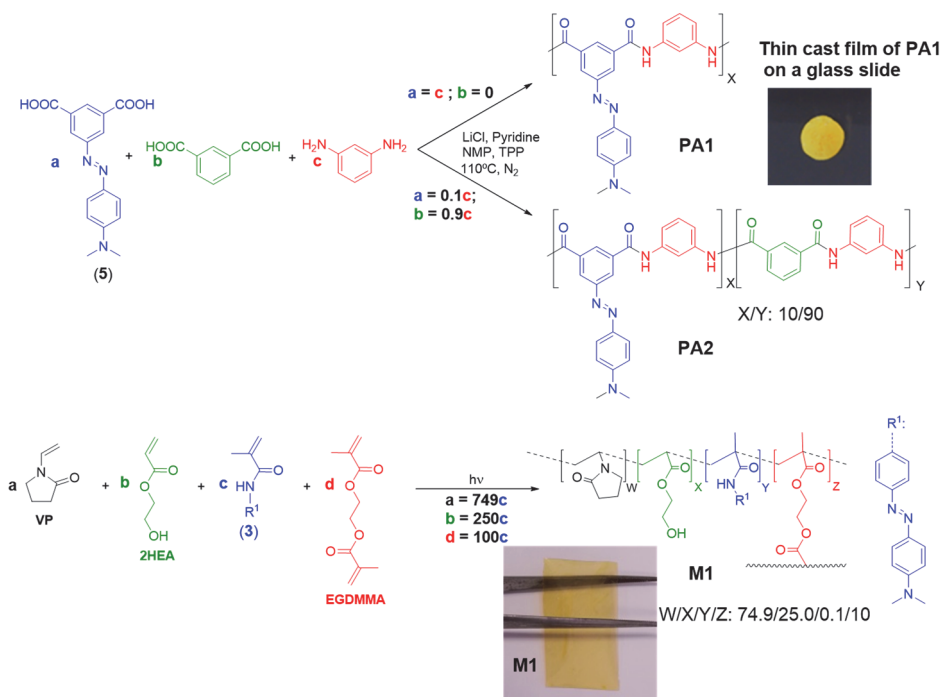
the solution was increased to a *pH* close to 1 by adding aliquots of diluted perchloric acid. After each addition, the *pH* was measured with a *pH* meter with a glass electrode, the membranes were allowed to equilibrate for 15 min, and the UV/Vis spectra were recorded. For higher acidities out of the range of the *pH* scale, vials containing 25 mL of perchloric acid of concentrations ranging from 0.1 to 3.5 M were prepared, and the membranes were successively immersed in them, starting from the lower acid concentration vial. After equilibrating the three films or membranes in each vial for 15 min, their UV/Vis spectra were recorded. The measurements were performed at 24°C. The colorimetric detection of acidic vapours was performed quantitatively as follows. The HCl vapour pressure of vapours from the head space of a fresh bottle of concentrated hydrochloric acid was calculated by titration with NaOH solution of known concentration. The titration was repeated five times and the results averaged. The membranes (**PA1** casted films and 5-mm discs cut from **M1**) were placed in a sealed quartz UV-cuvette using a homemade support. Then, increasing volumes of HCl vapours from the head space of the bottle were then added with a Hamilton micro syringe, and the UV/Vis spectra were recorded after equilibrating (see the response time subsection). The measurements were performed at 25°C.

Synthesis of sensory monomers and preparation of sensory materials

Monomers and polyamide model were prepared by previously described procedures schematically depicted in Scheme 1 (for experimental workup see Section S1, ESI).³⁹⁻⁴¹ The aromatic polyamide synthesis (**PA1** and **PA2**, Scheme 2), the crosslinked acrylic membrane preparation (**M1**, Scheme 2) and the coating of cotton and aramid fibres with the acidity sensory polymers (Table 1) were carried following previously methodologies (see Section S2, ESI).^{11,16,18,42,43}




















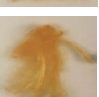
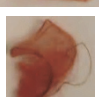


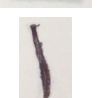


Scheme 1. Synthesis of monomers and model.



Scheme 2. Polymer structure and synthesis.

Table 1. Polyamide (PA1) and polyacrylic coated fibres, and visual sensing behaviour toward acid vapours.

	Polyamide coating (PA1)			Polyacrylic coating		
	Blank fibres	Coated fibres and coating, % ^{a)}	HCl vapour	Blank fibres	Coated fibres and coating, % ^{a)}	HCl vapour
Cotton fabric		 0.4			 96	
<i>m</i> -aramid yarns		 1.2			 674	
<i>p</i> -aramid fabric		 1.5			 121	
<i>p</i> -aramid yarns		 1.6			 321	

^{a)} Percentage of weight regain of blank samples upon coating.

Table 2. Viscosity, water sorption and solubility of materials.

Model or polymer	$\eta_{inh, a)}$ dLg ⁻¹	$\eta_{inh, b)}$ dLg ⁻¹	Water sorption		Solubility ^{e)}				
			% ^{c)}	% ^{d)}	DMSO, DMA, DMF	NMP	THF	CHCl ₃ , CHCl ₂ , EtOH	Acetone
Model	n.a.	n.a.	n.a.	n.a.	++	++	++	+	++
PA1	2.25	0.78	11	19	++	+	-	-	-
PA2	1.29	0.50	12	21	++	++	-	-	-
M1	n.a.	n.a.	37	53	n.a.	n.a.	n.a.	n.a.	n.a.

^{a)} Solvent = sulphuric acid (100%), temperature = 20°C, polymer concentration = 0.5 g/dL; n.a.: not applicable; ^{b)} solvent = NMP, temperature = 20°C, polymer concentration = 0.5 g/dL; n.a.: not applicable; ^{c)} polymeric samples in an atmosphere with a relative humidity of 65%; n.a.: not applicable; ^{d)} the water-swelling percentage (WSP) of membranes in pure water at 20°C; ^{e)} polymer concentration = 10 mg of polymer in 1 mL of solvent; ++ = soluble at room temperature; + = soluble on heating; +- = partially soluble; - = insoluble, n.a.: not applicable (crosslinked membranes).

Table 3. Thermal (TGA) and mechanical properties of materials.

Polymer	Thermal properties						Mechanical properties		
	N ₂ atmosphere			O ₂ atm.			Tensile strength, MPa	Young's Modulus, GPa	Elongation (%)
	T ₅ , ^{a)} °C	T ₁₀ , ^{b)} °C	Char yield, %	T ₅ , ^{a)} °C	T ₁₀ , ^{b)} °C	LOI ^{c)}			
PA1	330	360	50	330	400	37.5	60	1.54	13
PA2	400	456	64	412	464	43.1	50	1.34	11
M1	319	367	6	292	353	19.9	22	0.83	4

^{a)} 5% weight loss (T_5), 10% weight loss (T_{10}); ^{b)} at 800°C; ^{c)} limiting oxygen index, calculated from the TGA data ($LOI = 17.5 + 0.4 CR$, where CR is the char yield in% weight at 800°C under nitrogen).

Results and discussion

Overcoming the difficulty of sensing target molecules in pure water and in the gas phase

Organic molecules usually are water-insoluble and can barely be exploited in water media. Furthermore, the lack of mechanical properties of discrete molecules also impairs their applicability. Our main objective is sensing target molecules in water easily, i.e., using inexpensive and manageable solid systems that rapidly change their colour *in situ* upon interacting with the target in aqueous media, and that can be used by non-specialised personnel. For this purpose, we have designed organic probes that change their colour when exposed to different levels of acidity. Furthermore, the probes are aromatic diacids and acrylic monomers that allow for their polymerisation to render solid, handleable materials as films or membranes and coated fibres (both for use in commodity and high-tech smart textiles). Simultaneously, the copolymerisation of the probes with the proper monomers provides a macromolecular environment for sensing in water regardless of the water insolubility of the probes. The change of the colour

of the materials is clearly visible at given acid concentrations, permitting the broad determination of their acidities using the naked eye, which can be quantified in parallel using the UV/Vis technique. Furthermore, the materials change their colour in air in the presence of acid vapours, allowing for use of these materials in the preparation of coated fibres that could be used in PPE (personal protective equipment).

The strategy followed for the design of the colorimetric chemosensory units

The design of a colorimetric sensory motif for acidic media relies on a highly conjugated system that provides the chromophore and the link to an electron rich group capable of interacting with protons, preferably by being protonated. Protonation would then cause variation in the electron density of the conjugated sub-structure and, macroscopically, in the colour of the system.

In this study we have chosen an azo dye for two reasons: a) diazobenzene derivatives already have well-known dye characteristics, and b) the azo group is a weak base that can be protonated.³⁶

Moreover, the *N,N*-dimethylamino group, which is a stronger but still weak base, was chosen as a substituent in the *para* position of the 4-azobenzene ring. This group was chosen with the aim of using it as a primary protonation site at low *pH* and the azo motif as a second protonation site at an even lower *pH* as a way of expanding the acidity sensory range.

Materials preparation and characterisation

Both the sensory acrylic and condensation monomers, (3) and (4), respectively, were prepared easily and inexpensively using in several high-yield synthetic steps using widely available chemicals in proven organic reactions (Scheme 1). The ¹H and ¹³C NMR and FTIR data and the spectra

of the intermediates and monomers can be found in the ESI, Section S1. The potential applicability of the designed polyacrylic sensory membrane, **M1**, and even of the coating for commercial fibres, is highlighted by the fact that only 0.1% by weight of the sensory synthetic monomer is used in the preparation of the acid sensory materials, as will be described below, using 99.9 mol% of very inexpensive commercial comonomers. In a similar fashion, the sensory aromatic polyamides can be used to create an *m*-aramid-like structure as a homopolymer (**PA1**) or as a copolymer (**PA2**) using 10% by weight of the diacid sensory monomer (**5**). The inherent viscosity of the polymers was high enough to assure their high molecular weight, and their solubility good to allow their processability upon solution (Table 2). Furthermore, using a coating lower than 2% by weight, for conventional cotton and high-tech aramid fibres, smart textiles were successfully tested. The structure of the homopolymer and of the copolymer, especially considering the molar content of the sensory motifs, was in agreement with the ^1H NMR spectra (Figure 1).

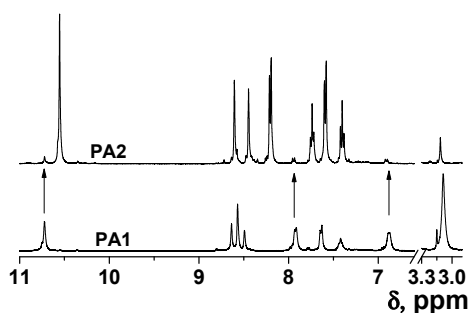


Figure 1. ^1H NMR of **PA1** and **PA2** (solvent = $\text{DMSO}-d_6$).

The polymer dense membranes, or films, were characterised as materials from both mechanical and thermal viewpoints. Mechanically, they were creasable and handleable: both for cast aromatic polyamide films prepared from **PA1** and **PA2** and for acrylic membrane **M1**. The aramids exhibited worthy Young's moduli and tensile strength for high-performance

polymer films prepared at a laboratory scale without orientation and post-thermal treatment (Table 3). In the same fashion, these properties were also excellent when testing the acrylic membrane.

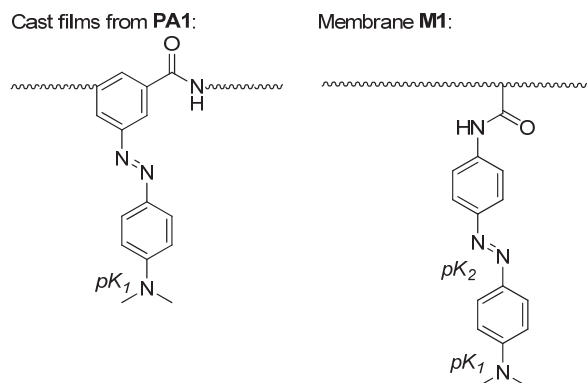
From the thermal resistance viewpoint, evaluated using TGA, the decomposition temperatures that resulted in a 5% weight loss under a nitrogen atmosphere (T_5) were approximately 330-400°C for aromatic polyamides and approximately 320 °C for **M1**. The T_5 of the aromatic homopolyamide **PA1** was low for this type of material^{11,12} due to the weight loss associated with the thermal degradation of the pendant azo group. Significantly, the LOI of aramids was high, which corresponds to the properties of high-thermal resistance materials (Table 3).

The films and membrane composition were designed to provide a high thermal, chemical and mechanical resistance in the case of polyamides with a relatively high water affinity provided by the polar amide groups and high hydrophilicity in the case of the crosslinked acrylic material (**M1**), i.e., gel behaviour. This allows the solvated hydrated protons, hydronium ions, to enter the membrane by diffusion and to reach and interact with the hydrophobic sensory motifs evenly distributed along the swelled membrane. The hydrophilic or hydrophobic character of the membrane is related to the water sorption, i.e., the moisture uptake at 65% RH, and to the water-swelling percentage (WSP). That is, its character is related to the weight percentage of water uptake by the films upon soaking until equilibrium in pure water at rt. These data are shown in Table 2, which, thus, confirms the properties for which they were designed.

The chemosensing mechanism

The weak basic character of both the tertiary aromatic amine and the azo groups of monomers (**3**) and (**4**) are responsible for the acidity sensing behaviour of the materials prepared herein (Scheme 3). Thus, the colour change visually observed for the materials when exposed to acidic media

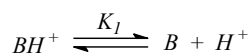
mainly arises from the protonation of these groups. It is this colour variation that permits the building of titration curves using the UV/vis technique as well as the qualitative visual determination of the acidity of the media using the naked eye.



Scheme 3. Protonation sites on the sensory motif of films, (each is marked with a pK label), which protonate upon increasing the acidity of the medium to a perchloric acid concentration of 3.5 M (the pK s are shown in Table 4).

The sensing mechanism has been analysed in terms of the deprotonation/protonation equilibrium of weak basic species. Quite notably, it is fairly unusual and uncommon to see studies that have been performed with these types of materials in the solid state both in air and immersed in water. The acrylic membrane **M1** is a gel material that swells in water, and the solvated hydronium ions can enter the water swelled membrane by diffusion, reaching the basic moieties of the pendant azobenzene derivative. Similarly, the low hydrated but hydrophilic nature of the thin polyamide films of **PA1** and **PA2** allow for the same diffusion and reaction processes. Additionally, in a comparable fashion, these materials can be hydrated in air due to the ambient relative humidity, and HCl vapours can then dissolved and transported into the membrane where the protonation processes occur.

The deprotonation/protonation equilibria can be described by,



where the equilibrium constant is

$$K_1 = \frac{a_B a_{H^+}}{a_{BH^+}} \quad (1)$$

and Eq. (1) can be rewritten as,

$$pK_1 = pH + \log \frac{[BH^+]}{[B]} - \log \frac{f_B}{f_{BH^+}} \quad (2)$$

where f represents the activity factors of the protonated species, BH^+ , and free base, B . Considering an ionisation ratio, I , as the ratio between the concentration of the protonated species and free base and ideal behaviour of the solutions, i.e., the activity coefficients are 1, Eq. (2) can be written as,

$$\log I = -pH + pK_1 \quad (3)$$

However, Eq. (3) allows for better results when expressed as^{44,45}

$$\log I = -n_1 pH + n_1 pK_1 \quad (4)$$

where n_1 gives an idea of the lack of ideality of the system. Eqs. (3) and (4) are the same for ideal systems where $n_1 = 1$. The ionisation ratio can be calculated from the absorbance values of UV/Vis measurements using Eq. (5), which can be obtained from the mass and absorbance balance, where AB , ABH^+ and A represent the absorbances of free base, protonated base, and the absorbance values at different pH for a given wavelength, λ , respectively. Substituting Eq. (5) into (4), Eq. (6) is obtained, which enables a nonlinear least squares fit of the sigmoid curve obtained from experimental measurements, known as the Chandler method.⁴⁶

$$I = \left(\frac{A - A_B}{A_{BH^+} - A} \right)_\lambda \quad (5)$$

$$A = \frac{A_B - A_{BH^+}}{1 + 10^{-n_1 pH + n_1 pK_1}} + A_{BH^+} \quad (6)$$

The acidity necessary to fully protonate weak bases is such that the concentration of protons in the medium is greater than 0.1 M, and the pH as a measure of the acidity of the medium is not useful. Moreover, when operating at increasingly acidic medium, the ionic strength of the medium increases, making the approach used by Debye-Hückel increasingly unsatisfactory. It is therefore necessary to define a quantitative scale to express the acidity of the medium. For this reason Hammett and Deyrup proposed an acidity function,⁴⁷ H_0 , representative of the acidity of the medium and independent of the nature of the indicator used as the reference in its definition and calculation. From a series of reference bases, S , the H_0 function is defined as:

$$H_0 = -\log \frac{a_{H^+} f_S}{f_{SH^+}} \quad (7)$$

If the base objects of study, B , fully or partially protonated in the acidic range in which the reference base is protonated, S , according to Hammett's hypothesis, must meet the following condition:

$$\frac{f_S}{f_{SH^+}} = \frac{f_B}{f_{BH^+}} \quad (8)$$

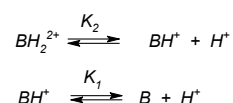
H_0 , in this case, depends only on the activity of protons because it is a measure of the acidity of the medium. Hammett and Deyrup calculated H_0 using a series of primary nitroanilines; their values are dependent only on the concentration of the mineral acid used. The correspondence of the calculated H_0 with the molar concentration of the acids used for this study, perchloric and hydrochloric acid, is shown in the ESI, Tables S1 and S2.^{48,49}

Following a similar reasoning to Eqs. (1) through (4), the corrected Hammett-Deyrup equation is proposed:^{45,50}

$$\log I = -n_i H_0 + n_i pK_i \quad (9)$$

Since the bases studied in this work are protonated in the high acidity region, in Eq. (6), the pH is replaced by H_0 where needed, i.e., when the acid concentration is higher than 0.1 M.

Bases with two protonation equilibria, such as membrane **M1**, can be described with two equilibrium constants:



In this work, these two equilibria overlap, i.e., the difference between their pK s is less than or equal to three units, indicating that both processes cannot be separated. To determine the values of the equilibrium constants by UV/vis, different wavelengths characteristic of each equilibrium constant are required. In the event that this is not possible, it is necessary to propose an alternative approach.

From the ratio of ionisation of the two equilibria obtained from Eq. (4), Eqs. (10) and (11) are obtained,

$$I_1 = \frac{[BH^+]}{[B]} = \left(\frac{a_{H^+}}{K_1} \right)^{n_1} \quad (10)$$

$$I_2 = \frac{[BH_2^{2+}]}{[BH^+]} = \left(\frac{a_{H^+}}{K_2} \right)^{n_2} \quad (11)$$

For convenience, the concentrations of B , BH^+ and BH_2^{2+} are henceforth represented by C_1 , C_2 , and C_3 , respectively. From a mass and absorbance balance, Eqs. (12) and (13) are obtained, where ε_1 , ε_2 and ε_3

are, respectively, the molar extinction coefficients of B , BH^+ and BH_2^{2+} . Using Eqs. (10) to (12), Eqs. (14) to (16) are obtained.

$$C_T = C_1 + C_2 + C_3 \quad (12)$$

$$A = \varepsilon_1 C_1 + \varepsilon_2 C_2 + \varepsilon_3 C_3 \quad (13)$$

$$C_2 = C_1 K_1^{-n_1} a_{H^+}^{n_1} \quad (14)$$

$$C_3 = C_1 K_1^{-n_1} K_2^{-n_2} a_{H^+}^{n_1+n_2} \quad (15)$$

$$C_1 = \frac{C_T}{1 + K_1^{-n_1} a_{H^+}^{n_1} + K_1^{-n_1} K_2^{-n_2} a_{H^+}^{n_1+n_2}} \quad (16)$$

By substituting Eqs. (14) to (16) in (13), Eq. (17) is obtained, where A_1 , A_2 and A_3 represent the absorbance of species B , BH^+ and BH_2^{2+} , respectively. The activity of the proton can be replaced by 10^{-pH} or 10^{-H_0} , depending on the acidity of the experiment, and K_i can be replaced by 10^{-pK_i} in Eq. (17). After performing a nonlinear least squares fit, this equation allows the attainment of the pK_s , n_i and A_i , as previously described.⁵¹

$$A = \frac{A_1 + A_2 K_1^{-n_1} a_{H^+}^{n_1} + A_3 K_1^{-n_1} K_2^{-n_2} a_{H^+}^{n_1+n_2}}{1 + K_1^{-n_1} a_{H^+}^{n_1} + K_1^{-n_1} K_2^{-n_2} a_{H^+}^{n_1+n_2}} \quad (17)$$

The behaviour of the materials as proton receptors, i.e., as sensory materials for high acidity media, is both highly dependent on the nature of the receptor moiety and film or membrane constitution, and on the measuring media, i.e., the acidity in water or acid vapours, as shown in Tables 4 and 5. These results arise from the UV/vis titration curves depicted in Figures 2 and 3 and in the ESI (Figures S9 and S10), and permit the design or tuning of the sensory materials for different applications and environments. Thus, for instance, the two protonation processes, in terms of pK_s , of the N,N -dimethylamino and azo groups are 1.78 and -0.5 for the acrylic membrane **M1** in water and -1.48 and -3.89 in the slightly hydrated

atmosphere corresponding to the vapour acidity measurements (a 24% by weight of hydration was assumed, in accordance with the water sorption studies, for calculations). In the case of aramid films, only the protonation of the *N,N*-dimethylamine group was observed in water with a $pK = 0.92$; two processes in the acidity vapour measurements were observed with pK values of -2.6 and -3.5. For these calculations, a hydration of 10% was used and no drastically different results were obtained using a higher and lower water content assumption (Table 5).

The complex nature of the protonated azo group was previously described by Jaffé and Gardner.³⁷ In relation to the *cis-trans* isomerisation, the process has no influence in our study because we mainly work under ambient light and thermal conditions, where the *trans* isomer is the predominant species, which was observed in our UV/vis and ¹H NMR studies. This is because the *trans* to *cis* isomerisation occurs under UV irradiation, and the *cis* to *trans* isomerisation occurs under visible light along with heating. Simultaneously, the latter process is much faster, by one order or magnitude, as reported by Tang *et al.*³¹ Additionally, acidic media have a well-known highly catalytic effect of when undergoing a *cis* to *trans* isomerisation.³⁶

The proposed protonation processes were also confirmed by ¹H NMR. Thus, the behaviour of the polyamide model compound (**5**) and the acrylic monomer (**3**) in a CD₃CN/D₂O (1.3/0.7 mL) solution upon acidification with DCI was studied using this technique. The first protonation process of the *N,N*-dimethylamino group was clearly seen for both compounds. The acidity constants were calculated in a similar way for the solid film shaped sensory materials. Details of the calculations and results are depicted in the ESI, Section S7. Unfortunately, it was not possible to increase the acidity in the NMR experiments to see further protonation processes for the acrylic monomer (**3**) or for model (**5**). The acidity constants, in terms of pK s, were in agreement with those of the solid materials in water considering that due to

the insolubility of (3) and (5) in water, the medium was mainly organic and that these are discrete molecules with high mobility. However, the sensory motifs in polymeric films or membranes are chemically anchored to a polymer structure within the solid state and, hence, have a highly restricted mobility.

Table 4. pK_s of **M1** and **PA1** in water obtained from Eqs. (6) and (17). The values between brackets are the pK_s calculated for monomers (3) and (4) using the program Marvin Suite.⁵²

Material	Calculated at				
	390 nm	418 nm	464 nm	499 nm	Average
M1	pK_1	1.69 ± 0.02	1.86 ± 0.02		1.78 ± 0.02 (3.58)
	n_1	1.01 ± 0.04	1.12 ± 0.07		1.06 ± 0.05
	pK_2	-0.4 ± 0.2	-0.54 ± 0.05		-0.5 ± 0.1 (0.11)
	n_2	0.45 ± 0.07	4 ± 2		1.1 ± 0.2 1.8 ± 0.8
	430 nm	550 nm			Average
PA1	pK	0.86 ± 0.04	0.98 ± 0.02		0.92 ± 0.03 (3.24)
	n	1.3 ± 0.1	1.5 ± 0.1		1.4 ± 0.1

Table 5. pK_s of **M1** (assuming a 24% of water, by weight) and **PA1** (10% of water, by weight) in an atmosphere of HCl vapours obtained from Eqs. (6) and (17).

Material	Calculated at				
	555 nm	426 nm	461 nm	570 nm	Average
M1	pK_1	-1.48			
	pK_2	-3.89			
PA1	pK_1	-2.7 (-2.9, -2.5) [§]	-2.5 (-2.7, -2.2) [§]	-2.6 (-2.8, -2.3) [§]	-2.6 (-2.8, -2.3) [§]
	pK_2		-3.5 (-3.6, -3.5)		

[§] The data between brackets corresponds to the water content of the film: 5%, left, and 15%, right.

Interference study

The selectivity of the sensory materials as colorimetric acidity sensors were tested in the presence of a broad set of salts (NaCl, KCl, $\text{CuSO}_4 \cdot 5\text{H}_2\text{O}$, $\text{Co}(\text{NO}_3)_2 \cdot 6\text{H}_2\text{O}$, $\text{Al}(\text{NO}_3)_3 \cdot 9\text{H}_2\text{O}$, $\text{Pb}(\text{ClO}_4)_4$, $\text{FeSO}_4 \cdot 7\text{H}_2\text{O}$,

LiCl, $\text{Zn}(\text{NO}_3)_2 \cdot 6\text{H}_2\text{O}$, $\text{Hg}(\text{NO}_3)_2 \cdot \text{H}_2\text{O}$, and $\text{Ni}(\text{NO}_3)_2 \cdot 6\text{H}_2\text{O}$). Thus, a solution of all these salts at a high concentration, 1×10^{-3} M of each, in 1M aqueous HClO_4 was used in this study. The UV/vis spectra of **M1** were obtained by dipping **M1** into this solution and, in parallel, into a pure solution of 1 M HClO_4 in water (Figure S14). The spectra were fairly similar, and slight changes were ascribed to the change in acidity caused by the acidic salts.

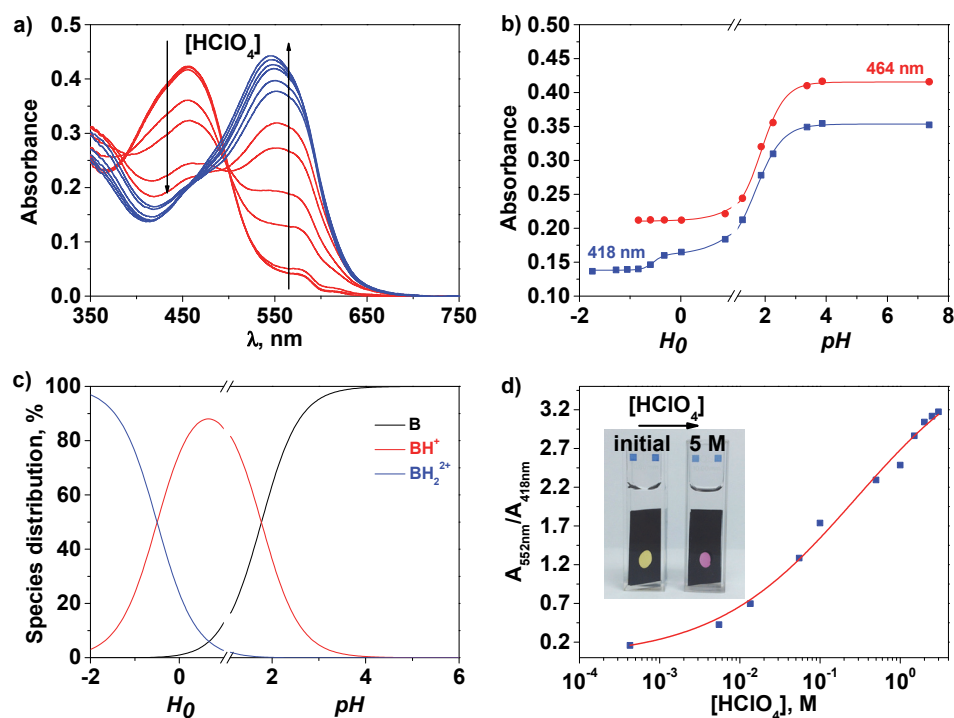


Figure 2. Titration of perchloric acid with membrane **M1** in Millipore-Q water using the UV/Vis technique: a) UV/Vis spectra showing the two protonation processes (low and higher acidity in red and blue, respectively); b) acidity absorbance relationship at 418 and 464 nm (continuous lines correspond to the fitting using Eqs. 17 and 6, respectively); c) species distribution using Eqs. 10-11, assigning a value of 100 to C_T ; d) ratiometric titration curve of perchloric acid ($[\text{HClO}_4]$ vs. absorbance at 552 and 418 nm ratio); inset: picture of the UV/vis cuvettes at the beginning and end of the experiment showing the colour change upon acidification of the medium.

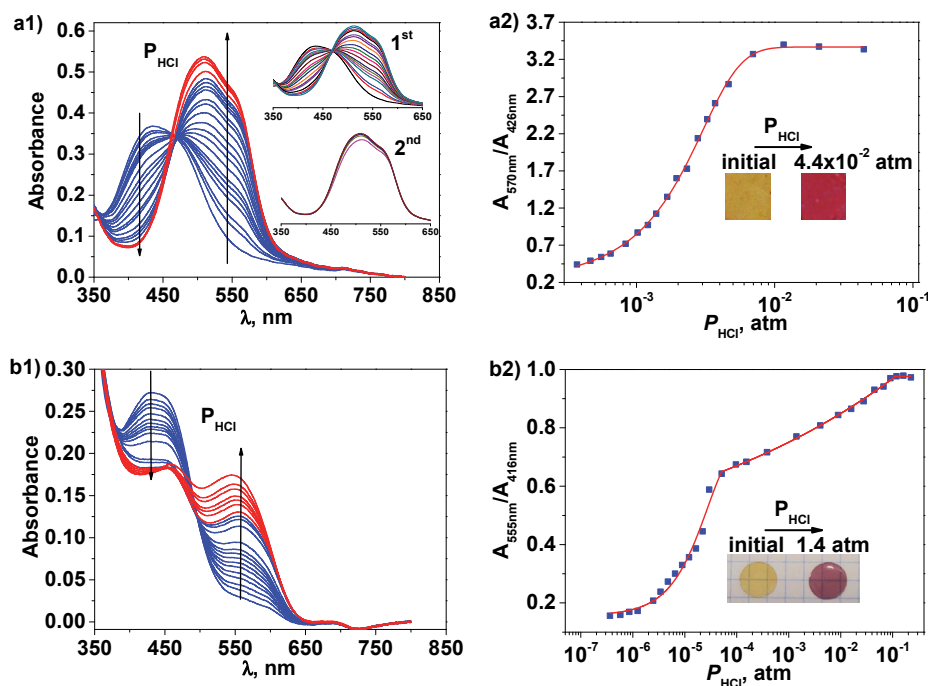


Figure 3. Titration of HCl vapours with the cast film of **PA1** and membrane **M1**: a1) **PA1**, UV/Vis spectra showing the two protonation processes (low and higher acidity in blue and red, respectively) (inset: first and second processes at low and higher acidity, respectively), a2) **PA1**, ratiometric titration curve of HCl vapours, in terms of partial pressure, vs. absorbance at 570 and 462 nm ratio (inset: picture of the film at the beginning and end of the experiment showing the colour change upon increasing the partial vapour pressure of HCl); b1) **M1**, UV/Vis spectra showing the two protonation processes (low and higher acidity in blue and red, respectively); b2) **M1**, ratiometric titration curve of HCl vapours, in terms of partial pressure, vs. absorbance at 555 and 416 nm ratio; inset: picture of membrane at the beginning and end of the experiment showing the colour change upon increasing the partial vapour pressure of HCl.

Reusing and stability of the sensory membranes in acidic media

The reusability of a material is a key parameter in its applicability both from sustainability and economy viewpoints. It is related to a material's chemical stability and reproducibility as well as to the recovery of the material.

Thus, the sensory materials, **M1** and **PA1**, were subjected periodically to 10 cycles of immersions in highly acidic water (4 M HClO₄)

followed by washing in pure water, without loss of performance and simultaneously with good reproducibility (Figure 4). The study with **PA1** was performed using a thin film (1.87 μm) prepared from casting over a microscope glass slide, which gave rise to an extremely short measuring-recovery cycle time of approximately 2 min; however, this process was approximately 17 min for **M1**, including a 2-min immersion in the acid medium and a 15-min wash. The differences most likely arise mainly from the thickness differences that influence the diffusion processes (Fick's law).

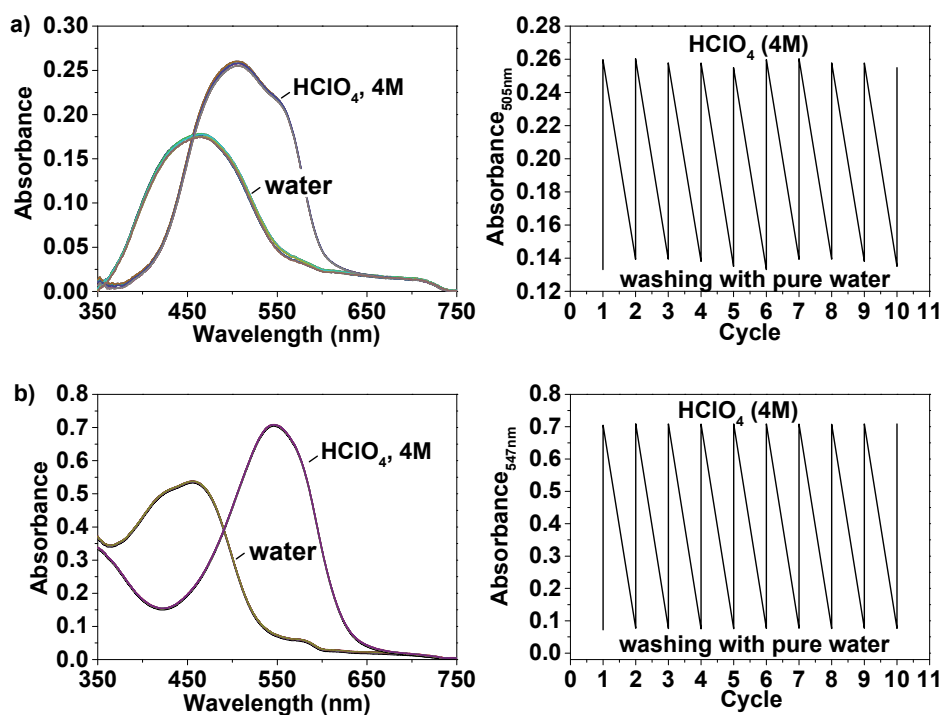


Figure 4. Reproducibility and reversibility of **M1** (b) and cast films of **PA1** (a) on a glass surface as acidity sensors analysed by UV/vis spectroscopy (left: UV/vis spectra; right: absorbance vs. measuring cycle). The measurements were performed by successive cycles of dipping the material in highly acidic water (4M HClO₄), followed by washing with pure water. The measuring-recovery cycle time was approximately 17 min for **M1**, which included a 2-min immersion in the acid medium and a 15-min wash, and approximately 2 min for **PA1**, which included a 2-min immersion in the acid medium, and the recovery was immediate after washing.

Response time

Sensors have to be not only accurate, reliable, and resistant to the environment, but rapid in their response for real live measurements; thus, response time is a key parameter for sensor performance. In this study, response time was determined by UV/vis spectroscopy as the time needed to achieve 99.8% of the absorbance variation (ESI, Figure S13). The colour change was immediate for polyamide films and lower than 3 min for the acrylic sensory membrane **M1**, and colour changes were clearly visible using only the naked eye in less than one minute. Figure S13 in the ESI also shows the stability of the measurement with time.

Sensing acidic aqueous media

The variation in the UV/vis spectra of membrane **M1** and polyamide cast films allowed for the construction of ratiometric titration curves as well as for the naked eye visualisation of increasing acidity, as shown in Figures 2d and S9 (ESI). **M1** shows a continuous change in the absorbance ratio at 552 and 418 nm (A_{552}/A_{418}) from a low perchloric concentration (4×10^{-4} M) to high acidities (3 M). On the other hand, the films prepared with **PA1** show continuous variation in the A_{550}/A_{408} ratio in the medium acidity range (from 2×10^{-3} to 1×10^{-2} M) (Figure S9 (ESI)). This sensing range is in agreement with the acidity constant or constants of the materials discussed above.

On the other hand, a 5-min exposure to the acidic media turned both materials from yellow to red, clearly permitting the visual qualitative evaluation of the acidity of the media (Figures 2d and S9 (ESI)).

Sensing acidic atmospheres

The detection and control of acids in the environment is important for health and safety at work, and also for environmental and industrial control. In this context, it is particularly important to be able to easily and quickly detect a

visual signal that indicates the presence of an acidic atmosphere.^{53,54} Within this frame, a 5-min exposure to hydrogen chloride gases of sensory film **PA1** and membrane **M1** turn the yellowish materials to red or purple. Moreover, similarly to aqueous media, a UV/vis ratiometric response was observed for partial HCl pressures ranging 4×10^{-4} - 1×10^{-2} atm for the former and 4×10^{-7} - 9×10^{-2} atm for the latter (Figures 3 and S10 (ESI)).

Smart fibres and fabrics as colorimetric acid sensors

Intelligent fabrics or smart labels made of smart fibres are promising materials for future and forthcoming applications as stand-alone systems in a number of advanced technological fields, such as sensors and actuators, energy storage tools, stimuli responsive materials, etc.^{18,55-57}

Within this context, we believe that smart textiles capable of sensing acidic media with macroscopic colour changes as a signal are promising materials. In this line, the coating of commercial fibres is a simple and straightforward way of economically transforming these fibres into smart fibres without impairing the weaving and wearable characteristics of the fabrics prepared with them. Thus, we have coated commodity cotton fabrics and high-tech *meta*- and *para*-aramid fabrics and yarns with acrylic and aramid sensory coatings, with a weight percent coating ranging from 0.4 to 1.6% in the case of the aramid and from 96 to 674% for the acrylic coatings. These coated yarns and fabrics changed their colour clearly upon exposure to HCl vapour from orange to pink-red for the aramid coating and to dark purple in the case of the acrylic coating, as depicted in Table 1.

Conclusions

Colorimetric sensory polymers sensitive toward acidic media, both in water and in the environment, have been designed and transformed or synthesised into manageable films or membranes, or even as acid-responsive

commodity and high-tech textiles that change their colour upon contact with an acidic aqueous atmosphere. These sensory materials are reusable; the materials are recovered by washing with water and are highly stable under acidic conditions for long periods of time. The polymeric materials were both aromatic polyamides and an acrylic network with gel behaviour. The polymers have covalently bonded conjugated azo groups and amino moieties in their pendant structure: the former as a colorimetric moiety and weak basic motif, and the latter also as a weak, but stronger, basic group and simultaneously as an electron donor or electron withdrawal group in its non-protonated and protonated forms. The pK_a s of the protonisable groups were different for the various polymers and also for the measurements in water and in air, and allowed for the detection of acidic media in water ranging from a concentration of perchloric acid of 1×10^{-2} to 3 M, and in air ranging from a vapour pressure of hydrogen chloride of 4×10^{-7} - 9×10^{-2} atm. Accordingly, the envisaged application includes intelligent textiles and tags for use in health and safety at work, along with applications for acidity control in industrial processes and laboratories and in the environment.

Acknowledgements

We gratefully acknowledge the financial support provided by the Spanish Ministerio de Economía y Competitividad-Feder (MAT2011-22544 and MAT2014-54137-R) and by the Consejería de Educación - Junta de Castilla y León (BU232U13).

Notes and references

Departamento de Química, Facultad de Ciencias, Universidad de Burgos, Plaza de Misael Bañuelos s/n, 09001 Burgos, Spain. Fax: (+) 34 947 258 831, Tel: (+) 34 947 258 085. E-mail: jmiguel@ubu.es.

Electronic Supplementary Information (ESI) available: experimental part (intermediate, monomer and material characterization, correlation between the acidity function (H_0) and the concentration of perchloric acid, titration of perchloric acid, titration of HCl vapours, pK_1 of monomer (**3**) and model (**5**) calculated by ^1H NMR, response time, and interference study. See DOI: 10.1039/b000000x/

- 1 R. G. Bates, *Determination of pH: Theory and Practice*, 2nd Ed., Wiley-Interscience, New York, 1973.
 - 2 D. Wencel, T. Abel, and C. McDonagh, Optical Chemical pH Sensors, *Anal. Chem.*, 2014, **86**, 15–29.
 - 3 Z. Jin, Y. Su and Y. Duan, *Sens. Actuators B*, 2000, **71**, 118–122.
 - 4 H.-X. Chen, X.-D. Wang, X.-H. Song, T.-Y. Zhou, Y.Q. Jiang and X. Chen, *Sens. Actuators B*, 2010, **146**, 278–282.
 - 5 D. K. Nordstrom, C. N. Alpers, C. J. Ptacek, D. W. Blowes, Negative pH and Extremely Acidic Mine Waters from Iron Mountain, California, *Environ. Sci. Technol.*, 2000, **34**, 254–258.
 - 6 K. J. Kuhn and J. T. Dyke, *Anal. Chem.*, 1996, **68**, 2890–2896.
 - 7 M. Shamsipur and G. Azimi, *Anal. Lett.*, 2001, **34**, 1603–1616.
 - 8 W. P. Carey and M. D. DeGrandpre, *Anal. Chem.*, 1989, **61**, 1674–1678.
 - 9 L. R. Allain, K. Sorasaene and Z. Xue, *Anal. Chem.*, 1997, **69**, 3076–3080.
 - 10 M.H. Noiré, L. Couston, E. Douarre and D. Pouy, *J. Sol-Gel Sci. Technol.*, 2000, **17**, 131–136.
 - 11 J. M. García, F. C. García, F. Serna and J. L. de la Peña, *Prog. Polym. Sci.*, 2010, **35**, 623–686.
 - 12 K. Marchildon, *Macromol. React. Eng.*, 2011, **5**, 22–54.
 - 13 M. Trigo-López, J. L. Pablos, F. C. García, F. Serna and J. M. García, *J. Polym. Sci., Part A: Polym. Chem.*, 2014, **52**, 1469–1477.
 - 14 M. Trigo-López, J. L. Barrio-Manso, F. Serna, F. C. García and J. M. García, *Macromol. Chem. Phys.*, 2013, **214**, 2223–223.
 - 15 S. Vallejos, A. Muñoz, S. Ibeas, F. Serna, F. C. García and J. M. García, *J. Mater. Chem. A*, 2013, **1**, 15435–15441.
 - 16 J. L. Pablos, M. Trigo-López, F. Serna, F. C. García and J. M. García, *Chem. Commun.*, 2014, **50**, 2484–2487.
 - 17 S. Vallejos, A. Munoz, S. Ibeas, F. Serna, F. C. García and J. M. García, *J. Hazard. Mater.*, 2014, **276**, 52–57.
 - 18 J. L. Pablos, M. Trigo-López, F. Serna, F. C. García and J. M. García, *RSC Adv.*, 2014, **4**, 25562–25568.
 - 19 O. Korostynska, K. Arshak, E. Gill and A. Arshak, *Sensors*, 2007, **7**, 3027–3042.
 - 20 T. A. Canada, L. R. Allain, D. B. Beach and Z. Xue, *Anal. Chem.*, 2002, **74**, 2535–2540.
-

- 21 Y. Tian, E. Fuller, S. Klug, F. Lee, F. Su, L. Zhang, S. Chao and D. R. Meldrum, *Sens. Actuators B*, 2013, **188**, 1–10.
 - 22 U.-W. Grummt, A. Pron, M. Zagorska and S. Lefrant, *Anal. Chim. Acta*, 1997, **357**, 253-259.
 - 23 Q.-J. Ma, H.-P. Li, F. Yang, J. Zhanga, X.-F. Wu, Y. Bai and X.-F. Li, *Sens. Actuators B*, 2012, **166–167**, 68–74.
 - 24 P. Hashemi and R. A. Zarjani, *Sens. Actuators B*, 2008, **135**, 112–115.
 - 25 D. Wencel, B.D. MacCraith and C. McDonagh, *Sens. Actuators B*, 2009, **139**, 208–213.
 - 26 Yordan Kostov and Stoyan Tzonkov, *Anal. Chim. Acta*, 1993, **280**, 15-19.
 - 27 S. Blair, M. P. Lowe, C. E. Mathieu, D. Parker, P. K. Senanayake and R. Katakya, *Inorg. Chem.*, 2001, **40**, 5860-5867.
 - 28 A. Lobnik, I. Oehme, I. Murkovic and O. S. Wolfbeis, *Anal. Chim. Acta*, 1998, 367, 159-165.
 - 29 A. A. Ensafi and A. Kazemzadeh, *Microchem. J.*, 1999, **63**, 381–388.
 - 30 S. Capel-Cuevas, M. P. Cuéllar, I. de Orbe-Payá, M.C. Pegalajar and L. F. Capitán-Vallvey, *Microchem. J.*, 2011, **97**, 225–233
 - 31 Q. Tang, X. Meng, H. Jiang, T. Zhou, C. Gong, X. Fu and S. Shi, *J. Mater. Chem.*, 2010, **20**, 9133-9139.
 - 32 N. Feng, G. Han, J. Dong, H. Wu, Y. Zheng and G. Wang, *J. Colloid. Interface. Sci.*, 2014, **421**, 15-21.
 - 33 L. Chen, S.-G. Li, Y.-P. Zhao, Y.-C. Wang and Q.-W. Wang, *J. Appl. Polym. Sci.*, 2005, **96**, 2163-2167.
 - 34 A. M. Sanchez and R. H. de Rosi, *J. Org. Chem.*, 1995, **60**, 2974-2976.
 - 35 A. M. Sanchez and R. H. de Rosi, *J. Org. Chem.*, 1996, **58**, 2094-2096.
 - 36 S. Ciccone and J. Halpern, *Can. J. Chem.*, 1959, **37**, 1903-1910.
 - 37 H. H. Jaffé and R. W. Gardner, *J. Am. Chem. Soc.*, 1958, **80**, 319-322.
 - 38 I. M. Klotz, H. A. Fiess, J. Y. Chen Ho and M. Melody, *J. Am. Chem. Soc.*, 1954, **76**, 5136-5140.
 - 39 S. Miao, H. Li, Q. Xu, N. Li, J. Zheng, R. Sun, J. Lu and C. M. Lic, *J. Mater. Chem.*, 2012, **22**, 16582-16589.
 - 40 C. D. Diakoumakos and J. A. Mikroyannidis, *J. Appl. Polym. Sci.*, 1998, **64**, 921-930.
 - 41 D. Ramachandran, C. C. Corten and M. W. Urban, *RSC. Adv.*, 2013, **3**, 9357-9364.
 - 42 J. L. Barrio-Manso, P. Calvo, F. C. García, J. L. Pablos, T. Torroba and J. M. García, *Polym. Chem.*, 2013, **4**, 4256-4264.
 - 43 J. L. Pablos, P. Estévez, A. Muñoz, S. Ibeas, F. Serna, F. C. García and J. M. García, *J. Mater. Chem. A*, 2015, **3**, 2833-2843
 - 44 B. García and J.M. Leal, *Collect. Czech. Chem. Commun.*, 1987, **52**, 299-307.
 - 45 B. García and J.C. Palacios, *Ver. Bunsen. Phys. Chem.* 1998, **92**, 696-700.
 - 46 W. D. Chandler and D. G. Lee, *Can. J. Chem.*, 1990, **68**, 1757-1761.
 - 47 L. Hammett and A.J. Deyrup, *J. Am., Chem. Soc.*, 1932, **54**, 2721-2739.
 - 48 K. Yates and H. Wai, *J. Am. Chem. Soc.*, 1964, **86**, 5408-5413.
 - 49 R. A. Cox, *Adv. Phys. Org. Chem.*, 2000, **35**, 1-66.
-

- 50 B. García, J. M. Leal, J. C. Palacios, L. A. Herrero, *J. Chem. Soc. Perkin Trans. 2*, 1988, 1759-1768.
 - 51 B. García, F. Secco, S. Ibeas, A. Muñoz, F. J. Hoyuelos, J. M. Leal, M.L. Senent, M. Venturini. *J. Org. Chem.*, 2007, **72**, 7832-7840.
 - 52 Marvin Suite software, ver. 6.2.1, ChemAxon Ltd (<http://www.chemaxon.com>), 2014.
 - 53 D. S. Ballantine Jr. and D. Callahan, *Talanta*, 1992, **39**, 1657-1667.
 - 54 M. G. Baron, R. Narayanaswamy and S. C. Thorpe, *Sens. Actuators B*, 1996, **34**, 511-515.
 - 55 L. Van Langenhove, C. Hertleer and A. Schwarz, *Smart Textiles: An Overview*, in *Intelligent Textiles and Clothing for Ballistic and NBC Protection*, NATO Science for Peace and Security Series B: Physics and Biophysics, eds. P. Kiekens and S. Jayaraman, Springer, Dordrecht, 2012, ch. 6, pp. 119-136.
 - 56 P. Westbroek, G. Priniotakis and P. Kiekens, *Intelligent/smart materials and textiles: an overview*, in *Analytical electrochemistry in textiles*, Woodhead Publishing Limited and CRC Press LLC: Cambridge: 2005, ch. 8, pp. 215-243.
 - 57 K. Cherenack and L. van Pieterse, *J. Appl. Phys.*, 2012, **112**, 091301.
-

CAPÍTULO 3

Polímeros de altas prestaciones

Más rápido, más fuerte, más ligero, más seguro... Estas exigencias siempre han llevado a los investigadores y a las empresas a la búsqueda y desarrollo de nuevos materiales para obtener productos de consumo que las satisfagan. Las poliamidas aromáticas se consideran materiales de altas prestaciones y se caracterizan por un comportamiento térmico y mecánico excepcional. Actualmente los trabajos del Grupo se dirigen hacia aplicaciones determinadas en Ciencia y Tecnología relacionadas con las propiedades que puedan aportar las características químicas o físicas de diseño específico de los nuevos polímeros. En este sentido se han sintetizado poliamidas aromáticas con coloración azul inherente y poliamidas con grupos funcionales en su estructura que mejoran las propiedades de las aramidas comerciales y que además permiten la preparación de polímeros a la carta de forma sencilla.

3.1. Introducción

Los materiales de altas prestaciones se caracterizan por presentar propiedades especiales; y es la combinación de una serie de propiedades lo que le hace tener un valor añadido a un determinado producto. Las características que suelen tener los polímeros de altas prestaciones incluyen alta resistencia térmica y a la llama, baja densidad, alta resistencia química, resistencia a la

hidrólisis y a la corrosión, buenas propiedades mecánicas, buen aislamiento eléctrico, facilidad de ser transformados, etc.

Los materiales de altas prestaciones se pueden clasificar, según su naturaleza, en: metálicos y aleaciones, cerámicos y vítreos, poliméricos y materiales compuestos. Los polímeros de altas prestaciones difieren de los plásticos estándar y de los plásticos de ingeniería principalmente en su estabilidad térmica y química y en sus propiedades mecánicas. Los polímeros de altas prestaciones generalmente son termoplásticos, y su temperatura continua de servicio (CST, *Continuous Service Temperature*), temperatura a la cual una determinada propiedad mecánica disminuye un 50% en un tiempo dado, está siempre por encima de los 150°C.⁸⁸

En un principio, la denominación de materiales de altas prestaciones comenzó a utilizarse para materiales que pudieran sustituir satisfactoriamente en algunas aplicaciones a metales tales como el aluminio. Sin embargo, las propiedades de los polímeros, a diferencia de las de los metales, se ven muy afectadas por la temperatura de trabajo, y sus propiedades mecánicas son dependientes del tiempo de aplicación del esfuerzo. En este sentido, los polímeros estarían en desventaja frente a los metales, pero sin embargo, presentan grandes ventajas sobre éstos dada su baja densidad, elevada resistencia química y ambiental, facilidad de procesado y diseño, y sencillez en la composición química de cara a la modificación a medida de las propiedades.

Generalmente los polímeros de altas prestaciones se obtienen por polimerización de monómeros que incorporan anillos bencénicos en su cadena principal. Estos anillos aromáticos dan rigidez a la cadena y confieren temperaturas de fusión muy elevadas, haciendo que el material pueda estar expuesto a altas temperaturas durante periodos de tiempo prolongados. Ejemplos de estos materiales son los polímeros de la familia de las poliimidias y

⁸⁸ E.A. Campo. *Thermal properties of polymeric materials* en "Selection of polymeric materials: how to select design properties from different standards", William Andrew Publishing, Norwich, 2008.

poliamidas, poliarilétercetonas, poliésteres aromáticos y polisulfonas, entre otros. Estos materiales tienen un coste elevado, son difíciles de procesar y se utilizan para la preparación de bienes de alto valor añadido.

3.1.1. Poliamidas aromáticas como materiales de altas prestaciones

Las poliamidas son polímeros que incorporan un grupo amida en su unidad estructural. Tanto los nailons (*nylons*) como las poliamidas aromáticas (o aramidas) se consideran polímeros de ingeniería, pero la estructura aromática de las aramidas confiere a estos polímeros unas características especiales que les hace menos sensibles a la oxidación y más resistentes a los disolventes y a la llama. Además tienen un buen comportamiento dieléctrico, propiedades no magnéticas, buena resistencia a la fatiga y excelente resistencia mecánica y térmica. Por lo tanto se les considera materiales de altas prestaciones.

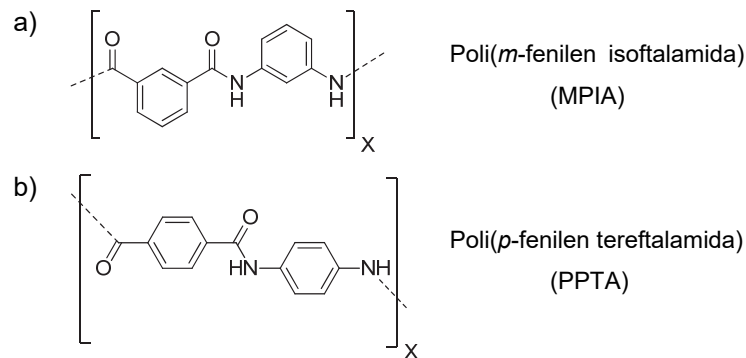


Figura 3.1. Estructura química de la MPIA (a) y la PPTA (b).

Las aramidas comerciales más conocidas son la poli(*m*-fenilen isoftalamida), MPIA, y la poli(*p*-fenilen tereftalamida), PPTA. Su estructura se muestra en la Figura 3.1. Estas poliamidas se pueden transformar en fibras sintéticas con aplicaciones tecnológicas en el campo de los recubrimientos y rellenos en la industria aeroespacial y de armamento, sustitución en asbestos, aislamiento eléctrico, chalecos antibalas, filtros industriales y tejidos deportivos, entre otras. Debido a su estructura química, hay un gran esfuerzo de

investigación dirigido a la explotación de las características de altas prestaciones de estos polímeros para obtener materiales electro o fotoluminiscentes, membranas de ósmosis inversa o membranas de intercambio iónico, materiales ópticamente activos, nanocompuestos, etc., con comportamientos mecánicos y térmicos superiores.

3.1.2. Propiedades de las poliamidas aromáticas

Las características de altas prestaciones de la PPTA son consecuencia de su estructura química. La estructura aromática con enlaces *para* orientados da lugar a macromoléculas rígidas con alta energía de cohesión y alta tendencia a la cristalinidad debido al establecimiento de puentes de hidrógeno intramoleculares a través de los grupos amida (Figura 3.2).⁸⁹⁻⁹² En consecuencia, una poliamida aromática con enlaces orientados en *meta*, la MPIA, produce una estructura menos lineal con la consiguiente reducción en la energía de cohesión y en cristalinidad, junto con una mayor solubilidad, lo que permite no solo su procesamiento en fibras y tejidos, sino también su utilización en forma de recubrimientos de alta resistencia.

La Tabla 3.1 resume las características físicas de las fibras de algunas poliamidas comerciales.⁹³⁻⁹⁶ Cabe destacar que las poliamidas aromáticas poseen baja inflamabilidad, gran resistencia térmica y puntos de fusión elevados, en muchos casos mayores de 500 °C, que se encuentran a

⁸⁹ H. H. Yang, *Kevlar aramid fiber*. John Wiley & Sons, Chichester, 1993.

⁹⁰ S. S. Kathiavelu, *Synth. Fib.* **2003**, 32, 12.

⁹¹ S. Reboullai, *Aramids high-performance fibres* en "Hearle JWS, Ed. Woodhead Publishing Limited series on fibres. CRC Press, Boca Raton, 2004.

⁹² V. Gabara, J. D. Hartzler, K-S. Lee, D. J. Rodino, H. H. Yang, *Aramid Fibers. Handbook of fiber chemistry*, en Lewin M, Ed. "International fiber science and technology series". Vol. 16, 3rd ed. CRC Taylor & Francis, 2007.

⁹³ J. Gallini. *Polyamides, aromatic* en "Encyclopedia of polymer science and technology", Vol. 3, John Wiley & Sons, Nueva York, 2005.

⁹⁴ S. Ozawa, K. Matsuda, *Aramid copolymer fibers* en "Handbook of fiber science and technology". Vol. 3, Marcel Dekker Inc., Nueva York, 1989.

⁹⁵ D. Tanner, J. A. Fitzgerald, P. G. Riewald, W. F. Knoff. *Aramid structure/property relationships and their role in applications development* en "Handbook of fiber science and technology", Vol 3, Marcel Dekker Inc., Nueva York, 1989.

⁹⁶ H. H. Yarn. *Nomex aramid fiber* en "Handbook of fiber science and technology", Vol 3, Marcel Dekker Inc., Nueva York, 1993.

veces por encima del punto de descomposición. Su elevada temperatura de transición vítrea T_g es consecuencia de la rigidez estructural y de los enlaces de hidrógeno. Estas mismas características son responsables de su solubilidad limitada y elevada resistencia química.

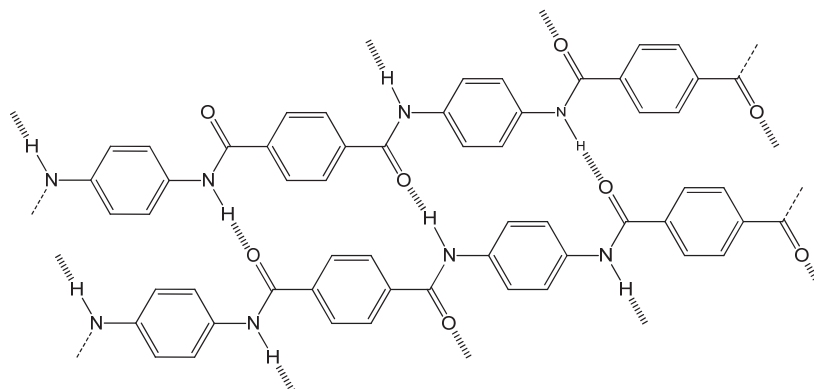


Figura 3.2. Formación de enlaces de hidrógeno intercatenarios en la PPTA.

Tabla 3.1. Propiedades de fibras de algunas poliamidas aromáticas comerciales.

Propiedad	Polímero	
	PMIA	PPTA
Densidad (g/cm ³)	1,38	1,44
Absorción de agua (%), a 65% HR ^a	5,2	3,9
Propiedades térmicas		
T_g (°C)	275	--
T_m (°C)	365 d ^b	> 500 d ^b
T_d (°C, en N ₂)	400-430	520-540
Propiedades mecánicas en tracción		
Resistencia a la tracción (MPa)	0,59-0,86	2,9-3,0
Modulo de Young (GPa)	7,9-12,1	70-112
Elongación (%)	20-45	2,4-3,6
Índice límite de oxígeno (L.O.I.)	29	29

a: humedad relativa.

b: descompone.

Los módulos elásticos y resistencias específicas son extremadamente altos como resultado de la alineación de la cadena polimérica en una dirección, con una distribución de la orientación a lo largo del eje muy estrecha. Por este

motivo las poliamidas aromáticas tienen una resistencia a la tracción comparable a la de los metales, y son más fuertes que los cables de acero y más rígidas que el vidrio.

Otro factor a tener en cuenta en las aramidas es la absorción de agua, presente generalmente en la atmósfera en la que se aplican. La capacidad relativamente alta de absorción de agua de las aramidas convencionales proviene de la interacción por puentes de hidrógeno de los grupos amida polares con las moléculas de agua.⁹⁷ Las cadenas laterales con grupos polares en los polímeros incrementan habitualmente la absorción de agua a través de nuevos puentes de hidrógeno con estas moléculas.

Estas propiedades hacen que estos materiales sean resistentes y tenaces, adecuados no sólo en aplicaciones como fibras textiles, sino también como materiales de ingeniería (fibras de alto módulo, refuerzo en mezclas de polímeros y materiales compuestos, etc.).

3.1.3. Diseño y síntesis de nuevos polímeros de altas prestaciones

Actualmente, la investigación básica en poliamidas aromáticas se lleva a cabo de dos maneras: a) tratando de resolver los problemas asociados a la elevada energía de cohesión de las aramidas que dan lugar a materiales difíciles de transformar debido a su extremadamente baja solubilidad y su excepcionalmente alta temperatura de transición vítrea; y b) expandiendo el alcance de sus aplicaciones como materiales de altas prestaciones en áreas nuevas, como materiales ópticos activos, luminiscentes, de intercambio iónico, resistentes a la llama y que puedan formar fibras. La manera de llevar esto a cabo es mediante: la introducción de grupos voluminosos laterales,⁹⁸⁻¹⁰³

⁹⁷ J. De Abajo, J. G. de la Campa, A. E. Lozano, J. Preston, *Polyisophthalamides (Enhancement of water-uptake)* en "Polymeric Materials Encyclopedia", Salamote, J.C. Ed., Vol. 8, 6325, Nueva York, 1996.

⁹⁸ J. F. Espeso, J. G. de la Campa, A. E. Lozano, J. de Abajo, *J. Polym. Sci. Part A Polym. Chem.* **2000**, *38*, 1014.

la incorporación de cadenas flexibles en el esqueleto de la poliamida, o la introducción de anillos *meta* orientados¹⁰⁴⁻¹⁰⁶ o asimétricamente sustituidos.¹⁰⁷⁻¹⁰⁹

Desde la experiencia previa, y siguiendo una de las líneas de investigación del Grupo de Polímeros, se orientó el trabajo a la obtención de poliamidas aromáticas con características físicas y/o químicas mejoradas respecto a las PPTA y la MPIA comerciales, con el objetivo de ampliar sus aplicaciones. La síntesis de estos nuevos polímeros se llevó a cabo mediante las dos vías de obtención comentadas en la introducción: la síntesis integral de nuevos monómeros y posterior polimerización y la modificación de polímeros existentes.

Por un lado se sintetizaron poliamidas aromáticas *meta*-orientadas con coloración azul inherente a partir de nuevos monómeros cromóforos y su posterior polimerización. Por otro lado se sintetizaron aramidas a partir de nuevos monómeros con grupos reactivos azida. La reactividad de los grupos azida permitió, mediante modificación de los polímeros sintetizados, la preparación de forma sencilla y rápida de materiales entrecruzados y de un gran número de poliamidas con distintos grupos laterales, tal y como se describe a lo largo de este capítulo.

⁹⁹ J. F. Espeso, E. Ferrero, J. G. de la Campa, A. E. Lozano, J. de Abajo, *J. Polym. Sci. Part A: Polym. Chem.* **2001**, 39, 475.

¹⁰⁰ D. J. Liaw, B. Y. Liaw, *Polymer* **2001**, 42, 839.

¹⁰¹ J. J. Ferreira, J. G. de la Campa, A. E. Lozano, J. de Abajo, J. Preston, *J. Polym. Sci. Part A: Polym. Chem.* **2007**, 45, 4671.

¹⁰² S. H. Hsiao, Y. M. Chang, *J. Polym. Sci. Part A Polym. Chem.* **2004**, 42, 4056.

¹⁰³ F. Serna, F. García, J. L. de la Peña, J. M. García, *High Perform. Polym.* **2008**, 20.

¹⁰⁴ J. M. García, J. G. de la Campa, G. Schwarz, J. de Abajo, *Macromol. Chem. Phys.* **2001**, 202, 1298.

¹⁰⁵ H. Nasr-Isfahani, K. Faghihi, N. Valikhani, *J. Appl. Polym. Sci.* **2009**, 111, 1769.

¹⁰⁶ M. C. E. J. Niesten, J. Feijen, R. J. Gaymans, *Polymer* **2000**, 41, 8487.

¹⁰⁷ S. Nakata, J. Brisson, *J. Polym. Sci. Part A Polym. Chem.* **1997**, 35, 2379.

¹⁰⁸ K. Faghihi, Z. Mozaffari, *J. Appl. Polym. Sci.* **2008**, 108, 1152.

¹⁰⁹ L. Li, O. Haba, T. Endo, M. Ueda, *High Perform. Polym.* **2001**, 13, 217.

3.2. Poliamidas aromáticas con coloración azul inherente

El color azul es el color más demandado en el mercado de las fibras de aramida para equipos de protección. Por ello, en el Grupo de Investigación se ha trabajado en la preparación de poliamidas aromáticas de altas prestaciones con coloración azul inherente, mediante la polimerización de una diamina que contiene el grupo cromogénico azadipirrometeno (ADPM) en su estructura con los monómeros comerciales *m*-fenilendiamina y cloruro de isoftaloilo. Las nuevas poliamidas azules obtenidas tienen mejores propiedades térmicas que la MPIA comercial.

3.2.1. Coloración de fibras de aramida y moléculas derivadas de azadipirrometenos

Las poliamidas aromáticas, o aramidas, se transforman generalmente en fibras para la elaboración de materiales de altas prestaciones, como tejidos de protección, papel aislante, materiales compuestos y recubrimientos. La tinción de estos materiales es compleja debido tanto a la propia estructura química que da lugar a fuertes interacciones intercatenarias, como a la alta cristalinidad, fomentada en el proceso de hilado de cara a la consecución de elevadas propiedades mecánicas y térmicas de las fibras. Por tanto, la producción de fibras de poliamidas aromáticas coloreadas es un tema de gran interés tecnológico, dadas las grandes dificultades que presenta su tinción.

En la producción a gran escala de fibras de aramida, la *meta*-aramida se tiñe mediante el uso de colorantes catiónicos y agentes químicos (*carriers*) para facilitar la penetración del colorante.¹¹⁰ A pesar de que la tintura catiónica permite obtener un gran rango de colores, la resistencia a la luz de este tipo de tintura no es elevada y se sitúa casi siempre en el límite bajo para los requerimientos de mercados y de usuarios exigentes.

¹¹⁰ M. R. Kim, H. Kim, J. J. Lee, *Fiber. Polym.* **2013**, *14*, 2038.

También es posible teñir de un modo más permanente y eficaz las aramidas mediante la inyección de sustancias colorantes que se añaden como un concentrado al polímero inmediatamente antes de la extrusión de la fibra. Este proceso se conoce como teñido en masa (*producer color*). Las ventajas de este procedimiento son que los procesos textiles no tienen que soportar los rigores de teñido, y la solidez del tinte es generalmente superior a la tintura catiónica tradicional.

Las poliamidas aromáticas coloreadas intrínsecamente se obtienen mediante anclaje de un cromóforo a su estructura.¹¹¹ De acuerdo con esto, se diseñó y sintetizó una diamina que presenta un cromóforo azul en su estructura, un derivado de azadipirrometeno, y que es el responsable del color azul de la poliamida.

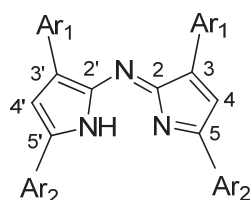


Figura 3.3. Núcleo de azadipirrometeno.

Los derivados de los azadipirrometenos (ADPM) son un tipo de cromóforos orgánicos azules descubiertos por Rogers en la década de 1940.¹¹² Son muy atractivos desde el punto de vista de sus propiedades ópticas, similares a las de los porfirinoides (cromóforos naturales de la clorofila). Los ADPM tienen muchas ventajas desde el punto de vista sintético comparado con los porfirinoides y al mismo tiempo mantienen una banda de absorción muy intensa (ϵ hasta $1 \times 10^5 \text{ M}^{-1} \text{ cm}^{-1}$) en la región del amarillo-rojo del espectro.¹¹³ Además es posible afinar las propiedades de color mediante la modificación de

¹¹¹ J. Eric Riordan and Hal. S. Blair, *Polymer* **1979**, *20*, 196.

¹¹² M. A. T. Rogers, *Nature* **1943**, *151*, 504.

¹¹³ A. Bessette, M. Cibian, F. Be' langer, D. De'silets and G. S. Hanan, *Phys. Chem. Chem. Phys.* **2014**, *16*, 22207.

los sustituyentes en el núcleo de ADPM (Figura 3.3), lo que les permite tener numerosas aplicaciones ópticas y electroquímicas en el campo de sensores, componentes de materiales activos a la luz, aparatos fotovoltaicos, etc.

3.2.2. Poliamidas con derivados de azadipirrometeno en su estructura

Se sintetizaron, mediante reacciones relativamente sencillas y con altos rendimiento, un monómero cromóforo y un modelo de poliamida derivados de azadipirrometeno (Figura 3.4). El modelo de poliamida se sintetizó para probar previamente la posibilidad de llevar a cabo la reacción de condensación sobre el monómero. El monómero cromóforo se utilizó para la preparación de las tres poliamidas aromáticas azules de la Figura 3.5 con un 0,1%, 1,0% y 10% en moles de unidad estructural que contiene el cromóforo, lo que permite modular la tonalidad. En este caso, las poliamidas se sintetizaron a baja temperatura por copolimerización con cloruro de isoftaloilo y *m*-fenilendiamina.

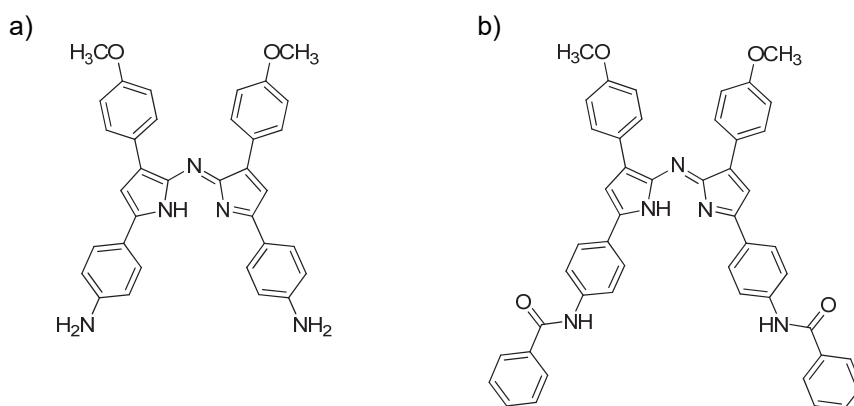


Figura 3.4. a) Estructura química del monómero cromóforo, y b) estructura química del modelo de poliamida

En general, la modificación de la estructura química de las aramidas para que posean características especiales conlleva una pérdida paralela de propiedades térmicas y mecánicas. Por lo tanto, es conveniente que la

proporción de grupos voluminosos en la cadena sea baja, $\leq 10\%$ en moles, para posibilitar la formación de enlaces de hidrógeno entre las cadenas, y por consiguiente su empaquetamiento molecular y su tendencia a la cristalinidad.

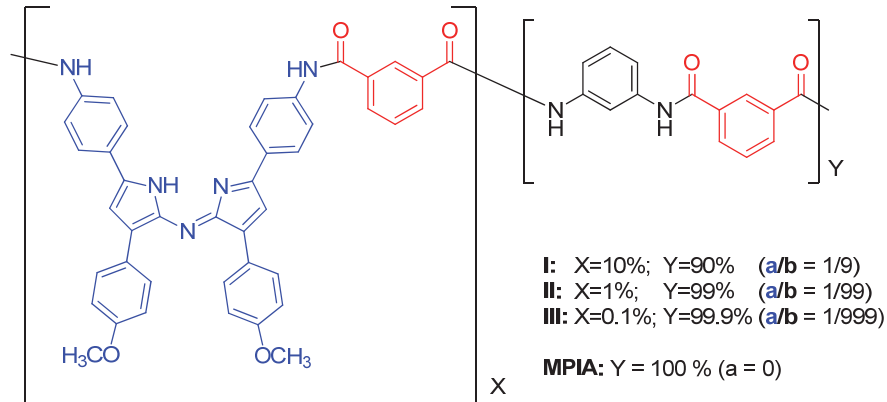


Figura 3.5. Estructura química de las poliamidas azules

La caracterización de los polímeros se puede abordar desde una doble vía: la puramente estructural, y la que implica la determinación del grado de conversión de la polimerización.¹¹⁴ Es conveniente resaltar que grados de conversión bajos dan lugar a polímeros con estructuras químicas correctas, desde el punto de vista del análisis mediante técnicas espectroscópicas, pero con pesos moleculares bajos y, por lo tanto, propiedades generales menores de las que se obtendrían con pesos moleculares altos. En el caso de las poliamidas azules sintetizadas, tanto la estructura química obtenida, como el peso molecular de las poliamidas determinado mediante la viscosidad inherente son correctos. Este hecho se traduce en la obtención de poliamidas con buenas propiedades mecánicas y térmicas; estas últimas incluso sorprendentemente mejoradas respecto a la MPIA comercial.

¹¹⁴ S. R. Sandler, W. Karo, J. Bonesteel, *Polymer Characterization* en "Polymer Synthesis and Characterization", E. M. Pearce eds., Academic Press, Nueva York, 1998.

3.2.3. Aplicaciones

El desarrollo de fibras que presenten una coloración inherente a la propia constitución química del material, y que por tanto no sea necesario someterlas a tinciones tras su producción, presenta un elevado interés industrial por dos motivos: simplifica un proceso industrial de producción de fibras coloreadas, ya que se suprime el paso de tinción de las fibras, y permite la obtención de un material con un color intrínseco mucho más homogéneo y duradero. Esto hace que las poliamidas aromáticas coloreadas tengan un valor añadido mayor.

Las fibras de poliamidas aromáticas se utilizan como materiales de altas prestaciones para la preparación de tejidos, por ejemplo. En este sentido el color azul es uno de los más demandados para la vestimenta en defensa civil, fuerzas de seguridad del estado y bomberos. Además la tonalidad de azul se puede modificar afinando las proporciones de unidad estructural que contiene el cromóforo. También es posible modificar el color del polímero mediante procesos redox que afectan al cromóforo, tal y como se ha visto en el estudio espectroelectroquímico realizado a uno de los polímeros en el que el máximo de absorbancia se desplaza de 700 a 775 nm tras la oxidación del núcleo de ADPM.

3.2.4 Resultados

A continuación se describen los resultados obtenidos a través de la transcripción íntegra del trabajo publicado.

❖ *Intrinsically colored wholly aromatic polyamides (aramids)*

Los detalles experimentales y de caracterización se encuentran en el material suplementario, cuya copia está disponible en el CD adjunto.

Intrinsically colored wholly aromatic polyamides (aramids)

Intrinsically colored wholly aromatic polyamides (aramids)

Miriam Trigo-López, Álvaro Miguel-Ortega, Saúl Vallejos, Asunción Muñoz, Daniel Izquierdo, Álvaro Colina, Félix Clemente García, José Miguel García.*

Departamento de Química, Facultad de Ciencias, Universidad de Burgos, Plaza de Misael Bañuelos s/n, 09001 Burgos, Spain. Email: jmiquel@ubu.es



This work describes the preparation of intrinsically blue-colored, high-performance aromatic polyamides (aramids). The color was achieved by preparing a diamine monomer containing a chromogenic azadipyrromethene (ADPM) core, which after polymerizing it with commercially available *m*-phenyleneisophthalamide and isophthaloyl chloride gave the blue-colored polyisophthalamide copolymers. These materials were structurally compared to commercialized and high-value-added *meta*-aramid fibers [poly(*m*-phenyleneisophthalamide), **MPIA**, brand names: NOMEX® and Teijinconex®]. Blue is the highest demanded color in the market of protective aramid fibers. The coloration efficiency of this special monomer is very high. Furthermore, the aramids showed even better thermal properties than commercial **MPIA**.

KEYWORDS: aramids; aromatic polyamides; high performance polymers; inherently colored polymers; intrinsically colored polymers; self-colored polymers.

1. Introduction

Wholly aromatic polyamides, usually termed as aramids, are high value-added high-performance materials. They are prepared and commercialized as outstanding thermally and mechanically resistant fibers. The commercial success of the aramids started in the 1960s with the discovery of the all-*para*-phenylene oriented aramid fiber, poly(*p*-phenylene terephthalamide), by Stephanie Kwolek at DuPont, which is commercialized under the trade name Kevlar®. Concomitantly, this put into the market the all-*meta*-phenylene oriented aramid fiber, MPIA, under the trade name Nomex®. Two decades later, the company Teijin made the only break-through in 50 years of commercial success of aramids with the commercialization of Technora®, the aramid with a copolymer structure comprising *meta*- and *para*-phenylene oriented rings, poly(*p*-phenylene-co-3,4'-oxydiphenylene terephthalamide).¹⁻⁶

Both the remarkable thermal and fire resistance, and the mechanical strength of aramids come from their chemical structure. Thus, the rigidity of the main polymer chain due to the wholly aromatic structure conjugated with the amide groups, the high average bond energy, along with the strong and highly directional interchain hydrogen bonds between amide moieties, provide the materials with extraordinary cohesive energy. The fibers are obtained by wet, dry or dry-jet wet spinning of aramid solutions. The properties of the fibers are physically enhanced by improving the rod-like structure and the percentage and quality of crystalline microdomains by cold and heat drawing after fiber spinning and coagulation. This increases the intermolecular packing and also the cohesive energy even further. The fibers are obtained as flogs, staple and continuous fibers that are used for

preparing yarns and fabrics for apparel (protective clothing such as fire, chemical and saw protection suits, and bullet-proof body armor), isolating paper, composites, and high temperature industrial filters, among others, covering the broad range of value-added products related with the following industrial sectors: transport (e.g., automotive and aerospace), oil and gas, protection and defense, telecom, and civil engineering.⁷⁻¹⁶

Although in some industrial applications (e.g., composites and hot gas filtration) the natural yellowish color of the fibers is used, generally most of the applications require colored fibers, specifically those related with apparels, carpets, drapes, etc. However, the aramid fibers have poor dyeing properties for the same reasons that make them extremely thermal and mechanical resistant, i.e., the dense molecular packaging, the cohesive energy, the molecular interactions and the chain orientation and crystallinity. Colored yarns can be obtained by dyeing the fibers or by dope dyed. In conventional dyeing of aramid fibers, the affinity toward conventional dyes has to be improved by expansion of the amorphous regions with the combination of swelling agents and extremely high temperatures, over 190°C.¹⁷ For this reason, the dope dyeing using pigments is usually preferred, and dope dyed yarns are usually used for garments woven with aramids. Anyhow, dyeing impairs the properties of the fibers and at the same time the resistance to fading is barely achieved.

Ideal color fastness of fibers is achieved by intrinsically, inherently or self-colored polymers.¹⁸⁻²¹ Inherently colored macromolecules are polymers with chromophores in their structure, i.e., polymers that have dye motifs chemically anchored. Accordingly, we designed and prepared a blue chromophore as an aromatic diamine monomer, and we used it to synthesize blue meta-aramids. The color hue was modified by tuning molar content of the chromophore monomer in relation with the conventional diamine monomer, i.e., *m*-phenylenediamine. The chromophore motifs

cannot migrate and are evenly distributed along the polymer chains due random copolymerization. Moreover, the impressive thermal properties of the aramids are even improved by using this colored monomer.

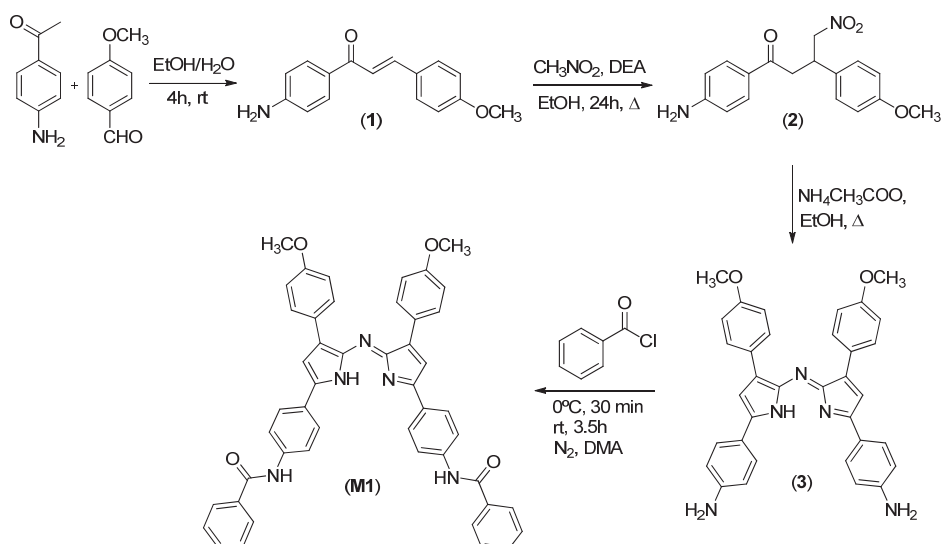
2. Experimental

All materials and solvents were commercially available and used as received, unless otherwise indicated. *p*-aminoacetophenone (99%, Aldrich), NaOH (99.9%, VWR-Prolabo), *p*-anisaldehyde ($\geq 98\%$, Merck), diethylamine (DEA) (98%, Aldrich), nitromethane ($\geq 95\%$, Aldrich), ammonium acetate (97%, Alfa Aesar), benzoyl chloride (99%, Aldrich), tetrabutylammonium hexafluorophosphate (TBAPF₆) (98%, Aldrich), ethanol (99.9%, VWR-Prolabo), methanol ($\geq 99.8\%$, Aldrich), dimethyl sulfoxide (DMSO) (99%, Prolabo), deuterated dimethyl sulfoxide (DMSO-*d*₆) (99.80D, VWR-Prolabo), and sulfuric acid (100%, Merck) were used as received. *N,N*-dimethylacetamide (DMA) ($\geq 99\%$, Aldrich) was vacuum distilled over phosphorous pentoxide twice and then stored over 4Å molecular sieves. *m*-phenylenediamine (MPD) is commercially available ($> 99\%$; Aldrich) and was purified by double vacuum sublimation. Isophthaloyl dichloride (ICL) ($> 99\%$, Aldrich) was purified by double crystallization from heptane (99.9%, VWR-Prolabo).

2.1. Synthesis

2.1.1. Synthesis of intermediates, monomer and model

The synthetic steps carried out to prepare monomer (**3**) and model (**M1**) are depicted in Scheme 1.



Scheme 1: Synthesis of monomer **(3)** and model **(M1)**.

Synthesis of (*E*)-1-(4-aminophenyl)-3-(4-methoxyphenyl)prop-2-en-1-one (1): A stirred mixture of 5.0 g (37 mmol) of *p*-aminoacetophenone, 140 mL of ethanol and 240 mL of aqueous NaOH 4M solution was brought to 0°C. 5.05 g (37 mmol) of *p*-anisaldehyde was added and the mixture was stirred at room temperature for 4 h. The flask was kept at 4 °C for 12 h, and then filtered off. The compound was dissolved in 300 mL of boiling methanol. The hot solution was filtered off and the solvent was evaporated to give compound **(1)**. Yield: 4.8 g (51%). M.p.: 120 ± 1 °C. ¹H NMR δ_H (400 MHz, DMSO-*d*₆, Me₄Si): 7.95 (2H, d, *J* 8.7 Hz, Ph); 7.83 (2H, d, *J* 8.8 Hz, Ph); 7.77 (1H, d, *J* 15.5 Hz, CH); 7.63 (1H, d, *J* 15.5 Hz, CH); 7.03 (2H, d, *J* 8.8 Hz, Ph); 6.65 (2H, d, *J* 8.8 Hz, Ph); 6.14 (2H, s, NH₂); 3.85 (3H, s, CH₃). ¹³C NMR, δ_C (100.6 MHz, DMSO-*d*₆, Me₄Si): 186.80, 161.74, 154.61, 142.24, 131.87, 131.17, 128.71, 126.46, 120.84, 115.23, 113.62, 56.24. EI-LRMS *m/z*: 253.11 (M⁺, 100), 252.10 (35), 238.08 (38), 225.11 (18), 210.08 (22), 161.06 (18), 145.05 (15), 120.04 (73), 92.05 (22), 65.04 (18). HRMS calcd. for (C₁₆H₁₅NO₂): 253.1103; Found: 253.1102. FT-IR [wavenumbers (cm⁻¹)]: ν_{NH2}: 3350; ν_{C=O}: 1640.

Synthesis of 1-(4-aminophenyl)-3-(4-methoxyphenyl)-4-nitrobutan-1-one (2): 1 g (3.95 mmol) of compound **(1)** and 2.041 mL (19.73 mmol) of DEA were mixed in a pressure tube together with 10 mL of ethanol. Then, 2.138 mL (39.5 mmol) of nitromethane was added to the mixture. The solution was refluxed for 24 h. The solvent was evaporated under vacuum and 20 mL of diethyl ether was added to the brown oil. A palid yellow solid was formed, and it was filtered off and air dried. Yield: 0.74 g (60%). M.p.: 99 ± 1 °C. ^1H NMR δ_{H} (400 MHz, DMSO- d_6 , Me $_4$ Si): 7.69 (2H, d, J 8.7 Hz, Ph); 7.30 (2H, d, J 8.6 Hz, Ph); 6.97 (2H, d, J 8.6 Hz, Ph); 6.58 (2H, d, J 8.7 Hz, Ph); 6.11 (2H, s, NH $_2$); 4.95 (1H, dd, J 12.7 Hz, J 5.6 Hz, CH $_2$ -NO $_2$); 4.82 (1H, dd, J 12.6 Hz, J 10.0 Hz, CH $_2$ -NO $_2$); 3.99 (1H, dd, J 9.6 Hz, J 6.1 Hz, CH); 3.74 (3H, s, CH $_3$); 3.35 (1H, dd, J 17.2 Hz, J 7.5 Hz, CH $_2$); 3.23 (1H, dd, J 17.1 Hz, J 6.8 Hz, CH $_2$). ^{13}C NMR, δ_{C} (100.6 MHz, DMSO- d_6 , Me $_4$ Si): 195.17, 159.15, 154.74, 132.99, 131.31, 129.73, 125.19, 114.70, 113.40, 80.98, 55.87. EI-LRMS m/z : 314.10 (M $^+$, <1), 268.10 (13), 239.10 (12), 134.06 (10), 121.03 (22), 120.03 (100), 106.05 (5). FT-IR [wavenumbers (cm $^{-1}$)]: ν_{NH_2} : 3364; $\nu_{\text{C=O}}$: 1622; δ_{NH_2} : 1596; $\nu_{\text{as NO}_2}$: 1580; $\nu_{\text{s NO}_2}$: 1349.

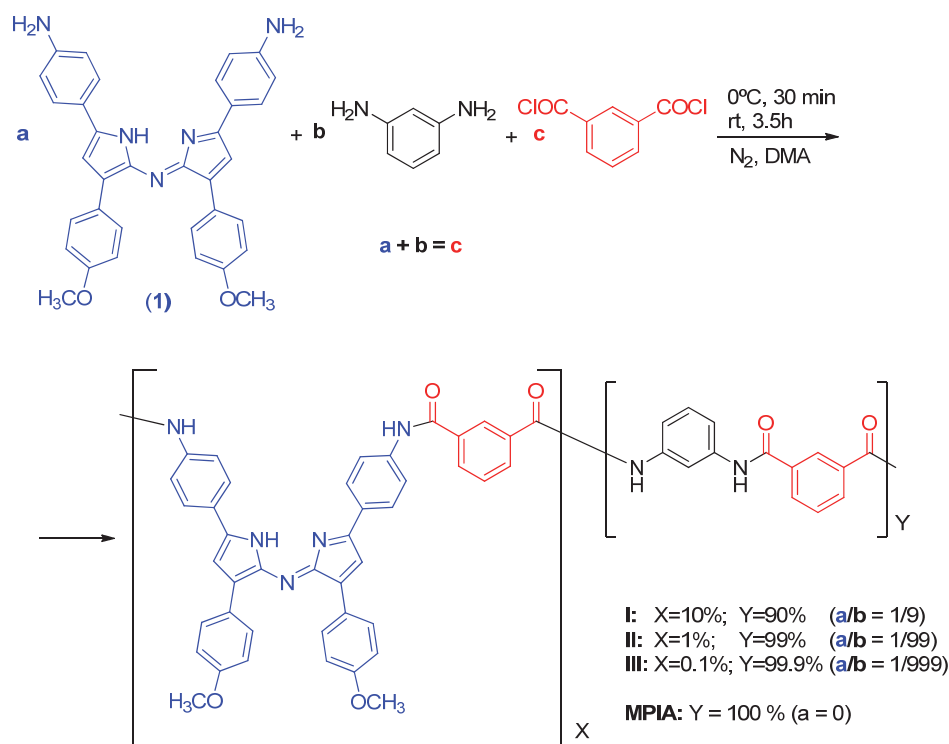
Synthesis of (Z)-5-(4-aminophenyl)-N-(5-(4-aminophenyl)-3-(4-methoxyphenyl)-2H-pyrrol-2-ylidene)-3-(4-methoxyphenyl)-1H-pyrrol-2-amine (3): Compound **(2)** (1 g, 3.18 mmol), ammonium acetate (8.309 g, 107.7 mmol) and ethanol (18 mL) were heated under reflux for 24 h in a pressure tube. The reaction solvent was evaporated under vacuum, and 50 mL of distilled water was added to the crude product. The mixture was stirred at room temperature for 10 min, and the green solid was filtered off and air dried. Yield: 0.67 g (80%). M.p.: 235 ± 1 °C (decomp.). ^1H NMR δ_{H} (400 MHz, DMSO- d_6 , Me $_4$ Si): 12.87 (1H, s, NH); 8.10 (4H, d, J 8.7 Hz, Ph); 7.78 (4H, d, J 8.6 Hz, Ph); 7.36 (2H, s, CH); 7.07 (4H, d, J 8.8 Hz, Ph); 6.78 (4H, d, J 8.6 Hz, Ph); 6.02 (4H, s, NH $_2$); 3.88 (6H, s, CH $_3$). ^{13}C NMR, δ_{C} (100.6 MHz, DMSO- d_6 , Me $_4$ Si): 159.99, 154.40, 152.30, 149.26, 140.51, 130.60, 128.98, 127.44, 119.77, 115.08, 114.72, 113.66, 56.13. EI-LRMS m/z : 539.23 (M $^+$,

100), 540.23 (40), 524.21 (8), 280.15 (6), 279.15 (26), 269.63 (16), 264.14 (20), 249.15 (6), 120.07 (6), 69.02 (5). HRMS calcd. for (C₃₄H₂₉N₅O₂): 539.2321; Found: 539.2310. FT-IR [wavenumbers (cm⁻¹)]: ν_{NH}: 3466, 3320, 3210; ν_{C=N}: 1627, 1594; δ_{NH2}: 1565, 1544.

Synthesis of model (M1): To a solution of benzoyl chloride (0.80 mmol, 0.112 g) in 0.6 mL of DMA at 0°C, 0.178 g (0.33 mmol) of compound **3** was added portionwise keeping vigorous stirring for 30 min under nitrogen, and then at room temperature for an additional 3.5 h. The final solution was slowly poured into distilled water, forming a dark blue solid that was filtered and washed thoroughly with water. Yield: 0.21 g (83%). ¹H NMR δ_H (400 MHz, DMSO-*d*₆, Me₄Si): 12.76 (1H, s, NH); 10.62 (2H, s, NH); 8.11-8.04 (14H, m, Ph); 7.69-7.57 (10H, m, Ph, CH); 7.05 (4H, d, *J* 8.8 Hz, Ph); 3.88 (6H, s, CH₃). ¹³C NMR, δ_C (100.6 MHz, DMSO-*d*₆, Me₄Si): 165.96, 159.62, 153.85, 141.54, 134.76, 131.97, 130.27, 128.72, 128.60, 127.91, 127.78, 127.55, 126.17, 125.97, 120.54, 114.07, 113.93, 55.31. EI-LRMS *m/z*: 747.28 (M⁺, 3), 628.26 (5), 384.20 (30), 383.20 (97), 368.19 (100), 353.17 (5), 279.17 (10), 278.17 (37), 263.16 (28), 181.04 (8), 169.04 (9), 131.04 (11), 119.04 (12), 105.09 (77). HRMS calcd. for (C₄₈H₃₇N₅O₄): 747.2846; Found: 747.2841. FT-IR [wavenumbers (cm⁻¹)]: ν_{NH}: 3283; ν_{C=O}: 1654; ν_{C-N}: 1243.

2.1.2. Synthesis of polymers

The preparation of copolyamides **I**, **II**, and **III** is schematically shown in Scheme 2. The synthesis of copolyamide **I** is described below as an illustrative example.



Scheme 2. Synthesis of copolyamides I, II and III.

A three necked flask with a nitrogen inlet and a mechanical stirrer was charged with 4.26 mL of DMA under a blanket of nitrogen at room temperature. Then, 0.23 g (0.426 mmol) of diamine **1** and 0.41 g (3.834 mmol) of MPD were added. The solution was stirred at room temperature until the solution of the diamine. The system was then cooled to 0 °C, and 0.86 g (4.260 mmol) of ICL was added portionwise (four equal amounts) over 5 min. The mixture was allowed to react under nitrogen at 0 °C for 30 min, and then at room temperature for additional 3.5 h. The final solution was slowly poured into distilled water, forming a dark blue, fibrous, swollen polymer precipitate that was filtered, washed thoroughly with water and acetone. The yield was quantitative.

2.2. Measurements

^1H and ^{13}C NMR spectra were recorded with a Varian Inova 400 spectrometer operating at 399.92 and 100.57 MHz, respectively, with deuterated dimethyl sulfoxide ($\text{DMSO-}d_6$) as solvent.

Infrared spectra (FT-IR) were recorded with a FT/IR-4200 FT-IR Jasco Spectrometer with an ATR-PRO410-S single reflection accessory. Low-resolution electron impact mass spectra (EI-LRMS) and high resolution electron impact mass spectra (EI-HRMS) were obtained at 70 eV on an Aligent 6890N mass spectrometer and on a Micromass AutoSpec mass spectrometer respectively.

Thermogravimetric analysis (TGA) data were recorded on a 5 mg sample under a nitrogen or oxygen atmosphere on a TA Instrument Q50 TGA analyzer at a scan rate of $10\text{ }^\circ\text{C min}^{-1}$. LOI was estimated using the experimental Van Krevelen equation, $\text{LOI} = 17.5 + 0.4 \text{ CR}$, where CR is the char yield weight percentage at 800°C , which was obtained from TGA measurements in a nitrogen atmosphere.²²

Melting points (m.p.) were visually determined with a Gallenkamp melting point apparatus.

UV/Vis spectroelectrochemical measurements were carried out using a SPELEC (DropSens), a commercial fully integrated synchronized spectroelectrochemical device. The light beam, supplied by a 360-2500 nm tungsten-halogen light source was both conducted to and collected from the spectroelectrochemical cell by a $200\text{ }\mu\text{m}$ reflection probe (RPROBE, DropSens). A standard three-electrode cell was used in all experiments, consisting of a commercial Pt working electrode, a Pt wire as auxiliary electrode and a homemade Ag/AgCl/KCl (3 M) reference electrode. The polymer was deposited on the Pt working electrode by drop casting.

Reflection UV/Vis data were recorded using a spectrometer QE-65000 (Ocean Optics) with a light beam supplied by an Avalight-DH-s-BAL Deuterium-halogen light source(Avantes), guided and collected by a reflection probe FCR-7IR200-2-2.5x100 (Avantes).

The polymer solubility was determined by mixing 10 mg of the polymer with 1mL of a solvent, followed by stirring for 24 h at 20°C. The polymer was considered soluble at room temperature if a homogeneous solution was obtained. If the polymer was not soluble, the system was heated to reflux to 2 h, and the polymer was considered soluble on heating if a homogeneous solution was obtained. Otherwise, the polymer was considered insoluble. The polymer inherent viscosities were measured with a Ubbelohde viscometer using *N*-methyl-2-pyrrolidone and sulfuric acid (100%) as solvents at 25 ± 0.1 °C and a polymer concentration of 0.5 g dL⁻¹.

Water sorption experiments were conducted gravimetrically at room temperature. 200 mg of the sample was dried at 60 °C for 24 h over phosphorus pentoxide, and the sample was placed in a closed box containing a saturated aqueous solution of NaNO₂ at 25 °C, which provided a relative humidity of 65%. The samples were weighed periodically over a period of 8 days until they equilibrated with their surroundings and presented no further changes in weight.

Polyamide films were prepared by evaporation of cast solutions of 12% by polymer weight in DMA. The solvent was eliminated by heating at 80 °C overnight. To determine the tensile properties of the polyamide, strips (5 mm in width and 30 mm in length) were cut from a polymer film of 551µm thickness for I on a SHIMADZU EZ Test Compact Table-Top Universal Tester at 20°C. Mechanical clamps were used and an extension rate of 5 mm min⁻¹ was applied using a gauge length of 9.44 mm. At least 6 samples were tested, and the data was then averaged.

3. Results and discussion

The preparation of inherently colored aromatic polyamides is a promising methodology for the exploitation of the high-performance thermal and mechanical properties of the aramids in the preparation of fibers for protective clothes. In this regard, it is advisable to modify as little as possible the aromatic nature of the main chain to maintain the outstanding properties of the aramids and at the same time achieving the new functionalities of the materials, i.e., permanent color in the development we are reporting, that increases even more their value added. In our case, we prepared a diamine monomer as novel blue chromophore for the preparation of a set of inherently blue copolyamides **I**, **II** and **III**, in which the color hue can be easily tuned by adjusting its feed percentage in the synthesis of the aramids. In our study, we have prepared aromatic copolyamides as **MPIA** derivatives with 0.1, 1.0 and 10.0% of structural units containing the chromophore (**3**) (Scheme 2).

In an initial approach to the preparation of the inherently colored polyamides we modeled the chemical modification reactions using a polyamide model to assure that the condensation reaction is carried out in a clean manner, i.e., without side reactions or any modification of the chromophore core.

For comparative purposes, some of the properties of the colored aramids are compared with those of the commercial *m*-aramid, **MPIA**, which we prepared following the standard procedure for aramid synthesis depicted in Scheme 2.

3.1. Polymer synthesis and characterization

The monomer (**3**) was prepared in a straightforward manner from commercially available materials, as shown in Scheme 1. The synthesis of

model **M1** (Scheme 1) was conducted according to a synthetic procedure similar to the one used in the preparation of the polymers (Scheme 2).

Thus, the preparation of the model containing the chromophore, **M1**, was easily achieved from (**3**) and benzoyl chloride. The FT-IR and ^1H and ^{13}C NMR spectra of the model confirm its structure and purity (Supporting information, Figure S4).

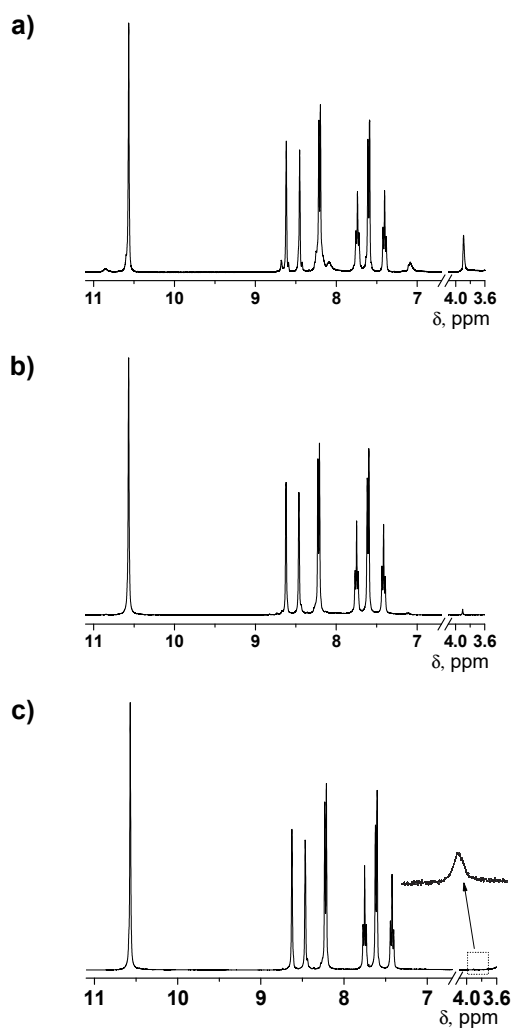


Figure 1. ^1H NMR spectra of copolyamides: a) I; b) II; and c) III.

As previously mentioned, aromatic copolyamides with a low percentage of modification of the structural units from the commercial aramids are interesting materials that can impart new properties and characteristics without penalizing their outstanding mechanical and thermal properties. The structure of the copolymers was in agreement with the NMR data (Figure 1) and the content of structural units corresponded with the feed molar ratio of the chromophore monomer (**3**), as per the integral ratio of the methyl protons of methoxy group (~3.9 ppm) to the aromatic region (7-9 ppm) in ^1H NMR spectra.

The chemical constitution limits the upper performance of materials. However, correct chemical structures do not guarantee the achievement of the highest properties, which are affected by different concomitant factors, such as molecular weight. This parameter is related with viscosity and in the field of high performance materials the inherent viscosity (η_{inh}) is usually studied for comparative purposes.

The viscosity is solvent dependent, and for this reason the inherent viscosity was measured in two different solvents (Table 1). Aramids with η_{inh} higher than 0.5 in NMP are usually considered as high molecular weight polymers, and our data are consistent with this approach.

Table 1. Inherent viscosity and water sorption of the polymers.

Polymer	η_{inh} (dL/g) [§]	Water uptake (%) ^{&}
I	0.76 (0.48)	7
II	1.15 (0.47)	7
III	1.03 (0.53)	7

[§] Polymer concentration = 0.5 g/dL; temperature = 30 °C; solvents: sulfuric acid 100% and NMP, the data obtained in NMP between brackets.

[&] Water sorption at 65% RH.

Polymers with polar groups absorb water from the environment, influencing their performance. The amide linkage of aramids is highly polar and its interaction with water molecules is highly favorable. The water sorption lowers the thermal transitions by weakening the amide-amide strong interactions impairing the electrical insulation, the mechanical, and the thermal properties. Conversely, a high water uptake is interesting for other technological fields in which aramids play an important role, such as membrane technology for water desalination, i.e., reverse osmosis membranes. The water sorption is limited by the aramid crystallinity. The prepared aramids absorb 7% by weight of water, a data fully comparable with laboratory prepared **MPIA** samples (the reported water uptake for commercial **MPIA** fibers is 5.2 %).⁷

The polymer **II** was characterized by time-resolved UV/Vis absorption spectroelectrochemistry. This multiple response technique allows us to obtain electrochemical and molecular information simultaneously. Polymer oxidation was studied using cyclic voltabsorptometry by scanning the potential between 0.00 V and +1.60 V at a scan rate of 0.02 V s⁻¹ in a 0.1 M TBAPF₆ acetonitrile solution. The cyclic voltammograms (Figure 2a) shows an ill-defined response providing little information on the oxidation process. However, the optical response is much more informative. Figure 2b shows the UV/Vis spectra in which a band centered at 775 nm evolves during the oxidation process. This band is related to the oxidation of the ADPM.²³ The corresponding voltabsorptogram at 775 nm is shown in Figure 2c. At lower potentials there is no change in the absorbance, but when the potential reaches a value of +0.70 V, the band centered at 775 nm starts to grow. At higher potentials the intensity of this band increases until the oxidation of the polymer is completed. As can be observed in Figure 2c, absorbance does not decrease in the backward scan and, therefore, the initial value of absorbance is not recovered after the oxidation, indicating that an irreversible oxidation of the polymer is taking place.

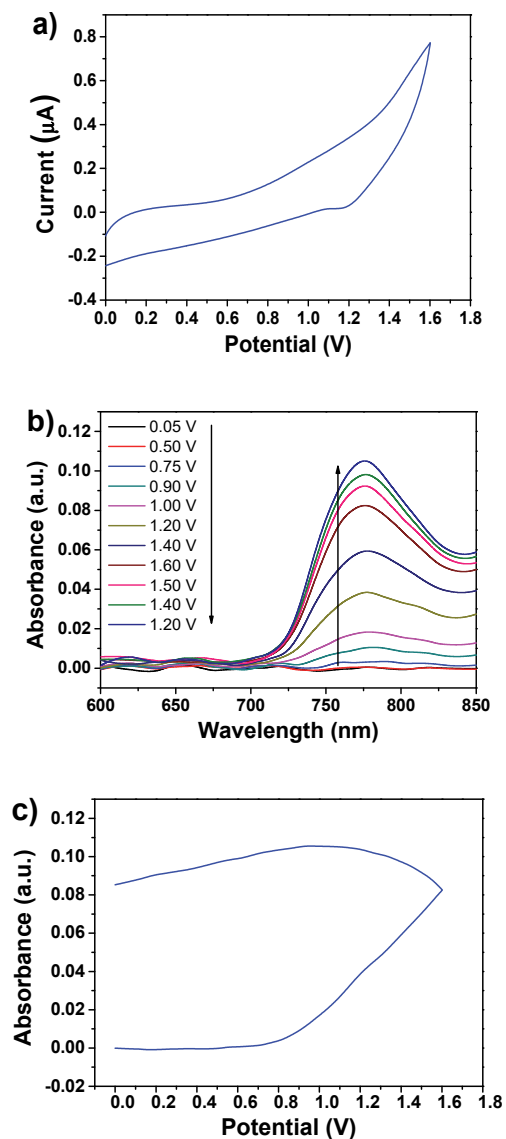


Figure 2. Electrochemical analysis of polymer II (film obtained by casting, 13 μm thickness): (a) Cyclic voltammogram obtained in 0.1 M TBAPF₆ acetonitrile solution. Potential was scanned between 0.00 V and +1.60 V at 0.020 V s⁻¹; (b) Evolution of the UV/Vis absorption spectra during the oxidation of the polymer; (c) Cyclic voltabsorptogram at 775 nm.

3.2. Solubility and water uptake

The lack of solubility has always been a drawback of polyamides and has limited their technological applications. However, the copolymers described in this work are highly soluble compared with aramids and can be dissolved at room temperature in polar aprotic solvents, such as NMP, DMSO, and DMA (Table 2). At this point, it is important to comment that the commercial **MPIA** is transformed into fibers by wet, dry or dry-jet wet spinning from a DMA solution of approximately 19.2% **MPIA**. As expected, the low-molecular-weight model is soluble in conventional organic solvents.

Table 2. Solubility of the polymers.[§]

Polymer	Solvents					
	DMSO, DMA	NMP, DMF	THF	Acetone	CHCl ₃ , CH ₂ Cl ₂ , EtOH	Cyclohexanone
I	++	++	-	-	-	-
II	++	++	-	-	-	-
III	++	+	-	-	-	-
MPIA	++	++	-	-	-	-
M1	++	++	++	+	+-	++

[§] Essay: 10 mg of polymer in 1 mL of solvent. Solubility: ++ = soluble at room temperature, + = soluble on heating, +- = partially soluble, - = insoluble.

Regarding the water uptake, the absorption of 7% by weight of water is similar to that of **MPIA**. This indicates that water affinity of the structural units containing the chromophore (**3**) of aramids **I**, **II** and **III** are similar to those of **MPIA**. Accordingly, this parameter will not affect the applicability of the materials as fibers in comparison with the commercial aramid fabrics.

3.3. Thermal and mechanical properties

The thermal resistance of the materials was considered to be related with the decomposition temperatures, in terms of weight loss, and with the char yield at a given temperature. The thermal resistance was evaluated using

TGA. The TGA data, summarized in Table 3, confirmed the good thermal stability of copolyamides, which surprisingly exhibited better thermal properties compared with the commercial aramid **MPIA**, which displayed 5% (T_5) and 10% (T_{10}) weight loss under nitrogen atmosphere of 432 and 452 °C, respectively.

Even more important than the weight loss at a given temperature is the minimum fraction of oxygen in a mixture of oxygen and nitrogen that will support combustion after ignition, that is, the LOI (limiting oxygen index), which is related to the char yield. The higher the char yield at 800 °C, the higher the LOI, and the better the flame resistance properties of the materials. LOI values higher than 21%, the oxygen content of air, will most likely not burn in an open-air situation. All LOI values are significantly higher than 21, and even higher than the LOI of **MPIA** calculated using the same method, which is 38. Considering this, the prepared materials have very good fireproof characteristics and must be considered as self-extinguishing materials.

In short, the results of the thermal behavior of the prepared aramids are quite shocking. We expected thermal property loss compared to commercial **MPIA** instead of an improvement. Remarkably, the improvement is more evident in oxidizing atmosphere (synthetic air) and even more striking in static thermogravimetric analysis at high temperature (350°C) (Figure 3).

The mechanical properties were similar to those of the reference *m*-aramid, **MPIA**, with tensile strength and Young's modulus of 51 and 1530 MPa, respectively, with elongation of 5 %.⁹ At this point, it is important to take into account that the measurements were carried out with lab-made un-oriented and thermally un-treated films prepared by casting.

Table 3. Thermal behavior of polymers I, II and III compared to MPIA.

Polymer	N ₂ atmosphere			O ₂ atmosphere (synthetic air)			
	T ₅ ^{a)} (°C)	T ₁₀ ^{b)} (°C)	CR ^{c)} (%)	T ₅ ^{a)} (°C)	T ₁₀ ^{b)} (°C)	CR ^{c)} (%)	LOI ^{d)}
I	416	448	58	427	462	-	41
II	444	463	56	451	482	1	40
III	449	472	60	451	480	-	42
MPIA	432	452	50	419	445	9	38

a) T₅: temperature at 5% weight loss is observed; b) T₁₀: temperature at 10% weight loss is observed; c) CR: char yield (%) at 800°C; d) Limiting oxygen index, calculated from the TGA data (LOI = 17.5 + 0.4 CR).

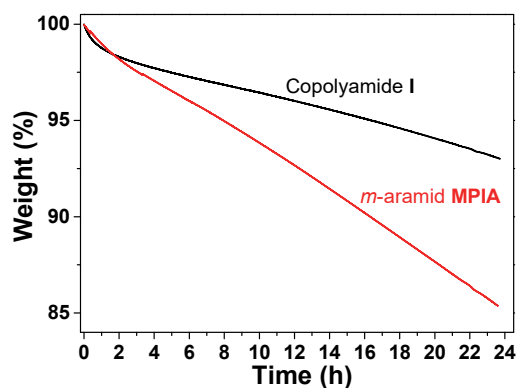


Figure 3. Weight loss of MPIA and aramid I after heating the polymers at 350 °C for 24 h in oxidizing (synthetic air) atmosphere.

3.4. Applicability of the intrinsically colored aramids

Colored commercial aramid fibers are highly demanded for protected apparels and are extremely expensive materials. However, the loss of color upon use is usual in all kind of fibers dyed using standard dyeing procedures. We have worked to solve this to increase even more the value added of the aramids and have reported a novel methodology to get inherently colored aromatic polyamides.

For this purpose we have chosen the blue color, which is usually associated with the apparels used in civil defense, e.g., state security forces and firefighters. The color hue can be tuned by means of increasing or decreasing the percentage of structural units containing the dye motifs (Figure 4). Moreover, different colors may be obtained by redox reaction affecting the chromophore motifs, as can be seen in the films with or without $\text{Al}(\text{NO}_3)_3 \cdot 9\text{H}_2\text{O}$ (Figure 5).

Research on yellow and red diamine monomers is on progress for the preparation of intrinsically colored aramids. With the correct copolymerization of the blue, red and yellow chromophores, the full color range will be available.

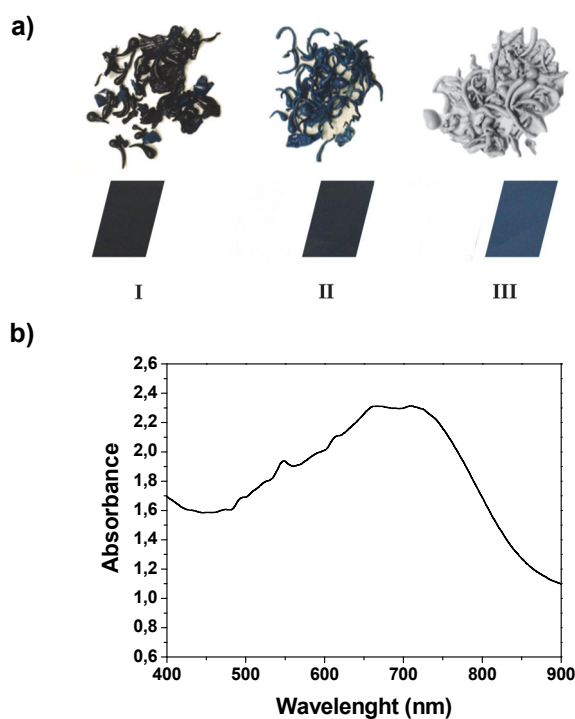


Figure 4. Color hue of the aramids as obtained upon precipitation after synthesis and films (a), and reflection Uv/vis spectrum (b) of polyamide II.

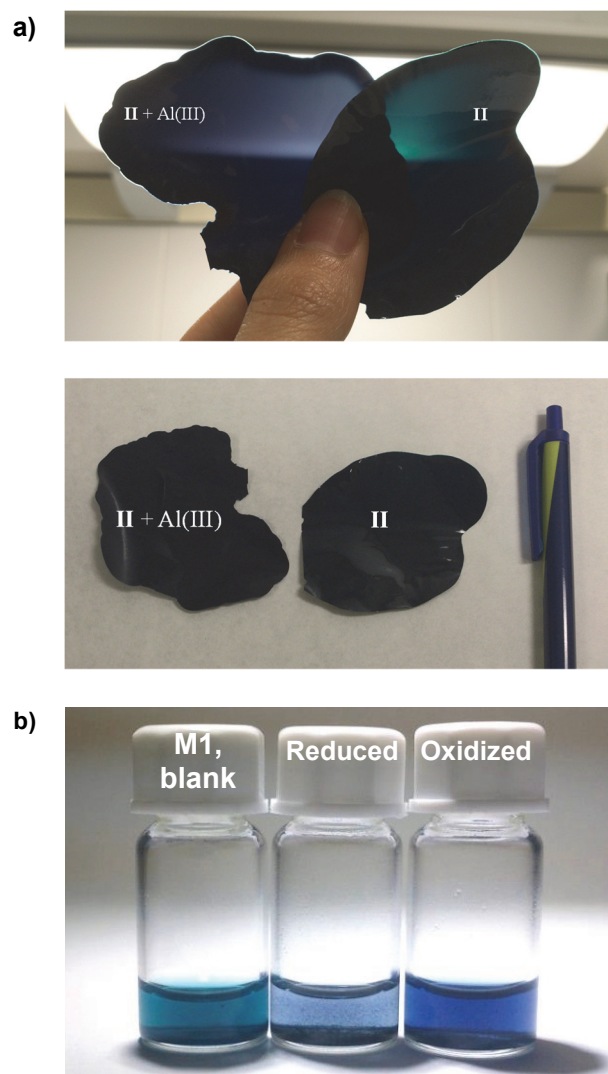


Figure 5. Aspect of polymer **II** and model **M1**: a) Color change upon adding $\text{Al}(\text{NO}_3)_3 \cdot 9\text{H}_2\text{O}$ to polymer **II**; b) color change upon reduction and oxidation (-1.3 V and 1.6 V respectively) of polyamide model **M1** in solution of acetonitrile ($5 \cdot 10^{-5}$ M).

4. Conclusions

We have synthesized a chromophore monomer that copolymerized with isophthaloyl dichloride and *m*-phenyldiamine results in a blue inherently colored wholly aromatic polyamide, specifically a *meta*-aramid. The blue is one of the highest demanded color in the market of protective aramid fibers. The coloration efficiency of this special monomer is very high. Moreover, it was intended to maintain the high mechanical and thermal properties of the reference aramids. Surprisingly, the thermal resistance has not only been maintained but notably improved. Furthermore, it has been demonstrated that the hue of the polyamide color can also be tuned by a redox process, and the evaluation of the application potential of this process is now under evaluation. Research is in progress for preparing yellow and red diamine monomers, and with the correct copolymerization of the described blue, and the forthcoming red and yellow chromophore monomers, the full color range will be available.

Acknowledgements

We gratefully acknowledge the financial support provided by the Spanish Ministerio de Economía y Competitividad-Feder (MAT2011-22544 and MAT2014-54137-R) and by the Consejería de Educación – Junta de Castilla y León (BU232U13).

Conflict of interest

A patent has been filled.

Supporting information

FT-IR, ¹H and ¹³C NMR of intermediates, monomer and model.

Notes and references

- 1 H.H. Yang, Kevlar Aramid Fiber, John Wiley & Sons, Chichester, 1993.
 - 2 H.H. Yang, Nomex aramid fiber, in *Handbook of fiber science and technology. Vol III: High technology fibers: part C*, ed. M. Lewin, J. Preston, Marcel Dekker Inc., New York, 1993, vol. 3, ch. 2, pp. 77-178.
 - 3 S. Rebouillan, Aramids, and A.R. Horrocks, H. Eichhorn, H. Schwaenke, N. Saville and C. Thomas, Thermally Resistant Fibres, in *High-performance fibres*, J.W.S. Hearle ed., CRC Press, Boca Raton, 2001, ch. 2 and 9.
 - 4 H.H. Yang, Aromatic high-strength fibers, Wiley, New York, 1989.
 - 5 S. Ozawa and K. Matsuda, Aramid copolymer fibers, in *Handbook of fiber science and technology. Vol III: High technology fibers: part B*, ed. M. Lewin, J. Preston, Marcel Dekker Inc., New York, 1989, vol. 3, ch. 1, pp. 1-34.
 - 6 D. Tanner, J.A. Fitzgerald, P.G. Riewald and W.F. Knoff, Aramid structure/property relationships and their role in applications development, in *Handbook of fiber science and technology. Vol III: High technology fibers: part B*, ed. M. Lewin, J. Preston, Marcel Dekker Inc., New York, 1989, vol. 3, ch. 2, pp. 35-80.
 - 7 J.M. García, F.C. García, F. Serna and J.L. de la Peña, *Prog. Polym. Sci.*, 2010, **35**, 623-686.
 - 8 K. Marchildon, *Macromol. React. Eng.* 2011, **5**, 22-54.
 - 9 M. Trigo-López, J.L. Barrio-Manso, F. Serna, F.C. García and J.M. García, Crosslinked Aromatic Polyamides: A Further Step in High-Performance Materials, *Macromol. Chem. Phys.*, 2013, **214**, 2223-2231.
 - 10 J. Gallini, Polyamides, aromatic, in *Encyclopedia of polymer science and technology*, John Wiley & Sons, New York, 2005, vol. 3, pp. 558-584.
 - 11 L. Vollbracht, Aromatic Polyamides, in *Comprehensive Polymer Science*, ed. G. Allen, B. Bevington, G.V. Eastmond, A. Ledwith, S. Russo, P. Sigwald, Pergamon Press, Oxford, 1989, vol. 5, ch. 22, pp. 373-383.
 - 12 J. Peterson, Aromatic Polyamides, in *Encyclopedia of Polymer Science and Engineering*, ed. H.F. Mark, N.M. Bikales, C.G. Overberger, G. Menges, John Wiley & Sons, Inc., New York, 1988, vol. 11, pp. 381-409.
 - 13 J.M. García, F.C. García, F. Serna and J.L. de la Peña, Aromatic Polyamides (Aramids), in *Handbook of Engineering and Specialty thermoplastics*, ed. S. Thomas and Visakh P.M., Wiley, Hoboken, 2012, ch. 6.
 - 14 S. Banerjee and S. Maji, High-Performance Processable Aromatic Polyamides, and M. Afshari, R. Kotek, P.G. Chen, High Performance Fibers, in *High Performance Polymers and Engineering Plastics*, V. Mittal Ed., Wiley, Hoboken, 2011, ch. 5 and 9.
 - 15 J.K. Fink, High performance polymers, William Andrew Inc, New York, 2008.
 - 16 P.E. Cassidy, Thermally stable polymers, Dekker, New York, 1980.
 - 17 E.-m. Kim, J.-h. Choi, Dyeing Properties and Color Fastness of 100 % *meta*-Aramid Fiber, *Fibers and Polymers* 2011, **12**, 484-490.
 - 18 B. Safabakhsh, A. Khosravi, K. Gharanjig, E. Kowsari, M. Khorassani and S.a Tafaghodi, Synthesis of a novel fluorescent coloured copolymer based on 4-butylthio-1,8-naphthalimide, *Color. Technol.*, 2012, **128**, 218-222
 - 19 J. Eric Riordan and Hal. S. Blair, Synthesis and characterization of inherently coloured azo polyamides, *Polymer*, 1979, **20**, 196-202.
-

- 20 S. Mallakpour, F. Rafiemanzelat and K. Faghihi, Synthesis and characterization of new self-colored thermally stable poly(amide-ether-urethane)s based on an azo dye and different diisocyanates, *Dyes Pigm.* 2007, **74**, 713-722.
 - 21 N.C. Tansil, L.D. Koh and M.-Y. Han, Functional Silk: Colored and Luminescent, *Adv. Mater.*, 2012, **24**, 1388-1397.
 - 22 D.W. van Krevelen, K. te Nijenhuis, *Properties of Polymers. Their Correlation with Chemical Structure; Their Numerical Estimation and Prediction from Additive Group Contributions*, 4th ed., Elsevier, Amsterdam, The Netherlands **2009**, pp. 855-857.
 - 23 A. N. Amin, M. E. El-Khouly, N. K. Subbaiyan, M. E. Zandler, M. Supur, S. Fukuzumi, F. D'Souza, *J. Phys. Chem. A*, 2011, **115**, 9810-9819.
-

3.3. Poliamidas aromáticas con grupos reactivos

Como se ha comentado anteriormente, las poliamidas aromáticas son materiales con propiedades térmicas y mecánicas excepcionales. La expansión de su campo de aplicación viene dado por la mejora de estas propiedades mediante distintos métodos entre los que se encuentra la introducción de grupos a la carta en la cadena principal. En este sentido, se han sintetizado polímeros con grupos reactivos azida en su estructura para preparar un polímero “madre” capaz de entrecruzar y de usarse para la preparación de muchos otros polímeros mediante la modificación de los grupos azida, de forma barata y sencilla.

3.3.1. Azidas aromáticas

Desde la preparación de la primera azida orgánica, la fenilazida, por Peter Griëß en el año 1864, estos intermedios flexibles y ricos en energía han suscitado un interés considerable, sobre todo a partir de la década de 1950, con la aparición de nuevas aplicaciones en la química de las acil, aril y alquil azidas.¹¹⁵ El interés comercial de estos compuestos comenzó con el uso de las azidas para síntesis de heterociclos como triazoles y tetrazoles, así como agentes de expansión y grupos funcionales en fármacos. La mayoría de las azidas son sustancias explosivas que descomponen con liberación de nitrógeno al aplicar algún tipo de energía, ya sea presión, impacto o calor. A pesar de sus propiedades explosivas, las azidas orgánicas son intermedios valiosos en síntesis orgánica. Se utilizan en cicloadición, síntesis de anilinas, y precursores de nitrenos.

Las azidas son grupos funcionales formados por tres nitrógenos con geometría lineal. La diversidad de las azidas viene determinada por sus propiedades fisicoquímicas, que se explican mediante una estructura

¹¹⁵ S. Bräse, C. Gil, K. Knepper, and V. Zimmermann, *Angew. Chem. Int. Ed.* **2005**, *44*, 5188.

mesomérica polar.¹⁰⁸ Las azidas aromáticas se estabilizan por conjugación del sistema aromático. Las estructuras dipolares *c* y *d*, también justifican la descomposición en el correspondiente nitreno y dinitrógeno, y la reactividad como dipolo-1,3 (Figura 3.6).

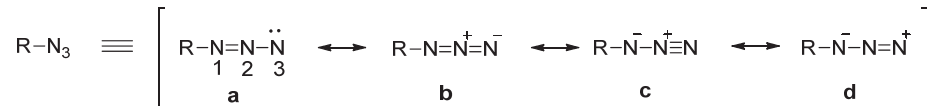


Figura 3.6. Estructuras resonantes del grupo azida.

La regioselectividad de su reactividad con electrófilos y nucleófilos se explica en relación a la estructura *d* (ataque en N^3 por nucleófilos, mientras que los electrófilos son atacados por N^1).

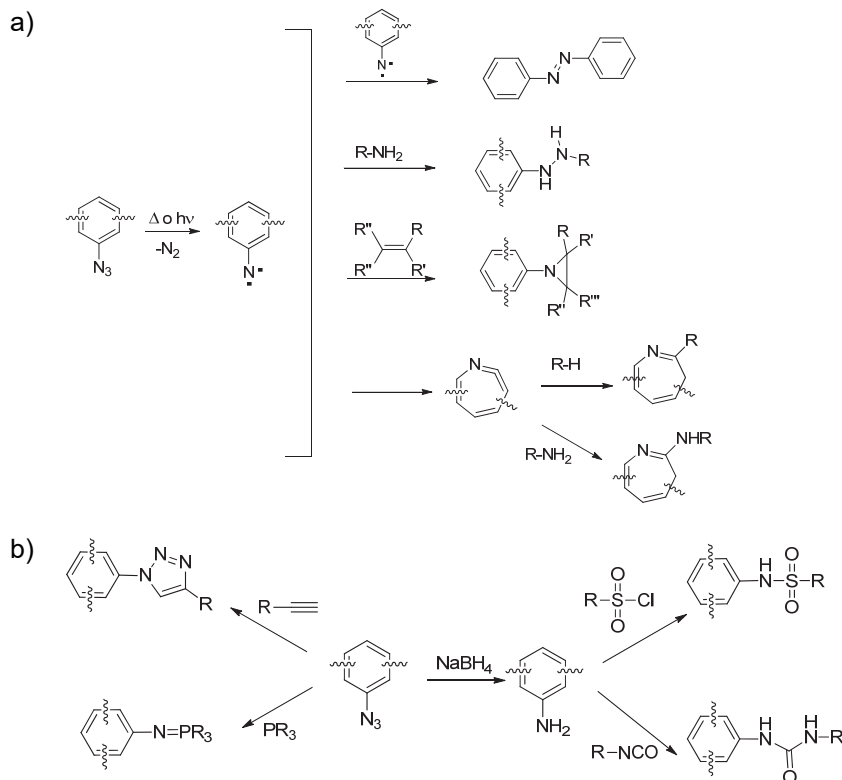


Figura 3.7. Ejemplos de la reactividad del grupo azida.

Las azidas reaccionan de forma muy distinta en diferentes condiciones de reacción. Ejemplos de la reactividad de este grupo vienen dados por la reactividad del nitreno por transformación de la azida (Figura 3.7a), así como por la reducción de la azida a amina para ampliar todavía más las numerosas posibilidades de reacción (Figura 3.7b).

3.3.2. Poliamidas aromáticas con grupos azida en su estructura

Hay tres maneras de mejorar las propiedades y las aplicaciones de las aramidas: la introducción de nuevos monómeros, la modificación de la estructura de un polímero existente y el entrecruzamiento.

En este apartado se han utilizado los tres métodos gracias a las posibilidades que ofrece el grupo azida. En un primer lugar se sintetizaron nuevos monómeros con grupos azida en su estructura para la preparación de aramidas. En segundo lugar, la presencia de estos grupos azida permitió el entrecruzamiento térmico de las cadenas de poliamida al transformarse en grupos reactivos nitreno. Por último, aunque la modificación química de las aramidas no es práctica debido a las restricciones por la solubilidad, en este caso se ha demostrado la facilidad de preparación de nuevas poliamidas por modificación química de las poliamidas con grupos azida en su estructura, posibilitando la obtención de materiales a la carta debido a la versatilidad del grupo azida.

El estudio de estas nuevas poliamidas ha dado lugar a dos trabajos. El primero trata de la síntesis a baja temperatura y caracterización de nuevas homopoliamidas y copoliamidas aromáticas (Figura 3.8) con distinta proporción de grupos azida y con propiedades térmicas y mecánicas muy similares a las de la MPIA preparada en las mismas condiciones. Tras un tratamiento térmico que consiste en calentar membranas densas de estas aramidas obtenidas por *casting*, por encima de los 150°C, las propiedades mecánicas, térmicas y de aislamiento eléctrico sufren una clara mejoría. El calentamiento de las

membranas produce un entrecruzamiento de las cadenas de poliamida con liberación de nitrógeno. Este hecho se ha comprobado mediante termogravimetría (pérdida de N_2), espectroscopia infrarroja por la desaparición del pico correspondiente al grupo azida, y por calorimetría diferencial de barrido donde se observa un proceso exotérmico debido a la transformación de los grupos azida en nitrenos.

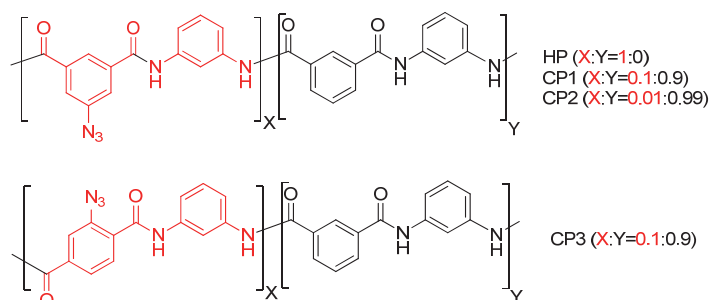


Figura 3.8. Poliamidas aromáticas sintetizadas con grupos azida en su estructura.

En un segundo trabajo, y con idea de expandir las aplicaciones de las poliamidas aromáticas, se utilizaron las poliamidas con grupos azida en la cadena principal como materiales de partida para la síntesis de otros polímeros de altas prestaciones por modificación química, rápida y sencilla, de estas poliamidas para obtener materiales a la carta. Inicialmente se sintetizó una estructura modelo para confirmar la posibilidad de preparar estas poliamidas a la carta y modular las condiciones de reacción, y se probó sobre ella la reducción de la azida a amina, así como una reacción “click” y una reacción con trifenilfosfina. El modelo con grupo amina obtenido se hizo reaccionar con un derivado de cloruro de sulfonilo y un isocianato. Finalmente, se llevaron a cabo las mismas reacciones con la copoliamida sintetizada anteriormente, que contiene un 10% de grupos azida en la cadena principal. Las nuevas poliamidas (Figura 3.9) se obtuvieron con buenos grados de conversión, buenas propiedades térmicas, y distintos grados de absorción de agua dependiendo de los grupos de la cadena lateral.

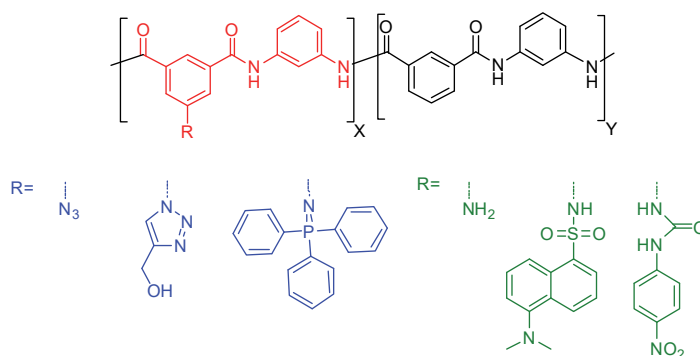


Figura 3.9. Nuevas poliamidas sintetizadas a partir de la poliamida madre con grupos azida.

3.3.3. Aplicaciones

El entrecruzamiento de las poliamidas aromáticas de forma barata y sencilla, tal como se ha realizado en este trabajo, se puede aplicar fácilmente en los procedimientos de producción de fibras actuales para mejorar las propiedades mecánicas térmicas y de aislamiento eléctrico de las fibras. Las aplicaciones de estas fibras entrecruzadas se pueden extender al campo de las tecnologías de protección avanzadas, como chalecos antibalas y trajes aislantes, productos de ingeniería civil, correas de transmisión, productos de protección anti-corte, etc.

La modificación de los grupos laterales de la cadena de las aramidas con grupos azida supone un procedimiento sencillo y rápido para la preparación de materiales a la carta. Dentro de la infinidad de posibilidades de funcionalización, se ha elegido utilizar como ejemplo una serie de grupos que habían sido empleados previamente para aplicaciones avanzadas, como el grupo con urea para la detección visual de distintos aniones,^{116,117} el grupo

¹¹⁶ N. San-José, A. Gómez-Valdemoro, S. Ibeas, F. C. García, F. Serna, J. M. García, *Supramol. Chem.* **2010**, 22, 325.

¹¹⁷ N. San-José, A. Gómez-Valdemoro, F. C. García, F. Serna, J. M. García, *J. Polym. Sci. Part A: Polym. Chem.* **2007**, 45, 4026.

fluorescente dansilo para sensores fluorogénicos de fluoruro,^{118,119} el grupo triazol para la extracción de cationes de medios acuosos,¹²⁰ la introducción de un grupo hidroxilo por ampliar la reactividad con alcoholes primarios, y los iminofosforanos en aplicaciones en biomedicina.¹²¹⁻¹²³

3.3.4. Resultados

A continuación se describen los resultados obtenidos a través de la transcripción íntegra de los trabajos publicados.

- ❖ *Crosslinked aromatic polyamides: a further step in high-performance materials*
- ❖ *Functional aramids: aromatic polyamides with reactive azido and amino group in the pendant structure*

Los detalles experimentales y de caracterización de los trabajos se encuentran en el material suplementario, cuya copia está disponible en el CD adjunto.

¹¹⁸ P. Estévez, H. El-Kaoutit, F. C. García, F. Serna, J. L. de la Peña, J. M. García, *J. Polym. Sci. Part A: Polym. Chem.* **2010**, *48*, 3823.

¹¹⁹ N. San-José, A. Gómez-Valdemoro, P. Estévez, F. C. García, F. Serna, J. M. García, *Eur. Polym. J.* **2008**, *44*, 3578.

¹²⁰ A. Gómez-Valdemoro, M. Trigo, S. Ibeas, F. C. García, F. Serna, J. M. García, *J. Polym. Sci. Part A: Polym. Chem.* **2011**, *49*, 3817.

¹²¹ L. Vela, M. Contel, L. Palomera, G. Azaceta, I. Marzo, *J. Inorg. Biochem.* **2011**, *105*, 1306.

¹²² M. Carreira, R. Calvo-Sanjuán, M. Sanaú, I. Marzo, M. Contel, *Organometallics* **2012**, *31*, 5772.

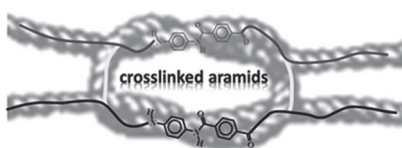
¹²³ S. Monge, B. Canniccionni, A. Graillot, J.-J. Robin, *Biomacromolecules* **2011**, *12*, 1973.

Crosslinked aromatic polyamides: A further step in high-performance materials

Crosslinked aromatic polyamides: A further step in high-performance materials

Miriam Trigo-López, José L. Barrio-Manso, Felipe Serna, Félix C. García, José M. García.*

Departamento de Química, Facultad de Ciencias, Universidad de Burgos. Plaza de Misael Banuelos s/n, E-09001 Burgos, Spain. Fax: +34947258831; Tel: +34947258085; E-mail: jmiquel@ubu.es.



This work aims to improve the outstanding thermal and mechanical properties of commercialized wholly aromatic polyamide fibers, i.e., aramids,

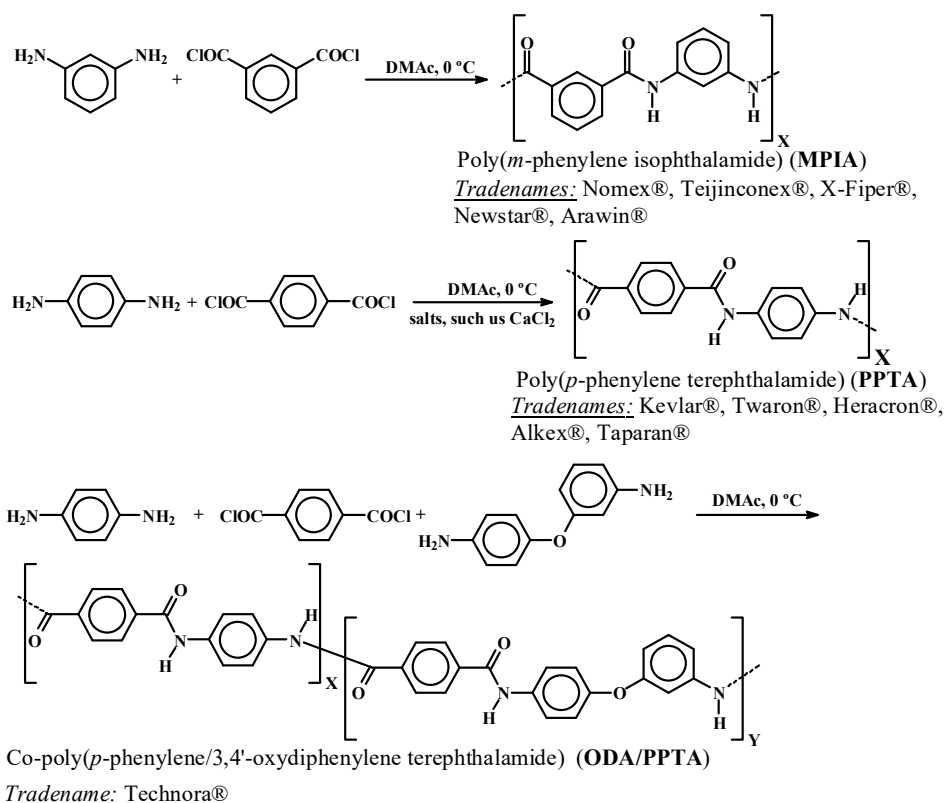
by crosslinking the materials. The introduction of a reactive azide group into the polymer structure leads to functional aramids. Crosslinking processes can be easily performed using an inexpensive thermal treatment after fiber spinning with current spin production facilities.

1. Introduction

The term high performance polymers originally stood for heat- and mechanical-resistant organic materials. New applications in advanced technologies have expanded this definition to include polymers that meet special requirements, such as extremely high clarity and chemical resistance, extraordinarily high or low adhesion, hydrophilicity or hydrophobicity, heat or electrical conductivity or special surface properties.^[1-3] Aromatic polyamides, wholly aromatic polyamides or aramids are polymers that can fulfill some of these criteria, specifically the original criteria that are related to outstanding heat and mechanical

properties, high chemical resistance and low dielectric constant. Thus, commercial aramids are used in every related industrial field with cutting-edge technologies and have been transformed into high-strength and flame-resistant fibers with broad applications in advanced industrial products, such as heat and cut-protection clothing, ballistic-protection products, specialty paper products, sport fabrics, transmission belts, friction products, industrial filters, membranes and specialty pipes. Comparing the properties of aramids to those of other synthetic yarns, the advantages of the former are related to their high tenacity and modulus of elasticity, low creep, good fatigue and thermal and chemical resistance. The advantages of aramids over steel mainly rely on their low density, high energy absorption, good fatigue and corrosion resistance, good dielectric behavior and non-magnetic characteristics.^[4-13]

Since the early discovery of aramids by the company DuPont in the late 1960s, the huge research efforts directed toward aromatic polyamides have not really improved the performance of the original structures.^[4] From a historical viewpoint, DuPont developed the first all-*para*-oriented aramid, poly(*p*-benzamide) (PPBA), which was marketed under the 'Fiber B' trade name. The production of PPBA was discontinued after a few years,^[14] and this polymer was replaced by poly(*p*-phenylene terephthalamide), PPTA, in 1970 under the trade name 'Kevlar®'.^[10-12] Simultaneously, in 1967, DuPont described and commercialized Nomex®, the all-*meta*-aramid poly(*m*-phenylene isophthalamide), MPIA.^[12,13] The only breakthrough of commercial importance was achieved twenty years later by Teijin Limited in 1987 by copolymerizing terephthaloyl dichloride (TPC) with *p*-phenylenediamine (PPD) and 3,4'-diaminodiphenyl ether (ODA), which led to a copolymer with enhanced solubility, ODA/PPTA, that was commercialized under the trade name Technora®.^[4,11] Scheme 1 shows the structures and synthesis of the above-mentioned marketed aramids.



Scheme 1. Synthesis, chemical structures and codes of the *meta*- and *para*-aromatic polyamides that are marketed today.

Although aramids are generally characterized by their thermal and mechanical resistance, *m*-aramids, fibers and yarns are characterized by their fire and thermal resistance (their limiting oxygen index, LOI = 30-32) and are specially suited for applications in heat and fire protection technologies,^[15] while *p*-aramids, fibers and yarns are used when their outstanding mechanical properties are required, e.g., in body protection such as cut-protection apparel and body armor.^[10] The latest marketed aramid, the copolymer ODA/PPT, offers a balance between the advantages

of *meta*- and *para*-materials.^[15] These properties can be attributed to their fully aromatic structure and amide linkages, which give rise to stiff rod-like macromolecular chains that interact with each other via strong and highly directional hydrogen bonds. These interactions favor the development of effective crystalline domains, which give rise to an extremely high cohesive energy due to effective and compact intermolecular packing.^[4]

There are three ways to chemically improve some of the properties of aramids: (a) by introducing new monomers, (b) by chemically modifying the structure of existing polymers and (c) by crosslinking.^[4] The first way has been extensively exploited in basic research, mainly by introducing flexible bonds into the main chain and bulky side groups to improve the solubility by diminishing the cohesive energy and rigidity; this process leads to a concomitant undesired loss of thermal or mechanical resistance.^[4] The only example of commercial success with this strategy was the copolymer ODA/PPTA.^[15]

The chemical modification of aramids is not practical due to solubility restrictions. Therefore, crosslinking is usually used to improve the mechanical, thermal and chemical resistance of organic polymers, although this strategy has scarcely been used for aramids due to economic and technical difficulties. For instance, the thermal crosslinking of aromatic polyamides by means of thermal treatment of functionalized aramids (with arylene carboxylic acid and hydroxyl groups,^[16] benzocyclobutenes,^[17,18] enamionitriles^[19] or active aryl halides^[20]), and of aramids containing poly(meth)acrylic acid (PAA) as a crosslinking agent, has been described.^[21] Following this approach, we propose the preparation of functional, crosslinkable aromatic polyamides that can easily scaled up to current fiber production technologies, i.e., dry, wet or dry-jet wet spinning, to enhance the mechanical, thermal and electrical isolation properties of the fibers.

2. Experimental Section

2.1. Materials

All of the materials and solvents are commercially available and were used as received unless otherwise indicated. 5-Aminoisophthalic acid (Aldrich, 94%) and 5-aminoterephthalic acid (Aldrich, 99%) were used as received. *N,N*-dimethylacetamide (DMAc, Aldrich) was vacuum-distilled over phosphorous pentoxide twice and then stored over 4 Å molecular sieves. *m*-Phenylenediamine (MPD) is commercially available (Aldrich, >99%) and was purified by double vacuum sublimation. Isophthalic (ICL) and terephthaloyl (TCL) dichloride (Aldrich, >99%) were purified by double crystallization from dry heptane.

2.2. Techniques and Conditions

2.2.1. Chemical Characterization of the Polymers, Copolymers, and Monomers

Nuclear magnetic resonance spectra, ^1H and ^{13}C NMR, were recorded with a Varian Inova 400 spectrometer operating at 399.92 and 100.57 MHz, respectively, with deuterated dimethyl sulfoxide ($\text{DMSO-}d_6$) as a solvent; infrared spectra, FT-IR, were recorded with a Nicolet Impact spectrometer or a JASCO FT/IR-4100 fitted with a PIKE TECH "Miracle" ATR; low-resolution electron impact mass spectra, EI-LRMS, were obtained at 70 eV on an Agilent 6890N mass spectrometer.

2.2.2. Thermal Characterization of the Polymers and Copolymers

Differential Scanning Calorimetry (DSC) data were obtained using a Perkin-Elmer DSC Pyris I analyzer with 10 mg of sample under a nitrogen atmosphere. Thermogravimetric analysis data, TGA, were recorded for a

5 mg sample under a nitrogen atmosphere on a TA Instrument Q50 TGA analyzer at a scan rate of 10°C/min; limiting oxygen index, LOI, was estimated using the experimental Van Krevelen equation^[25] $LOI = 17.5 + 0.4 CR$, where CR is the char yield in % weight at 800°C, which was obtained from TGA measurements in a nitrogen atmosphere.

2.2.3. Solubility and Viscosity

The polymer solubility was determined by mixing 10 mg of the polymer with 1 mL of a solvent, followed by stirring for 24 h at 20°C. The polymer was considered soluble at room temperature if a homogeneous solution was obtained. If the polymer was not soluble, the system was heated to reflux for 2 h, and the polymer was considered soluble on heating if a homogeneous solution was obtained. Otherwise, the polymer was considered insoluble or partially soluble; the polymer inherent viscosities were measured with a Ubbelohde viscometer using sulfuric acid (96%) as a solvent at $30.0 \pm 0.1^\circ\text{C}$ and at a polymer concentration of 0.5 g/dL.

2.2.4. Mechanical and Electrical Properties

To determine the tensile properties of the polymers, strips (5 mm wide and 30 mm long) were cut from the polymer dense films with a 30-45 μm thickness on a Hounsfield H10KM Universal Testing Dynamometer at 20°C. Mechanical clamps were used, and an extension rate of 5 mm/min was applied using a gauge length of 10 mm. At least six samples were tested for each polymer, and the data were then averaged; the frequency-dependent dielectric constant is simply the square of the refractive index in a non-magnetic medium ($n = \sqrt{\epsilon_r \mu_r}$, where n is the refractive index, ϵ_r is the relative permittivity and μ_r is the relative permeability, which is close to 1 at optical frequencies, so $n \approx \sqrt{\epsilon_r}$). The refractive index was determined using Brewster's law. Brewster's angle was the angle at which the intensity of the polarized reflected laser light from the aramid film surface reached a minimum.

2.3. Procedures

2.3.1. Synthesis of 5-Azidoisophthalic Acid

In a beaker, 73 mmol of 5-aminoisophthalic acid was placed with 100 mL of water, and 18 mL of HCl (37%) was added dropwise. The mixture was cooled in an ice bath at 0-5°C. In 25 mL of distilled water, 75.3 mmol of NaNO₂ was dissolved and added dropwise to the mixture, which was stirred for 30 minutes. Then, 73 mmol of NaN₃ was dissolved in 25 mL of distilled water and added dropwise to the mixture. A solid was formed, and gas evolution was observed, making it difficult to keep stirring. The mixture was stirred until gas evolution was no longer detected. The product was then filtered, washed with distilled water and dried at room temperature. Yield: 85%. M.p.: 250°C. ¹H NMR δ_H (400 MHz, DMSO-*d*₆, Me₄Si): 13.20 (2H, s, COOH); 8.23 (1H, s, Ph); 7.73 (2H, s, Ph). ¹³C NMR δ_C (100.6 MHz, DMSO-*d*₆, Me₄Si): 166.77, 141.54, 133.99, 127.17, 124.33. EI-LRMS *m/z*: 207 (M⁺, 13), 179 (100), 123 (65), 105 (15), 90 (10), 89 (24), 78 (45), 64 (45), 63 (92), 52 (29), 45 (58). FTIR [wavenumbers (cm⁻¹)]: ν_{acid O-H}: broadband (3090); ν_{AS, N=N⁺=N⁻}: 2122; ν_{C=O}: 1715.

2.3.2. Synthesis of 5-Azidoisophthaloyl Dichloride (1)

In a round-bottom flask, 24 mmol of 5-azidoisophthalic acid was added with approximately 50 mL of SOCl₂. A few drops of DMF were added as catalysts. The mixture was heated at 75°C and stirred for 30 minutes. The solution was then vacuum distilled. The obtained solid was crystallized in approximately 150 mL of dry heptane. A second crystallization was conducted by adding a few drops of SOCl₂ to the hexane to assure the absence of water. The solid was dried under vacuum to prevent its exposure to sunlight and/or humidity. Yield: 43%. M.p.: 63°C. ¹H NMR δ_H (400 MHz, DMSO-*d*₆, Me₄Si): 8.20 (1H, s, Ph); 7.75 (2H, s, Ph). ¹³C NMR δ_C (100.6

MHz, DMSO-*d*₆, Me₄Si): 165.19, 142.02, 132.62, 127.17, 125.14. EI-LRMS *m/z*: 244 (M⁺, 15), 217(100), 153 (65), 126 (15), 90 (12), 89 (22), 78 (46), 64 (43), 63 (90). FTIR [wavenumbers (cm⁻¹)]: $\nu_{\text{acid O-H}}$: broadband (3069); $\nu_{\text{AS, N=N}^+=\text{N}^-}$: 2114; $\nu_{\text{C=O}}$: 1748.

2.3.3. Synthesis of 2-Azidoterephthalic Acid

In a beaker, 13.8 mmol of 2-aminoterphthalic acid was dissolved in 70 mL of NMP, and 3.5 mL of HCl (37%) was added dropwise. The mixture was cooled in an ice bath at 0-5°C. In 15 mL of distilled water, 14.5 mmol of NaNO₂ was dissolved and added dropwise to the mixture, which was stirred for 10 minutes. Then, 13.8 mmol of NaN₃ was dissolved in 20 mL of distilled water and added dropwise to the mixture. A gas evolution was observed and a yellow-milky solution was formed, then 70 mL of distilled water was added. The solid thus formed was filtered, and washed with distilled water. The solid was extracted with methanol, and the solvent was removed. A yellow solid was obtained. Yield: 40%. M.p.: 220°C (decomp). ¹H NMR δ_{H} (400 MHz, DMSO-*d*₆, Me₄Si): 13.54 (2H, s, COOH); 7.87 (1H, s, Ph); 7.79 (2H, m, Ph). ¹³C NMR δ_{C} (100.6 MHz, DMSO-*d*₆, Me₄Si): 167.17, 139.94, 135.66, 132.30, 128.67, 126.42, 122,12. EI-LRMS *m/z*: 207 (M⁺, 3), 106 (53), 105 (22), 91 (100), 77 (14), 65 (5), 63 (4), 51 (8). FTIR [wavenumbers (cm⁻¹)]: $\nu_{\text{acid O-H}}$: broadband (2979); $\nu_{\text{AS, N=N}^+=\text{N}^-}$: 2129; $\nu_{\text{C=O}}$: 1710.

2.3.4. Synthesis of 2-Azidoterephthaloyl Chloride (2)

In a round-bottom flask, 24 mmol of 2-azidoisophthalic acid was added with approximately 50 mL of SOCl₂. A few drops of DMF were added as catalysts. The mixture was heated at 75°C and stirred for 30 minutes. The solution was then vacuum distilled. The obtained solid was crystallized in approximately 150 mL of dry heptane. A second crystallization was conducted by adding a few drops of SOCl₂ to the hexane to assure the

absence of water. The solid was dried under vacuum to prevent its exposure to sunlight and/or humidity. Yield: 43%. M.p.: 51°C. ^1H NMR δ_{H} (400 MHz, DMSO- d_6 , Me $_4$ Si): 7.86 (1H, s, Ph); 7.79 (2H, m, Ph) ^{13}C NMR δ_{C} (100.6 MHz, DMSO- d_6 , Me $_4$ Si): 166.80, 166.78, 129.89, 135.47, 132.23, 128.55, 126.37, 122.03. EI-LRMS m/z : 244 (M^+ , 5), 215 (70), 180 (100), 152 (32), 124 (93), 117 (16), 97 (13), 88 (17), 62 (27). FTIR [wavenumbers (cm^{-1})]: $\nu_{\text{AS, N=N}^+=\text{N}^-}$: 2129; $\nu_{\text{C=O}}$: 1739.

2.3.5. Polyamide Model

To a solution of 1.45 mL of NMP (5% LiCl) and aniline (1.44 mmol), 0.72 mmol 5-azidoisophthaloyl dichloride was added at 0°C under a nitrogen blanket. A vigorous stirring was maintained for 30 minutes. The mixture was kept at room temperature for 4 hours, precipitated in water and washed until pH 7 was reached. Yield: 80%. M.p.: 285°C. ^1H NMR δ_{H} (400 MHz, DMSO- d_6 , Me $_4$ Si): 10.52 (2H, s, NH); 8.43 (1H, s, Ph); 7.9 (2H, s, Ph); 7.85 (4H, d, J 7.99, Ph); 7.42 (4H, m, Ph); 7.17 (2H, m, Ph). ^{13}C NMR δ_{C} (100.6 MHz, DMSO- d_6 , Me $_4$ Si): 164.95, 141.11, 139.77, 137.75, 129.61, 124.95, 124.67, 121.96, 121.49. EI-LRMS m/z : 357 (M^+ , 100), 328 (10), 239 (20), 208 (45), 184 (50), 146 (60), 120 (10), 93 (15), 77 (25). FTIR [wavenumbers (cm^{-1})]: $\nu_{\text{N-H}}$: broadband (3444); $\nu_{\text{AS, N=N}^+=\text{N}^-}$: 2119; $\nu_{\text{C=O}}$: 1644.

2.3.6. Synthesis of the Reference *m*-Aramid Poly(*m*-phenylene isophthalamide) (MPIA)

A 200 mL, double-walled glass flask with a nitrogen inlet and a mechanical stirrer was charged with 80 mL of *N,N*-dimethylacetamide under a blanket of nitrogen at room temperature. Then, 4.326 g (40 mmol) of *m*-phenylenediamine was added. The solution was stirred at room temperature until a diamine solution was obtained. The system was then cooled to 0°C using a circulating system. Then, 8.121 g (40 mmol) of isophthaloyl

dichloride was added portionwise (four equal amounts) over 5 min, and the mixture was allowed to react under nitrogen at 0°C for 30 min and then at 20°C for an additional 3.5 h. The final solution was slowly poured into 800 mL of distilled water, forming a white, fibrous, swollen polymer precipitate that was filtered, washed thoroughly with water and dried in a vacuum oven at 70°C overnight. The yield was nearly quantitative. The inherent viscosity, which was obtained in sulfuric acid at a concentration of 0.5 g/dL and at 30°C, was 2.1 dL/g.

2.3.7. *Synthesis of the Polymer Poly[(m-phenylene 5-azidoisophthalamide)-co-(m-phenylene isophthalamide)] (CP1)*

The preparation of the homopolyamide followed the procedure that was described for MPIA. The polyamide was prepared in a similar fashion using a 1:1 molar ratio of 5-azidoisophthaloyl dichloride and MPD.

2.3.8. *Synthesis of the Polymer Poly[(m-phenylene 5-azidoisophthalamide)-co-(m-phenylene isophthalamide)] (CP1)*

The preparation of the homopolyamide followed the procedure that was described for **MPIA**. The copolyamide was prepared in a similar fashion using a 0.9:0.1:1.0 molar ratio of isophthaloyl dichloride, 5-azidoisophthaloyl dichloride and MPD.

2.3.9. *Synthesis of the Polymer Poly[(m-phenylene 5-azidoisophthalamide)-co-(m-phenylene isophthalamide)] (CP2)*

The preparation of the homopolyamide followed the procedure that was described for MPDI. The copolyamide was prepared in a similar fashion using a 0.99:0.01:1.00 molar ratio of IPC, 5-azidoisophthaloyl dichloride and MPD.

2.3.10. Synthesis of the Polymer poly[(*m*-phenylene 2-azidoterephthalamide)-co-(*m*-phenylene isophthalamide) (CP3)]

The preparation of the homopolyamide followed the procedure that was described for **MPIA**. The copolyamide was prepared in a similar fashion using a 0.9:0.1:1.0 molar mixture of IPC, 2-azidoterephthaloyl dichloride and MPD.

The NMR and IR spectra of polymers can be found in the Supporting Information (SI).

2.3.11. Polymer Films. General Procedure

Polymers and copolymers with *m*-oriented rings were soluble enough to be transformed into dense polymer films using the conventional casting technique. Polymer films were prepared by evaporating the cast solutions in *N,N*-dimethylacetamide. Solutions of 7% by polymer weight were obtained. The solvent was eliminated by heating the solution at a temperature of 60°C for 6 h in an air-circulating oven and then at 100°C for 4 hours under vacuum (1 mmHg).

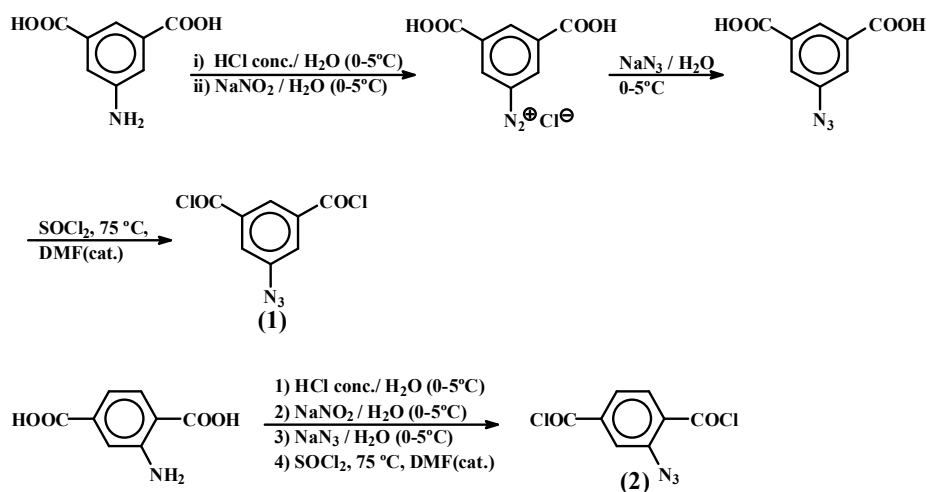
2.3.12. Crosslinking Procedure (Thermal Treatment)

The materials, in the form of dense films that were obtained by *casting*, were heated in air at 240°C for 10 min. Then, the thermal and mechanical properties were evaluated.

3. Results and Discussion

Thus, we propose the preparation of functional, crosslinkable aromatic polyamides by preparing a copolymer that contains the reactive azide group in the main polymer chain. Considering the way in which aromatic polyamides are commercially synthesized (Scheme 1), we prepared two

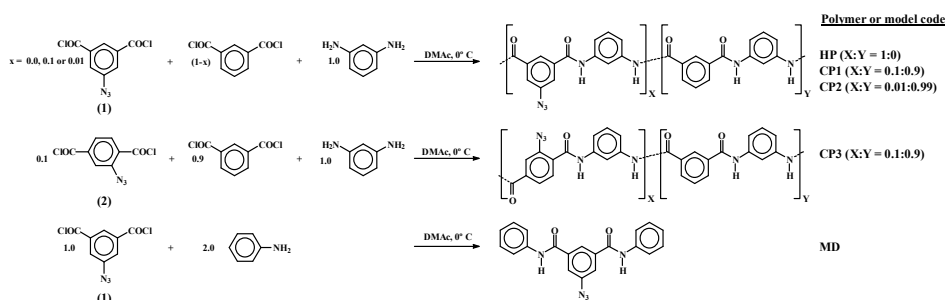
aromatic diacid dichlorides that contain the azide group, i.e., 5-azidoisophthalic (**1**) and 2-azidoterephthalic (**2**) dichlorides, which were designed to prepare fully *meta*- and *para*-aramids. However, at the present stage, these monomers have only been tested in *m*-aramid structures for solubility reasons. These monomers were prepared in a straight, cheap, easy and clean manner from commercial 5-aminoisophthalic and 2-aminoterephthalic acids, as depicted in **Scheme 2**. The validity of a difunctional compound as a condensation monomer can be determined in different ways. The simplest and most effective way is the preparation of a polymer model with good yield and without byproducts. The excellent characteristics of 5-azidoisophthaloyl dichloride as a condensation monomer were exemplified by the preparation of the corresponding model upon reaction with aniline under polymerization-like conditions (Scheme 3).



Scheme 2. Reactive monomer synthesis.

Polymerization was performed following the standard industrial procedures, i.e., the reaction of the diacid dichlorides and aromatic diamine comonomers in a polar aprotic solvent, such as DMAc, at a low temperature,

and yielded quantitatively high-purity copolymers. The absence of a side reaction was previously tested by preparing an easily characterizable model compound (**MD**). The polymer structures and codes are depicted in Scheme 3, and their NMR spectra are reported in the SI. A homopolymer (**HP**) and three copolymers (**CP1**, **CP2** and **CP3**) were prepared by the low temperature reaction of the comonomers in dry DMAc under an inert atmosphere. For comparison purposes, commercialized MPIA was also prepared. The polymers were obtained as white, fibrous, swollen precipitates by pouring the reaction solution into distilled water. Precipitation is the standard procedure for isolating aramids in the lab.^[4] The procedure differed from the industrial preparation of MPIA fibers, in which the dope solution is obtained from the reaction medium by neutralizing the evolved HCl with Ca(OH)₂, filtering the medium and heating it to 80°C. Finally, the fibers are spun following one of the standard spinning procedures, i.e., dry, wet or dry-jet wet spinning, followed by washing and cold and hot fiber drawing and finishing.^[2,9,12]



Scheme 3. Synthesis of crosslinkable aromatic copolyamides.

The polymer viscosities were high, greater than 1.29 dL/g (Table 1), and the NMR and IR spectra exhibited clean signals that corresponded to the polymer or copolymer structures (SI). The solubility was good (Table 1), which is most likely the most important weakness of these materials despite the overall strength of aramids; this quality impairs their applicability in fields others than fibers.^[4]

From a practical viewpoint, the crosslinking of a polymer should increase the properties of interest without impairing other properties. Thus, it is advisable to introduce crosslinking groups in a small molar proportion. We prepared copolymers with crosslinking azide groups in molar concentrations of 10% (**CP1** and **CP3**) and 1% (**CP2**) of the structural units. For comparison and characterization purposes, we also synthesized a homopolymer (**HP**) that contained the azide group in all of the structural units.

Table 1. Inherent viscosities and solubilities of the polymers.

Polymer	$\eta_{inh}^{b)}$ (dLg ⁻¹)	Solubility ^{a)}						
		H ₂ SO ₄	DMAc	DMF	NMP	DMSO	CHCl ₃ , EtOH	THF
HP	1.29	++	++	+	++	++	-	-
CP1	2.04	++	++	+	++	++	-	-
CP2	1.65	++	++	+	++	++	-	-
CP3	1.69	++	++	+	++	++	-	-
MD	--	++	++	++	++	++	-	+

^{a)} polymer concentration = 10 mg of polymer in 1 mL of solvent; ++ = soluble at room temperature; + = soluble on heating; +- = partially soluble; - = insoluble; ^{b)} solvent = sulfuric acid (96%), temperature = 30°C, polymer concentration = 0.5 g/dL.

Polymer films were prepared to evaluate their thermal and mechanical properties following the standard *casting* procedure. Upon heating the films at 240°C for 10 min (the prefix “*tt*” of the polymer and copolymer codes indicates a thermal treatment), all of the materials became insoluble due to the crosslinking process that was ascribed to the transformation of the azide moieties into highly reactive nitrene groups, which exhibit a reactivity similar to those of carbenes. Nitrenes undergo different reactions with aromatic rings and with functional groups, which give rise to insertions, additions to multiple bonds, rearrangements, abstraction and dimerization reactions and ring expansion products (see SI, Scheme S1).^[22-24] The insolubility of the films in all of the solvents, including a strong acid, after thermal treatment clearly confirms the crosslinking of the

materials. Even the more insoluble commercial aramids, the *para*-aramids, are soluble in sulfuric acid. Moreover, a second proof of the transformation can be found by monitoring the disappearance of the free azide groups using FTIR. The characteristic absorption band of the azide group at 2109 cm^{-1} disappeared after thermal treatment. As an illustrative example, Figure 1 shows the FT-IR spectra of the films that were prepared from **HP** and from **CP1** before and after thermal treatment.

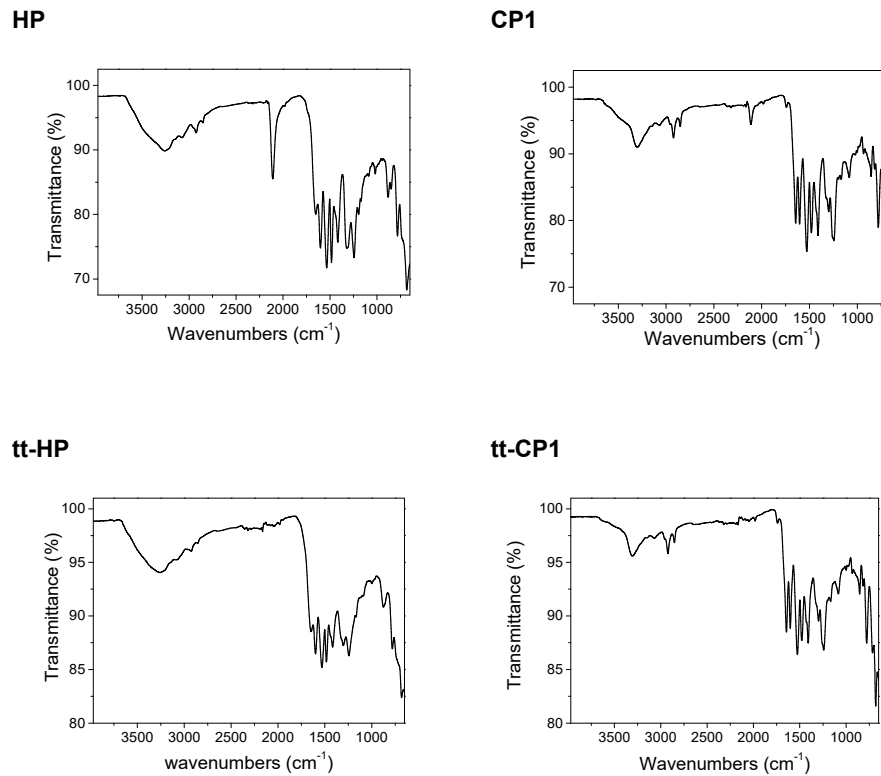


Figure 1. Comparison of the FT-IR spectra of the heat-treated (**tt-HP** and **tt-CP1**) and untreated (**HP** and **CP1**) polymers.

Accordingly, the thermal treatment of the polymers and copolymers above 150°C led to the crosslinking of the polymer materials; the higher the temperature, the shorter the time needed to complete crosslinking. This fact

can be observed in the TGA data (Table 2), in which the homopolymer **HP** exhibits a T_5 close to 200°C. The weight loss is ascribed to the transformation of the azide in the nitrene groups, which occurs with the concomitant crosslinking and evolution of a N_2 molecule per azide moiety.

Table 2. Thermal TGA data (nitrogen atmosphere) of the polymer and copolymer membranes prior to and after 10 minutes at 240°C.

Polymer	Without thermal treatment				Polymer	Heated at 240°C for 10 min			
	T5a) (°C)	T10b) (°C)	Char yield (%)	LOIc)		T5a) (°C)	T10b) (°C)	Char yield (%)	LOIc)
MPIA	432	452	50	37					
HP	194 ^{d)}	275 ^{d)}	55	39	tt-HP	439	471	59	41
CP1	437	456	54	39	tt-CP1	435	454	56	40
CP2	421	454	50	38	tt-CP2	435	457	58	41
CP3	421	458	56	40	tt-CP3	433	457	58	41

a) 5% weight loss (T_5), 10% weight loss (T_{10}); b) at 800°C; c) limiting oxygen index, calculated from the TGA data^[25] ($LOI = 17.5 + 0.4 CR$, where CR is the char yield in % weight at 800°C); d) the low values correspond to the weight loss corresponding to the decomposition of the azide group to render the nitrene, with a loss of a nitrogen molecule (N_2) per azide group. This loss is specially significant for homopolymer HP.

The films exhibited good thermal behavior similar to that of the reference *m*-aramid that was prepared for comparison, **MPIA**, while the thermal treatment of the films led to materials with much better thermal and fire resistance, specially considering the improvement in the char yield at 800°C and the estimated limiting oxygen index (LOI). The LOI values that were calculated from the char yields are higher than those measured for aramids^[25] but are valuable for comparison purposes. These improvements can be ascribed to the lower probability of volatile residue formation in the crosslinked materials upon the thermal breakage of one of more covalent bonds. This conclusion was supported by isothermal TGA analysis. Both **MPIA** and **HP** were heated from 50 to 350°C at 10°C/min and the weight of each sample was recorded. Then, the polymers were kept at constant temperature, 350°C, for 24h under oxidizing atmosphere (synthetic air). The

weight losses of **MPIA** and **ttHP** were 15 and 10%, respectively, showing the good heat resistance improvement of the crosslinked materials compared with the reference aramid. The cross-linking was seen by DSC, where exothermic processes were observed in parallel to the weight losses, ascribed to the transformation of the azide into the nitrene groups, as depicted in Figure 2 for **CP3**.

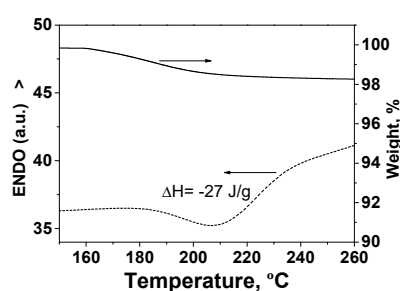


Figure 2. DSC (dash line) and TGA (solid line) of polymer **CP3** around the crosslinking temperature.

The mechanical properties of the films (Table 3) are in agreement with previous results that were obtained for unoriented aramid films, which were prepared by casting on a lab scale.^[26] The results of the thermally untreated films, in terms of their Young's modulus and tensile strength, are fully comparable with those obtained for the reference polymer **MPIA**. However, the mechanical properties of **CP3** are lower than those of **CP1**. Regarding this point, we speculate with the fact that azides in ortho position to amide groups can give rise to intrachain hydrogen azide-amide bonds, leading to a 6 member rings where the amide hydrogen is bonded to the azide nitrogen linked to aromatic ring, thus impairing chain packaging and diminishing the interchain hydrogen bonds, responsible of the outstanding mechanical properties of the aramids. The polymer thermal treatments, i.e., the crosslinking, induced a large improvement in these parameters, as expected.

Table 3. Mechanical properties of the polymer and copolymer films without and with thermal treatment at 240°C (10 min).

Polymer	Without thermal treatment		Polymer	Heated at 240°C for 10 min	
	Young's Modulus (GPa)	Tensile Strength (MPa)		Young's Modulus (GPa)	Tensile Strength (MPa)
MPIA	1.4	63			
HP	1.5	67	tt-HP	2.7	126
CP1	1.4	59	tt-CP1	2.9	127
CP2	1.4	73	tt-CP2	1.7	84
CP3	1.0	48	tt-CP3	1.1	64

The crosslinking process also improves the electrical isolation properties of the aramids. Thus, the relative dielectric constant (ϵ_r) of the **tt-CP1** films was lower than that of **MPIA** ($\epsilon_{r, \text{tt-CP1}} = 2.47 \pm 0.15$, $\epsilon_{r, \text{tt-MPDI}} = 2.99 \pm 0.15$). This result is important, specially for *m*-aramid, because the global *m*-aramid fiber market indicates that electrical insulation paper is the most important fiber-consuming market, followed closely by protective clothing; the later also includes electric arc protective apparel.

Considering the current aramid fiber production technology, the thermal crosslinking of aramids can be easily achieved in the dry, wet and dry-jet wet spinning processes, specially in the later because the initial water-wet fiber is obtained from a slightly heated dope solution (temperature $\sim 80^\circ\text{C}$, solvent = sulfuric acid for *p*-aramids or DMAc for *m*-aramids and aromatic copolyamides, polymer concentration $\sim 19\%$, salt –usually CaCl_2 -concentration $\sim 9\%$). Thus, crosslinking could be performed after the washing and stretching procedures, along with or sequential to the tow drawing and crystallization/finishing steps. Considering the dry spinning procedure, the initial heating of the spun dope at approximately 400°C would initially produce fully or partially crosslinked fibers prior to the initial washing and stretching procedures.

4. Conclusion

In short, we have addressed a cheap and simple way to crosslink aromatic polyamides that can easily be applied to current fiber production technologies, i.e., dry, wet or dry-jet wet spinning, to enhance the mechanical, thermal and electrical isolation properties of the fibers. These properties are key parameters of a successful aramid fiber, mainly in regard to advanced protection technologies, e.g., ballistic applications and electrical protection apparel, civil engineering products, composites, conveyor and transmission belts, hot gas filtration bags, cut-protection products, elastomer reinforcements, engineering plastics, friction products, heat-protection products, optical fiber cables, reinforced pipes, hoses, ropes and cables, sealing materials, specialty paper products, tires, adhesives, sealants and coatings. A PCT patent has been filed (applicant: University of Burgos).

Supporting Information

Supporting Information is available online from Wiley InterScience or from the author

Acknowledgements

The authors gratefully acknowledge the financial support that was provided by the Spanish Ministerio de Economía y Competitividad – Feder (MAT2011-22544) and by the Consejería de Educación - Junta de Castilla y León. We also wish to thank Prof. Angel Ballesteros and Ms. M^a Jesús Riaño of the Department of Physics of the University of Burgos for measuring the refractive index of the polyamide films.

Keyword: aromatic polyamides, aramids, crosslinking, mechanical properties, thermal properties

References and notes

- [1] V. Mittal, *High Performance Polymers: An Overview*, in *High Performance Polymers and Engineering Plastics*, Ed.: V. Mittal, Scrivener Publishing LLC, Salem **2011**, Ch. 1.
 - [2] S. Rebouillat, "Aramids", in *High Performance Fibres*, J.W.S. Hearle Ed., Woodhead Publishing Ltd and CRC Press LLC, Boca Raton **2000**.
 - [3] J.K. Fink, *High performance polymers*, William Andrew Inc., New York **2008**.
 - [4] J.M. García, F.C. García, F. Serna, J.L. de la Peña, *Prog. Polym. Sci.* **2010**, *35*, 623.
 - [5] D.J. Liaw, P.N. Hsu, W.H. Chen, S.L. Lin, *Macromolecules* **2002**, *35*, 4669.
 - [6] D.J. Liaw, F.C. Chang, M.K. Leung, M.Y. Chou, K. Muellen, *Macromolecule* **2005**, *38*, 4024.
 - [7] K.L. Wang, M.A. Kakimoto, M. Jikey, *High Perform. Polym.* **2005**, *17*, 225.
 - [8] J.M. García, F.C. García, F. Serna, J.L. de la Peña, "Aromatic Polyamides", in *Handbook of Engineering and Specialty Thermoplastics*, Vol. 4, S. Thomas, Visakh P.M., Eds., Wiley, Salem **2012**, Ch. 6.
 - [9] J. Gallini, "Polyamides, aromatic", in *Encyclopedia of polymer science and technology*, Vol. 3, John Wiley & Sons, New York **2005**, Pp. 558-584.
 - [10] H.H. Yang, *Kevlar Aramid Fiber*, John Wiley & Sons, Chichester **1993**.
 - [11] H.H. Yang, *Aromatic high-strength fibers*, Wiley, New York **1989**.
 - [12] V. Gabara, J.D. Hartzler, K.-S. Lee, D. J. Rodini, H.H. Yang, "Aramid Fibers", in *Handbook of fiber Chemistry*, 3th edition, M. Lewin, Ed., CRC Press, Boca Raton **2007**, Ch.13.
 - [13] H.H. Yang, "Nomex aramid fiber", in: *Handbook of fiber science and technology*, Vol. III, *High Technology Fibers, Part C*, Marcel Dekker Inc., New York, **1993**, Cp. 2.
 - [14] R.J. Gaymans, "Polyamides", in: *Synthetic Methods in Step-Growth Polymers*, M.E. Rogers, T.E. Long, Eds., John Wiley & Sons, Inc., Hoboken **2003**, ch. 3.
 - [15] S. Bourbigot, X. Flambard, *Fire Mater.* **2002**, *26*, 155.
 - [16] NL. WO2009130244 (2008), Teijin Aramid B.V., invs.: J. Bos, W.H.J. Nijenhuis.
 - [17] L.J. Markoski, K.A. Walker, G.A. Deeter, G.E. Spilman, D.C. Martin, J.S. Moore, *Chem. Mater.*, **1993**, *5*, 248
 - [18] L.-S. Tan, N. Venkatasubramanian, *J. Polym. Sci. Part A: Polym. Chem.* **1996**, *34*, 3539.
 - [19] Y.J. Kim, I.S. Chung, I. In, S.Y. Kim, *Polymer*, **2005**, *46*, 3992.
 - [20] W. Seeeny, *J. Polym. Sci. Part A: Polym. Chem.* **1992**, *30*, 1111.
 - [21] NL. WO2008028605 (2006), Teijin Aramid B.V., invs.: J. Bos, S.C. Noordewier.
 - [22] M.B. Smith, J. March, in: *March's Advanced Organic Chemistry: Reactions, Mechanisms and Structure*, 6th Ed., Wiley & Sons, Hoboken **2007**, ch 5.
 - [23] S. Bräse, C. Gil, K. Knepper, V. Zimmermann, *Angew. Chem. Int. Ed.* **2005**, *44*, 5188.
 - [24] F. Budyka, M.M. Kantor, M.V. Alfimov, *Russ. Chem. Rev.* **1992**, *61*, 25.
 - [25] D. W. Van Krevelen and K. te Nijenhuis, *Properties of Polymers. Their Correlation with Chemical Structure; Their Numerical Estimation and Prediction from Additive Group Contributions*, 4th edition, Elsevier, Amsterdam **2009**, pp. 855-57.
 - [26] A. Gómez-Valdemoro, N. San-José, F.C. García, J.L. de la Peña, F. Serna, J.M. Garcia, *Poly. Chem.* **2010**, *1*, 1291.
-

Functional Aramids: Aromatic Polyamides with Reactive Azido and Amino Groups in the Pendant Structure

Functional Aramids: Aromatic Polyamides with Reactive Azido and Amino Groups in the Pendant Structure

Miriam Trigo-López, Jesús Luis Pablos, Félix Clemente García, Felipe Serna, José Miguel García*

Departamento de Química, Facultad de Ciencias, Universidad de Burgos. Plaza de Misael Banuelos s/n, E-09001 Burgos, Spain. Fax: +34947258831; Tel: +34947258085; web: sites.google.com/site/grupodepolimeros/ Correspondence to: J. M. García (E-mail: jmiguel@ubu.es)

Additional Supporting Information may be found in the online version of this article.

The structure of the high performance aromatic polyamides, also known as aramids, was modified to render functional polymers by the introduction of primary amine and azide functional groups in the main polymer chain. These materials were prepared as parent polymers for future use in the simple and inexpensive preparation of other high performance materials by the chemical derivatization of the primary amine and azide groups using their well-known and broad reactivity. The potential of the parent aramids was exemplified with the preparation of four novel functional aramids containing the fluorescent dansyl group, the anion and cation receptors urea and triazole with free primary alcohol functional groups, and the iminophosphorane ligand for forthcoming synthetic processes.

KEYWORDS: aramids, aromatic polyamides, functional polymers, functionalization of polymers, high performance materials, modification

Introduction

Wholly aromatic polyamides, or aramids, are materials with superior thermal and mechanical properties belonging to the high performance polymer family. Aramids have an extremely low solubility and a melting temperature

Journal of Polymer Science Part A: Polymer Chemistry **2014**, *52*, 1469–1477

above their decomposition temperature; these properties, along with their difficult synthesis, impair their application to the fiber fields for fire and mechanical protection garments and for advanced composite materials.¹⁻⁴ The only commercial breakthrough in the aramid field after the introduction nearly five decades ago of poly(*m*-phenylene isophthalamide), MPIA, and poly(*p*-phenylene terephthalamide), PPTA, by DuPont was the introduction of the copolymer poly[(*p*-phenylene terephthalamide)-co-(3,4'-oxydiphenylene terephthalamide)], ODA/PPTA, by the Teijin Group in the late 1980s.

Accordingly, the expansion of the application fields of these materials is twofold: through the increment of the thermal and mechanical performance of the currently commercialized aramids, by crosslinking,⁵ for example; or through the inexpensive and simple preparation of functional materials that impart innovative properties while concomitantly exploiting their outstanding thermal and mechanical behavior. Following the latter approach, we prepared aramids with azido and amino groups in the pendant structure. These aramids can be easily modified to render materials with a la carte functional groups exploiting the reactivity of these groups. As illustrative examples of the envisaged potential of the parent functional aramids, we prepared from the parent polymer materials containing fluorescent dansyl groups with potential applications as high-tech luminescent converters (LUCO) or electrochromic materials,⁶⁻¹⁸ the anion and cation receptors urea and triazole with free primary alcohol functional groups for sensing applications,¹⁹⁻²³ and iminophosphorane as the ligand for the preparation of hybrid materials with a potential application in the biomedical field.²⁴⁻²⁶

Experimental

All materials and solvents were commercially available and used as received, unless otherwise indicated: NaBH₄ (≥96%, Aldrich), propargyl

alcohol (99%, Alfa Aesar), $\text{CuSO}_4 \cdot 5\text{H}_2\text{O}$ ($\geq 99\%$, VWR-Prolabo), sodium L(+)-Ascorbate ($\geq 99\%$, VWR-Prolabo), triphenylphosphine ($\geq 95\%$, Sigma-Aldrich), dansyl chloride ($\geq 99\%$, Sigma-Aldrich), 4-nitrophenyl isocyanate (97%, Aldrich), diethyl ether (99.9%, VWR-Prolabo), *N,N*-dimethylacetamide (DMA, $\geq 99.9\%$, Aldrich). 5-Azidoisophthaloyl dichloride and 5-azido-*N1,N3*-diphenylisophthalamide (**M1**) were prepared and purified following previously described procedures.⁵

Measurements

^1H and ^{13}C NMR spectra were recorded with a Varian Inova 400 spectrometer operating at 399.92 and 100.57 MHz, respectively, with deuterated dimethylsulfoxide ($\text{DMSO-}d_6$) as the solvent.

Infrared spectra (FT-IR) were recorded with a FT/IR-4200 FT-IR Jasco Spectrometer with an ATR-PRO410-S single reflection accessory. Low-resolution electron impact mass spectra (EI-LRMS) were obtained at 70 eV on an Agilent 6890N mass spectrometer. Thermogravimetric analysis (TGA) data were recorded for a 5 mg sample under a nitrogen or oxygen atmosphere on a TA Instrument Q50 TGA analyzer at a scan rate of $10^\circ\text{C min}^{-1}$. The LOI was estimated using the following experimental Van Krevelen equation: $\text{LOI} = 17.5 + 0.4 \text{ CR}$, where CR is the char yield weight percentage at 800°C , which was obtained from the TGA measurements under a nitrogen atmosphere.

UV/Vis spectra were recorded using a Varian Cary3-Bio UV/Vis spectrophotometer. Fluorescence spectra were recorded using a Hitachi F-7000 fluorescence spectrophotometer.

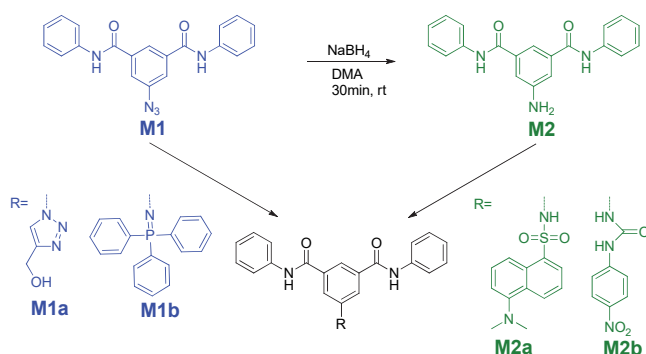
The polymer solubility was determined by mixing 10 mg of the polymer with 1 mL of a solvent followed by stirring for 24 h at 20°C . The polymer was considered soluble at room temperature if a homogenous

solution was obtained. If the polymer was insoluble at room temperature, the system was heated to reflux for 2 h, and the polymer was considered soluble on heating if a homogenous solution was obtained. Otherwise, the polymer was considered insoluble. The inherent viscosity, η_{inh} , of the polymers was measured with an Ubbelohde viscometer using sulfuric acid (96%) as the solvents at $30^{\circ}\text{C} \pm 0.1^{\circ}\text{C}$ and a polymer concentration of 0.5 g dL^{-1} . The intrinsic viscosity, $[\eta]$, was calculated measuring the η_{inh} at different polymer concentrations ($0.5, 0.3, 0.1,$ and 0.05 g dL^{-1}) using sulfuric acid (96%) as the solvents at $30^{\circ}\text{C} \pm 0.1^{\circ}\text{C}$ and extrapolating to zero concentration. The number average molecular weight (M_w) was calculated from $[\eta]$ using the Mark-Houwink-Sakurada equation ($[\eta]=kM_w^{\alpha}$) and the viscometric constants of MPIA ($k = 0.00013 \text{ dL g}^{-1}$; $\alpha = 0.84$).⁴

Water sorption experiments were conducted gravimetrically. The sample (200 mg) was dried at 60°C for 24 h over phosphorus pentoxide, and the sample was placed in a closed box containing a saturated aqueous solution of NaNO_2 at 20°C , which provided a relative humidity of 65%. The samples were weighed periodically over a period of 8 days until they equilibrated with their surroundings and presented no further changes in weight.

Synthesis and characterization of the model compounds and polymers

The syntheses of the model compounds were achieved by chemical modifications of 5-azido-*N*1,*N*3-diphenylisophthalamide (**M1**) (Scheme 1).



Scheme 1. Synthesis of the model compounds

Synthesis of 5-amino-N1,N3-diphenylisophthalamide (M2). First, 2.7 mmol 5-azido-N1,N3-diphenylisophthalamide (**M1**) is dissolved in 5 mL of DMA. To this mixture is added 5.4 mmol of NaBH₄; the mixture is stirred for approximately 30 minutes and then poured into 200 mL of water. The formed solid is washed with water. Yield: 93%. M.p.: 241°C. ¹H-NMR (399.9 MHz, DMSO-*d*₆, δ): 10.26 (s, 2H, NH); 7.81 (d, *J* = 7.6 Hz, 4H, Ph); 7.66 (t, *J* = 1.4 Hz, 1H, Ph); 7.38 (t, *J* = 7.9 Hz, 4H, Ph); 7.30 (d, *J* = 1.5 Hz, 2H, Ph); 7.13 (t, *J* = 7.4 Hz, 2H, Ph); 5.64 (s, 2H, NH₂). ¹³C-NMR, (100.6 MHz, DMSO-*d*₆, δ): 166.86, 149.86, 140.16, 137.06, 129.53, 124.48, 121.15, 116.59, 114.8. EI-LRMS (*m/z* (%)): 331 (50) [M⁺], 240 (20), 239 (100), 211 (6), 185 (13), 166 (5), 119 (5), 91 (12), 65 (7). FTIR (KBr) [Wavenumbers (cm⁻¹)]: ν_{N-H}: 3305; ν_{NH2}: 3335, 3239; ν_{C=O}: 1633; δ_{N-H}: 1592.

Synthesis of 5-(4-(hydroxymethyl)-1H-1,2,3-triazol-1-yl)-N1,N3-diphenylisophthalamide (M1a). A mixture of **M1** (1 mmol) and propargyl alcohol (1 mmol) in DMA/H₂O (5/1, v/v) in the presence of 5 mol % CuSO₄·5H₂O with 10 mol % sodium ascorbate as the in situ reducing agent to generate the active Cu(I) species was stirred at 60°C for 24 hours. The mixture was then precipitated in water, filtered off and washed with distilled water. Yield: 65%. M.p.: 199°C. ¹H-NMR (399.9 MHz, DMSO-*d*₆, δ): 11.63 (s, 2H, NH); 8.93 (s, 1H, CH triazol); 8.71 (s, 2H, Ph); 8.66 (d, *J* = 1.2 Hz, 1H, Ph); 7.85 (d, *J* = 8.4 Hz, 4H, Ph); 7.44 (t, *J* = 7.5 Hz, 4H, Ph); 7.19 (t, *J* = 7.8 Hz, 2H, Ph);

5.47 (t, $J = 5.5$ Hz, 1H, CH₂); 4.72 (d, $J = 5.5$ Hz, 2H, OH). ¹³C-NMR, (100.6 MHz, DMSO-*d*₆, δ): 164.78, 150.56, 139.70, 137.76, 137.72, 129.69, 127.76, 125.08, 122.68, 122.37, 121.47, 55.96. EI-LRMS (m/z (%)): 413 (30) [M⁺], 385 (40), 368 (37), 294 (20), 293 (100), 221 (13), 144 (10), 93 (7), 78 (18), 62 (19). FTIR (KBr) [Wavenumbers (cm⁻¹): $\nu_{\text{N-H, O-H}}$: broadband 3284; $\nu_{\text{C=O}}$:1644; $\delta_{\text{N-H}}$:1537.

Synthesis of N1,N3-diphenyl-5-((triphenylphosphoranylidene)amino)-isophthalamide (M1b). To 1 mmol of **M1** was added 10 mL of ether and placed in a capped round-bottom flask along with 3 mmol of triphenylphosphine dissolved in 10 mL of ether. The mixture is stirred for 48 h. The solid is filtered off and washed with ether. Yield: 91%. M.p.: 269°C. ¹H-NMR (399.9 MHz, DMSO-*d*₆, δ): 10.20 (s, 2H, NH); 7.87-7.75 (m, 11H, Ph); 7.71-7.61 (m, 10H, Ph); 7.41 (s, 2H, Ar H); 7.36 (t, $J = 7.9$, 3H, Ph); 7.12 (t, $J = 7.4$ Hz, 2H, Ph). ¹³C-NMR, (100.6 MHz, DMSO-*d*₆, δ): 166.64, 152.54, 140.16, 136.57, 133.21, 133.19, 133.14, 133.04, 131.16, 130.18, 130.01, 129.89, 129.59, 129.45, 125.58, 125.58, 125.39, 124.41, 121.17, 116.01. EI-LRMS (m/z (%)): 591 (100) [M⁺], 499 (17), 471 (13), 353 (38), 352 (35), 263 (12), 262 (57), 185 (11), 183 (37), 108 (11). FTIR (KBr) [Wavenumbers (cm⁻¹): $\nu_{\text{N-H}}$: 3284; $\nu_{\text{Ar C-H}}$: (3056); $\nu_{\text{C=O}}$:1644; $\nu_{\text{P=H}}$:1365.

Synthesis of 5-dansylamino-N1,N3-diphenylisophthalamide (M2a): **M2** (1 mmol) is dissolved in 3.5 mL of DMA under a nitrogen blanket. Then, the solution is cooled at 0°C in an ice-bath. To this mixture is added 1.1 mmol of dansyl chloride, and the mixture is stirred for 30 minutes at 0°C, then for another 4 h at room temperature and at 50°C overnight. The mixture is then poured into water, filtered off and washed with water. Yield: 74%. M.p.: 185°C. ¹H-NMR (399.9 MHz, DMSO-*d*₆, δ): 11.18 (s, 1H, NH-SO₂-); 10.41 (s, 2H, NH); 8.51 (d, $J = 8.6$ Hz, 1H, naph); 8.45 (d, $J = 8.6$ Hz, 1H, naph); 8.31 (d, $J = 7.3$ Hz, 1H, naph); 8.21 (s, 1H, Ph); 7.81 (s, 2H, Ph); 7.77 (d, $J = 8.3$ Hz, 4H, Ph); 7.73-7.66 (dt, $J = 10.8$ Hz, $J = 8.0$ Hz, 2H, naph); 7.39 (t, $J =$

7.8 Hz, 4H, Ph); 7.33 (d, $J = 7.6$ Hz, 1H, naph); 7.15 (t, $J = 7.4$ Hz, 2H, Ph); 2.85 (s, 6H, CH₃). ¹³C-NMR, (100.6 MHz, DMSO-*d*₆, δ): 165.47, 152.21, 139.76, 139.28, 137.08, 135.42, 131.31, 130.67, 129.88, 129.82, 129.58, 129.34, 124.82, 124.56, 122.06, 121.56, 121.19, 119.55, 116.46, 46.00. EI-LRMS (m/z (%)): 564 (100) [M⁺], 565 (39), 550 (37), 331 (38), 239 (73), 170 (40), 168 (31), 156 (17), 127 (10), 115 (10), 93 (12). FTIR (KBr) [Wavenumbers (cm⁻¹): ν_{N-H} : 3363, 3237; $\nu_{Ar C-H}$: 3056, 2946; $\nu_{C=O}$: 1640; δ_{N-H} : 1573, ν_{SO_2-NH} (As, S): 1336, 1136. The quantum yield (Φ) was 0.34 and was calculated according to the literature.²⁷ The measurements were performed at an excitation wavelength of 360 nm with quinine sulfate as the standard.

Synthesis of 5-(3-(4-nitrophenyl)ureido)-N1,N3-diphenylisophthalamide

(M2b): **M2** (1 mmol) is dissolved in 3.5 mL of DMA under a nitrogen blanket. The solution is cooled at 0°C in an ice-bath. To the solution is added 1.1 mmol of 4-nitrophenyl isocyanate, and the mixture is stirred for 30 minutes at 0°C, then for another 4 h at room temperature, and at 50°C overnight. The mixture is then poured into water, filtered off and washed with water. Yield: 81%. M.p.: 271°C. ¹H-NMR (399.9 MHz, DMSO-*d*₆, δ): 10.47 (s, 2H, NH); 9.61 (s, 1H, NH-urea); 9.40 (s, 1H, NH-urea); 8.27-8.23 (m, 5H, Ph); 7.84 (d, $J = 7.7$ Hz, 4H, Ph); 7.79 (d, $J = 9.2$ Hz, 2H, Ph); 7.42 (t, $J = 7.9$ Hz, 4H, Ph); 7.17 (t, $J = 7.4$ Hz, 2H, Ph). ¹³C-NMR, (100.6 MHz, DMSO-*d*₆, δ): 166.02, 153.02, 147.06, 142.17, 140.42, 139.96, 136.94, 129.62, 126.07, 124.77, 121.80, 121.54, 121.27, 118.70. EI-LRMS (m/z (%)): 331 (37) [M⁺], 239 (61), 185 (11), 164 (35), 138 (85), 119 (57), 108 (51), 91 (56), 78 (42). FTIR (KBr) [Wavenumbers (cm⁻¹): ν_{N-H} : broadband 3316; $\nu_{Ar C-H}$: 3092; $\nu_{C=O}$: 1713, 1640; δ_{N-H} : 1594; ν_{NO_2} (As, S): 1535, 1325.

Syntheses of the polyamides

The preparation of the parent copolyamide **CP1** (Scheme 2) was performed following the conventional solution low temperature polycondensation

method from 5-azidoisophthaloyl dichloride, isophthaloyl dichloride, and *m*-phenylenediamine ($\eta_{inh} = 1.25 \text{ dL g}^{-1}$; $[\eta] = 1.32 \text{ dL g}^{-1}$; $M_w = 5.9 \times 10^4$).⁵

Parent copolyamide CP2. To a solution of 1 g of copolyamide **CP1** in 5 mL of DMA, 0.5 g of NaBH₄ is added. The mixture is stirred for 30 min at room temperature, and then poured into water, forming a white, fibrous, swollen polymer precipitate that was filtered and washed thoroughly with water. Yield: 93%; $\eta_{inh} = 1.12 \text{ dL g}^{-1}$; $[\eta] = 1.36 \text{ dL g}^{-1}$; $M_w = 6.1 \times 10^4$).⁵

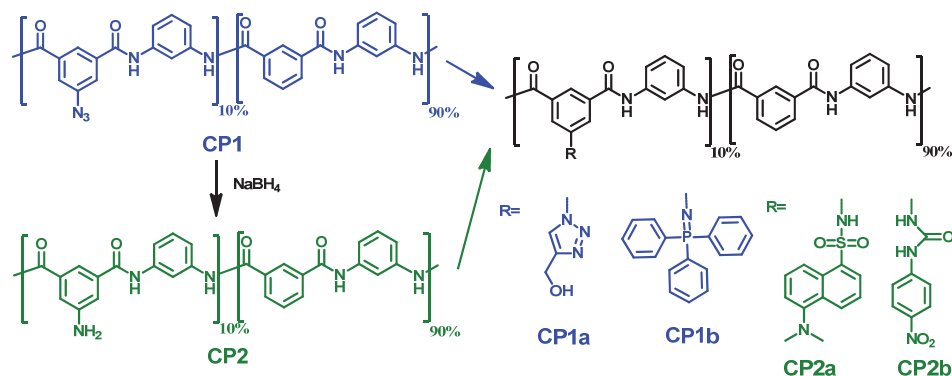
Synthesis of copolyamide CP1a. To a solution of 0.2 g of copolyamide **CP1** in 16 mL of DMA/H₂O (15/1, v/v) was added 1 equivalent of propargyl alcohol along with 5 mol % of CuSO₄·5H₂O and 10 mol % sodium ascorbate. The mixture is stirred at 60°C for 24 hours and then precipitated in water, filtered off and washed with distilled water. Yield: 68%.

Synthesis of copolyamide CP1b. Copolyamide **CP1** (0.2 g) is dissolved in 5 mL of DMA and stirred for 24 h along with 2 equivalents of triphenylphosphine. The mixture is poured into water, and the polymer is then filtered off and washed with acetone. Yield 92%.

Synthesis of copolyamide CP2a. Copolyamide **CP2** (0.2 g) is dissolved in 5 mL of DMA under a nitrogen blanket. The solution is cooled at 0°C in an ice-bath. To the mixture is added 1.1 equivalents of dansyl chloride, and the mixture is stirred for 30 minutes at 0°C, then for another 4 h at room temperature, and at 80°C overnight. The mixture is then poured into water, filtered off and washed with water. Yield: 81%.

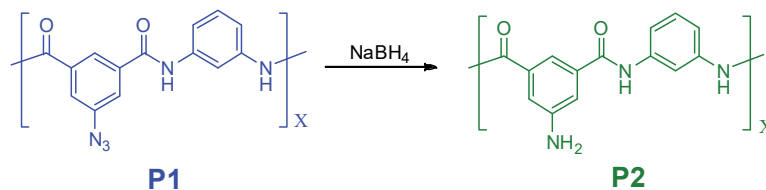
Synthesis of copolyamide CP2b. Copolyamide **CP2** (0.2 g) is dissolved in 5 mL of DMA under a nitrogen blanket. The solution is cooled at 0°C in an ice-bath. To the solution is added 1.1 equivalents of 4-nitrophenyl isocyanate, and the mixture is stirred for 30 minutes at 0°C, then for another

4 h at room temperature, and at 80°C overnight. The mixture is then poured into water, filtered off and washed with water. Yield: 84%.



Scheme 2. Syntheses of the copolyamides.

The preparation of the parent homopolyamides **P1** (Scheme 3) was prepared following a previously described procedure.⁵ The synthesis of homopolyamide **P1a** was achieved following the procedure described for the preparation of **CP2** from 1 g of **P1** using 5 mL of DMA and 0.27 g of NaBH₄. Yield: 87%.



Scheme 3. Syntheses of the homopolyamides.

Results and discussion

The preparation of the functional aromatic polyamides is a promising method for the exploitation of the high performance thermal and mechanical properties of the aramids beyond the preparation of fibers for protective clothes, composite materials and electrical isolating paper. In this regard, it

is advisable to modify as little as possible the aromatic nature of the main chain to maintain the outstanding properties of the aramids and to simultaneously modify the aramid as much as possible to give new functionalities to the materials. In our case, we prepared parent copolyamides with two reactive and easily modifiable chemical azide and amine groups in 10% of the structural units. As an example of the potential of this strategy, we modified these groups to produce four different copolymers with completely different characteristics.

Model and polymer synthesis

In an initial approach to the preparation of the parent functional polyamides and their subsequent modification to render different aramids with *a la carte* properties, we modeled the chemical modification reactions using polyamide models. Thus, the preparation of the first parent model containing the azide groups, **M1**, was easily achieved from 5-azidoisophthaloyl chloride and aniline, and its reduction rendered the parent model containing the free amine group, **M2**. The click reaction of **M1** with propargyl alcohol rendered a model with 4-(hydroxymethyl)-1*H*-1,2,3-triazol groups, **M1a**, and its reaction with triphenylphosphine rendered, via the Staudinger reaction, the model with the iminophosphorane residue **M1b** (Scheme 1). The model **M2** showed the typical reactions of primary aromatic amines, and the reaction with a sulfonylchloride derivative and an isocyanate group rendered the models **M2a** and **M2b** with sulfonamide and ureido groups, as shown in Scheme 1. The modification of **M1** to give **M2** and the reaction performed to introduce a different functionality were achieved in good yield and with inexpensive, simple and reliable organic reactions. The IR and ¹H and ¹³C NMR spectra of all of the models are depicted in the supporting information, Figures S1-S6.

As previously mentioned, aromatic copolyamides with a low percentage of modification of the structural units of the commercial aramids

are interesting materials that can impart new properties and characteristics without penalizing their outstanding mechanical and thermal properties. We also prepared the homopolyamides with azide and amine groups, **P1** and **P2**, respectively (Scheme 2), for comparative ^1H NMR studies and to demonstrate the possibility of increasing the percentage of the structural units containing the free functional groups up to 100%. The ^1H NMR spectra of copolymers **CP1** and **CP2** show the signals corresponding to the two structural units (Figure 1) with the correct integrals, which can be easily observed for the two main amide signals, whereas the homopolymers **P1** and **P2** have only one amide signal. Moreover, the splitting of the amide signals (the red asterisks in Figure 1) indicates a random copolymerization, as expected.²⁸ The full FT-IR spectra and the ^{13}C and ^1H NMR spectra of the materials can be found in the supporting information, Figures S7-S14.

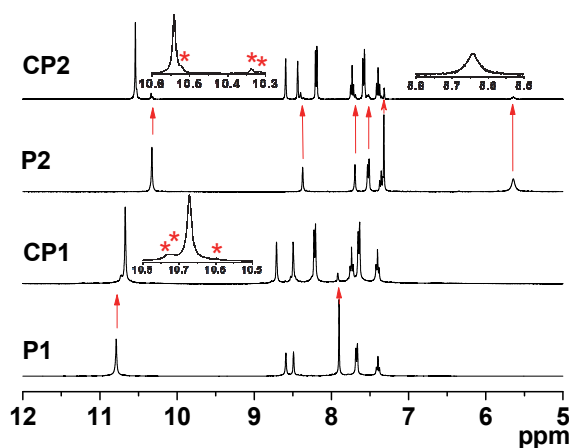


Figure 1. ^1H NMR spectra of homopolymers **P1** and **P2** and copolymers **CP1** and **CP2**.

Optical properties

Regarding the optical properties in solution, the solutions of the models in THF are colorless or pale yellow (Figure 2), and the solution containing the well-known dansyl fluorophore **M2a** exhibits a strong fluorescence at 507 nm

upon irradiation at 350 nm, whereas the other solutions are non or weakly blue fluorescent. On the other hand, tough and creasable cast films obtained from DMA of the polyamides were yellowish (Figure 3) and the polymer CP2a was fluorescent (Figure 3). Pictures taken to the raw polymer materials and films are shown in the supporting information, Figure S15.

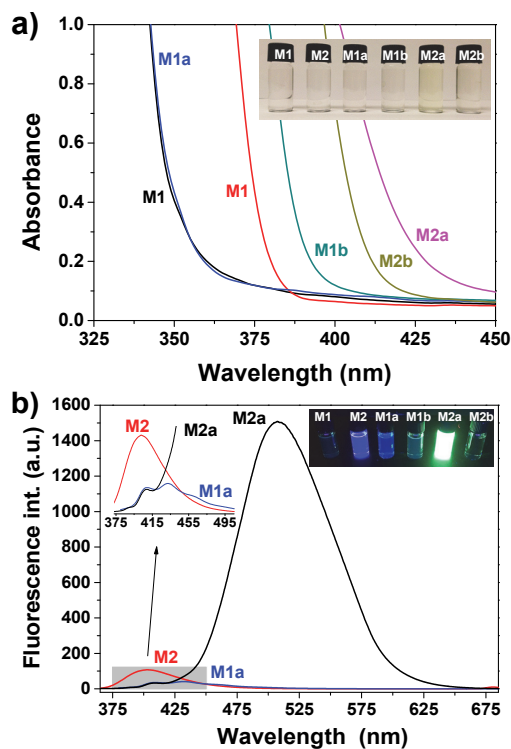


Figure 2. The fluorescence and colorimetric behavior of the polyamide models in the THF solution ($2.30 \cdot 10^{-3}$ M): a) UV/Vis spectra (inset: picture obtained under visible light); b) fluorescence spectra at an excitation wavelength of 370, 340 and 350 nm for **M1a**, **M2** and **M2a**, respectively (inset: picture of all of the models obtained under UV irradiation at 366 nm).

Solubility and water sorption

The materials are highly soluble for aramids and can be dissolved at room temperature in polar aprotic solvents, such as NMP, DMSO and DMA (Table

1). Note that solubility has always been a drawback of polyamides and has limited their technological applications. In addition, the MPIA is transformed into fibers by wet, dry or dry-jet wet spinning from a DMA solution of approximately 19.2% MPIA. As expected, the low molecular weight models are soluble in conventional organic solvents.

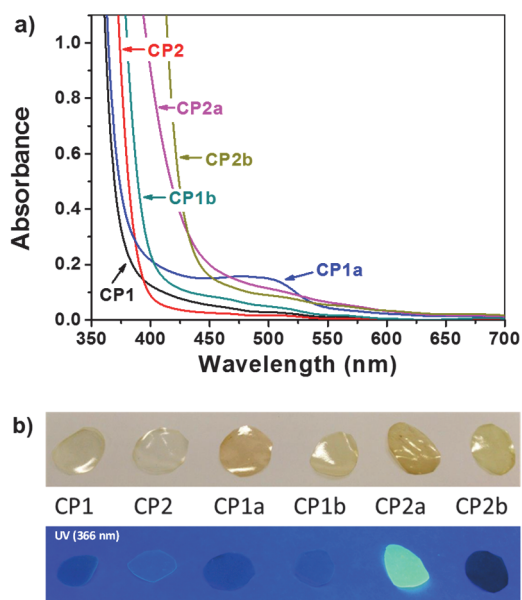


Figure 3. The fluorescence and colorimetric behavior of the polyamide films: a) UV/Vis spectra; b) picture obtained under visible light (top) and under UV irradiation at 366 nm (bottom).

The water uptake from the environment is an important parameter for polar polymers because it influences their performance. In aramids, the water molecules interact with the amide groups, weakening the amide–amide interactions, lowering cohesive energy of the materials and, consequently, their high thermal transitions, mechanical properties, and electrical insulation characteristics.²³ In contrast, in other advanced technological fields, such as reverse-osmosis membrane technology, greater water sorption is generally associated with better performance.

Considering the conventional uptake of 1.2 moles of water per structural unit of the commercial MPIA under an atmosphere of 65% RH at 25°C, the homopolymer **P1** showed a similar behavior, and this water sorption increased to 1.8 molecules of water per structural unit upon reduction of the azide to the amine group to render **P2**. These data are in agreement with the higher water affinity of the primary amine moieties compared with the azide moieties. Similarly, the introduction of bulky side residues with polar groups, such as the dansyl moieties with amine and sulfonamide groups, resulted in an uptake of 2.1 molecules of water per hypothetical structural unit.

Table 1. The inherent viscosities and solubilities of the models and the polymers

Model or polymer	Water uptake		Solubility ^b					
	Weight, %	Water Molecules per structural unit ^c	NMP, DMSO, and DMA	DMF	THF	CHCl ₃ , CH ₂ Cl ₂	EtOH	Acetone
M1	–	–	++	++	+	–	–	–
M2	–	–	++	++	++	–	++	++
M1a	–	–	++	++	++	+–	++	+
M1b	–	–	++	++	++	++	++	+
M2a	–	–	++	++	++	++	++	++
M2b	–	–	++	++	+–	–	+–	++
P1	8.6	1.3	++	+	–	–	–	–
P2	12.5	1.8	++	++	–	–	–	–
CP1	10.0	1.4	++	+	–	–	–	–
CP2	10.6	1.4	++	++	–	–	–	–
CP1a	8.1	1.1	++	++	–	–	–	–
CP1b	9.2	1.4	++	++	–	–	–	–
CP2a	14.0	2.1	++	++	–	–	–	–
CP2b	10.1	1.5	++	++	–	–	–	–

^a Relative humidity of 65%, temperature = 20°C.

^b Polymer concentration = 10 mg of polymer in 1 mL of solvent; ++ = soluble at room temperature; + = soluble on heating; +– = partially soluble; – = insoluble; ^{b)} solvent = sulfuric acid (96%), temperature = 30°C, polymer concentration = 0.5 g/dL. NMP = *N*-methylpyrrolidone, DMSO = dimethyl sulfoxide, THF = tetrahydrofuran, DMF = *N,N*-dimethylformamide.

^c In copolymers, a hypothetical structural unit is calculated by considering the relative weight of the two structural units that comprise the copolyamides (Scheme 2).

Thermal resistance

The thermal resistance of the materials was considered to be related to the decomposition temperatures in terms of weight loss and with the char yield at a given temperature. The thermal resistance was evaluated using thermogravimetric analysis (TGA). The TGA data, summarized in Table 2, confirmed the good thermal stability of the parent copolymers **CP1** and **CP2**, which exhibited no thermal properties compared with the commercial aramid MPIA, which displayed a 5% (T_5) and 10% (T_{10}) weight loss under nitrogen atmosphere at 432 and 452°C, respectively.⁵ The decomposition temperatures of the homopolymer **P1** containing an azide group were very low, approximately 200°C due to the thermal decomposition of the azide to initially render the highly reactive nitrene group with the concomitant loss of nitrogen molecules. The chemical reduction of this group to a primary amine rendered **P2**, which exhibited a thermal behavior similar to that of MPIA and to the parent copolyamides **CP1** and **CP2**. The behavior of the functional copolymer obtained from the parent copolyamides **CP1** and **CP2** showed a behavior intimately related to the new pendant structures and, for example, the thermally labile urea groups diminished the T_5 value to 296°C.

Table 2. Thermal TGA data of the polymers in an inert (N_2) and an oxidizing (synthetic air) atmosphere.

Polymer	N_2 atmosphere			O_2 atmosphere (synthetic air)			LOI ^c
	T_5^a (°C)	T_{10}^b (°C)	CR (%)	T_5^a (°C)	T_{10}^b (°C)	CR (%)	
P1	203	207	49	205	210	1	37
P2	424	461	53	427	461	1	39
CP1	437	456	54	423	468	3	37
CP2	439	459	56	433	467	1	40
CP1a	317	433	46	309	422	1	36
CP1b	375	423	49	350	392	1	37
CP2a	401	429	49	411	456	4	37
CP2b	296	436	41	293	424	3	34

^a 5% Weight loss (T_5), 10% weight loss (T_{10});^b at 800°C.

^c Limiting oxygen index, calculated from the TGA data.

Even more important than the weight loss at a given temperature is the minimum fraction of oxygen in a mixture of oxygen and nitrogen that will support combustion after ignition, i.e., the LOI, which is related to the char yield. The higher the char yield at 800°C, the higher the LOI, and the better the flame resistance properties of the materials. LOI values higher than 21%, the oxygen content of air, will most likely not burn in an open-air situation. Considering that all of the LOI values are significantly higher than 21 and that the LOI of MPIA, calculated using the same method, is 37, the materials have very good fireproof characteristics and must be considered as self-extinguishing materials.

Envisaged potential of the materials

The goal of this study is the preparation of parent high performance polymers easily modifiable for the preparation of new functional materials with a la carte properties. To illustrate the potential preparation of different functional aramids from the parent compounds, **CP1** and **CP2**, four pendant groups were introduced using inexpensive and straightforward reactions. Among the introduced groups, we primarily chose those that we have previously studied for advanced applications. For example, aromatic polyamides with pendant 4-nitrophenyuredido moieties have been studied as colorimetric chemosensory materials for the visual detection of different anions.^{21,29} Similarly, aramids with pendant fluorescence groups, such as the dansyl and other groups, were studied as fluorescent materials and potential LUCO and fluorescent chemosensors for different anions, such as fluoride.^{8,19} Regarding the lighting and backlighting applications of the LUCO materials, Figure 4 shows the CIE chromaticity coordinates for copolymer **CP2a** that were calculated from the fluorescence spectra using the CIE 1931 color matching functions (x and y).³⁰ The CIE color space, or color model, is a numerical model that represents the color spectrum visible to the “average human”, and x and y are used to specify colors in practice. Similarly,

polymers containing pendant triazole moieties have been studied in the removal and sensing of cations from aqueous media, although not with polymers having a main aromatic polyamide chain.²² Moreover, the introduction of primary hydroxyl groups (**CP1a**) opens new possibilities regarding the simple reaction of primary alcohols. In addition, other groups, such as iminophosphorane, show potential for application in biomedicine²⁴⁻²⁶ and as intermediates for other reactions, such as the Sataudinger or the aza-Wittig reactions, including solid or heterogeneous phase reactions.^{31,32}

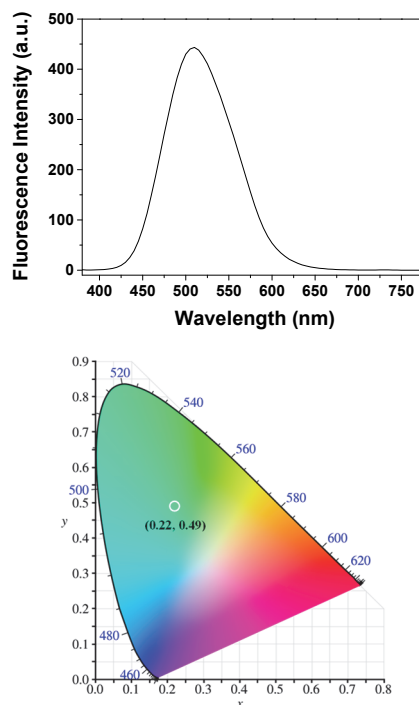


Figure 4. Top: The fluorescence spectra of copolyamide **CP2a** in the solid state (film), which showed an emission maximum at 510 nm. Bottom: CIE 1931 xy chromaticity diagram (Wikipedia commons, public domain image, http://commons.wikimedia.org/wiki/File:CIE1931xy_blank.svg) along with the observed color. Conditions: $\lambda_{ex.} = 365$ nm; Scan speed: 1200 nm/min.

Conclusions

We prepared aromatic polyamides, known as aramids, with primary amine and azide groups. These polymers behave as parent polyamides for the fast, inexpensive and easy preparation of a broad number of aramids with different functionalities to achieve materials with a la carte properties. The derivatization of the parent polyamides can be performed simply due to the exploitation of the reactivity of the primary amino and azide groups. As examples of derivatization, aramids containing fluorescent dansyl groups with potential applications as high-tech luminescent converters or electrochromic materials, the anion and cation receptors urea and triazole with free primary alcohol functional groups for sensing applications, and the iminophosphorane ligand for the preparation of hybrid materials with potential applications in the biomedical field or as an intermediate for other synthetic processes were reported.

Acknowledgements

We gratefully acknowledge the financial support provided by the Spanish Ministerio de Economía y Competitividad-Feder (MAT2011-22544) and by the Consejería de Educación-Junta de Castilla y León (BU232U13).

References and notes

- 1 J. M. García, F. C. García, F. Serna, J. L. de la Peña, *Prog. Polym. Sci.* **2010**, 35, 623-686.
 - 2 K. Marchildon, *Macromol. React. Eng.* **2011**, 5, 22-54.
-

- 3 L. Vollbracht, In *Aromatic Polyamides*; G. Allen, B. Bevington, G. V. Eastmond, A. Ledwith, S. Russo, P. Sigwald eds.; *Comprehensive Polymer Science*, Vol. 5; Pergamon Press: Oxford, 1989; pp 375-86.
- 4 J. Gallini, In *Polyamides aromatic*; H.F. Mark, J. I. Kroschwitz eds.; *Encyclopedia of polymer science and technology*, Vol 3; John Wiley and Sons: New York, 1989; pp 558-584.
- 5 M. Trigo-López, J. L. Barrio-Manso, F. Serna, F. C. García, J. M. García, *Macromol. Chem. Phys.* **2013**, *214*, 2223–2231.
- 6 X. Huang, S. Han, W. Huang, X. Liu, *Chem. Soc. Rev.* **2013**, *42*, 173-201.
- 7 J. de Wild, A. Meijerink, J. K. Rath, W. G. J. H. M. van Sarka, R. E. I. Schroppa, *Energy Environ. Sci.* **2011**, *4*, 4835-4848.
- 8 P. Estévez, H. El-Kaoutit, F. C. García, F. Serna, J. L. de la Peña, J. M. García, *J. Polym. Sci. Part A: Polym. Chem.* **2010**, *48*, 3823-3833.
- 9 P. Uthirakumar, C.-H. CH, E. K. Suh, Y.-S. Lee, *React. Funct. Polym.* **2007**, *67*, 341-347.
- 10 H. Cankaya, R. Kilci, A. Sennaroglu, E. Yilgor, I. Yilgor, *J. Appl. Polym. Sci.* **2010**, *117*, 378-383.
- 11 P. Uthirakumar, C. H. Hong, E. K. Suh, S. Y. Lee, *Chem. Mater.* **2006**, *18*, 4990-4992.
- 12 C. W. Chang, G. S. Liou, *J. Mater. Chem.* **2008**, *18*, 5638-5646.
- 13 S. H. Cheng, S. H. Hsiao, T. H. Su, G. S. Liou, *Macromolecules* **2005**, *38*, 307-316.
- 14 S. H. Hsiao, H. M. Wang, P. C. Chang, Y. R. Kung, T. M. Lee, *J. Polym. Res.* **2013**, *20*, 154.
- 15 S. H. Hsiao, H. M. Wang, P. C. Chang, Y. R. Kung, T. M. Lee, *J. Polym. Sci. Part A: Polym. Chem.* **2013**, *51*, 2925-2938.
- 16 G. S. Liou, H. S. Hsiao, N. K. Huang, Y. L. Yang, *Macromolecules* **2006**, *39*, 5337-5346.
- 17 Y. C. Kung, H. S. Hsiao, *J. Polym. Sci. Part A: Polym. Chem.* **2011**, *49*, 4830-4840.
- 18 Y. C. Kung, H. S. Hsiao, *J. Polym. Sci. Part A: Polym. Chem.* **2011**, *49*, 3475-3490.
- 19 N. San-José, A. Gómez-Valdemoro, P. Estévez, F. C. García, F. Serna, J. M. García, *Eur. Polym. J.* **2008**, *44*, 3578-3587.
- 20 N. San-José, A. Gómez-Valdemoro, V. Calderón, J. L. de la Peña, F. Serna, F. C. García, J. M. García, *Supramol. Chem.* **2009**, *21*, 337-343.
- 21 N. San-José, A. Gómez-Valdemoro, S. Ibeas, F. C. García, F. Serna, J. M. García, *Supramol. Chem.* **2010**, *22*, 325-338.
- 22 A. Gómez-Valdemoro, M. Trigo, S. Ibeas, F. C. García, F. Serna, J. M. García, *J. Polym. Sci. Part A: Polym. Chem.* **2011**, *49*, 3817-3825.
- 23 A. Gómez-Valdemoro, N. San-José, F. C. García, J. L. de la Peña, F. Serna, J. M. García, *Polym. Chem.* **2010**, *1*, 1291-1301.
- 24 L. Vela, M. Contel, L. Palomera, G. Azaceta, I. Marzo, *J. Inorg. Biochem.* **2011**, *105*, 1306-1313.
- 25 M. Carreira, R. Calvo-Sanjuán, M. Sanaú, I. Marzo, M. Contel, *Organometallics* **2012**, *31*, 5772-5781.
- 26 S. Monge, B. Canniccioni, A. Graillet, J.-J. Robin, *Biomacromolecules* **2011**, *12*, 1973-1982.
- 27 A. M. Brouwer, Standards for photoluminescence quantum yield measurements in solution (IUPAC Technical Report), *Pure Appl. Chem.* **2011**, *83*, 2213-2228.
- 28 J. L. Barrio-Manso, P. Calvo, F. C. García, J. L. Pablos, T. Torroba, J. M. García, *Polym. Chem.* **2013**, *4*, 4256-4264.
- 29 N. San-José, A. Gómez-Valdemoro, F. C. García, F. Serna, J. M. García, *J. Polym. Sci. Part A: Polym. Chem.* **2007**, *45*, 4026–4036.

- 30 International Commission on Illumination (<http://cie.co.at/>). The colour matching parameters were downloaded for free from the CIE web page (<http://files.cie.co.at/204.xls>). Access date: November 8, 2013.
- 31 P. Molina, M. J. Villaplana, *Synthesis* **1994**, 1197-1218
- 32 Ali Ramazani, A. Souldozi, *ARKIVOC* 2008, *xvi*, 235-242.

CONCLUSIONS

The use of analyte receptors in aqueous media regardless of the chemical nature of the receptor and its affinity towards the medium can be achieved by means of chemically immobilizing them into hydrophilic polymeric materials. Additionally, the polymer structure can be designed in order to provide an adequate diffusion into the sensory material and to achieve a suitable response time and effective selectivity in the analyte-receptor interaction.

The improvement of their mechanical, thermal and optical properties can further expand the applications of aramids. These improvements are achieved by chemically modifying the main chain of aramids containing functional groups or by introducing groups that provide special physical or chemical features to the materials.

The specific conclusions resulting from this work are the following:

- The design of vinyl monomers with pendant receptors containing fluorenone, 1,2,3-triazole, primary, secondary and tertiary amines, azobenzenes and terpyridines enables the preparation of linear and crosslinked polymers, as well as smart fabrics, that can be used as sensory materials.
 - The chemical design of the polymer structures to be used as chromogenic and fluorogenic sensors permits the preparation of manageable materials with good mechanical properties to be used in aqueous media and in air.
-

- The sensitivity and manageability of the polymers can be adjusted to meet concrete technological requirements.
 - The modification of aromatic polyamides with chromophore or reactive groups is a strategy to prepare high performance materials with improved characteristics that broaden their applicability.
 - The modification of aromatic polyamides, under strict chemical control, allows for the good mechanical performance of the commercially available aramids, improving their thermal behavior and providing enough solubility to be transformed in finished products.
 - The design and synthesis of polymers with target molecules receptors led to the preparation of sensory chromogenic and fluorogenic materials towards explosives (TNT), metal cations, high acidity, water and humidity. These materials were obtained as films, linear copolymers or coated fabrics.
 - Aramids with azido groups in their main structure were synthesized, showing improved thermal, mechanical and reactivity properties compared to commercial meta-oriented aramids. An intrinsically blue colored aramid with improved thermal properties was also obtained by introducing a chromophore in the main chain of meta-aramids.
-

ANEXO

Resumen de méritos

A continuación se recogen las publicaciones científicas, patentes, aportaciones a congresos y estancias en centros extranjeros llevadas a cabo durante la realización de esta Tesis doctoral:

Publicaciones Científicas directamente relacionadas con esta Tesis

- 1) Crosslinked aromatic polyamides: A further step in high-performance materials. M. Trigo-Lopez, J. L. Barrio-Manso, F. Serna, F. C. García, J. M. García, *Macromolecular Chemistry and Physics* **2013**, 214, 2223.
 - 2) Solid Sensory Polymer Kit for the Easy and Rapid Determination of the Concentration of Water in Organic Solvents and Ambient Humidity. M. Trigo-Lopez, A. Muñoz, S. Ibeas, F. C. García, F. Serna, J. M. García, *Sensors and Actuators: B. Chemical* **2014**, 191, 233.
 - 3) Water soluble polymers, solid polymer membranes, and coated fibres as smart sensory materials for the naked eye detection and quantification of TNT in aqueous media, J. L. Pablos, M. Trigo-Lopez, F. Serna, F. C. García, J. M. García, *Chemical Communications* **2014**, 50, 2484.
 - 4) Functional Aramids: Aromatic Polyamides with Reactive Azido and Amino Groups in the Pendant Structure. M. Trigo-Lopez, J. L. Pablos, F. C. García, F. Serna, J. M. García, *Journal of Polymer Science Part A: Polymer Chemistry*, **2014**, 52, 1469.
 - 5) Solid polymer substrates and smart fibres for the selective visual detection of TNT both in vapour and in aqueous media. J. L. Pablos, M. Trigo-Lopez, F. Serna, F. C. García, J. M. García, *RSC Advances* **2014**, 4, 25562.
 - 6) Aromatic polyamides and acrylic polymers as solid sensory materials and smart coated fibres for high acidity colorimetric sensing. M. Trigo-López, J. L. Pablos, A. Muñoz, S. Ibeas, F. Serna, F. C. García, J. M. García, *Polymer Chemistry* **2015**, 6, 3110.
 - 7) Intrinsically colored wholly aromatic polyamides (aramids). M. Trigo-Lopez, A. Miguel-Ortega, S. Vallejos, A. Muñoz, D. Izquierdo, A. Colina, F. C. García, J. M. García, *Dyes and Pigments* **2015**, 122, 177.
 - 8) Colorimetric detection of Fe(III), Co(II), Cu(II) and Sn(II) in 100% water by acrylic polymers with pendant terpyridine motifs for analytical and forensic applications. M. Trigo-López, A. Muñoz, S. Ibeas, F. C. García, F. Serna, and J. M. García. Artículo enviado para su publicación.
-

Publicaciones Científicas indirectamente relacionadas con esta Tesis

- 1) Recent Patents on Aromatic Polyamides. M. Trigo-Lopez, P. Estevez, N. San-Jose, A. Gomez-Valdemoro, F. C. García, F. Serna, J. L. de la Peña, J. M. García, *Recent Patents on Materials Science* **2009**, 2, 190.
- 2) Acrylic copolymers with pendant 1,2,4-triazole moieties as colorimetric sensory materials and solid phases for the removal and sensing of cations from aqueous media. A. Gomez-Valdemoro, M. Trigo, S. Ibeas, F. C. García, F. Serna, J. M. García, *Journal of Polymer Science Part A: Polymer Chemistry* **2011**, 49, 3817.

Capítulos de libros

- 1) M. Trigo, J. L. Pablos, F. C. García, J. M. García, *Aromatic Polyamides en "Handbook of Thermoplastics"*, 2nd Edition, Edited by: O. Olabisi, CRC Press, Boca Raton, 2015.

Propiedad intelectual. Patentes

- 1) S. Vallejos, P. Estévez, M. Trigo, H. El Kaoutit, S. Ibeas, A. Muñoz, F. García, F. Serna, J. L. de la Peña, J. M. García, *Monómeros vinílicos y membranas poliméricas densas como sensores fluorogénicos de cationes pesados y de moléculas biológicas*, Universidad de Burgos. 2011, solicitud n°: P201100041.
 - 2) M. Trigo, S. Vallejos, P. Estévez, S. Ibeas, A. Muñoz, F. García, F. Serna, J. L. de la Peña, J. M. García, *Sensores fluorogénicos de humedad y de agua en disolventes orgánicos*, Universidad de Burgos. 2012, patente n°: ES2461354.
 - 3) S. Vallejos, M. Trigo, J. L. Pablos, M. A. Muñoz, F. C. García, F. Serna, J. M. García, *Sensor colorimétrico de hierro en medios acuosos y biológicos, como aguas industriales, vino, y sangre*, Universidad de Burgos. 2013, solicitud n°: P201300575.
 - 4) J. M. García, F. C. García, F. Serna, J. L. de la Peña, M. Trigo, P. A. Estévez, S. Vallejos, R. Ferrer, *Cross-linked aramid*, First Jet International LTD (China). 2013, patente n°: WO 2013/190023.
 - 5) J. L. Pablos, M. Trigo, S. Vallejos, M. A. Muñoz, L. A. Sarabia, M. C. Ortiz, A. Mendía, F. C. García, F. Serna, J. M. García, *Materiales poliméricos*
-

para la detección colorimétrica visual y cuantificación de explosivos nitroaromáticos y utilización de los mismos, Universidad de Burgos. 2013, solicitud nº: P201301187.

- 6) J. L. Pablos, M. Trigo, S. Vallejos, M. A. Muñoz, L. A. Sarabia, M. C Ortiz, A. Mendía, F. C. García, F. Serna, J. M. García, *Materiales poliméricos sólidos para la detección fluorogénica de explosivos nitroderivados y utilización de los mismos*, Universidad de Burgos. 2014, solicitud nº: P201400073.
- 7) F. C. García, A. Mendía, J. M. García, M. Trigo, F. Serna, S. Vallejos, P. Martínez, J. L. Pablos, M. A. Muñoz, M. J. Rojo, *Sensores cromogénicos para aminas*, Universidad de Burgos. 2014, solicitud nº: P201400595.
- 8) M. Trigo López, A. Mendía Jalón, F. Serna Arenas, A. Miguel Ortega, R. Ferrer Rullán, J. M. García Pérez, A. Muñoz Santamaría, S. Vallejos Calzada, J. L. Pablos Lagartos, F. C. García García, *Poliamidas aromáticas con coloración inherente y utilización de las mismas*, Universidad de Burgos. 2015, solicitud nº: P201500153

Trabajos presentados en congresos

- 1) M. A. Alonso Lomillo; O. Domínguez-Renedo; A. Gil; S. Hernández; M. Trigo; M. Tejero; M. J. Arcos-Martínez, *Disposable Biosensors for Biogenic Amines Determination*, presentación póster, *Euro Analysis 2009*, Innsbruck (Austria), 6-10 de septiembre de 2009
 - 2) V. Tricio, M. Trigo, O. Munguira, R. Vitoria, A. Minguito, R. Góngora, *Una experiencia de aprendizaje utilizando actividades de investigación orientada*, presentación oral, *Innovación Docente en Química 2009 (INDOQUIM 2009)*, Burgos (España), 16-18 de septiembre de 2009
 - 3) M. Trigo; A. Gómez; F. García; J. M. García. *Monómeros diamina azoderivados del pirazol como sensores colorimétricos de Fe(III) y Hg(II)* presentación póster, *IV Workshop on Sensors and Molecular Recognition* Valencia (España) 8-9 julio de 2010. Libro de resúmenes: 71
 - 4) M. Trigo, J. A. Simón, V. Tricio. *Estudio comparativo de monografías "Ciencias para el Mundo Contemporáneo". Preparación y diseño y de una propuesta de actividades para la enseñanza en secundaria*, presentación oral, VI Jornadas sobre enseñanza de la física. *Análisis de la puesta en marcha del Máster de Secundaria en la especialidad de Física y Química*, Burgos (España), 27 y 28 de mayo de 2011.
-

- 5) P. Estévez, S. Vallejos, H. El Kaoutit, M. Trigo, F. Serna, F. García, J.L. de la Peña, J.M. García, *Síntesis de resinas urea-formaldehído con baja Emisión de formaldehído y su aplicación en la Fabricación de tableros de partículas*, presentación oral, *XVI French-Spanish Meeting of Organic Chemistry*, Burgos (España), 19-24 de junio de 2011, Libro de resúmenes: 32.
 - 6) S. Vallejos, P. Estévez, H. El Kaoutit, M. Trigo, F. Serna, F. García, J. L. de la Peña, J. M. García, *Sensory coumarin-containing polymers*, presentación póster, *XVI French-Spanish Meeting of Organic Chemistry*, Burgos (España), 19-24 de junio de 2011, Libro de resúmenes: 74.
 - 7) M. Trigo, A. Gómez, P. Estévez, S. Vallejos, H. El Kaoutit, F. Serna, F. García, J. L. de la Peña, J. M. García, *Linear and crosslinked acrylic polymers bearing pendant receptor motifs. Application to the extraction/elimination of heavy metals from aqueous media*, presentación póster, *XVI French-Spanish Meeting of Organic Chemistry*, Burgos (España), 19-24 de junio de 2011, Libro de resúmenes: 75.
 - 8) M. Trigo, S. Vallejos, P. Estévez, H. El Kaoutit, F. Serna, J. L. de la Peña, F. García, J. M. García, *Fluorogenic and chromogenic polymer Chemosensors*, presentación póster, *XVI French-Spanish Meeting of Organic Chemistry*, Burgos (España), 19-24 de junio de 2011, Libro de resúmenes: 61.
 - 9) H. El Kaoutit, P. Estévez, S. Vallejos, M. Trigo, F. García, F. Serna, J. L. de la Peña, J. M. García, *Aromatic polyamides with pendant fluorene moieties as sensory materials for the colorimetric and fluorogenic sensing of analytes*, presentación póster, *XVI French-Spanish Meeting of Organic Chemistry*, Burgos (España), 19-24 de junio de 2011, Libro de resúmenes: 70.
 - 10) S. Vallejos, P. Estévez, H. El Kaoutit, M. Trigo, F. Serna, F. García, J. L. de la Peña; J. M. García, *Working with water insoluble organic molecules in aqueous media: piperazinedione derivative containing polymers as sensory materials for the fluorogenic sensing of biomolecules*, presentación oral, *European Polymer Congress – European Polymer Federation (EPF)*, Granada (España), 26-30 de junio de 2011, Libro de resúmenes: T4, OP24.
 - 11) P. Estévez, S. Vallejos, H. El Kaoutit, M. Trigo, F. Serna, F. García, J. L. de la Peña, J. M. García, *Synthesis of Low Formaldehyde Emission Urea-Formaldehyde Resins and Their Application to the Manufacturing of*
-

-
- Particleboards*, presentación póster, *European Polymer Congress – European Polymer Federation (EPF)*, Granada (España), 26-30 de junio de 2011, Libro de resúmenes: T1, 31.
- 12) S. Vallejos, P. Estévez, H. El Kaoutit, M. Trigo, F. Serna, F. García, J. L. de la Peña, J. M. García, *Sensory Coumarin-Containing Polymers*, presentación póster, *European Polymer Congress – European Polymer Federation (EPF)*, Granada (España), 26-30 de junio de 2011, Libro de resúmenes: T4, 114.
 - 13) M. Trigo, A. Valdemoro, P. Estévez, S. Vallejos, H. El Kaoutit, F. Serna, F. García, J. L. de la Peña, J. M. García, *Novel Polymetacrylamides Containing a Triazole Moiety. Application to the Extraction/Elimination of Metal Cations from Aqueous Media*, presentación póster, *European Polymer Congress – European Polymer Federation (EPF)*, Granada (España), 26-30 de junio de 2011, Libro de resúmenes: T4, 125.
 - 14) H. El Kaoutit, P. Estévez, S. Vallejos, M. Trigo, F. García, F. Serna, J. L. de la Peña, J. M. García, *Fluorene-derivative containing polymers as sensory materials for the colorimetric and fluorogenic sensing of analytes*, presentación póster, *European Polymer Congress – European Polymer Federation (EPF)*, Granada (España), 26-30 de junio de 2011, Libro de resúmenes: T4, 132.
 - 15) P. Estévez, H. El Kaoutit, S. Vallejos, M. Trigo, F. García, F. Serna, J. L. de la Peña; J. M. García, *Copolímero que contiene un derivado de pirimidina en su estructura como sensor colorimétrico de mercurio en agua*, presentación oral, *V Workshop on Sensors and Molecular Recognition*, Valencia (España), 1-3 de julio de 2011, Libro de resúmenes: 19.
 - 16) M. Trigo, P. Estévez, S. Vallejos, H. El Kaoutit, F. Serna, F. García, J. L. de la Peña, J. M. García, *Reacciones “Click” en la síntesis de monómeros acrílicos*, presentación oral, *Jóvenes Investigadores en Polímeros (JIP)*, Islantilla (España), 22-26 de abril de 2012, Libro de resúmenes: 105.
 - 17) S. Vallejos, P. Estévez, M. Trigo, H. El Kaoutit, F. Serna, F. García; J. L. de la Peña, J. M. García, *Polímeros sensores derivados de la 8-hidoxiquinolina*, presentación oral, *Jóvenes investigadores en Polímeros (JIP)*, Islantilla (España), 22-26 de abril de 2012, Libro de resúmenes: 107
 - 18) T. Torroba, J. García, B. Díaz de Greñu, P. Calvo; J. M. García, S. Vallejos, F. C. García, M. Trigo, *Materiales fluorogénicos para la detección medioambiental de compuestos neurotóxicos*, presentación oral, *VIII*
-

Reunión Científica de Bioinorgánica, Burgos (España), 7-10 de julio de 2013.

- 20) A. Muñoz, S. Ibeas, S. Vallejos, M. Trigo, J. L. Pablos, A. Mendia, F. García, J. M. García, *Study of Some Complexation Reactions in the Design and Synthesis of New Hybrid Polymeric Materials*, presentación oral, *International simposium on metal complexes*, Burgos (España), 16-20 de junio de 2013.
- 21) J. García, B. Diaz de Greñu, P. Calvo, J. M. García, S. Vallejos, F. García, M. Trigo, T. Torroba, *Fluorogenic materials for the environmental detection of neurotoxic compounds*, presentación póster, *International simposium on metal complexes*, Burgos (España), 16-20 de junio de 2013.
- 22) M. A. Muñoz; M. Trigo; E. González; Jesús G.-Ruiz; D. Ibañez; D. Izquierdo; F. C. García; J. M. García, *Spectroelectrochemistry of different palladium containing polymers*. presentación póster, *XXXV Reunión del grupo de electroquímica de la Real Sociedad Española de Química y 1er simposio E3 del Mediterráneo: Electroquímica para la energía y el medio ambiente*, Burgos, España 14-16 julio de 2014
- 23) J. L. Pablos, M. Trigo, S. Vallejos, F. Serna, F. C. García, J. M. García, *Polímeros sensores y tejidos inteligentes para la detección colorimétrica de TNT en medio acuoso y fase vapor*, presentación oral, *XIII Reunión del Grupo Especializado de Polímeros (GEP) de la RSEQ y RSEF*, Girona (España), 7-10 de septiembre de 2014, Libro de resúmenes: 55, ISBN: 978-84-697-0702-9.
- 24) M. Trigo-López; J. L. Pablos; A. Muñoz; S. Ibeas; F. Serna; F. Clemente García; J. M. García. *Sensory membranes and coated fibers for high acidity colorimetric sensing*, presentación oral, *XI Simposio de Investigadores Jóvenes*, Bilbao (España), 4-7 de noviembre de 2014, Libro de resúmenes: 92.

Estancias en centros de I+D+i públicos o privados

- 1) University of California, Santa Barbara (E.E.U.U.) en Materials Research Laboratory del 27/06/2014 al 05/10/2014, bajo la dirección del Prof. Craig J. Hawker.
-